[redacted]

CENTRAL RESEARCH LIBRARY
DOCUMENT COLLECTION

ORNL 1575
Special

AEC RESEARCH AND DEVELOPMENT REPORT

MARTIN MARIETTA ENERGY SYSTEMS LIBRARIES
3 4456 0349499 3

LABORATORY RECORDS

REPORT OF THE 1953 SUMMER SHIELDING SESSION

DECLASSIFIED
Classification Changed To:
By Authority Of: 9.24.70
By: 2.10.71

REFERENCE COPY
DO NOT REMOVE FROM LIBRARY

OAK RIDGE NATIONAL LABORATORY
OPERATED BY
CARBIDE AND CARBON CHEMICALS COMPANY
A DIVISION OF UNION CARBIDE AND CARBON CORPORATION
UCC
POST OFFICE BOX P
OAK RIDGE, TENNESSEE

[redacted]

[redacted]

ORNL-1575

This document consists of 417 pages.
Copy 56 of 255 copies. Series A.

Contract No. W-7405-eng-26

REPORT OF THE 1953 SUMMER SHIELDING SESSION

Participating Personnel

F. H. Abernathy, ORNL
R. Aronson, NDA
E. P. Blizard, ORNL
C. F. deGanahl, Pratt and Whitney
A. Fraas, ORNL
H. Goldstein, NDA
R. Greene, Curtiss-Wright
D. C. Hamilton, Convair
Julius Jonas, Lockheed
John LaMarsh, Pratt and Whitney
B. P. Leonard, Convair
R. Mela, NDA
T. R. Mitchell, GE-ANP
M. Neustadt, Lockheed
R. Olason, Boeing
H. Reese, Curtiss-Wright
R. H. Ritchie, ORNL
A. Simon, ORNL
H. E. Stern, Convair
C. L. Storrs, GE-ANP
T. A. Welton, ORNL
H. P. Yockey, ORNL

Editors

E. P. Blizard, ORNL
H. Goldstein, NDA

[redacted]

DATE ISSUED

[redacted]

JUN 14 1954

[redacted]

CARBIDE AND CARBON CHEMICALS COMPANY
A Division of Union Carbide and Carbon Corporation
Post Office Box P
Oak Ridge, Tennessee

[redacted]

MARTIN MARIETTA ENERGY SYSTEMS LIBRARIES

3 4456 0349499 3

[redacted]

ORNL-1575
Special

Internal Distribution

1. H. Bethe (consultant)
2. D. S. Billington
3. E. [illegible]. Blizard
4. C. [illegible] Center
5. R. [illegible] Charpie
6. C. [illegible] Clifford
7. G. T. Chapman
8. R. G. Cochran
9. J. B. [illegible]ee
10. L. B. [illegible]let
11. W. K. [illegible]en
12. A. P. F[illegible]as
13. S. Glass[illegible]ne (consultant)
14. A. Holla[illegible]er
15. A. S. Hou[illegible]holder
16. H. E. Hung[illegible]rd
17. W. H. Jord[illegible]
18. J. A. Lane
19. C. E. Lars[illegible]
20. R. S. Livi[illegible]on
21. W. D. Man[illegible]
22. F. C. Ma[illegible]nsc[illegible]in
23. J. L. M[illegible]m
24. K. Z. M[illegible]rgan
25. F. H. [illegible]urray
26. R. H. [illegible]itchie
27. A. S[illegible]on
28. A. [illegible] Snell
29. H. [illegible] Stern
30. C. [illegible]. Storrs
31. J. A. Swartout
32. [illegible] H. Taylor
33. [illegible] M. Warde
34. [illegible]. M. Weinberg
35. T. A. Welton
36. E. P. Wigner (consult[illegible]t)
37. G. C. Williams
38. H. P. Yockey
39-[illegible]4. ANP Library
4[illegible]50. Laboratory Records Depa[illegible]ment
51. Laboratory Records, ORN[illegible].C.
52. Health Physics Library
53. Metallurgy Library
54. Reactor Experimental Engi[illegible]ering Library
55-59. Central Research Library
60-149. ORSORT

[redacted]

[redacted]

External Distribution

150. Air Force Engineering Office, Oak Ridge
151. Air Force Plant Representative, Burbank
152. Air Force Plant Representative, Seattle
153. Air Force Plant Representative, Wood-Ridge
154. ANP Project Office, Fort Worth
155-157. Argonne National Laboratory (Kermit Anderson, J. W. Butler)
158. Armed Forces Special Weapons Project (Sandia)
159. Armed Forces Special Weapons Project, Washington (E. C. Lauer)
160-168. Atomic Energy Commission, Washington (Col. M. J. Nielsen, Col. T. A. Redfield, C. R. Horner, A. F. Thompson)
169. Battelle Memorial Institute
170. Boeing Airplane Company (R. Olason)
171. Brookhaven National Laboratory (M. Fox)
172. Bureau of Aeronautics (R. Zirkind)
173. Bureau of Ships (T. Rockwell)
174. California Research and Development Company
175. Carbide and Carbon Chemicals Company (Y-12 Plant)
176. Chief of Naval Research
177. Commonwealth Edison Company
178-180. Convair, Fort Worth (R. N. Little)
181. Convair, San Diego (H. Helms)
182-183. Curtiss-Wright Corporation, Wright Aeronautical Division (C. Campbell, H. Reese)
184. Department of the Navy, Op-362
185. Detroit Edison Company
186. duPont Company, Augusta
187. duPont Company, Wilmington
188. Foster Wheeler Corporation
189. General Dynamics Corp., Electric Boat Division (E. L. Ozapek)
190-192. General Electric Company, APP (T. R. Mitchell)
193. General Electric Company, Richland
194. Glen L. Martin Company (T. L. Nagey)
195-196. Knolls Atomic Power Laboratory (H. E. Stone, L. H. Weinberg)
197. Lockheed Aircraft Company (J. Vanas)
198. Lockland Area Office
199. Los Alamos Scientific Laboratory
200. Materials Laboratory (WADC) (Col. P. L. Hill)
201. Monsanto Chemical Company
202. National Advisory Committee for Aeronautics, Cleveland (A. Silverstein)
203. National Advisory Committee for Aeronautics, Washington
204. Naval Research Laboratory (W. R. Faust)

[redacted]

[redacted]

205. North American Aviation, Inc.
206-209. Nuclear Development Associates, Inc. (H. Goldstein, R. Mela, R. Aronson)
210-214. Nuclear Powered Aircraft Branch, Weapon Systems Division (WADC) (Col. C. D. Gasser)
215. Oak Ridge Operations (K. Kasschau)
216. Patent Branch, Washington
217. Phillips Petroleum Company
218-221. Powerplant Laboratory (WADC) (A. M. Nelson, F. M. Westfall)
222-231. Pratt and Whitney Aircraft Division (Fox Project) (C. F. deGarmo)
232. Rand Corporation
233. San Francisco Operations Office
234. USAF Headquarters
235. U. S. Naval Radiological Defense Laboratory
236. University of California Radiation Laboratory, Berkeley
237. University of California Radiation Laboratory, Livermore
238. Walter Kidde Nuclear Laboratories, Inc.
239-240. Westinghouse Electric Corporation (J. J. Taylor)
241-255. Technical Information Service, Oak Ridge

[redacted]

[redacted]

TABLE OF CONTENTS

		Page
	ABSTRACT	1
	SUMMARY	3
I.	INTRODUCTION	9
II.	PROBLEMS ENCOUNTERED IN SHIELDING NUCLEAR-POWERED AIRPLANES	11
	A. Schematic Discussion of a Nuclear-Powered Airplane and Its Pertinent Shield	13
	1. Basic Statement of the Problem	13
	2. Basic Approach to the Problem	15
	B. Shield Designs for Particular Reactor Cycles	17
	1. Reflector-Moderated Reactor (RMR)	17
	2. Supercritical Water Reactor (SCWR)	23
	3. Direct Cycle Reactor (DCR)	31
	4. Summary of Cycle Configurations	41
III.	METHODS AND TECHNIQUES OF SHIELD DESIGN	43
	A. Specification of Allowable Radiation Levels	45
	1. Factors Involved in Setting Maximum Permissible Exposures	45
	2. Effects of Crew Exposure to Reactor Radiation	52
	3. Conclusions	57
	4. Discussion of Health Physics Instrumentation and Units of Measurement	58
	B. Design of Reactor Shields by Comparison with Bulk Shielding Measurements	67
	1. Semianalytical Method of Shield Design	67
	Spherical reactor and shield	69
	Finite circular slab source	80
	Cylindrical reactors	81
	Discussion of method	83

[redacted]

[redacted]

Page

2. The Homogeneous Shield Method. 84
   Plane isotropic source in infinite medium 85
   Disk source to infinite plane transformation (Hurwitz transformation). 87
   Disk source to point transformation. 90
   Plane to sphere transformation 90
   Plane to cylinder transformation 91
   Geometry for partially specified attenuation functions. 92
   Comparison of source strengths 96

3. Assumptions Involved in the Comparison Methods 105
   Homogeneous shield method. 105
   Semianalytical shield method 108
   Summary. 112

4. Recipes for the Application of the Comparison Methods. 114
   Fast neutrons. 114
   Primary gamma rays 117
   Dose away from the reactor 120

C. Heating in Shields 121

D. Unfamiliar Shield Materials and Their Evaluation 139

1. Characteristics of a Good Shielding Material 140

2. Methods of Evaluation. 143

3. Light Hydrogenous Materials Considered for Comparison. 153

4. Results of Comparisons 158

5. Conclusions. 164

E. Calculation of Crew Compartment Dose 167

1. Direct Path Radiation. 167

2. Air-Scattered Radiation. 170
   Basic assumptions. 170
   Gamma-ray scattering 172
   Neutron scattering 214
   Validity of basic assumptions. 227

F. Radiations Due to Fission Products 233

1. Activation of Coolants from Delayed Neutrons 233

2. Gamma Rays from Fission Decay Products 233

[redacted]

[redacted]

Page

G. Structure and Ground Scattering. 237

1. Single Scatter Method for Thin Structural Members. . . 238

2. Albedo Method for Thick Structural Members 244

3. Ground Scattering. 248

H. Ducts and Internal Voids in Shields. 255

1. Attenuation of Neutrons by Air Ducts in Shields (Theory) 255

2. Effect of Internal Voids on Neutron Attenuation. . . . 261

3. Attenuation of Gamma Rays by Air Ducts and Voids . . . 262

I. Interaction of Shield Weights and Aircraft Performance . . 263

1. Airplane and Shield Design Relationships 263

2. Effects of Shield Weight on Airplane Configuration . . 269

J. Ground Handling of Aircraft with Unit and Divided Shields. 279

IV. APPLICATION OF SHIELD DESIGN METHODS TO THE REFLECTOR-MODERATED REACTOR 285

A. Summary of the Lid Tank Tests. 288

B. Design Procedure for the Reactor Shield. 293

1. Scale-up of Lid Tank Measurements 293

2. Sample Shield Design Calculation 302

C. Dose from Gamma Activity in Heat Exchanger 311

1. Method 1 312

2. Method 2 315

3. Sample Calculation Illustrating Method 1 316

D. Delayed Neutron Activation of Sodium in the Heat Exchanger 321

1. Heat Exchanger with Black Boundaries 323

2. Heat Exchanger with Gray Boundaries. 325

3. Unloaded Heat Exchanger for Transparent Curtain. . . . 326

[redacted]

[redacted]

Page

4. Unloaded Heat Exchanger for Black Curtain 328

5. Loaded Heat Exchanger for Transparent Curtain 330

6. Loaded Heat Exchanger for Black Curtain 332

7. Sample Calculations 333

E. Shield Patches. 343

F. Replacement of Water with Hydrocarbon Fuel. 347

G. Shield Cooling. 351

H. Design Procedure for the Crew Compartment Shield. 353

1. Assumptions and Basic Data. 353

2. Design Procedure. 355

3. Conclusions 359

I. Results 363

V. RECOMMENDATIONS FOR FUTURE RESEARCH 377

1. Determination of Tolerance Dose 379

2. Improvement of Computational Methods. 380

3. Experimental Program. 382

4. Shield Design Studies 384

VI. TRENDS IN SHIELD DESIGN 385

VII. BIBLIOGRAPHY AND ACKNOWLEDGMENTS. 399

[redacted]

[redacted]

ABSTRACT

The direct, supercritical water, and reflector-moderated circulating fluorides aircraft reactor cycles are described with particular attention being called to the shielding problems they present. Recommended procedures are then presented for aircraft shield design. Biological tolerances are first discussed. Next, two methods are described to derive design information from bulk shielding experiments, and these are compared and evaluated. Neither is infallible but they have different limitations. Recipes are given for solution of some of the more common attenuation problems. A section follows on the calculation of heating in shields.

The possibilities of shield improvement by use of the more unfamiliar materials are examined, with many suggested candidates. The calculation of air scattering and crew shield penetration is treated for typical crew shield designs, the method presented being illustrative of a way in which it is possible to design quickly for any degree of dividedness.

Methods are described for treatment of fission product activity, structure and ground scattering, and ducts through shields. The interaction of shield weights and airplane performance is discussed in the light of modern nuclear-powered airplane designs, and problems of ground handling are pointed out with some suggestions for their solution.

The foregoing design methods are then applied to the circulating fused fluoride reflector-moderated reactor and a series of representative shield weights are evolved. A special problem treated only in this section is a calculation of activation of a secondary coolant by delayed neutrons released by the fuel in the heat exchanger.

[redacted]

Recommendations are made for future research, particularly in biological effects of radiation, computational methods, new experiments, and design studies. Trends in shield design are discussed, it being pointed out that the calculational methods in particular are showing more promise of applicability than ever before, much thanks to the better basic data and more powerful calculating machinery.

SUMMARY

This document purports to give the best available methods of aircraft shield design. It represents the results of a concerted effort on the part of representatives of seven interested technical organizations, primarily during June of 1953, but including some subsequent improvements and additions which have become available up to the time of publishing. In all of the work the aim has been to illustrate methods rather than to develop actual designs.

To insure concentration of effort on important problems, the several schemes currently in favor for achieving a nuclear-powered airplane were first studied and the problems associated with their shield designs were delineated.

The reflector-moderated reactor is a circulating fluoride fuel reactor in which the moderation is accomplished largely in a beryllium reflector region which blankets the core. The advantage of this scheme is that the reflector-moderator is effectively the first part of the shield and the reactive core is kept quite small. The fluoride fuel gives up its heat to a secondary coolant, probably liquid sodium, in a heat exchanger which is wrapped around outside of the reflector. This heat exchanger also assists in shielding. Outside of the heat exchanger is a steel container, and this is followed by a fairly thick (~6-in.) layer of lead. A_t the outside of this lead layer is a thin layer of boron (perhaps B^{10}), and a quite thick layer of borated water.

The basic attenuation of this arrangement of reactor and shield has been determined by bulk shielding experiments on a facility such as the ORNL Lid Tank. Special problems which are not solved in such a series of tests have

to do with the radioactivity in the heat exchanger. The fission product gamma rays are a very poorly known source since the very short half-life emitters, which have not been investigated, are involved. In addition, the delayed neutron emitters cause the sodium to become activated. This problem was given special attention during the session.

The supercritical water reactor uses fixed fuel cooled by supercritical water which transfers its heat to a second fluid in an external heat exchanger. Special problems for this reactor include the activity (both neutron and gamma) of the water, the cooling of the shield, and the cooling of the pressure shell. For the latter, calculations of energy deposition in shield and pressure vessel are particularly important.

The third reactor type considered was the so-called direct cycle reactor being studied by General Electric (Evendale). Special problems associated with this cycle have primarily to do with the large air ducts which are necessary. No new developments appeared during the session in the methods of calculation of duct attenuation. Some attention was given, however, to engine arrangements which would ease the air-flow problem. These, however, have not been given a thoroughgoing analysis by the full engineering complement at GE.

The section on methods and techniques of shield design is opened with a review of the situation with regard to the tolerable radiation dose. This information is of course basic to any shield design and the proper choice of tolerance dose is not obvious. In addition to the collection of that information which is available for making the choice, some recommendations are made regarding the choice of plane crew and of the shield arrangement. It is proposed that genetic and late effects can be minimized

by choosing older men to operate the plane. Some consideration is given to the desirability of using additional shielding for the more sensitive organs such as the eyes and the gonads.

Considerable attention was paid to the problem of interpreting bulk shielding experiments and applying their results to actual shield designs. In the so-called semianalytic method attenuation is taken to be characteristic of the materials on the line-of-sight from an element of source to the detector (at the crew position). This allows a spherically symmetric variation of shield material in spherical geometry and correspondingly regular variations for other geometries.

Another method, strictly applicable only to homogeneous reactor-shield regions, which has been in use for some time, was examined, improved, evaluated, and compared to the semianalytic method. The two methods are quite different in approach, and although neither is exact, the fact that they agree in most cases of interest is of considerable comfort. From these methods useful recipes for shield design were derived and presented, including treatments to be applied in calculation of heating in shields.

A rather broad look was given to the field of the more unusual shield materials. Systematic study of various classes of compounds such as the saturated hydrocarbons revealed optimum chemical compounds. The lithium compounds were also examined in some detail, with particular emphasis on LiH. This compound offers a definite weight advantage over water, for example, although it is surely less convenient to use.

Methods for intercomparison of shield materials were developed and used, taking account not only of the better neutron attenuation which the hydrogenous materials afford, but also of the penalty which must be paid in additional lead for the poorer gamma-ray attenuation.

The methods for calculation of crew compartment dose in a divided shield are laid out as completely as possible. Much of the work has appeared previously in the Reactor Handbook, but there is some extension of that work. The validity of the methods is critically examined and some effort was expended in estimating the amount by which the estimates are conservative. Structure and ground scattering are treated in much the same way.

The phenomenological theory of the effect of air ducts on shield attenuation is given much as it was for the Reactor Handbook. The emphasis is on inclusion of useful results with a rather briefer treatment of the proofs.

The interaction of shield weights and aircraft performance was studied as a revision and extension of the work of the Technical Advisory Board (1950).[1] More attention was paid to the differences in airplane configuration between those with unit and divided shield power plants. Similarly in the study of ground handling methods the contrast was drawn on the basis of degree of dividedness. Of course the divided shield leads to more difficult ground handling problems, but the thick crew shield promises considerable advantage in case of an accident in which radioactive materials are spread about.

The methods described in the report are illustrated insofar as is possible in actual calculations for reflector-moderated reactor (RMR) shields. A number of cases are calculated to show the variation in weight and size with the several design parameters. Of special interest is a calculation of the activation of sodium in the heat exchanger due to the delayed neutrons released there by the circulating fuel.

(1) "Report of the Technical Advisory Board," ANP-52 (Aug. 4, 1950).

In recommendations for future research it is pointed out that essentially no actual aircraft shielding experience has been obtained to date and that no shield designs can be considered as firm until at least a full-scale mockup has been tested. Accordingly, this is an essential next order of business. Further than this is the need for much other experimental work which will enable refinement of designs. Calculational methods which show promise are also listed as likely places for future effort.

A section on trends in shield design recalls the recommendation of the 1950 Shielding Board for a divided shield. This recommendation has been followed in most aircraft shield designs during the last three years, although the degree of division fluctuates with core size. Present efforts are toward a modified version of the divided shield, which places enough shielding at the reactor to prevent excessive radiation fields around the plane but which does not completely surrender the weight savings of the divided shield. It is predicted that weight savings in the future will be largely accomplished by utilizing lighter shielding materials. It is also pointed out that there have been significant improvements in the tools available to the shield designer, with many more anticipated for the next new years. The Lid Tank Shielding Facility has been supplemented by the Bulk Shielding Facility, which began operation in 1950, and the Tower Shielding Facility which begins operation in early 1954. The testing of full-scale mockups in these facilities together with improved instrumentation will continue to lend assurance to shield designs. Interpretation of such shielding measurements has already confirmed the utility of the removal cross section concept, provided a basis for a semi-empirical duct theory, formalized a method of shield optimization, and promises to add much more

in the future. Measurements of slant penetration of gamma rays at NBS and BNL have also proven directly helpful for crew shield design. Because badly needed microscopic nuclear data and high-speed computing machines have been made available, great strides have been made in fundamental shielding research during the last three years. There are, of course, many problems yet to be tackled, and the form of shield design in the future cannot be predicted. The over-all program, as presently conceived, appears adequate to insure the successful performance of a shield constructed for a nuclear-powered airplane provided only that the myriad of engineering details do not overload the basic design.

I. INTRODUCTION

Although many aircraft shields have been designed, some regions of uncertainty continue to admit a freedom of judgment which is uncomfortably large. With numerous groups engaged in this field it is inevitable that the freedom be exercised in different ways with corresponding diversity in the shield configurations and weight estimates. Since standardization of the design methods would considerably minimize this diversity, it was felt that representatives from several organizations should meet with this as their prime objective. Accordingly, a 1953 Summer Shielding Session was held at Oak Ridge National Laboratory, and the conclusions of the group on standardization and tangent problems are presented in this report.

During the study period of four weeks it became quite clear that the situation was not simple. In many of the problems it was not a case of merely choosing among a variety of methods, but rather turned into a desperate casting about for one that was reasonably satisfactory. In these instances the alleviating research is indicated and recommended for early consideration. In addition, an interim choice of method is made with clear notation of its temporary nature and the seriousness of the hiatus which it covers.

The situation was not all so black. In many cases more than one adequate method was available and in these it was possible to standardize to some extent. It is to be emphasized, however, that the report which follows should be constantly subject to review and amendment. The Session participants have no intention of arrogating to themselves the right to standardize the field except by default.

In order to insure that the deliberations of the Session were concentrated in the most important regions, shield designs for three reactor cycles were studied to indicate not only the gamut of the problems encountered, but also their relative importance to the aircraft. In addition, to illustrate the design methods and to exhibit the variations in shield configurations with several basic parameters, a rather complete shield analysis (but of course not a completely detailed design) was carried out for the fused salt reflector-moderated reactor (RMR).

Although this report is largely a presentation of studies which are unquestionably shielding, two border problems were also considered, albeit cursorily. One of these, the discussion of the interplay between the shield weight or its distribution and the configuration of the airplane, shows how at least one airplane company (Boeing) uses shielding information in the evolution of an aircraft design. The other border problem is the specification of a tolerable dose and this is included to indicate the frustration which shielding personnel experience in attempting to make their designs realistic in this respect.

II. PROBLEMS ENCOUNTERED IN SHIELDING NUCLEAR-POWERED AIRPLANES

II-A. SCHEMATIC DISCUSSION OF A NUCLEAR-POWERED AIRPLANE AND ITS PERTINENT SHIELD

1. Basic Statement of the Problem

Nuclear power for aircraft propulsion implies a reactor which inevitably is a source of biologically damaging radiation. The problem is to interpose materials and arrange the airplane so that the crew and other sensitive components are not subjected to excessive radiation.

The reactor itself is always potentially the most important source. Fast neutrons and gamma rays leak from it and both must be attenuated. In addition, the neutrons on being scattered or absorbed, can produce gamma rays and these must likewise be attenuated. The reactor must be cooled, and the coolant can become activated, so that on emergence it constitutes another secondary source. If the fuel is circulated the delayed neutrons will be released where they can activate a secondary coolant. In addition, the structure itself may become activated by the leaking neutrons. All these sources, both primary and secondary, must be known.

Of equal importance is a knowledge of the sensitivity of the crew and parts of the airplane to radiation. That of humans is known within rather poorly defined limits. Less is known about the sensitivity of electronic equipment, and practically nothing is known about the susceptibility of boron-shielded machinery (engines, etc.) for becoming activated. These areas of ignorance, while very inconvenient, do not render shield designing impossible since the uncertainties that they introduce in shield weight are not out of reason.

Other information which is needed for shield design would include an evaluation of the inconvenience of a large radiation field around the

airplane, as well as of the activation of various components such as the turbojets. Lesser problems such as the interference of nuclear radiation with communications systems and the detectability resulting from a radiation-induced visible light will affect the design to some extent.

Besides the basic problems described above there are some which are characteristic of the shield itself. The shield becomes heated by the radiation it is attenuating and hence must be cooled. This requirement usually militates for a liquid component which can be circulated to a heat exchanger. The shield may also suffer radiation damage and this precludes the use of complicated molecules in the higher radiation fields since these are essentially impossible to recombine by simple means. By containing a compound such as LiH in a gas-tight space it is quite easy to limit the dissociation since recombination will compensate for the radiation-induced decomposition. It is not hard to imagine that no simple analogous process exists to preserve $(CH_3)_4NBH_4$.

The reactor coolant must be passed through the shield and openings must be provided for this. The worst problem of this sort occurs of course with gas-cooled shields, since the ducts are then largest and the coolant is most transparent to radiation. Similarly, if the crew is shielded some provision must usually be made for seeing out and for this the use of lead glass and water shielding may be contemplated.

2. Basic Approach to the Problem

Probably the most fundamental decision which must be made in the evolution of a shield design is the location of the shield. That is to say, it must be decided whether the shield material is to be located around the reactor, around the crew, in between as a shadow shield, or in some combination of these. It can be shown quite clearly that a shadow shield per se is not enough because of the high scattered flux which the air introduces. It is also true that for the sizes of reactor and crew compartments and for the separation distances which are contemplated that the lightest shields are those in which two asymmetric shields are used, one around the crew and the other around the reactor. This arrangement is of course that commonly called a divided shield. There is no question that a divided shield would be used in almost every case if the only criterion were crew protection for minimum weight.

Other considerations mentioned above, however, militate for placing a greater fraction of the shielding at the reactor to reduce the general radiation level about the plane. This of course eases many of the problems such as ground handling, engine activation, and payload protection. The situation in which all the shielding is at the reactor is that in which a unit shield is used. This is not to say that the ground handling problem is thereby eliminated, since the reactor-crew separation distance is relied on for an attenuation of about 70. In other words, with reactor at full power the dose rate at the reactor shield exterior will be 70 times that at the crew position, so that many ground handling problems are seriously affected.

There has been considerable effort expended recently, some of it reported here, toward a modified divided shield in which low weight and

handling ease are compromised. It is thus possible to eliminate the activation of the engines and other components, to reduce the servicing problems, and in general to ease the other divided shield disadvantages.

In general, the smaller the reactor core the less divided will be the optimum weight shield, so that for the comparatively small reflector-moderated reactor the penalty for easing handling problems is not excessive, at least for the lower end of the power range.

The various reactor shields which have been studied by this group are discussed in more detail in the next section.

II-B. SHIELD DESIGNS FOR PARTICULAR REACTOR CYCLES

1. Reflector-Moderated Reactor (RMR)

The basic design of the reflector-moderated reactor was developed[1] to make the reactor, intermediate heat exchanger, and shield a very closely integrated unit with shielding considerations paramount. The salient problem was the reduction of the activation of the secondary fluid to a tolerable level while at the same time keeping the weight of the "completely engineered" reactor--heat exchanger-shield assembly fairly close to that of an ideal unit shield. This was accomplished by employing an unusually thick reflector followed by a layer of boron or boron carbide. Fortunately, such an arrangement also satisfies other major shielding requirements. The leakage of neutrons from the core to the pressure shell is reduced to the point where secondary gamma production in the pressure shell region is relatively minor. In addition, virtually all of the energy (99.98%) released by fission in the reactor is converted into heat in the high-temperature zone enclosed by the pressure shell. Thus the amount of heat generated in the relatively low-temperature shield region is very small and hence the shield cooling system imposes an almost negligible weight and drag penalty. Finally, the neutron and gamma flux can be reduced to a level such that radiation damage to shielding materials just outside the lead region should not be serious.

A typical layout of the design is given in Fig. II-B-1 in which a vertical cross section through the reactor core, moderator, and heat exchanger shows a

(1) The evolution of this design is covered by A. P. Fraas, "Three Reactor--Heat Exchanger--Shield Arrangements for Use with Fused Fluoride Circulating Fuel," Y-F15-10 (June 30, 1952).

series of four concentric shells, each of which is a surface of revolution. The two inner shells surround the fuel region at the center (i.e., the core of the reactor) and separate it from the beryllium "island" and the outer beryllium reflector. The fuel circulates downward through this region where the fissioning takes place and then downward and outward to the entrance of the spherical shell heat exchanger that lies between the moderator outer shell and the main pressure shell. It then flows upward between the tubes in the heat exchanger into two mixed-flow pumps at the top. From the pumps it is discharged inward to the top of the annular passage leading back to the reactor core. The fuel pumps are sump-type pumps located in the expansion tank at the top. The total fuel volume in the system for this design would be approximately 7 cu ft, of which approximately 1.3 cu ft would be in the reactor core and 1.0 cu ft in the expansion tank. Most of the balance would be in the interstices between the tubes in the heat exchanger.

The moderator is cooled by sodium which flows downward through passages in the beryllium and back upward through the annular space between the beryllium and the enclosing shells. Two centrifugal pumps at the top circulate the sodium first through the moderator and then through the small semi-toroidal Na-to-NaK heat exchangers around the outer periphery of the pump-expansion tank region. These heat exchangers are necessary because the sodium in passing through the high thermal-neutron flux in the moderator is rendered far too active to be allowed to flow outside of the shield.

Inconel was chosen as the primary material of construction because of the readily fabricated materials tested to date it seems to be the most resistant to fluoride corrosion. Beryllium was chosen as the moderator material partly because it seems to be the best material obtainable from

[redacted]
DWG. 18743

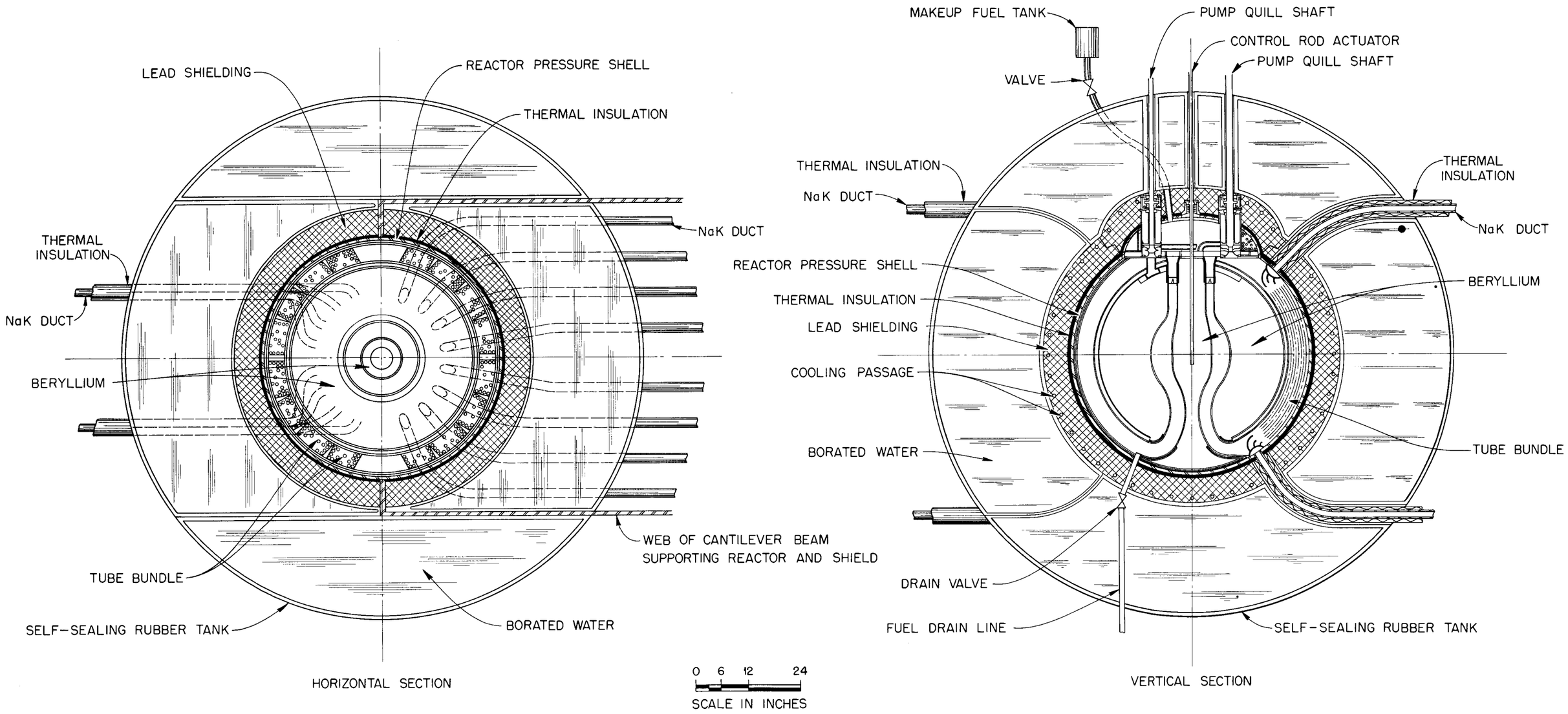

Fig. II-B-1. Cross Sections of Reflector-Moderated Reactor.

both shielding and critical mass standpoints, and partly because its physical properties appear to be superior to any other material that might be used in that location except graphite. It was decided that the vase-shaped island in the center should be used because it reduces the critical mass and improves the power distribution in the fuel region, and because it promises to give the simplest and most desirable fuel passage from the hydrodynamic standpoint. The 12 in. thick beryllium reflector followed by 1 in. of B_4C was chosen originally to keep the neutron flux escaping to the heat exchanger region to a level approximately equal to that of the delayed neutron flux from the circulating fuel in that region. (It has since been demonstrated that this thickness is the minimum permissible to satisfy criticality requirements and should be no greater from the shielding standpoint. It was also found that a considerable weight saving can be achieved by substituting 0.13 in. of B^{10} for the 1 in. of B_4C.)

The spherical shell heat exchanger that makes possible the compact layout of the reactor--heat exchanger assembly is based on the use of tube bundles curved in such a way that the tube spacing is uniform irrespective of "latitude."[2] The individual tube bundles terminate in headers that, before the tubes are welded in place, resemble shower heads.

The fuel-to-NaK heat exchanger presents some special problems peculiar to this design. The material in the spherical shell intermediate heat exchanger is roughly 30% fuel, 30% Inconel, and 40% NaK by volume. It is about 70% as effective as water for the removal of fast neutrons so that it is of real value from the shielding standpoint. The delayed neutrons and the decay gammas from the circulating fuel in the heat exchanger might appear to

(2) A. P. Fraas and M. E. LaVerne, "Heat Exchanger Design Charts," ORNL-1330 (Dec. 7, 1952).

pose a serious handicap. However, the delayed neutrons from this region, having an energy of only about 1/2 Mev, have an attenuation length much shorter than the corresponding attenuation length for radiation from the core. Thus from the outer surface of the shield the intermediate heat exchanger appears as a much less intense source of neutron radiation than the more deeply buried reactor core. The short-half-lived fission-product decay gammas present a more serious problem. In general, they appear to be a less important source of radiation than the secondary gammas from the pressure shell and the lead, but they must be included in the calculations.

Figure II-B-1 shows both a horizontal and a vertical cross section through a representative reactor-shield assembly. The shield was designed so that it might be inserted through an opening 6.7 ft wide in the bottom of the fuselage. Thus it would lend itself to installation in the bomb bay of the B-36 just aft of the main spar, for example. Two cantilever beams placed on 6-ft centers were employed as the primary structure. The front ends of these cantilever beams could be bolted or pinned to fittings on the rear spar while the reactor and the shield structure would be attached to the rear ends. The shield structure would be divided into six major sections, each of which would consist of an inner layer of lead and an outer tank of rubber that would be filled with borated water. The top and bottom sections would be separated from the four in the central region by surfaces of revolution passing through the centerlines of the NaK ducts that penetrate the shield. Two large bowl-shaped rubber tanks would be placed at either side. These could be deflated while the power plant was being inserted in the airplane and then could be filled with water after the power plant was in place. The top section of the shield would be pierced by five tubes. Four of these tubes would carry quill shafts to transmit power from bleed-off air turbines to the pumps at the top of the reactor, while the fifth would carry the control rod actuating mechanism.

2. Supercritical Water Reactor (SCWR)

A representative supercritical water airplane propulsive system has been studied from the shielding point of view. Neither the over-all system nor its components, the airplane, engines, reactor, or shield, can be considered as engineered designs; however, they do serve as a rough framework within which the problems involved in producing an efficient biological shield for this type of propulsion system can be examined. It should further be noted that the studies from which this shield resulted were performed before the 1953 Summer Shielding Session and that unfortunately time did not permit revision of the shield where indicated by the conclusions of this session.

Reactor

The 400-megawatt reactor core assembly is a 2.5 ft diameter by 2.5 ft long right circular cylinder. It is surrounded by a water reflector of non-uniform thickness and density such that the outer edge of the reflector is essentially spherical. Some 200 uranium-bearing stainless steel fuel elements running the length of the cylinder between circular tube sheets at each end are arranged radially in such a pattern as to provide an essentially flat flux distribution across the reactor. The reactor is moderated by water flowing between the fuel elements, and the heat is removed by water flowing through the fuel elements parallel to the axis of the cylinder. Reactor control is obtained by moderator water density control through temperature and it is contemplated that control rods will not be required. The reactor operates at approximately 5500 psi, which is above the critical pressure for water so that no boiling takes place. Water enters the reactor at approximately 460°F and leaves at 1000°F. During the life of the reactor the reflector and moderator densities vary from approximately 0.4 to 0.8 g/cc and

it is presently believed that a core life of the order of 500 hr can be obtained. The core consists of approximately 12.0% stainless steel and 88% water by volume. A schematic diagram of the SCWR is given in Fig. II-B-2.

Pressure Shell and Thermal Shield

Containing the high pressure requires a rather heavy pressure shell operating at relatively high temperatures. From a weight standpoint it would be desirable to keep the enclosed volume to a minimum by placing the shell directly around the reflector. However, in this case the pressure shell would be subject to an intolerable operating temperature and very large thermal stresses due to radiation heating in the shell itself. Thus a layer of borated stainless steel balls is wrapped around the reflector as a thermal shield. The balls, of course, carry no load and are sufficiently small, approximately 0.25 in. in diameter, to provide a large amount of cooling surface, and inlet water is continuously filtered through them to carry away the heat. In this typical case the thermal shield is about 6.5 in. thick and consists of about 30% water and 70% stainless steel by volume. Water enters the thermal shield at its outside surface from a thin passage between the thermal shield and the inside of the pressure shell which it also cools. After passing through the thermal shield this water joins the reflector and moderator water and finally flows through the fuel tubes so that the heat rejected by the pressure shell and thermal shield is usefully absorbed by the working fluid. The 5 ft diameter pressure shell is spherical, and approximately 2 in. thick, with considerable reinforcement in local areas where the support structure is attached and the three or four water inlet and outlet lines penetrate the shell. Analytical studies, partly supported by Lid Tank experiment, have shown that the thermal shield, although it does not suppress secondary gamma rays completely, is quite efficient as gamma shielding from the biological point of view. For the

DRAWN FROM PWAC-39, COURTESY PRATT AND WHITNEY AIRCRAFT CORPORATION

[redacted]
ORNL-LR-DWG 417

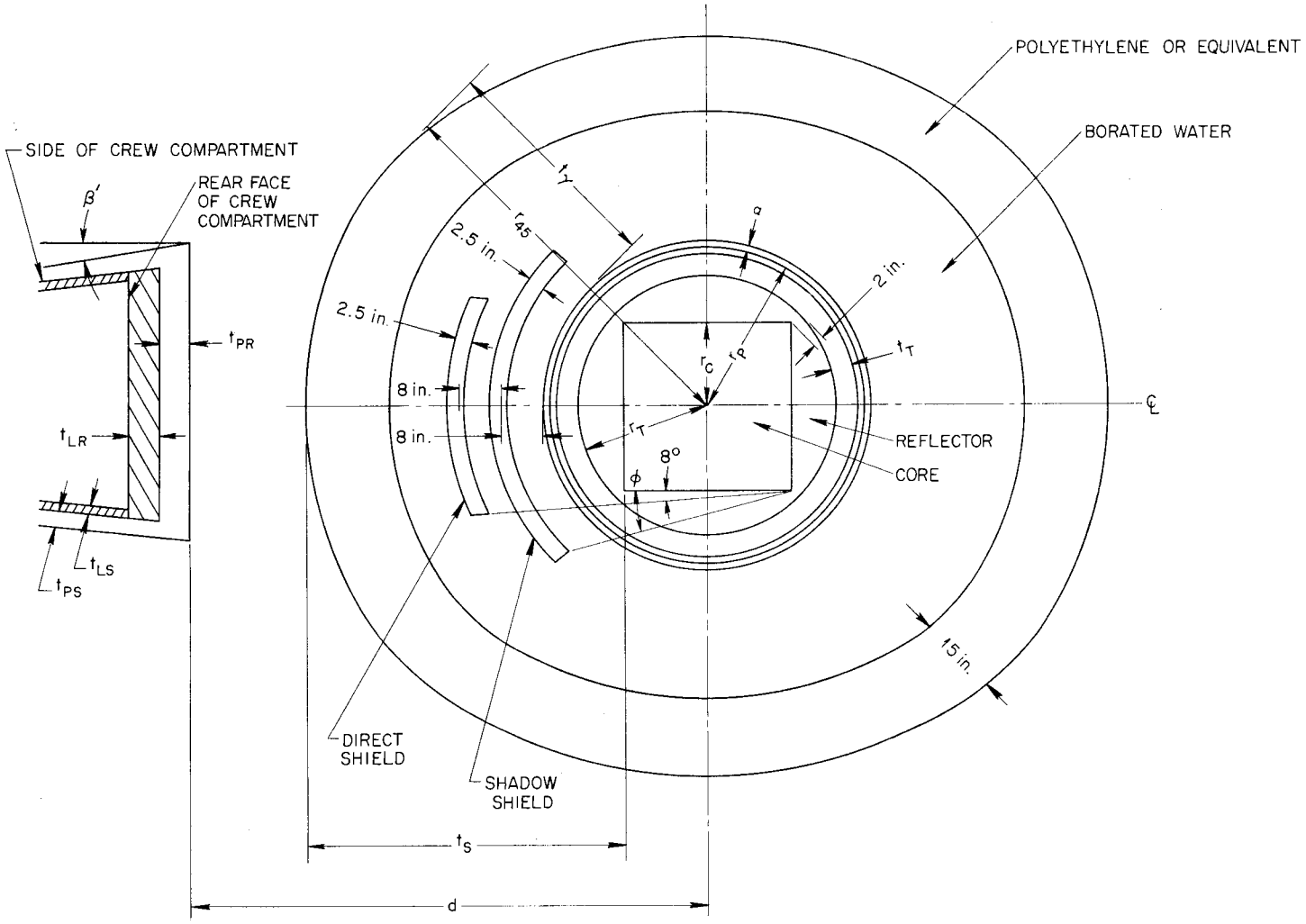

a = Thickness of Pressure Shell (in.)

c = Core (Steel + Water + Uranium)

d = Distance from Center of Reactor to Rear Face of Crew Compartment (ft)

r_C = Radius of Core (ft)

r_P = Radius of Pressure Shell (ft)

r_T = Inner Radius of Thermal Shield (ft)

r_{45} = Distance from Center of Reactor to Outside of Reactor Shield at 45 Degrees from Axis of Airplane (ft)

t_{LR} = Thickness of Lead on Rear of Crew Compartment (in.)

t_{LS} = Thickness of Lead on Sides of Crew Compartment (in.)

t_{PR} = Thickness of Plastic on Rear of Crew Compartment (in.)

t_{PS} = Thickness of Plastic on Sides of Crew Compartment (in.)

t_S = Actual Shield Thickness at Front of Reactor (ft)

t_T = Thickness of Thermal Shield (in.) (Porous Steel, 2/3 Steel by Volume)

T_γ = Thickness of Hydrogenous Material Outside of Pressure Shell (ft)

β' = Half-Angle of Taper of Sides of Crew Compartment (degrees)

φ = Shadow Shield Half-Angle (degrees)

Fig. II-B-2. Divided Shield System for Supercritical Water Reactor (SCWR).

particular crew shield and reactor geometry used here, the weight of stainless steel in the thermal shield and pressure shell required to reduce the crew dose by a specified amount is substantially equivalent to the weight of lead required on the crew shield to obtain the same reduction. Thus the pressure shell requirements fix a lower limit to thermal shield thickness, but somewhat thicker thermal shields can be used to reduce the amount of gamma shield division to a considerable extent with little or no weight penalty. It has been found that cooling the pressure shell on the inside only, with a small amount of thermal insulation between the shell outside surface and the shield water results in the most satisfactory temperature distribution in the shell.

Biological Shield

In the divided shield configuration given here as an example, the gamma shielding outside the pressure shell consists only of two lead dishes facing the crew compartment. The inner dish serves as both a direct shield for the rear of the crew compartment and a shadow shield, having an angle of 20° measured to the rear corner of the reactor core. The outer dish serves as direct shielding primarily with an angle of 8° measured in the same fashion. The dishes are each approximately 2.5 in. thick and are separated from the pressure shell and each other by about 8 in. to provide cooling and to reduce secondary gamma production in the lead. No attempt has been made to optimize either the shadow angle or attenuation of these dishes as yet.

The pressure shell is surrounded by a tank of borated water, which in turn is surrounded by a layer of some plastic such as polyethylene. A steel shell between the water and plastic is stressed so as to permit replacing the water with a high density material for ground handling provided an auxiliary cup-shaped support is placed under the shell to carry the weight. Some neutron shadow shielding is provided by shaping the external layer of plastic so that the flux in the forward direction is 1/8 of that over the rear hemisphere with a gradual increase from 0 to 90°.

Support Structure and Ducting

The pressure shell is supported by a conical truss hanging from the main wing spar box. The water tank is supported from this same truss by a circular stiffening ring which connects with each truss member where it intersects the tank surface. The lead shadow dishes are hung from truss work extending to the pressure shell. One exit and two or three inlet pipes are required. These penetrate the shield in the rear hemisphere following large radius bends to provide pipe flexibility.

Airplane and Engines

From the over-all shield point of view little need be said concerning the details of the airplane and engine configurations. The reactor mentioned here would be of sufficient power to drive a sea level Mach 0.9 bomber carrying a payload of 20,000 lb through two steam turbine ducted blower engines. For shield design each engine can be considered to consist of a condenser containing approximately 1,000 lb of water, 15,000 lb of stainless steel, and 4,000 lb of aluminum distributed inside a cube roughly 12 ft on a side. A reasonable airplane configuration for this task results in separation distances of 50 ft from the center of the reactor to the rear face of the crew compartment, and approximately 90 ft from the condensers to the crew compartment. A five-man crew would probably be required for this airplane and a mission length of 25 hr would give a radius of over 8,000 miles.

Crew Compartment

For simplicity a schematic crew compartment having a 50 sq ft rear face, a 250 sq ft side area, and a 25 sq ft front face has been used as representative of what would be required for airplanes of this general type. Tapering the crew compartment from rear to front results in an increase of the effective

shadow shield angle and in this particular case permitted an engine arrangement such that the active condensers did not have a direct view of the crew compartment sides. A taper of 8° half-angle was assumed for the crew compartment considered here. Lead was used as gamma and borated polyethylene as neutron shielding material. A dose rate of 1.0 rem/hr was assumed, and calculations indicated that the minimum weight resulted when 80% of the dose was taken through the compartment sidewalls as scattered radiation and 20% through the rear face as direct radiation. From the weight point of view alone, it was similarly determined that 50% of the dose in rem/hr should be taken in gammas and 50% in fast neutrons using the conventional RBE of 10.

Shield Weights

Weights estimated by Pratt and Whitney for the shield described above cannot be considered as corresponding to an engineered shield, nor are they entirely up to date as far as shield design techniques are concerned. They are included herein primarily to give a rough scale to the problem.

Pressure Shell and Contents	18,000 lb
Reactor Neutron Shielding and Shadow Dishes	39,400
Structure and Piping	5,000
Crew Compartment	26,400
Total	88,800 lb

Special Problems

The following section describes briefly these aspects of the over-all shield problem in which significant differences exist between the SCWR and other systems which are being considered for aircraft propulsion.

High Reactor Operating Pressure. The necessity for a highly stressed pressure shell operating in an intense radiation field makes the entire question of radiation heating close to the reactor of great importance to

this cycle. Procedures which are perfectly adequate for prediction of dosages at large distances from the core may well be unsatisfactory for use in analyzing the temperature distributions which will exist in the thermal shield and pressure shell, and efficient design requires that these distributions be known with considerable accuracy.

Studies have shown that the pressure shell and thermal shield are not weight penalties in themselves. That is, the weights of iron involved appear to pay their way as shield material at least as efficiently as does lead on a reasonably sized crew compartment.

Water Activity. Two reactions, the $O^{16}(n,p)N^{16}$ which gives a hard gamma emitter with about a 7.5-sec half life and the $O^{17}(n,p)N^{17}$ which results in a 1-Mev neutron emitter with a half life of about 4 sec, are the important water activations from the shield point of view. The prediction of the equilibrium level of water activity during operation is a complex problem since it depends upon rather precise knowledge of the activation flux at all points throughout the core and reflector and a detailed picture of water residence times at these points. Only rough estimates have been possible to date. These indicate that the gamma activity, while not negligible, does not require a large weight penalty for a divided shield. The neutron activity appears to be negligible for a divided shield core as far as crew dose is concerned, but the amount of activity in the condenser materials caused by these neutrons over a long period of operation has not been investigated as yet.

Shield Cooling. Since the protection of the pressure shell requires a considerable amount of thermal shielding, and since the heat released in this thermal shield is carried away by the working fluid, the heat removal

problem for the biological shield is not large. For a 400-megawatt core it is estimated that approximately 1.5×10^6 BTU/hr or about 0.1% of the total reactor power must be dissipated. While this is still a large amount of heat in absolute terms, it appears that adequate heat exchangers can be placed within the ducted blower power plants so that no drag increment will accrue to the airplane in cooling the biological shield.

Ducting. Ducts or pipes must penetrate the reactor biological shield to carry away the heat from the reactor core. The flow scheme for the SCWR has not been completely developed but it appears that either two or three inlet pipes and one exit pipe are required. The inlet pipes carry water at approximately 0.85 g/cc and the exit pipe water at about 0.13 g/cc. The inlet pipes have an inside diameter of approximately 5 in. and are not considered to affect the shield at all. The exit pipe is larger, about 7 in. in inside diameter, and may have some local effect on the shield since the fluid density is so low. However, it is anticipated that all the piping can be located on the side of the reactor away from the crew and that pipe flexibility considerations will demand indirect paths through the shield so that the piping will compromise the shield to an essentially negligible extent.

3. Direct Cycle Reactor (DCR)

The third reactor cycle which has been chosen for study is the direct or air-cooled reactor cycle. In this cycle quite different emphasis is placed on the several shield design problems as a direct result of the particular requirements of this type of reactor. In order to accomplish the necessary transfer of heat the reactor is made quite large compared to those specified for the other cycles, and it contains a large void volume. The shield must make accommodations for air ducts of considerable size, which must be kept short to avoid large pressure drops. On the other hand, this cycle is potentially capable of extremely high-temperature operation, which makes it especially suitable for applications where high speed rather than long operation is required. Thus, a small crew compartment can be used, and there is considerable incentive to place a great deal of shielding around the crew, rather than the reactor.

Reactor

As an example of a direct cycle reactor and shield, the AC-2, a GE-ANP conceptual design* has been selected. The reactor, roughly 3 1/2 ft diameter by 3 ft long, consists of a hexagonal array of cylindrical tubes containing a small amount of uranium, possibly in a nichrome wire screen. Air passing through these tubes is heated and used for propulsion. The space between the tubes is filled with water or alkyl-benzene as a moderator. The functions of reflection and control are provided by beryllium cylinders around the periphery of the reactor. Rotation of these cylinders exposes a boron-coated surface to the reactor to reduce reactivity. This reactor configuration is sketched in Fig. II-B-3.

---

* Subsequently discarded.

SECRET
DWG. 20502

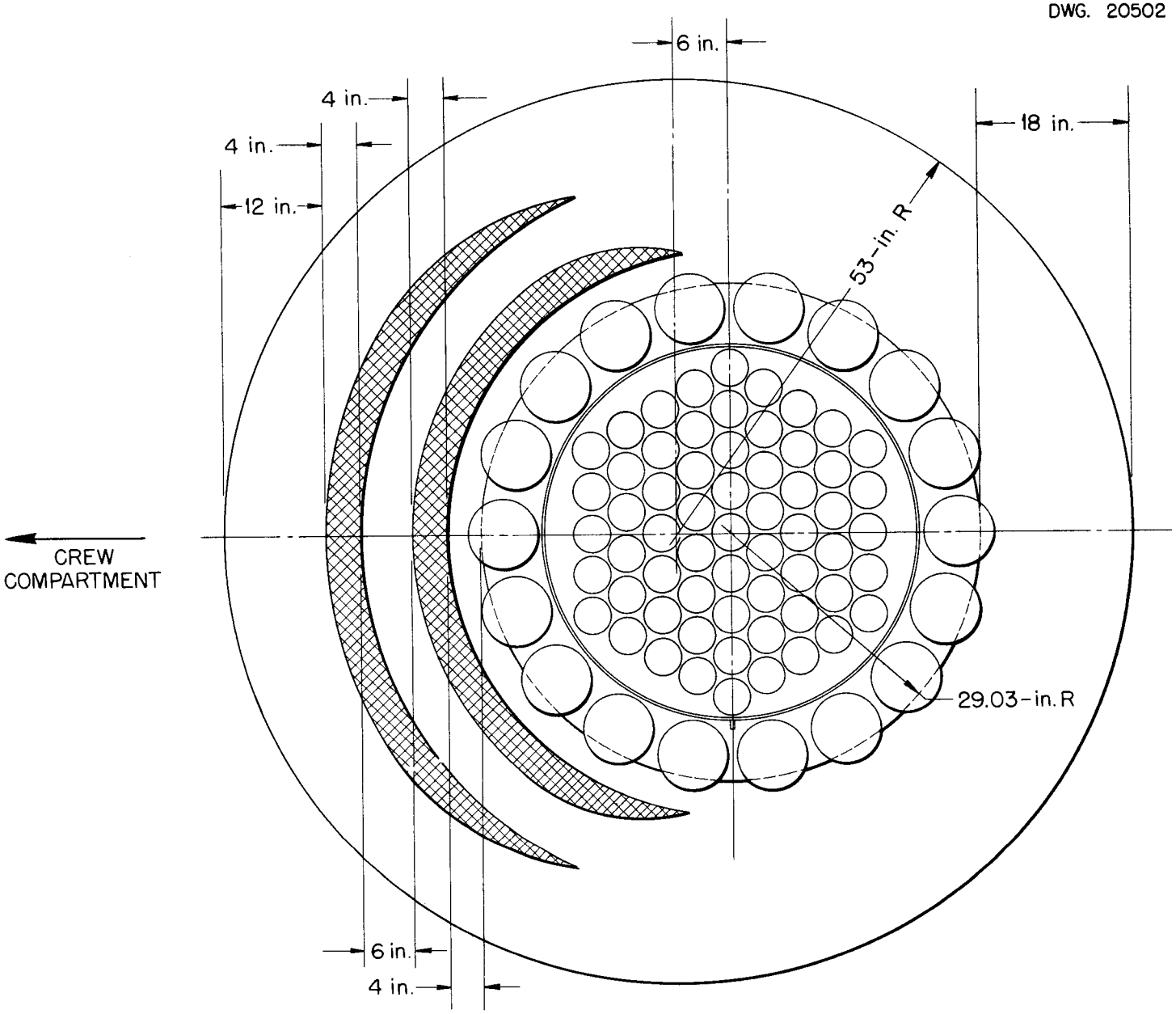

Fig. II-B-3. Vertical Cross Section of Direct Cycle Reactor Shield.

The reactor is oriented in the airframe with its axis of symmetry at right angles to the direction of flight and is flanked by two turbojets. The air passes through the shield in 61 bent cylindrical ducts. An unusual feature is that air from each compressor passes through the reactor and out the opposite turbine. The reactor power is 160 megawatts; air flows through the reactor at Mach 0.2; and the turbine inlet temperature is 1750°F.

Reactor-Shield Geometry

Figures II-B-3 and II-B-4 show the reactor-shield geometries based on preliminary calculations. No calculations have been made of mechanical structure or weights. The reactor is placed eccentrically in a cylindrical water tank, the axes of the two cylinders being displaced 6 in. to increase the forward shielding. The resulting neutron shield thickness varies from 38 in. at the front to 26 in. at the rear. From each end of the reactor the bundle of air ducts leads out and back to the turbojets. The minimum diameter of each duct is set by pressure drop considerations and is assumed to be 3.25 in. A gamma shadow shield in the form of two lead partial ellipsoids is placed in front of the reactor. Each of these is 4 in. thick at the center and tapers toward the extremities.

Crew Compartment Shield

Since the total length of mission contemplated is about 6 to 8 hr, it was felt unnecessary to make provisions for relief of crew members or for their shifting of position. This in turn made possible a small crew compartment, which for this design was taken as a cylinder 5 ft in diameter and 12 ft long. With this small crew compartment it was clearly worth while to place a comparatively large fraction of the shielding materials for both gammas and neutrons around the crew.

[redacted] DWG. 20501

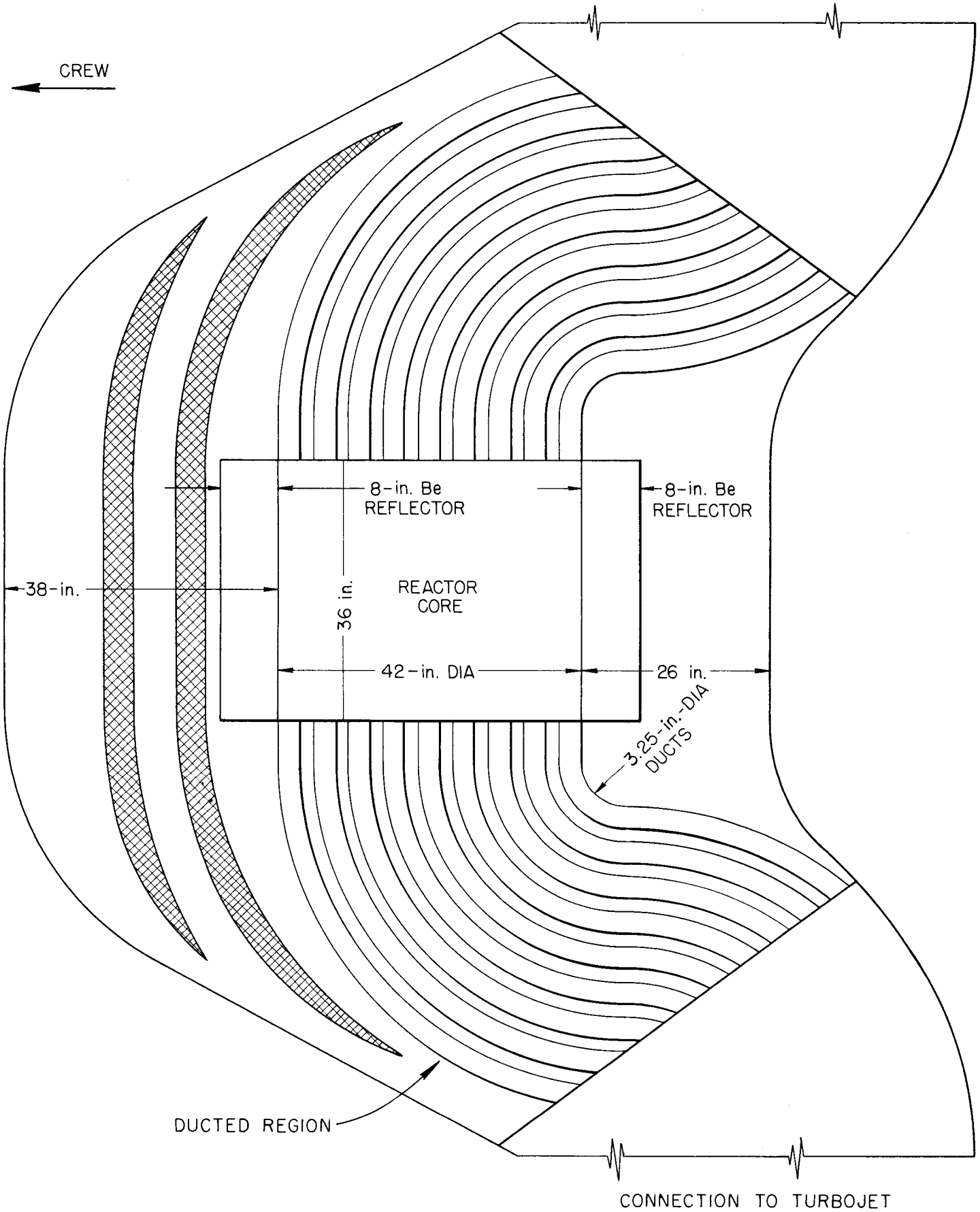

Fig. II-B-4. Plan View of Direct Cycle Reactor Shield.

The crew shield was designed to allow 1/4 rem/hr total dose rate, made up of 0.162 r/hr of gamma radiation (70% scattered) and 0.0088 rep/hr (80% scattered) of fast-neutron radiation, with a reactor-crew separation of 50 ft and standard sea level conditions. No provision was made for ground or structure scattering save the avoidance of extremely asymmetric neutron shielding on the reactor.

The crew compartment is shielded with 13.8 in. of plastic and 0.5 in. of lead at the sides, 10 in. of plastic and 0.25 in. of lead at the front, and 30 in. of plastic backed with 2 in. of lead at the rear.

Shield Thicknesses

The shield thicknesses were determined as far as possible by the method of direct comparison with experimental configurations. The first step was to choose the appropriate amount of water for attenuation of the direct neutrons. This was read directly from the BSF pure water data,(3) using an inverse-distance-squared relation to take into account the reactor-crew separation, and the ratios of power and leakage of the AC-2 and BSF reactors. The leakage was taken to be proportional to λ/t, where λ is the fast-neutron relaxation length in the core, and t, the "thickness" of the reactor, is only properly defined in the case of a plane-surfaced reactor. This is entirely equivalent to using the ratios of power densities, relaxation lengths, and frontal areas. Since the AC-2 presents a curved, rather than plane, surface toward the crew, there is some ambiguity in the application of this recipe, which could perhaps be eliminated by the more sophisticated treatments of section III-B of this report.

(3) H. E. Hungerford, "Bulk Shielding Facility Data Work Sheets," CF-52-2-37 (Feb., 1952).

The direct gamma dose was next determined from the same BSF data, making essentially the same corrections. Since this dose was, of course, far in excess of the amount desired, lead was used to replace some of the water in both reactor and crew shields, the total thickness being ascertained from Lid Tank data.(4) In order to prevent excessive secondary gamma formation, the lead on the reactor had to be laminated and separated from the reactor by borated water. The optimum manner of doing this should be determined by a special experiment, including at the same time such engineering features as are required to support the lead, but it is not anticipated that such an experiment would cause an important change in the estimates of the effectiveness or weight of such a highly divided shield as this.

The total thicknesses of shielding material as determined above were divided between the reactor and crew shields by a series of successive approximations with the objective of achieving minimum weight consistent with avoiding spectacular asymmetry of the reactor neutron shield and insurmountable activation and ground handling problems. This division was accomplished as a final step at the same time that the apportionment of total dose between neutrons and gammas and between direct and scattered radiation was made.

Calculation of Air-Scattered Dose

The air-scattered neutron dosage rate was calculated by assuming "line-of-sight" emission of neutrons from the reactor shield, isotropic scattering in air, and crew shield penetration as observed in the air scattering experiments in the BSF.(5) Thus, neglecting air attenuation and multiple scattering,

(4) C. E. Clifford, "Gamma Attenuation Behind 3.8-, 7.6-, and 11.4-cm Solid Lead Shadow Shields in Pure Water as a Function of Water Reflector Thicknesses," CF-52-5-163 (May 20, 1952).

(5) H. E. Hungerford, "The Skyshine Experiments at the Bulk Shielding Facility," ORNL-1611.

the equation for the air-scattered neutron flux arriving at the outside of the crew compartment is written

$$I(D) = \frac{N_o n \sigma}{8\pi D} \int_{\psi=0}^{\pi} \int_{\beta=0}^{\pi-\psi} d\beta \, d\psi$$

where

D = reactor-crew separation distance, 15 m,

$I(D)$ = air-scattered neutron flux arriving at outside of crew compartment (neutrons/cm^2 . sec),

N_o = isotropic source strength (neutrons/sec),

n = nuclear density of air; 5.1×10^{19} nuclei/cc at room temperature and at sea level,

σ = average scattering cross section for 6-Mev neutrons, 1.28×10^{-24} cm^2,

ψ = angle between reactor-crew axis and direction of neutron emission from reactor shield,

β = angle between reactor-crew axis and direction of neutron incidence on crew shield.

When integrated over β this becomes

$$I(D) = \frac{N_o n \sigma}{8\pi D} \int_{\psi=0}^{\pi} (\pi - \psi) \, d\psi$$

From this equation it can be seen that, for an isotropic source, the contribution to the air-scattered dosage rate at the crew varies with ψ as $(\pi - \psi)$. It is clear, then, that an optimum reactor shield design of this type should provide enough more shielding against low ψ neutrons to approximately equalize their importance to that of the neutrons emitted at higher angles. This was performed by displacing the axes of the cylindrical reactor

core and shield. The air-scattered neutron dose is then calculated by measuring the minimum water thicknesses "seen" by neutrons which penetrate the reactor shield at various angles without scattering, and comparing these to the minimum thickness at some angle ψ to which the calculation is normalized, say 90°. The $(\pi - \psi)$ vs ψ curve is then adjusted at various angles of ψ by the excess or insufficient attenuation afforded by the difference in thickness occurring at the normalization angle and the angle in question. Finally, integration over ψ is performed under the adjusted curve and this value is used in conjunction with a value for the source strength, N_o, which is calculated under the assumption that the reactor shield emits just as many neutrons per unit solid angle in all directions as it does in the direction to which the calculation was normalized. A 6-in. displacement of reactor core and shield axes yielded an adjusted $(\pi - \psi)$ vs. ψ curve which seemed reasonable, particularly when it is borne in mind that the air scattering of 6- to 8-Mev neutrons is likely to be preferentially forward.

The scattered gamma dose could not be determined so easily, however, since it was advantageous to use a very asymmetric gamma shield which resulted in a factor of 10^4 between the attenuation of gammas on the front and the sides. Since a volume source cannot cast a sharp shadow, and since a good shadow shield must surely taper gradually at the edges, no attempt was made to use the notion of an "effective shadow angle." Instead, the total gamma production of the reactor was determined, and these gammas were assumed to emanate from several point sources placed throughout the reactor, but primarily near the surface, for conservatism. Scale drawings were next constructed, using an arbitrarily tapered lead shield. Assuming line-of-sight penetration, gamma emission as a function of angle was determined for the various point sources

and combined with the NDA calculations (section III-E) to give the dose in the crew compartment. An improved tapered lead shield could then be designed and the process repeated, rapidly converging on a far better taper than was likely to remain after mechanical design of the shield. More numerous "point sources" could of course be used for improved accuracy.

Design of Air Ducts

The air ducts, which did not penetrate the gamma shield, were designed in accordance with the Simon-Clifford formula given in section III-H of this report. That is, they were assumed to have only a density-reducing effect on the shield, which was appropriately thickened to maintain the original attenuation.

Conclusions

One of the inherent advantages of the direct cycle is that activation of the coolants is not important. The primary coolant, air, becomes slightly activated because of its argon content, and accidentally so in the event of fuel element failure. However, the thick crew shield is ample protection in either case. The moderator, which is actually a secondary coolant, presents a more serious problem. However, the heat exchanger used to cool this fluid is small enough to permit placing it behind the reactor and so using the reactor shielding as a shadow shield. The radiation from the moderator is small compared to that escaping from the sides of the reactor, as a result of the highly divided shield configuration.

A number of problems have not been completely resolved in this design. The assumption of line-of-sight penetration of gammas is not realistic and is perhaps dangerous since a slight forward scatter upon leaving the reactor shield would increase markedly the probability of air scattering into the crew compartment. The assumption of isotropic neutron air scattering,

although probably conservative, can no doubt be improved. Structure scattering may prove to be more important than anticipated. The calculation of slant attenuation of neutrons in the crew shield is not on very firm ground, and is particularly important when the crew shield is thick. These problems should all be solved readily by the Tower Shielding Facility.

The penetration of neutrons through air ducts, though well understood for single ducts, presents some difficulties in the case of many closely packed ducts. That such a configuration can be made to exhibit the characteristics of a region of reduced density has yet to be demonstrated for ducts greater than 2 in. in diameter.

The direct cycle, because of the relatively thin reactor shield, introduces some serious questions in connection with after-shutdown radiation-induced activities, and radiation damage. Not only must these effects be calculated with some care, but it is possible that the shield design may have to be compromised in order to provide satisfactory solutions.

A final point which is often overlooked is that an "ideal shield" such as this one is frequently unrecognizable after engineering analysis. What at first appears to be a fine design may prove so difficult to construct in accordance with the somewhat rigorous requirements of aviation application that its final weight is extremely disappointing. For example, steel may have to be substituted for lead, with unfortunate shielding consequences. The problem of developing shield materials which possess enough structural integrity to permit a simple engineered design requires some attention.

4. Summary of Reactor Cycle Configurations

To facilitate comparison of the shields described for the various cycles in the foregoing text, Table II-B-1 is included. It is intended primarily to highlight the differences in design problems. The information in the table was largely current during the summer of 1953, but it should be noted that the designs were chosen to illustrate the shield design methods and nothing more.

Table II-B-1. Summary of Reactor Cycle Configurations

	RMR	SCWR	DCR
Fuel	Uranium in fluorides	Uranium in stainless steel	Uranium in nichrome or ceramics
Moderator	Beryllium	Supercritical water	Water (alkyl-benzene)
Coolant	Fuel-to-NaK	Supercritical water	Air
Reflector	Beryllium	Water	Beryllium (water)
Dose	0.1 rem/hr[a]	1 rem/hr	0.25 to 1.0 rem/hr
Airplane and Mission	Chemically augmented[a]	Mach 0.9, sea level, 24 hr	Mach 1.5, 60,000 ft, 8 hr
Power	150 megawatts[a]	400 megawatts	160 megawatts
Core size	1.5 ft diam[a]	2.5 ft diam	42 in. diam x 36 in.
Crew compartment	8 ft diam x 10 ft, 5 ft diam x 10 ft	8 ft diam x 10 ft	5 ft diam x 12 ft

a These specifications are typical of the current thought but are of course in no way to be considered settled.

III. METHODS AND TECHNIQUES OF SHIELD DESIGN

III-A. SPECIFICATION OF ALLOWABLE RADIATION LEVELS

Flight and ground handling crews must of course be properly shielded from the reactor of a nuclear-powered aircraft; therefore, one of the first needs of a shield designer is a specification of the radiation levels to which the crews may be subjected. Obviously, the higher the allowed levels the lower the over-all shield weight. To date the tolerance limits have not been completely defined and the tentative dose levels have been on the conservative side. While considerable progress has been made in developing light-weight shields using these tentative tolerance limits, the study of radiation effects is continuing and much remains to be done. To put this problem in its proper light the nature of radiation effects must first be described.

1. Factors Involved in Setting Maximum Permissible Exposures

Radiation is an insult to the body. It should be remembered, however, that there are other insults which present parallel problems in determining other maximum permissible exposures. For instance, each new medical drug which is introduced for use on human beings must be studied first with laboratory animals. If, to obtain a desired improvement in the condition of a patient, it is considered necessary to administer the drug in quantities large enough so that toxicity may be a factor, the first clinical uses will ordinarily be limited to cases in which the patient is already in some danger. By the same token radiation exposure in radiological therapy will greatly exceed the values permissible in occupational exposure.

Questions relating to the establishment of permissible radiation exposure levels are being studied by the use of many of the same techniques that are employed for these related situations. It should be borne in mind in the following discussion that considerable experience has been accumulated in the

general field. The use of laboratory animals and the extrapolation to man has been successfully carried out for other body insults. It is not unlikely that similar methods can be found which will be successful for radiation exposure also.

It is not often realized that the health physics, radiobiology, and radiology fields are as old as the study of X rays and radioactivity itself.(1) In the earliest experiments it was discovered that radiations could produce burns, and cause and cure cancer. The cases of the Joachimstal uranium miners and the radium dial painters resulted in a great impetus to research in this field. As physical and medical interest gathered force and as high-voltage machines were developed more discoveries were made in these sciences. A major effort was started by the Manhattan Project and continued by the Atomic Energy Commission.

The fact that reliable answers to questions of radiation tolerance posed by the ANP Program are not yet available reflects the immensity of these questions rather than the scale of effort which has been expended on their solution. Furthermore, one should be cautious about believing that one particular experiment will give the required results. Those tolerance limits in which confidence can be placed are covered by regulations of the National and International Radiation Protection Committees and represent the opinion of leaders in the fields of health physics, radiobiology and radiology.* These

(1) K. Z. Morgan, "Radiation Safety Measures in an Atomic Energy Plant," Eng. J. 31, No. 3 (1948).

* The work of the Advisory Committee on X ray and Radium Protection is sponsored by the Bureau of Standards. Particular attention is called to the work of Subcommittee 1, Permissible Dose from External Sources; Subcommittee 3, X rays up to Two Million Volts; Subcommittee 4, Heavy Particles; and Subcommittee 5, Electrons, Gamma Rays, and X rays Above Two Million Volts. The reports of these Subcommittees will appear as publications of the Bureau of Standards.

levels are probably too conservative to use as crew tolerances in an aircraft. Rather than attempt to expand the information, it is intended to define the problem more accurately than has been done heretofore, to indicate how far present knowledge will take us, and to determine what are the most glaring gaps in the required information.

In the meantime, for the purposes of this report, it shall be assumed that dose rates of 1, 0.25, and 0.1 rem/hr will be of interest for studies of manned nuclear-propelled aircraft. The relative biological effectiveness of fast neutrons relative to gamma rays will be taken as 10.

As long as the present situation exists wherein nuclear-powered aircraft performance depends critically on shield weight there will be a strong incentive to set the flight crew exposure levels at as high a value as the risks will make acceptable. In order to do this, the risk must be known as a function of radiation composition, intensity, fractionation, and total accumulated dose. It will be presumed that exposure of maintenance crews will follow the practice established for occupational exposure as long as this group has the character and composition of other workers with radioactive materials. The flight crew exposure presents a special problem. If a portion of the maintenance crew were carefully selected and controlled then these might be given doses comparable to those of the flight crew.

Since the flight crew exposure is to be maximized let us consider how this may be done. The effects of the exposure will be manifested in the individual and in his descendents. Consider first the genetic problem.

The Genetic Problem

When a male animal suffers radiation of the gonads[2] the principal damage is to the mature and generating sperm and to cells which are precursors of sperm cells. Studies have been made of the genetic effects in the sperm of mice exposed to doses in the neighborhood of the median lethal dose. The progeny fall into at least four distinct groups (a) dominant lethal, (b) sterile, (c) semisterile, and (d) fertile. The dominant lethals die in the early embryonic stages. The sterile and semisterile groups total 35% of the three live-born groups following a dose of about 700 r of X rays in mice. The semisterile offspring produce three types of progeny. The first type consists of embryos which die in various stages of development. The other two types, which occur in equal number, fall in the semisterile and fertile groups mentioned above.

The effects mentioned so far are the result of major chromosomal aberrations induced in the sperm. Gene mutations are also induced but it is more important to consider the occurrence of these in the precursor cells.

Russell concludes[2] that when these facts are related to man those individuals who receive a large dose of radiation should refrain from procreating for about two months, during which period the sperm will be replaced by sperm that are free of major chromosomal aberrations although they will not be free of gene mutations and possibly minor chromosomal aberrations.

Next consider the damage to the precursors of the sperm cells. These cells will produce sperm throughout the reproductive life of the individual. The damage is cumulative and so this factor is one which may set a total dose

(2) W. L. Russell, "Mammalian Radiation Genetics," Symposium on Radiobiology, Oberlin College, p. 427, Wiley, New York, 1952.

rather than a dose rate during exposure. The damage of importance probably occurs in the genes. It has been thought in the past that most gene mutations were recessive and would not assert themselves for many generations so that connection with the irradiated individual would be lost. It is true that this is part of the picture and the problem here is to maintain the average total dose in the population below about 10 r during the fertile period of life.

It is likely that the number of individuals irradiated as flight crew members of nuclear-powered airplanes will be small enough, and the total dose set by other factors will be low enough so that the average total dose in the population will not be affected. However, recent work(3) indicates that there is also a perceptible decrease in vigor and viability in the immediate offspring. It is quite possible that a total dose to one parent of 300 rem will constitute a hazard which cannot be ignored. The occupationally accepted dose rate of 0.3 rem per week allows the accumulation of 450 rem in the 30-yr period (age 15 to 45) of normal fertility.

The considerations described above are likely to set a rather lower total dose than would be set by damage to the individual. It is possible, other factors permitting, to design around this problem by crew selection. Certain criteria (age, family size, age of wife, etc.) can be set up by study of vital statistics pertinent to the group under consideration so that very few additional children will be produced by members of the group chosen. It is not necessary that procreation be avoided entirely. If the group is properly selected with other factors considered, of course, the number of children born after the exposure of the father will automatically be small and the genetic hazard can thus be avoided.

---

(3) W. R. Russell and L. B. Russell, private communication concerning unpublished work.

The Mitotic Rate Problem

There is ample experimental evidence to show that the tissue with a high rate of cell division (mitotic rate) is more radiosensitive than tissue with a low mitotic rate. The mitotic rate reduces as a man or animal ages and so more radio resistance develops. Among the most serious problems are the late effects. Typical late effects are the incidence of leukemia and various malignancies. In the older man, say about 35 yr, these conditions have 10 to 15 fewer years to develop before normal senility. The advantages of choosing men as old as other requirements will permit, therefore, are threefold: (a) it minimizes the genetic problem, (b) it provides a more radio resistant individual, and (c) it decreases the hazard from late effects.

Partial Shielding of Most Sensitive Body Organs

Another possible means of increasing the dose permissible from that suitable for a simple random population total body picture lies in partial shielding. Certain organs of the body are more radiosensitive than others, or certain organs respond more to the cumulative dose. Increased radiation tolerance is found if the blood-forming tissue in the bone marrow and spleen tissue is shielded. The head and hands are relatively less sensitive to gamma rays. On the other hand the neutrons have a high RBE* for the eyes and the cataractogenic reaction responds to the cumulative dose. It appears that the placing of partial shielding material about the seat so the thighs, trunk, and eyes receive extra protection may result in weight savings in the crew shield. The total dose which may be tolerated by the extremities if the trunk is protected is close to the median lethal dose for total body exposure. Shielding of certain organs by the rest of the body is important. Experiments at the ORNL Health Physics Division by C. A. Mills[4] indicate that

(4) C. A. Mills, "Fast Neutron Dosimetry in a Small Tissue Equivalent Phantom," to be published in Nucleonics.

* Relative biological effect (see page 61).

the shielding afforded by the brain to the eyes from a neutron source located to the back is about a factor of three in dose rate reduction.

Evaluation of such possible weight savings is best done as a semiempirical study of phantoms inside a crew shield mockup such as will be used at the ORNL Tower Shielding Facility.(5) A detailed study of the dose to each organ will be required before a reliable set of tolerance regulations and dose schedule can be drawn.

Although most of the biological damage attributed to fast neutrons is the result of proton and heavy particle recoil in the tissue, the capture gamma dose arising from neutrons absorbed in the men and equipment inside the crew compartment will have to be considered. Reference is made to the Los Alamos slow neutron work(6) where the "intra-mouse dose" was found to be appreciable. This effect was also found important in the evaluation of exposure to men in the reactor experiment accidents.(7)

Preventive Treatment

Considerable study is being made of substances of possible use in the prophylaxis and therapy of radiation syndrome. Some early success has been achieved(8) but there is insufficient experience to use these drugs on humans. The possibility of success in this direction should not now be counted on by the shield designer, but it should be kept in mind as a highly valuable practical result which may come from fundamental research.

(5) E. P. Blizard, "The Tower Shielding Facility," Reactor Sci. Tech. 3, No. 2, p. 279, TID-2009 (1953).
(6) James T. Brennan et al., "The Biological Effectiveness of Thermal Neutrons on Mice," LA-1408 (Feb. 15, 1952).
(7) J. G. Hoffman, "Radiation Doses in the Pajarito Accident of May 21, 1946," LA-687 (May 26, 1948).
(8) M. C. Fishler et al., "Therapeutic Effect of Rat Bone Marrow Injection in Rats Exposed to Lethal Whole-Body X Radiation," USNRDL-410 (Sept. 8, 1953).

2. Effects of Crew Exposure to Reactor Radiation

Ionizing radiation can be divided for the present purposes rather neatly into two classes according to whether the ionization density along a particle track is high or low. Neutrons, of course, do not ionize but produce fast protons either from recoil or (n,p) capture in nitrogen. Recoil particles of carbon, oxygen, and nitrogen produce an appreciable contribution. Thermal neutrons also produce 2.2-Mev gamma rays by hydrogen capture in soft tissue. Except for the capture and inelastic scattering gamma rays, the dose produced indirectly from neutrons lies in the heavily ionizing group. Gamma rays and X rays ionize directly and also produce high-speed electrons which contribute to the low ionization density group.

If an organism is subjected to a mixture of the two types of ionizers, the dose from each must be considered separately. The high ionization density radiation is characterized by a greater biological effect than a simple comparison on the basis of energy deposition would suggest. These radiations are said to have high RBE (relative biological effect). The values are usually quoted relative to gamma rays from radium or 250-kv X rays. There is evidence that for some purposes the neutron and gamma doses in rems may be added. This hypothesis, while it is widely applied here and elsewhere, should be used with caution since the threshold dose and RBE may vary from one effect to another.(9)

In order to know the expected biological effect from an exposure or series of exposures it is necessary to know the exact distribution of dose. It is usually sufficient to specify the RBE of each radiation, the total dose, the

(9) R. E. Zirkle, "Radiobiological Additivity of Various Ionizing Radiations," Am. J. Roentgenol. Radium Therapy 63, p. 170 (1950).

dose rate, and the interval between exposures. For some biological effects there will be better recovery from a given total dose if it is fractionated, and for some of these effects fractionation of a neutron dose is less effective than fractionation of X ray and gamma doses. The recovery is more probable in general if the radiation has a low RBE. The fact that dose from neutrons appears to show no recovery for some of the important biological effects is one of the reasons why the neutron dose must be kept as low as practicable.

From the work of R. S. Stone[10] and J. C. Larkin, Jr., and from various accidental exposures, there are about 274 human beings who have been exposed to neutron and gamma irradiation. There are also several thousand victims of the Hiroshima and Nagasaki bombing. The dose received by this latter group is often in question but much good descriptive information can be expected from studying them. Thus, it is seen that there is considerable information available on humans. Let us consider specific radiation syndromes.

Radiation Cataract

The present status of knowledge about radiation cataract in humans has been summarized by W. T. Ham.[11] The cataract is a defect of the lens of the eye which obscures the vision. Examination of the lens with the slit lamp shows a number of vacuoles or granules scattered or clumped about the anterior pole of the lens. A low grade cataract may be seen by the slit lamp but still not interfere with the patient's vision. As the vacuoles or granules become more dense they scatter or absorb more light until eventually vision is obscured.

Ham concludes that until more information is available on the human eye 10 to 20 rep of fast neutrons and 500 r of gamma rays should be regarded as a dose

(10) Stone, R. S., "Neutron Therapy and Specific Ionization," Am. J. Roentgenol. Radium Therapy 59, p. 771 (1948).
(11) W. T. Ham. Jr., "Radiation Cataracts," Arch. Opthalmol. (Chicago) 50, p. 618 (1953).

capable of producing lens opacities which may interfere with vision. Since the head contains a negligible fraction of the blood-forming tissues and hence its radiation cannot contribute to leukemia, the effect on the eye is the controlling factor, and consequently very high doses of gamma rays may be tolerated if the neutron dose is kept low. The value of 25 is recommended for the RBE of fast neutrons for cataract production because of the evidence given in Ham's paper. Because of the timing of the present work, an RBE of 10 is used elsewhere in this report, in conformity with earlier concepts. The neutron doses to the eyes of the four individuals in the ZPR-1 reactor accident[12] are 16.2, 9.1, 5.1 and 0.8 rep. Since this is one of the few cases where humans have received a dose under known conditions, the progress of these cases will be very imformative.

Cataracts also occur in old age and therefore a good deal of medical and surgical experience has been acquired in their treatment. Success in restoring sight has been achieved by removing the lens and the use of correcting glasses. Many people who have senile or radiation cataracts lead normal useful lives. While no one should permit hemself to be exposed to a cataractogenic dose, nevertheless, many cataracts can be treated successfully. This remark does not so far apply to any other radiation effects.

Sperm Count

Probably the most sensitive indication of excessive radiation is the sperm count. Rather than varying a few percent the sperm count will change by orders of magnitude. This question is discussed by Oakes and Lushbaugh[13] relative to a patient exposed to the Pajarito accident. The sperm count has been followed in detail and complete recovery was achieved. The libido is known not to be affected directly by radiation.

(12) R. O. Brittan *et al.*, "Technical Review of ZPR-1 Accidental Transient: The Power Excursion, Exposures, and Clinical Data," ANL-4971 (Jan. 26, 1953).

(13) W. R. Oakes and C. C. Lushbaugh, "Course of Testicular Energy Following Accidental Exposure to Nuclear Radiatons; Report of a Case," Radiology 59, p. 737 (1952).

Late Effects of Radiation

Together with radiation genetic problems the late effects of radiation are probably least well understood and most insidious in their results of all problems in radiation damage. Furthermore, neutrons have very high RBE's for these effects. Although too little research has been done in this field, the information which does exist is extremely significant. The principal work is that of R. S. Stone[10] and J. C. Larkin, Jr.; P. S. Henshaw, E. F. Riley, and G. E. Stapleton;[14] and also E. Lorenz.[15] Some recent results of A. C. Upton and J. Furth[16] confirm this work.

Stone and Larkin attempted to treat cancer with fast neutrons. They failed largely because the capacity of normal tissue to repair itself is destroyed and because the RBE of the late effects is so much higher than that of early effects (such as erythema). The values of RBE given by Stone and Larkin are shown in Table III-A-1. A more recent value[17] of the "n" unit is used, namely, 1 n = 2 rep.

The authors quoted above concur in giving high values of RBE for neutrons using the late effects as the indicator. Attention should be directed to the fact that the RBE for late effects from neutron irradiation may be closer to 20 than 10 for younger men of age 20 to 40 as opposed to that for patients in the age range studied by Stone and Larkin. Their patients ranged in age at the time of treatment (when mentioned in ref. 10) from 49 to 72. The data of Stone and

(14) P. S. Henshaw, E. F. Riley, and G. E. Stapleton, "The Biologic Effects of Pile Radiations," Radiology 49, p. 349 (1947).
(15) E. Lorenz, "Some Biologic Effects of Long Continued Irradiation," Am. J. Roentgenol. Radium Therapy 63, p. 176 (1950).
(16) A. C. Upton and J. Furth, reported at Meeting of Radiation Research Society, June, 1953, Iowa State College.
(17) H. H. Rossi, "The n Unit and Energy Absorption in Tissue," Radiology 61, p. 93 (1953). (N.B.: The n unit is no longer regarded as a proper means of reporting neutron dose.)

Table III-A-1. Relative Biological Effectiveness of Neutrons

Subject	Result of Exposure	RBE	Remarks and Conditions of Experiment	Reference
Man	Skin erythema	2.5-3.5	Cyclotron fast neutrons on face and forearm.	a
	Late effects	7	Estimated from neutron therapy.	a
	Lens opacity	25	Estimated from data on man and animals.	b
Mouse	Life span shortened (delayed lethality)	3.6	Reactor neutrons single dose.	c
		17	Reactor neutrons fractionated dose (0.23 rep/day caused 18% shorter life).	c
	Acute lethality	2	Cyclotron neutrons.	a
	Dominant lethal mutations	8	Cyclotron neutrons.	d
Rabbit	Epilation	2	Cyclotron neutrons.	a

a R. S. Stone, "Neutron Therapy and Specific Ionization," Am. J. Roentgenol. Radium Therapy 59, No. 6, p. 771 (1948).
b W. T. Ham, Jr., "Radiation Cataracts," Arch. Opthalmol. (Chicago)50, p. 618 (1953)
c P. S. Henshaw, E. F. Riley, and G. E. Stapleton, "The Biologic Effects of Pile Radiation," Radiology 49, p. 349 (1947).
d W. L. Russell, L. B. Russell, J. S. Gower, and C. W. Sheppard, "Neutron Induced Dominant Lethals in the Mouse," Genetics 38, p. 688 (1953); see also Recordings of Genetic Society of America, No. 22, p. 98 (1953).

Larkin on humans which gives an RBE for late effects of 7 should be considered to be in agreement with that of Henshaw, Riley and Stapleton[14] who give a value of RBE for late effects on mice of 17.

3. Conclusions

As a result of the above discussion the following conclusions are drawn pertaining to high radiation exposure of personnel in the ANP Program:

(1) It is desirable to choose men as old as other requirements will permit.

(2) It is desirable to choose the group so that very few additional children will be born.

(3) The shield designer should plan to cast design choices and contingencies in such a way that neutron dose will be lower than the design specification. This should be done even at the expense of a larger gamma dose or some increase over minimum shield weight design.

(4) The total neutron dose to the eye should not exceed 20 rep in the life of an individual.

4. Discussion of Health Physics Instrumentation and Units of Measurement

Instrumentation -- Bragg-Gray Principle

Ionizing radiation such as comes from a nuclear reactor may be characterized in many ways. In the fields of health physics, radiobiology, radiation chemistry, and radiology, the quantity correlated with the effect studied is the energy deposited per unit mass of medium, and this is called the dose. The amount of such energy is too small to be measured directly for most applications (that is in a calorimeter), so recourse is made to instruments designed according to the Bragg-Gray principle.(18) This principle states that the energy loss $(dE/dm)_b$ of ionizing radiation absorbed per unit of mass of a given medium is related to the energy absorbed in a small gas-filled cavity in the medium according to the following expression:

$$\left(\frac{dE}{dm}\right)_b = P_b W_g J_g$$

where

P_b = relative mass stopping power of the medium with respect to the gas,

W_g = average energy required to produce an ion pair in the gas,

J_g = number of ion pairs produced per unit mass of the gas in the cavity (the quantity that is usually determined experimentally).

It should be emphasized that in order for this principle to hold, the gas cavity must be small compared to the range of the ionizing particles and both W_g and P_b must be independent of the energy of the radiation. The Bragg-Gray principle can be applied to a chamber for which the walls and gas are of the same material, e.g., air or tissue equivalent, provided that the cavity is small compared to the range in the gas of the ionizing particles.

(18) L. H. Gray, "An Ionization Method for the Absolute Measurement of Gamma-Ray Energy," Proc. Roy. Soc. (London) 156 A, p. 578 (1936).

Examples of such instruments are the Victoreen thimble chambers, the graphite-wall ionization chamber, and the Hurst neutron dosimeter. Photographic film is a satisfactory X-ray and gamma-ray dosimeter when suitably calibrated against a Bragg-Gray instrument. Geiger and scintillation counters do not measure dose, although a scintillator with an integrating sensing circuit may measure something proportional to dose.

It should be pointed out that a properly used Bragg-Gray instrument makes it possible to measure heat absorption in a shield at low power. The neutron and gamma contributions can be measured separately and independently.

Definition of Units and Terms Commonly Used in Health Physics

Roentgen (r). That quantity of X or gamma radiation such that the associated corpuscular emission per 0.001293 g of air (1 cc of air at $0^{\circ}C$ and 760 mm Hg) produces, in air, ions carrying 1 esu of quantity of electricity of either sign (see Table III-A-2). The roentgen is not recognized above 3 Mev.(19)

Roentgen Equivalent Physical (rep). That amount of ionizing radiation of any type that loses energy at the point in question in soft tissue to the extent of 93 ergs per gram. It is approximately equal to 1 r of about 200-kv X radiation in soft tissue.

Rad. An ionizing radiation unit corresponding to a loss of energy in any medium of 100 ergs per gram.

Roentgen Equivalent Man (rem). That amount of ionizing radiation of any type that produces the same damage to man as 1 r of about 200-kv X radiation. (1 rem = $\frac{1}{(RBE)}$ rep. It should be noted that when the physical dose is measured in rad units in tissue, the approximate definition is used: 1 rem $\doteq \frac{1}{(RBE)}$ rad,

(19) "Recommendations of the International Commission on Radiological Protection and of the International Commission on Radiological Units, 1950," Handbook 47, p. 24, National Bureau of Standards (June 29, 1951).

Table III-A-2. Conversion Factors for X or Gamma-Ray Absorption in Air

Values Corresponding to 1 r	
Absorbed in 1 cc of Air	Absorbed in 1 g of Air
1 esu/cc	773.4 esu/g
2.083×10^{9} ion pairs/cc	1.611×10^{12} ion pairs/g
3.336×10^{-10} coulombs/cc	2.58×10^{-7} coulombs/g
6.77×10^{10} ev/cc	5.23×10^{13} ev/g
0.108 ergs/cc	83.8 ergs/g
1.08×10^{-8} joules/cc	8.38×10^{-6} joules/g
2.59×10^{-9} cal/cc	2.00×10^{-6} cal/g

The rem is not a physical quantity. It is the product of a unit (rep) and a scale factor (RBE) used to indicate biological damage due to measured exposures of radiations of different quality or mixtures of radiations. The use of the rem is controversial so that care should be used in specifying exactly how the values are obtained in a particular application.

Relative Biological Effectiveness (RBE). The biological effectiveness of any type or energy of ionizing radiation in producing a specific biological damage (e.g., leukemia, anemia, sterility, carcinogenesis, cataracts, shortening of life span, etc.) relative to damage produced by equivalent energy deposition by X or gamma radiation of about 200 kv. It is given frequently as an average value in the common energy range of a particular type of ion (see Table III-A-3).

Conversion of Dose to Flux. The equations used to convert dose to flux are as follows:

$$1\ \text{r} = \frac{2.08 \times 10^3 W_a}{(\mu - \sigma_s)_a E} = \frac{6.77 \times 10^4}{(\mu - \sigma_s)_a E}\ \text{photons/cm}^2\ \text{(below 3 Mev)}^{(19)}$$

$$1\ \text{r/hr} = \frac{0.576 W_a}{(\mu - \sigma_s)_a E} = \frac{0.576 \times 32.5}{3.35 \times 10^{-5} E} = \frac{5.6 \times 10^{5*}}{E}\ \text{photons/cm}^2\ \text{sec (below 3 Mev)}^{(19)}$$

$$1\ \text{rep} = 2.3 \times 10^9\ \text{thermal neutrons/cm}^2\ \text{(in soft tissue)}$$

$$1\ \text{rep/hr} = 6.4 \times 10^5\ \text{thermal neutrons/cm}^2\ \text{sec (in soft tissue)}$$

where

W_a = average energy per ion pair,

$(\mu - \sigma_s)_a$ = total coefficient of absorption minus the compton scattering coefficient[20] of energy E (Mev) in air.

(20) G. R. White, "X Ray Attenuation Coefficients from 10 Kev to 100 Mev," NBS-1003 (May 13, 1952); W. S. Snyder and J. L. Powell, "Absorption of γ-Rays," ORNL-421 (March, 1950), also issued as AECD-2739; W. Heitler, Quantum Theory of Radiation, Oxford Univ. Press, New York, 1944.

* Final approximate equation correct from 0.07 to 2.0 Mev within about 12%.

Table III-A-3. Laboratory Values of Maximum Permissible Exposure to Various Types of Ionizing Radiation[a]

Type of Radiation	Maximum Permissible Exposure			RBE	Approximate Flux for an 8-hr Exposure
	mr/wk	mrep/wk	mrem/wk		
X or Gamma Rays	300		300	1	4000 photons/cm^2·sec of 1 Mev
Beta Rays		300	300	1	94 electrons/cm^2·sec of 1 Mev
Thermal Neutrons		120	300	2.5[b]	1800 n_t/cm^2·sec of 0.02 ev
Fast Neutrons		30	300	~10	42 n_f/cm^2·sec of 2 Mev
Protons		30	300	10	- - - - - - - - - - - - -
Alpha Particles		30	300	10	0.009 α/cm^2·sec of 5 Mev
Recoils (O, C, N, etc.)		15	300	20	- - - - - - - - - - - - -

a If the "mrad" unit is used in place of the "mrep" unit, the values given in these tables will remain unchanged. The "rep" corresponds to an energy loss in tissue of 93 ergs/g and the "rad" corresponds to an energy loss of 100 ergs/g in any medium, and use of the "rad" would correspond to an increase of about 7.5% in the permissible energy dose to tissue, less than the accuracy claimed for these values.

b This value is based on calculations of W. S. Snyder, "Calculations for Maximum Permissible Exposure to Thermal Neutrons," Nucleonics 6, p. 46 (1950), and relates to the calculation of dose from the multiple collision of neutrons in a large mass of tissue (man). For the single collision case where the dose is calculated for a small object the RBE is equal to 5.

Dose Measurements with Ion Chamber. The dose rate as measured with an ion chamber is given by the equation,[21]

$$\text{rep/hr} = 8.3 \times 10^{11} \frac{WITP_m}{vp}$$

where

I = current (amps) flowing between the electrodes in the gas,

v = volume of gas (cc),

p = gas pressure (mm Hg),

T = gas temperature (^{o}K) when sufficient voltage is applied to collect all the ions produced by the radiation and there is no gas multiplication.

If air is used in the ion chamber, the energy per ion pair, W, is equal approximately to 32.5 ev in the case of beta, gamma, X and electron radiation and approximately 35 ev in the case of proton and alpha radiation. The stopping power, P_m, of tissue relative to air is equal approximately to 1.13 for beta, gamma, X and electron radiation and 1.2 for proton and alpha radiation.

The above equation gives the dose rate in roentgens per hour if it is applied to X and gamma radiation and is multiplied by 93/84, and if P_m is set equal to 1. It gives the dose rate in rad per hour if it is multiplied by 93/100 and if P_m is set equal to 1.

Maximum Exposure. Dose values for maximum permissible exposures are given in Tables III-A-4 and III-A-5.

(21) K. Z. Morgan, "Health Physics," Handbook on Physics, to be published by the National Research Council.

Table III-A-4. Neutron Dose Values

Neutron Energy (Mev)	Normal Incident Flux[a] for 0.3 rem/wk (n/cm^2 sec)	International Maximum Permissible Value (n/cm^2 sec)	Flux to Dose Conversion Factors	
			rep/(n/cm^2)	rem/(n/cm^2)
10	26	30	8.0×10^{-7}	8.0×10^{-8}
5	26	30	8.0×10^{-7}	8.0×10^{-8}
4	30	30	6.9×10^{-7}	6.9×10^{-8}
3	35	30	5.9×10^{-7}	5.9×10^{-8}
2	42	40	5.0×10^{-7}	5.0×10^{-8}
1	58	60	3.6×10^{-7}	3.6×10^{-8}
0.5	82	80	2.54×10^{-7}	2.54×10^{-8}
0.1	220	200	9.5×10^{-6}	9.5×10^{-7}
0.01	1000	1000	2.1×10^{-11}	2.1×10^{-12}
10^{-5}	--	1000	2.1×10^{-11}	2.1×10^{-12}
2.5×10^{-8} (thermal)	1800	2000	1.15×10^{-11}	1.15×10^{-12}

a Fast-neutron values are based on calculations by W. S. Snyder in a paper, "Calculated Depth Dose Curves in Tissue for Broad Beams of Fast Neutrons," submitted for publication in Brit. J. Radiology. Refer also to J. H. Tait, "Calculation of the Energy Deposition by Fast Neutrons in Soft Tissue," Brit. J. Radiology 23, No. 269, p. 282 (1950). These calculations are for neutrons incident normally on a 30-cm thick slab of flesh. The values obtained are sensitive to the geometry and care should be exercised in their use. Snyder is extending the study to other geometrical configurations.

Table III-A-5. Values of Maximum Permissible Weekly Occupational Exposure of Body Organs of Adults[a]

Body Organ	Type of Radiation						
	X or Gamma Rays (mr)	Beta Rays or Electrons (mrep)	Protons (mrep)	Fast Neutrons (mrep)	Thermal Neutrons (mrep)	Alpha Particles (mrep)	Recoil Particles (O,C,N) (mrep)
Total Body	300	300	30	~30	~120	30	15
In the Skin[b]							
Total body	600-1500[c]	600-1500[c]	150	~150	~450	150	75
Head and neck	1500	1500	150	30-150[c]	120-450[a]	150	75
Hand, forearms, and feet	1500	1500	150	150	60	150	75
Eyes[d]	450	300	30	~30	~120	30	15
Gonads[e]	300 (or 300 mrep)	300	30	~30	~120	30	15
Blood-forming Organs[e]	~400	300	30	~30	~120	30	15
Intermediate Tissue[c,f]	400-1500	300-1500	30-150	30-150	120-450	30-150	15-75

a See footnote (a), Table III-A-3; also "Permissible Dose from External Sources," Handbook 55, National Bureau of Standards.

b The minimum thickness of the epidermis is taken as 0.07 mm.

c The higher limit must not be used unless shielding or localization of the radiation can be provided so that the exposure limits to other critical tissues are not exceeded.

d The average depth of the sensitive portion of the lens of the eye is considered to be at 3 mm.

e The average depth of the ovaries, testes, and blood-forming organs are considered to be 7, 1, and 5 cm, respectively.

f "Intermediate" tissue is considered to be that between the surface of the body and a depth of 5 cm (excluding the lens of the eye and the testes).

III-B. DESIGN OF REACTOR SHIELDS BY COMPARISON WITH BULK SHIELDING MEASUREMENTS

1. Semianalytical Method of Shield Design

The analytical method of shield design, in the most ambitious sense, implies a knowledge of the fundamental cross sections of all the components of a shield and a subsequent calculation of the dose in the actual geometry of the problem. Such a calculation is unlikely to be made in the near future.

A more practical approach to an analytic calculation is provided by the concept(1) of the removal cross section and by our recently acquired knowledge of the buildup factors for gamma rays in various media.(2) Even with this information, however, an application to a specific problem remains difficult because of the integrations over the source regions which must be performed in complicated geometries. In many shielding applications, however, the reactor core and shield may be assumed to have regular shapes and to vary in composition in a simple fashion. In such situations, it is possible to perform the integrations over the geometry and to express the final doses in a form which is flexible and useful for shield designs and comparisons.

A first approach to this problem was made by Ascoli(3) who obtained approximate expressions for the dose of neutrons and gamma rays at the outside of a spherical shield surrounding a spherical reactor. An expression for the

(1) R. D. Albert and T. A. Welton, "A Simplified Theory of Neutron Attenuation and Its Application to Reactor Shield Design," WAPD-15 (Nov. 30, 1950); the presently used definition is given in "Physics Division Quarterly Progress Report for Period Ending December 20, 1952," ORNL-1477, p. 4.

(2) H. Goldstein, J. E. Wilkins, Jr., and Stanley Preiser, "Interim Report on the NDA-NBS Calculations of Gamma Ray Penetration," NDA Memo 15C-20 (Sept. 8, 1953); U. Fano, "Gamma-Ray Attenuation," Nucleonics 11, No. 8, 8 (1953).

(3) "Report of the Technical Advisory Board to the Technical Committee of the Aircraft Nuclear Propulsion Program," ANP-52, p. 196 (Aug. 4, 1950).

secondary gamma dose was also given. Unfortunately, no details of the derivations and no discussion of the use of the results in shield design were reported.

The analytic method has recently been considered by A. Simon, T. A. Welton, R. Aronson and H. Goldstein ["The Semianalytic Method of Shield Design," ORNL-1571 (in preparation); hereinafter referred to as SWAG] with the result that a general method for treating regular shield geometries was obtained. In particular, the results for the special case of the flux outside of a spherical reactor core and shield were obtained and differ somewhat from those given by Ascoli.(3) Analytical results in SWAG also include the geometries corresponding to a finite disk source, a cylindrical reactor (both near the flat face and the rounded sides) as well as expressions for the secondary dose. A method of using these expressions, the so-called "semianalytic" method of shield design, together with the results of bulk shielding mockups, is described in SWAG and also in section III-B-4.

In the remainder of this section, expressions for the geometries noted above will be derived. An expression for the secondary gamma-ray dose in the spherical case will also be obtained. Except in the case of the formula for the secondary gamma-ray dose, we shall refer to all radiations as neutrons. The results are equally valid, of course, for primary gamma-ray doses.

The following basic assumptions and notations are applicable to each of the cases described:

(1) The reactor core is assumed to be homogeneous with a rate of neutron production n_o (neutrons/cm^3 sec) which is constant over the core.

(2) The cross section in the core is denoted by σ_o; it is also assumed that there is no buildup in the core.

(3) The attenuation in the shield is assumed to be exponential; the buildup in the shield is later introduced in an approximate fashion.

(4) Only first-flight neutrons are considered; in the secondary gamma-ray case this means first-flight neutrons to the point of capture or inelastic scattering and first-flight gamma rays to the detector.

It will always be advantageous to choose the coordinates for the integration over the reactor core to be the neutron trajectory R and some associated polar angles. The complete dependence on R of the resulting integrand is then simply $\exp(-\sigma_o R)$ and this integration may be performed immediately. This point will be made clear by the calculations below.

Spherical Reactor and Shield

The reactor core is of radius a. The shield is assumed to vary radially in an arbitrary manner with a cross section denoted by $\sigma(r)$. The outer radius of the shield is b. The dose of neutrons at a point r' is then

$$F(r') = n_o \iiint \frac{R^2\, dR\, d(\cos\theta)\, d\phi}{4\pi R^2}\, e^{-\int_1^2 \sigma(r) ds} \tag{1}$$

where the geometry is shown in Fig. III-B-1. Here ds is an element of length along the path from point 1 to point 2. The angle ϕ is an azimuthal angle which may be integrated immediately. Now we have

$$r^2 = s^2 + r'^2 - 2sr' \cos\theta$$

$$\therefore\ s = r' \cos\theta - \sqrt{r^2 - r'^2 \sin^2\theta}$$

or

$$ds = \frac{-r\, dr}{\sqrt{r^2 - r'^2 \sin^2\theta}} \tag{2}$$

The path length inside the reactor core is

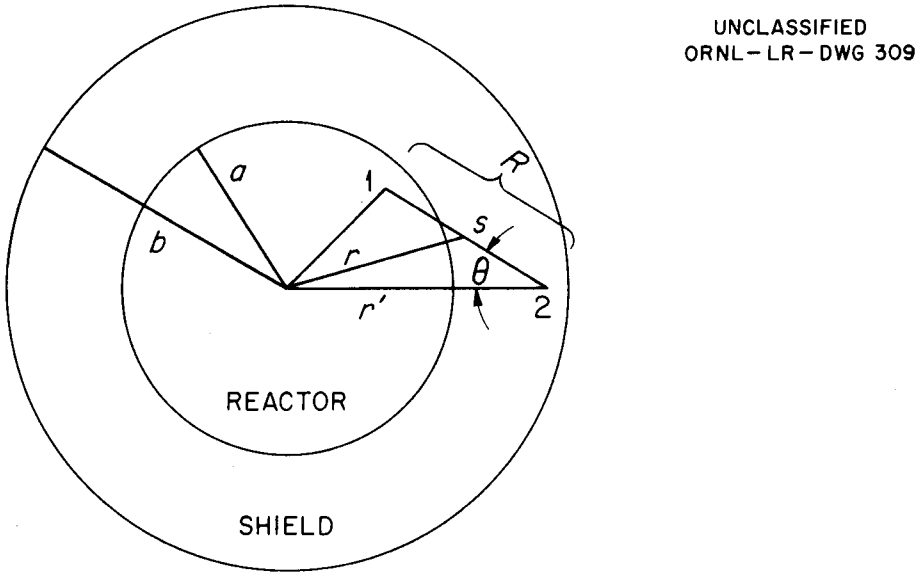

Fig. III-B-1. Geometry for Spherical Reactor and Shield.

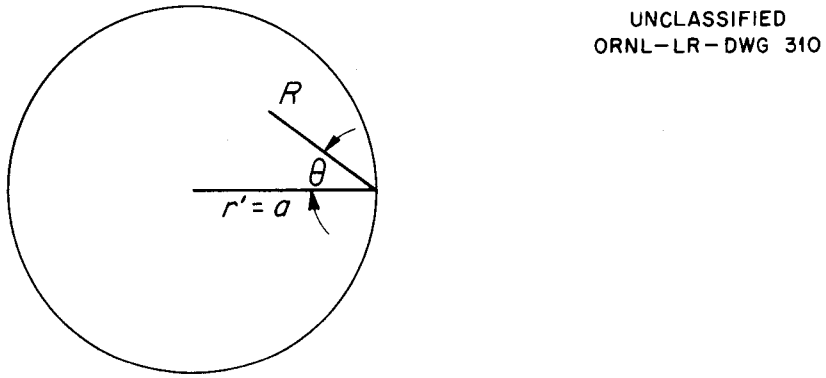

Fig. III-B-2. Geometry for Spherical Reactor where $r' = a$.

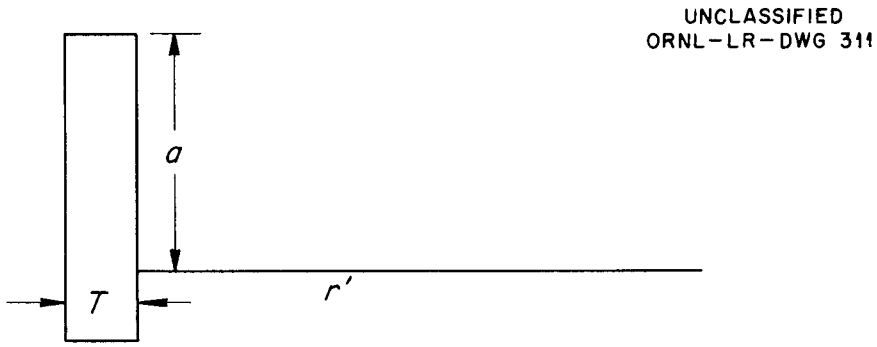

Fig. III-B-3. Geometry for Finite Circular Slab Source.

$$R - r' \cos\theta + \sqrt{a^2 - r'^2 \sin^2\theta} \tag{3}$$

Combining these relations, we have

$$\int_1^2 \sigma ds = \sigma_o \left[R - r' \cos\theta + \sqrt{a^2 - r'^2 \sin^2\theta} \right] + \int_a^{r'} \frac{\sigma(r) r \, dr}{\sqrt{r^2 - r'^2 \sin^2\theta}}$$

Equation (1) now becomes

$$F(r') = \frac{n_o}{2} \int_{\sqrt{1 - \frac{a^2}{r'^2}}}^{1} d(\cos\theta) \, e^{-\int_a^{r'} \frac{\sigma(r) r \, dr}{\sqrt{r^2 - r'^2 \sin^2\theta}}}$$

$$\times \int_{r'\cos\theta - \sqrt{a^2 - r'^2 \sin^2\theta}}^{r'\cos\theta + \sqrt{a^2 - r'^2 \sin^2\theta}} dR \quad e^{-\sigma_o (R - r'\cos\theta + \sqrt{a^2 - r'^2 \sin^2\theta})} \tag{4}$$

Note the characteristic simple exponential dependence on R which was mentioned above. Integrating over R, the result becomes

$$F(r') = \frac{n_o}{2\sigma_o} \int_{\sqrt{1 - \frac{a^2}{r'^2}}}^{1} d(\cos\theta) \left(1 - e^{-2\sigma_o \sqrt{a^2 - r'^2 \sin^2\theta}} \right)$$

$$\times \; e^{-\int_a^{r'} \frac{\sigma(r) \, r \, dr}{\sqrt{r^2 - r'^2 \sin^2\theta}}} \tag{5}$$

Equation (5) is still an exact expression. At this point, a single approximation is needed to obtain the final result. Since $r' \sin\theta \leq a \leq r$, we expand the square roots in a binomial expansion and keep two terms.

$$\sqrt{a^2 - r'^2 \sin^2\theta} \cong a - \frac{1}{2}\frac{r'^2}{a}\sin^2\theta$$

$$(r^2 - r'^2 \sin^2\theta)^{-1/2} \cong \frac{1}{r}\left(1 + \frac{1}{2}\frac{r'^2}{r^2}\sin^2\theta\right) \tag{6}$$

This approximation will be an excellent one for thick shields since in this case the dominant contributions to the dose will come from regions of integration corresponding to $r' \sin\theta << a$. As the point r' approaches the surface of the reactor core, the approximation becomes worse. However, even right at the core surface, $r' = a$, it will be shown below that the error is never worse than 30% and usually is completely negligible.

Combining Eqs. (5) and (6), we have

$$F(r') \cong \frac{n_o}{2\sigma_o} e^{-\int_a^{r'} \sigma dr} \int_{\sqrt{1 - \frac{a^2}{r'^2}}}^{1} e^{-\left(1/2 \int_a^{r'} \frac{r'^2}{r^2} \sigma dr\right)\sin^2\theta}$$

$$\times \left(1 - e^{-2\sigma_o a} e^{+\sigma_o a (r'^2/a^2)\sin^2\theta}\right) d(\cos\theta)$$

Let us define

$$\alpha(r') = \frac{1}{2}\int_a^{r'} \frac{r'^2}{r^2}\sigma\, dr$$

$$\beta(r') = \alpha(r') - \sigma_o a \frac{r'^2}{a^2} \tag{7}$$

Now

$$I(\alpha) = \int_{\sqrt{1-a^2/r'^2}}^{1} d(\cos\theta)\, e^{-\alpha\sin^2\theta} = e^{-\alpha} \int_{\sqrt{1-a^2/r'^2}}^{1} dt\, e^{\alpha t^2}$$

$$= \frac{e^{-\alpha}}{\sqrt{\alpha}} \int_{\sqrt{\alpha}\sqrt{1-a^2/r'^2}}^{\sqrt{\alpha}} dy\, e^{y^2} \qquad \text{for } \alpha > 0$$

The function

$$y(x) = \frac{e^{-x^2}}{x} \int_0^x e^{t^2}\, dt$$

has been tabulated by S. Sakamoto[4] and is reproduced in Table III-B-1. In terms of this function we have

$$I(\alpha) = \left[y(\sqrt{\alpha}) - \sqrt{1 - \frac{a^2}{r'^2}}\; e^{-\alpha\, a^2/r'^2}\; y\left(\sqrt{\alpha}\sqrt{1 - \frac{a^2}{r'^2}}\right)\right] \quad \text{for } \alpha > 0 \qquad (8)$$

The entire result for the flux can now be written

$$F(r') \cong \frac{n_o}{2\sigma_o}\, e^{-\int_a^{r'} \sigma\, dr} \left[I(\alpha) - e^{-2\sigma_o a}\, I(\beta) \right] \qquad (9)$$

One further point should be mentioned. Although α is always positive, β may be negative. In this case

$$I(\beta) = \int_{\sqrt{1-a^2/r'^2}}^{1} d(\cos\theta) e^{+|\beta|\sin^2\theta} = e^{|\beta|} \int_{\sqrt{1-a^2/r'^2}}^{1} dt\, e^{-|\beta| t^2}$$

---

(4) S. Sakamoto, "Tafel der Funktionen $y = e^{-x^2}/x \int_0^x e^{\alpha^2}\, d\alpha$ und $z = e^{-x^2} \int_0^x e^{\alpha^2}\, d\alpha$ im Intervall $x = 0$ bis $x = 10$," Ber. Verhandl. Akad. Wiss. Leipzig, Math-naturw. Kl. 80, 217 (1928).

or

$$I(\beta) = \frac{e^{|\beta|}}{\sqrt{|\beta|}}\left[\int_0^{\sqrt{|\beta|}} dt\, e^{-t^2} - \int_0^{\sqrt{|\beta|(1-a^2/r'^2)}} dt\, e^{-t^2}\right] \text{ for } \beta<0 \qquad (10)$$

The meaning of the second term $e^{-2\sigma_0 a}I(\beta)$ is clear. This is a negative source on the back face of the reactor, correcting for the fact that the core is not opaque. In many physical problems $\sigma_0 a >> 1$ and the "back-face" correction will be small or negligible.

Equation (9) for the flux takes on a simple form if the reactor shield is thick ($\alpha >> 1$ and $a^2/r'^2 << 1$). For large x, the y function takes the form

$$y(x) \dashrightarrow \frac{1}{2x^2}$$

Hence

$$I(\alpha) \dashrightarrow \frac{1 - e^{-\alpha a^2/r'^2}}{2\alpha}$$

and

$$F(r') \dashrightarrow \frac{n_0 a^2}{2\sigma_0 r'^2} e^{-\int_a^{r'} \sigma dr} \left\{ \frac{1 - e^{-(1/2)\int_a^{r'} (a^2/r^2)\sigma dr}}{\int_a^{r'} a^2/r^2\, \sigma dr} - \frac{e^{-2\sigma_0 a}\left[1 - e^{+\sigma_0 a - (1/2)\int_a^{r'} (a^2/r^2)\sigma dr}\right]}{\int_a^{r'} a^2/r^2\, \sigma dr - 2\sigma_0 a} \right\} \qquad (11)$$

This result reduces to Ascoli's result [Ref. (3), p. 197] if the back-face correction is neglected and if one assumes that

$$\frac{1}{2}\int_a^{r'} \frac{a^2}{r^2}\, \sigma dr >> 1$$

TABLE III-B-1. TABLE OF THE FUNCTIONS $y = \frac{e^{-x^2}}{x}\int_0^x e^{a^2}\,da$ AND $z = e^{-x^2}\int_0^x e^{a^2}\,da$ IN THE INTERVAL $x = 0$ TO $x = 10$

[Reprint from S. Sakamoto, *Ber. Verhandl. Akad. Wiss. Leipzig, Math-Naturw. Kl.* 80, 217 (1928).]

x	y	z	x	y	z	x	y	z	x	y	z	x	y	z	x	y	z
0,00	1,0000	0,0000	0,35	0,9221	0,3227	0,70	0,7293	0,5105	1,05	0,5076	0,5330	1,40	0,3261	0,4565	1,75	0,2056	0,3598
0,01	0,9999	0,0100	0,36	0,9178	0,3304	0,71	0,7229	0,5133	1,06	0,5017	0,5318	1,41	0,3218	0,4537	1,76	0,2029	0,3571
0,02	0,9997	0,0200	0,37	0,9134	0,3380	0,72	0,7165	0,5159	1,07	0,4958	0,5305	1,42	0,3175	0,4509	1,77	0,2003	0,3545
0,03	0,9994	0,0300	0,38	0,9090	0,3454	0,73	0,7101	0,5184	1,08	0,4900	0,5292	1,43	0,3133	0,4480	1,78	0,1977	0,3519
0,04	0,9989	0,0400	0,39	0,9045	0,3528	0,74	0,7037	0,5207	1,09	0,4842	0,5278	1,44	0,3092	0,4452	1,79	0,1952	0,3494
0,05	0,9983	0,0499	0,40	0,8999	0,3599	0,75	0,6973	0,5230	1,10	0,4784	0,5262	1,45	0,3051	0,4424	1,80	0,1927	0,3468
0,06	0,9976	0,0599	0,41	0,8952	0,3670	0,76	0,6909	0,5251	1,11	0,4727	0,5247	1,46	0,3011	0,4396	1,81	0,1903	0,3444
0,07	0,9967	0,0698	0,42	0,8904	0,3740	0,77	0,6845	0,5271	1,12	0,4670	0,5230	1,47	0,2971	0,4367	1,82	0,1879	0,3420
0,08	0,9957	0,0797	0,43	0,8855	0,3808	0,78	0,6781	0,5289	1,13	0,4613	0,5213	1,48	0,2932	0,4339	1,83	0,1856	0,3396
0,09	0,9946	0,0895	0,44	0,8805	0,3874	0,79	0,6716	0,5306	1,14	0,4556	0,5194	1,49	0,2893	0,4311	1,84	0,1833	0,3373
0,10	0,9934	0,0993	0,45	0,8754	0,3939	0,80	0,6651	0,5321	1,15	0,4500	0,5175	1,50	0,2855	0,4283	1,85	0,1811	0,3350
0,11	0,9920	0,1091	0,46	0,8702	0,4003	0,81	0,6586	0,5335	1,16	0,4445	0,5156	1,51	0,2818	0,4255	1,86	0,1789	0,3327
0,12	0,9904	0,1188	0,47	0,8649	0,4065	0,82	0,6520	0,5347	1,17	0,4390	0,5136	1,52	0,2781	0,4227	1,87	0,1767	0,3304
0,13	0,9887	0,1285	0,48	0,8596	0,4126	0,83	0,6455	0,5358	1,18	0,4335	0,5115	1,53	0,2744	0,4198	1,88	0,1745	0,3280
0,14	0,9869	0,1382	0,49	0,8543	0,4186	0,84	0,6390	0,5368	1,19	0,4281	0,5094	1,54	0,2708	0,4170	1,89	0,1723	0,3256
0,15	0,9850	0,1478	0,50	0,8489	0,4244	0,85	0,6325	0,5376	1,20	0,4227	0,5073	1,55	0,2672	0,4142	1,90	0,1702	0,3233
0,16	0,9830	0,1573	0,51	0,8434	0,4301	0,86	0,6261	0,5384	1,21	0,4174	0,5051	1,56	0,2637	0,4114	1,91	0,1680	0,3209
0,17	0,9809	0,1668	0,52	0,8378	0,4357	0,87	0,6197	0,5391	1,22	0,4122	0,5029	1,57	0,2602	0,4085	1,92	0,1659	0,3186
0,18	0,9787	0,1762	0,53	0,8322	0,4411	0,88	0,6134	0,5398	1,23	0,4070	0,5006	1,58	0,2567	0,4056	1,93	0,1639	0,3163
0,19	0,9763	0,1855	0,54	0,8265	0,4463	0,89	0,6071	0,5403	1,24	0,4018	0,4982	1,59	0,2533	0,4028	1,94	0,1619	0,3141
0,20	0,9738	0,1948	0,55	0,8207	0,4514	0,90	0,6008	0,5407	1,25	0,3967	0,4959	1,60	0,2500	0,4000	1,95	0,1600	0,3120
0,21	0,9711	0,2039	0,56	0,8149	0,4563	0,91	0,5945	0,5410	1,26	0,3916	0,4934	1,61	0,2468	0,3973	1,96	0,1581	0,3098
0,22	0,9683	0,2130	0,57	0,8090	0,4611	0,92	0,5882	0,5411	1,27	0,3866	0,4910	1,62	0,2436	0,3946	1,97	0,1562	0,3077
0,23	0,9654	0,2220	0,58	0,8031	0,4658	0,93	0,5819	0,5412	1,28	0,3816	0,4885	1,63	0,2404	0,3919	1,98	0,1543	0,3056
0,24	0,9624	0,2310	0,59	0,7972	0,4704	0,94	0,5756	0,5411	1,29	0,3767	0,4859	1,64	0,2373	0,3892	1,99	0,1525	0,3035
0,25	0,9593	0,2398	0,60	0,7913	0,4748	0,95	0,5693	0,5408	1,30	0,3719	0,4834	1,65	0,2342	0,3865	2,00	0,1507	0,3014
0,26	0,9561	0,2486	0,61	0,7853	0,4790	0,96	0,5630	0,5405	1,31	0,3671	0,4809	1,66	0,2312	0,3838	2,01	0,1489	0,2993
0,27	0,9528	0,2573	0,62	0,7792	0,4831	0,97	0,5567	0,5400	1,32	0,3624	0,4784	1,67	0,2282	0,3811	2,02	0,1471	0,2972
0,28	0,9494	0,2658	0,63	0,7731	0,4870	0,98	0,5505	0,5395	1,33	0,3577	0,4758	1,68	0,2253	0,3785	2,03	0,1454	0,2952
0,29	0,9458	0,2743	0,64	0,7669	0,4908	0,99	0,5443	0,5389	1,34	0,3531	0,4732	1,69	0,2224	0,3758	2,04	0,1437	0,2931
0,30	0,9421	0,28 26	0,65	0,7607	0,4945	1,00	0,5381	0,5381	1,35	0,3485	0,4705	1,70	0,2195	0,3731	2,05	0,1420	0,2911
0,31	0,9383	0,2909	0,66	0,7545	0,4980	1,01	0,5319	0,5372	1,36	0,3440	0,4678	1,71	0,2166	0,3704	2,06	0,1404	0,2892
0,32	0,9344	0,2990	0,67	0,7482	0,5013	1,02	0,5258	0,5363	1,37	0,3395	0,4651	1,72	0,2138	0,3677	2,07	0,1388	0,2873
0,33	0,9304	0,3070	0,68	0,7419	0,5045	1,03	0,5197	0,5353	1,38	0,3350	0,4623	1,73	0,2110	0,3650	2,08	0,1372	0,2854
0,34	0,9263	0,3149	0,69	0,7356	0,5076	1,04	0,5136	0,5342	1,39	0,3305	0,4594	1,74	0,2083	0,3624	2,09	0,1357	0,2835

TABLE III-B-1 (continued).

x	y	z	x	y	z	x	y	z	x	y	z	x	y	z	x	y	z
2,10	0,1341	0,2816	2,45	0,0936	0,2293	2,80	0,0691	0,1935	3,15	0,0535	0,1684	3,50	0,0427	0,1496	3,60	0,0403	0,1449
2,11	0,1326	0,2798	2,46	0,0927	0,2281	2,81	0,0685	0,1926	3,16	0,0531	0,1678	3,51	0,0425	0,1491			
2,12	0,1312	0,2781	2,47	0,0918	0,2268	2,82	0,0680	0,1918	3,17	0,0527	0,1672	3,52	0,0422	0,1486	4,00	0,0323	0,1293
2,13	0,1297	0,2763	2,48	0,0909	0,2256	2,83	0,0675	0,1909	3,18	0,0524	0,1666	3,53	0,0420	0,1482	4,50	0,0254	0,1141
2,14	0,1283	0,2745	2,49	0,0901	0,2244	2,84	0,0669	0,1901	3,19	0,0520	0,1660	3,54	0,0417	0,1477	5,00	0,0204	0,1021
2,15	0,1268	0,2727	2,50	0,0893	0,2232	2,85	0,0664	0,1893	3,20	0,0517	0,1654	3,55	0,0415	0,1473	6,00	0,0141	0,0845
2,16	0,1254	0,2710	2,51	0,0885	0,2221	2,86	0,0659	0,1885	3,21	0,0514	0,1649	3,56	0,0412	0,1468			
2,17	0,1241	0,2693	2,52	0,0877	0,2210	2,87	0,0654	0,1877	3,22	0,0510	0,1643	3,57	0,0410	0,1463	8,00	0,0079	0,0630
2,18	0,1228	0,2677	2,53	0,0869	0,2199	2,88	0,0649	0,1869	3,23	0,0507	0,1637	3,58	0,0407	0,1458	10,00	0,0050	0,0503
2,19	0,1215	0,2661	2,54	0,0861	0,2187	2,89	0,0644	0,1861	3,24	0,0503	0,1631	3,59	0,0405	0,1454			
2,20	0,1202	0,2645	2,55	0,0853	0,2176	2,90	0,0639	0,1854	3,25	0,0500	0,1626						
2,21	0,1189	0,2628	2,56	0,0846	0,2165	2,91	0,0635	0,1847	3,26	0,0497	0,1620						
2,22	0,1176	0,2611	2,57	0,0838	0,2154	2,92	0,0630	0,1840	3,27	0,0494	0,1614						
2,23	0,1163	0,2595	2,58	0,0831	0,2143	2,93	0,0625	0,1832	3,28	0,0490	0,1609						
2,24	0,1151	0,2579	2,59	0,0823	0,2132	2,94	0,0621	0,1825	3,29	0,0487	0,1603						
2,25	0,1139	0,2563	2,60	0,0816	0,2122	2,95	0,0616	0,1818	3,30	0,0484	0,1598						
2,26	0,1127	0,2547	2,61	0,0809	0,2112	2,96	0,0612	0,1811	3,31	0,0481	0,1592						
2,27	0,1115	0,2531	2,62	0,0802	0,2101	2,97	0,0607	0,1803	3,32	0,0478	0,1587						
2,28	0,1104	0,2516	2,63	0,0795	0,2091	2,98	0,0603	0,1796	3,33	0,0475	0,1581						
2,29	0,1092	0,2501	2,64	0,0788	0,2080	2,99	0,0598	0,1789	3,34	0,0472	0,1576						
2,30	0,1081	0,2486	2,65	0,0781	0,2069	3,00	0,0594	0,1782	3,35	0,0469	0,1571						
2,31	0,1070	0,2472	2,66	0,0774	0,2059	3,01	0,0590	0,1775	3,36	0,0466	0,1566						
2,32	0,1059	0,2458	2,67	0,0767	0,2049	3,02	0,0585	0,1768	3,37	0,0463	0,1561						
2,33	0,1049	0,2444	2,68	0,0761	0,2040	3,03	0,0581	0,1761	3,38	0,0460	0,1556						
2,34	0,1039	0,2430	2,69	0,0755	0,2030	3,04	0,0577	0,1754	3,39	0,0457	0,1551						
2,35	0,1028	0,2416	2,70	0,0748	0,2020	3,05	0,0573	0,1748	3,40	0,0455	0,1546						
2,36	0,1018	0,2403	2,71	0,0742	0,2011	3,06	0,0569	0,1741	3,41	0,0452	0,1541						
2,37	0,1009	0,2391	2,72	0,0736	0,2002	3,07	0,0565	0,1735	3,42	0,0449	0,1536						
2,38	0,0999	0,2378	2,73	0,0730	0,1993	3,08	0,0561	0,1728	3,43	0,0446	0,1530						
2,39	0,0990	0,2366	2,74	0,0724	0,1984	3,09	0,0557	0,1722	3,44	0,0443	0,1525						
2,40	0,0981	0,2354	2,75	0,0718	0,1975	3,10	0,0553	0,1715	3,45	0,0441	0,1520						
2,41	0,0972	0,2342	2,76	0,0713	0,1967	3,11	0,0549	0,1709	3,46	0,0438	0,1515						
2,42	0,0963	0,2330	2,77	0,0707	0,1959	3,12	0,0546	0,1702	3,47	0,0435	0,1510						
2,43	0,0954	0,2318	2,78	0,0702	0,1951	3,13	0,0542	0,1696	3,48	0,0433	0,1505						
2,44	0,0945	0,2306	2,79	0,0696	0,1943	3,14	0,0538	0,1690	3,49	0,0430	0,1501						

Aus der leicht abzuleitenden Gleichung

$$\frac{dz}{dx} = 1 - 2zx$$

findet man die Annäherungsformeln

$$z = \frac{x}{2x^2-1} + \frac{2x}{(2x^2-1)^3}$$

$$y = \frac{1}{2x^2-1} + \frac{2}{(2x^2-1)^3}$$

die mit größer werdendem Argument immer brauchbarer werden und für $x = 3{,}6$ noch die vierte Stelle richtig liefern.

This last assumption is often incorrect, as for example in the attenuation of gamma rays by a water shield. Note that r' need not be inside the shield radius ($r' \leq b$). If $r' \geq b$, the previous formulas are all valid simply by regarding $\sigma(r)$ as being zero for $r > b$. The essential difference of Eq. (11) from the corresponding result for a slab geometry (see below, page 78) lies in the term $\int \frac{\sigma dr}{r^2}$ which weights the different regions of the shield unequally. This term will be referred to as a "curvature correction" for the sphere.

As was mentioned above, the validity of the binomial expansion decreases as $r' \rightarrow a$. The worst case is at $r' = a$. At this point, it is possible to solve the geometrical problem (see Fig. III-B-2) without a binomial expansion:

$$F(a) = \frac{n_o}{2} \int_0^1 d(\cos\theta) \int_0^{2a\cos\theta} dR\, e^{-\sigma_o R}$$

$$= \frac{n_o}{2\sigma_o} \int_0^1 dx(1 - e^{-2\sigma_o ax}) = \frac{n_o}{2\sigma_o}\left[1 - \frac{1}{2\sigma_o a}(1 - e^{-2\sigma_o a})\right] \tag{12}$$

Let us compare this with the result of Eq. (9). Now as $x \rightarrow 0$, $y(x) \rightarrow 1$; and hence as $\alpha \rightarrow 0$, $I(x) \rightarrow 1$. Also $\beta \rightarrow -\sigma_o a$, and

$$I(\beta) \longrightarrow \frac{e^{\sigma_o a}}{\sqrt{\sigma_o a}} \int_0^{\sqrt{\sigma_o a}} e^{-t^2} dt$$

$$F(a) \cong \frac{n_o}{2\sigma_o}\left(1 - \frac{e^{-\sigma_o a}}{\sqrt{\sigma_o a}} \int_0^{\sigma_o a} e^{-t^2} dt\right) \tag{13}$$

The ratio of Eq. (13) to Eq. (12) is then

$$R\,\frac{\text{approx.}}{\text{exact}} = \frac{1 - \dfrac{e^{-\sigma_o a}}{\sqrt{\sigma_o a}} \displaystyle\int_0^{\sqrt{\sigma_o a}} e^{-t^2}dt}{1 - \dfrac{1}{2\sigma_o a}\left(1 - e^{-2\sigma_o a}\right)}$$

When the reactor core is opaque ($\sigma_o a >> 1$) this ratio is unity, even at the surface of the reactor! The worst case is in the limit of a transparent reactor ($\sigma_o a = 0$). This limiting value is easily seen to be 4/3. Hence it is clear that the binomial expansion will be an exceedingly good approximation in all cases of interest.

An interesting point is that one obtains the leakage from a sphere by going to the limit of no shield ($\sigma = 0$) in Eq. 9. The flux* is then

$$F(r') = \frac{n_o a^2}{2\sigma_o r'^2}\left[\frac{1}{2} + \frac{e^{-2\sigma_o a}}{2\sigma_o a}\left(1 - e^{\sigma_o a}\right)\right]$$

The flux at r' with no self-shielding would be

$$F = n_o \frac{\frac{4}{3}\pi a^3}{4\pi r'^2} = \frac{n_o a^3}{3r'^2}$$

Hence the leakage is

$$f \cong \frac{3}{4\sigma_o a}\left[1 + \frac{e^{-2\sigma_o a}}{\sigma_o a}\left(1 - e^{\sigma_o a}\right)\right] \tag{14}$$

This differs from the exact result(5)

$$f = \frac{3}{4\sigma_o a}\left[1 - \frac{1}{2(\sigma_o a)^2} + \frac{e^{-2\sigma_o a}}{2(\sigma_o a)^2}\left(1 + 2\sigma_o a\right)\right]$$

by only 12 percent at most.

(5) See for example H. Hurwitz in "Report of the Physics Section for December 1952, January and February 1953," Knolls Atomic Power Laboratory, KAPL-909, p. 19.

* For $r' >> a$ the flux approaches the correct density.

Secondary Gamma-Ray Dose from a Spherical Reactor and Shield. This calculation follows a manner very similar to that for the primary dose. The neutron flux F(r) in the shield is given by Eq. (9). The cross section in the shield for the conversion of neutrons into gamma rays is denoted by $\sigma_i(r)$ and the cross section for the resultant gamma ray by $\eta(r)$. With these definitions, the secondary gamma-ray dose at r' is

$$F(r') = \frac{n_o}{4\sigma_o} \int_a^{r'} e^{-\int_a^r \sigma dr} e^{-\int_r^{r'} \eta dr} \sigma_i(r)$$

$$\times \left[I(\alpha) - I(\beta) e^{-2\sigma_o a} \right] I(\gamma) dr \tag{15}$$

where

$$\gamma = \frac{1}{2} \int_r^{r'} \frac{r'^2}{r''^2} \eta(r'') dr''$$

$$\alpha = \frac{1}{2} \int_a^r \frac{r^2 \sigma(r'')}{r''^2} dr''$$

$$\beta = \alpha - \sigma_o a \frac{r^2}{a^2}$$

The details of this derivation may be found in SWAG.

If the point r' is far away, the quantity γ must be large and

$$I(\gamma) \longrightarrow \frac{1}{2\gamma} = \frac{1}{r'^2 \int_a^b \frac{\eta(r'')}{r''^2} dr''}$$

where b is the outer radius of the shield.

Finite Circular Slab Source

Although solutions for this problem have been obtained many times before, the result is included here because of its relation to the Lid Tank Shielding Facility source and because of its use in the semianalytic method of shield design. The geometry is shown in Fig. III-B-3. Once again the source strength of neutrons n_o is assumed constant in the core, as is the core cross section σ_o. The shield is assumed to have a slab geometry with a cross section given by $\sigma(r)$. The result for the flux at r' (cf. SWAG) is easily seen to be

$$F(r') = \frac{n_o}{2\sigma_o}\left[E_2(\alpha) - \frac{r'}{\sqrt{r'^2 + a^2}}\, E_2\left(\frac{\sqrt{r'^2 + a^2}}{r'}\,\alpha\right) - E_2(\beta) + \frac{r'}{\sqrt{r'^2 + a^2}}\, E_2\left(\frac{\sqrt{r'^2 + a^2}}{r'}\,\beta\right)\right] \tag{16}$$

where

$$\alpha = \int_0^{r'} \sigma dr$$

$$\beta = \alpha + \sigma_o T$$

$$E_2(x) = \int_1^{\infty} dt\; t^{-2}\, e^{-tx}$$

The functions $E_2(x)$ are tabulated by G. Placzek.(6) At large thicknesses of material, $\alpha >> 1$ and $\beta >> 1$, and

(6) G. Placzek and Gertrude Blanch, "The Functions $E_n(x) = \int_1^{\infty} e^{-xu}\, u^{-n}\, du$ and Their Fourier and Laplace Transforms," Montreal Laboratory, MT-1.

$$E_2(x) \longrightarrow \frac{e^{-x}}{x} \quad (1 - 2/x + 6/x^2 - \ldots\ldots) \qquad \text{for } x >> 1$$

Hence, Eq. (16) becomes

$$F(r') \longrightarrow \frac{n_o}{2\sigma_o} \; \frac{e^{\int_o^{r'} \sigma dr}}{\int_o^{r'} \sigma dr} \left\{ \left[1 - e^{-(1/2)(a^2/r'^2) \int_o^{r'} \sigma dr} \right] - \frac{\int_o^{r'} \sigma dr e^{-\sigma_o T}}{\int_o^{r'} \sigma dr + \sigma_o T} \left[1 - e^{-(1/2)(a^2/r'^2)\left(\int_o^{r'} \sigma dr + \sigma_o T\right)} \right] \right\} \tag{17}$$

The second term in the brackets is clearly the "back effect." The quantity $(1/2)(a^2/r'^2) \int_o^{r'} \sigma dr'$ is the measure of whether the source appears more like an infinite plane or a point source, the infinite plane corresponding to $(1/2)(a^2/r'^2) \int_o^{r'} \sigma dr'$ large, and the point source to this quantity very small.

Cylindrical Reactors

Geometry near Flat Face. The shield near the flat face of a cylindrical reactor can usually be taken to have a slab geometry. This problem is then simply the finite circular slab source which has already been solved if one ignores the back-face correction. Detailed corrections for the shape of the back faces can indeed be made and this is done in SWAG. These corrections are not of interest unless one is close to a fairly transparent reactor.

Geometry near Round Face. The problem in this case is to find the flux $F(r')$ at a point which is a radial distance r' from the center of a cylindrical core. The cylinder is taken to be of radius a and length 2b. The cross section in the shield $\sigma(r)$ varies only with radial distance from the cylinder.

Two approximations in addition to the binomial expansion are required in order to obtain a workable solution to this problem. The first one requires the neglect of the back-face contribution. Hence the result given below is not applicable to very transparent cores. The second one approximates the integral

$$\int_0^{\sin^{-1}y} e^{-\alpha \sin^2 t}\, dt \cong \frac{1}{\sqrt{\alpha}} \sqrt{\frac{\pi}{4}}\ \mathrm{erf}(y\sqrt{\alpha})$$

where

$$\mathrm{erf}(x) = \frac{2}{\sqrt{\pi}} \int_0^x e^{-t^2}\, dt$$

The result may then be written in terms of a single integral which can be evaluated by numerical means:

$$F(r') = \frac{n_o}{2\sigma_o\sqrt{\pi}\left(\frac{1}{2}\int_a^{r'} \frac{r'^2}{r^2}\,\sigma dr\right)^{1/2}} \int_0^{\tan^{-1}(b/r')} d\phi \cos^{3/2}\phi$$

$$\times\ \mathrm{erf}\left[\left(\frac{1}{2\cos\phi}\int_a^{r'} \frac{a^2}{r^2}\,\sigma dr\right)^{1/2}\right] e^{-\int_a^{r'}\sigma dr/\cos\phi} \qquad (18)$$

This result takes on a simple form for the special case of a distant point ($r' >> b$). In this case

$$F(r') \longrightarrow \frac{n_o ba}{2\sigma_o \sqrt{\pi}\, r'^2 \sqrt{\alpha}} \; \mathrm{erf}(\sqrt{\alpha}) e^{-\int_a^r \sigma \sim dr} \tag{19}$$

where

$$\alpha = \frac{1}{2} \int_a^{r'} \frac{a^2}{r^2} \; \sigma \sim dr$$

Discussion of the Method

A detailed analysis of the assumptions and drawbacks of the analytic method are presented below in section III-B-3. At this point we shall briefly call attention to some of them. One obvious point is that this method does not take account of buildup. This defect may be partly remedied by including the buildup as a multiplying factor with a value characteristic of the normal (or shortest) shield penetration. Another point is that the method assumes a first-flight kernel (which is exponential). Multiple scatterings could conceivably be more important in some geometries. Finally it should be remarked that none of the formulas contain any energy dependence. This is not a real defect since the analytic formulas can be immediately modified to the form of an energy dependent cross section with an integral over the source energy spectrum. In practice, for thick shields, a single source energy will be dominant and this extension is not necessary. These points are all discussed further below.

2. The Homogeneous Shield Method[7]

A second method of shield design is possible when the medium is homogeneous. In this method, which has been in use for some time, no assumption is made of exponential attenuation and buildup is included. With it the dose that would be measured by an isotropic detector far from the source of radiation can be computed, the procedure being essentially as follows:

(1) The reactor core is replaced by a thin isotropic source on the surface of the reactor which gives the same dose at large distances.

(2) The response of an isotropic detector to a test source (the BSR or the Lid Tank source plate) is measured experimentally.

(3) The response of the detector for the equivalent surface source is inferred from the experimental results by use of the transformations described below.

The transformation theorems will be derived first. They are used to predict the dose to be expected from an isotropic source of one geometry in terms of the dose from an isotropic source of another geometry. Following this will be a discussion of how a volume source is replaced by an isotropic surface source.

To derive the transformation theorems one assumes an isotropic surface source imbedded in an infinite homogeneous, isotropic medium. The response of an isotropic detector to an infinitesimal element of isotropic source depends in this case only on the separation distance between them. In this section a unit source strength per unit area is assumed. One then writes for a point source of arbitrary strength

(7) This section is taken in large part from Reactor Science and Technology, TID-2002, Vol. 2, No. 2 (August, 1952), p. 73; also E. P. Blizard, "Introduction to Shield Design, Parts I and II," CF-51-10-70 (1952).

$$D_{Pt}(R) = SG(R) \tag{1}$$

where

D_{Pt} = detector response to a point isotropic source,

R = distance between source and detector,

S = source strength,

$G(R)$ = response of detector to a unit point source at distance R.

Plane Isotropic Source in Infinite Medium

In this case the source is assumed infinitely thin, all in one plane, of unit strength emitted isotropically per unit area of source per unit time, and imbedded in an infinite uniform medium (see Fig. III-B-4). The response of the isotropic detector at a distance z away from the infinite source, $D_{P\ell}(x,\infty)$, is now calculated:

$$D_{P\ell}(z,\infty) = \int_{\rho=0}^{\infty} G(R)\ 2\pi\rho\ d\rho$$

where

$$R^2 = \rho^2 + z^2,$$

$$2R\ dR = 2\rho\ d\rho;$$

therefore

$$D_{P\ell}(z,\infty) = 2\pi \int_{z}^{\infty} G(R)\ R\ dR \tag{2}$$

The relation between point and plane source geometries is obtained by differentiating Eq. (2),

$$\frac{d}{dz} D_{P\ell}(z,\infty) = -2\pi z\ G(z) \tag{3}$$

UNCLASSIFIED
ORNL-LR-DWG 312

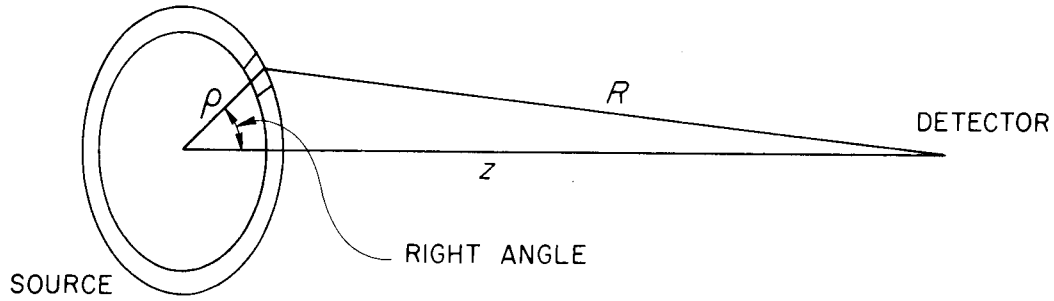

Fig. III-B-4. Plane-Source Geometry.

UNCLASSIFIED
DWG 17071A

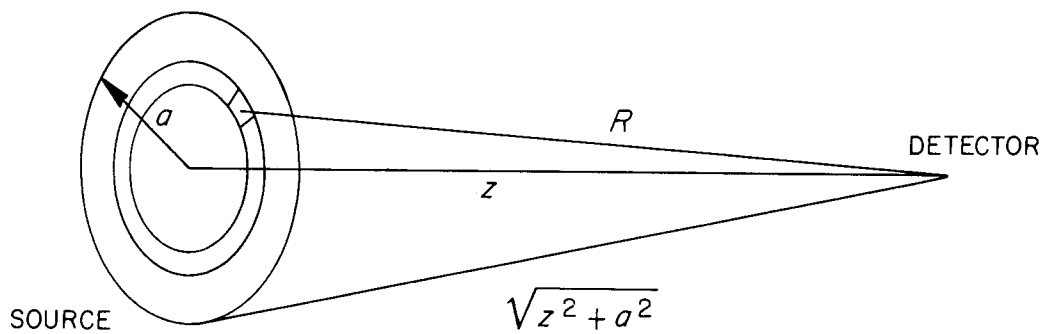

Fig. III-B-5. Geometry for Disk to Plane Transformation.

UNCLASSIFIED
ORNL-LR-DWG 313

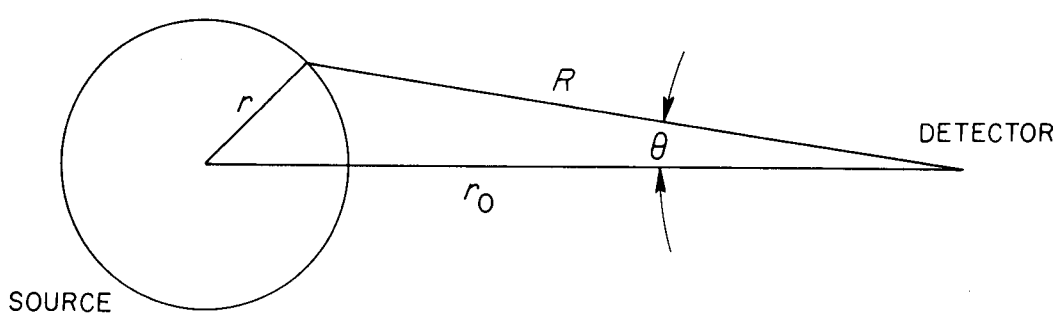

Fig. III-B-6. Geometry for Plane to Sphere Transformation.

Disk Source to Infinite Plane Transformation (Hurwitz Transformation)

By quite similar manipulation one can compute the dose to be expected with an infinite plane source in terms of measurements on the axis of a finite disk source. Both sources are assumed to have unit strength per unit area and to be isotropic.

The response of the detector to a disk source of radius a (see Fig. III-B-5) at a distance z from the source along the axis is

$$D_{P\ell}(z,a) = \int_{\rho=0}^{a} G(R)\, 2\pi\rho\, d\rho$$

or

$$D_{P\ell}(z,a) = 2\pi \int_{z}^{\sqrt{z^2+a^2}} G(R)\, R\, dR \tag{4}$$

For an infinite plane source this becomes

$$D_{P\ell}(z,\infty) = 2\pi \int_{z}^{\infty} G(R)\, R\, dR$$

$$= 2\pi \sum_{\nu=0}^{\infty} \int_{z^2+\nu a^2}^{\sqrt{z^2+(\nu+1)a^2}} G(R)\, R\, dR$$

$$= \sum_{\nu=0}^{\infty} D_{P\ell}(\sqrt{z^2 + \nu a^2},\ a) \tag{5}$$

Thus the response of the detector to an infinite plane source is just the sum of the responses to a disk source at distances $\sqrt{z^2 + \nu a^2}$, $\nu = 0,1,2,\ldots$

For $a >> \lambda$ (where λ is the relaxation length of the plane data), the series converges quickly. If the dose on the disk axis can be well represented in the region beyond some distance z by

$$D_{P\ell}(z,a) = D_{P\ell}(z_o,a)\, e^{-\frac{z-z_o}{\lambda}}$$

then the exact expression, Eq. (5), can be approximated for $z \gtrsim z_o$ by the inequality

$$1 + \alpha > \frac{D_{P\ell}(z,\infty)}{D_{P\ell}(z,a)} \gtrsim \frac{1}{2} + \alpha$$

where

$$\alpha = \frac{2\lambda^2}{a^2}\,(1 + z/\lambda).$$

To see this, consider

$$\frac{D_{P\ell}(t,\infty)}{D_{P\ell}(z,a)} = \frac{\sum_{\nu=0}^{\infty} D_{P\ell}(\sqrt{z^2+\nu a^2},\, a)}{D_{P\ell}(z,a)} = \frac{\sum_{\nu=0}^{\infty} D_{P\ell}(z,a)\, e^{-(\sqrt{z^2+\nu a^2}\,-z)/\lambda}}{D_{P\ell}(z,a)}$$

$$= e^{z/\lambda} \sum_{\nu=0}^{\infty} e^{-\sqrt{z^2+\nu a^2}\,/\lambda}$$

Since the exponential in the above expression is a monotonic decreasing function of ν, a lower bound L can be found for the summation, as follows:

$$e^{z/\lambda} \sum_{\nu=0}^{\infty} e^{-\sqrt{z^2+\nu a^2}\,/\lambda} > e^{z/\lambda} \sum_{\nu=0}^{\infty} \int_{\eta=\nu}^{\nu+1} e^{-\sqrt{z^2+\eta a^2}\,/\lambda}\, d\eta$$

$$= e^{z/\lambda} \int_{\eta=0}^{\infty} e^{-\sqrt{z^2+\eta a^2}\,/\lambda}\, d\eta = L$$

Carrying out the integration, one has

$$L = \frac{2\lambda^2}{a^2}\left[1 + \frac{z}{\lambda}\right]$$

An upper bound U can be obtained as follows:

$$U = 1 + e^{z/\lambda}\sum_{\nu=1}^{\infty}\int_{\eta=\nu}^{\nu+1} e^{-\sqrt{z^2+(\eta-1)a^2}}\,d\eta = 1 + e^{z/\lambda}\int_{\eta=1}^{\infty} e^{-\sqrt{z^2+(\eta-1)a^2}}\,d\eta$$

Geometrically, this is equivalent to shifting the approximating lower curve one unit to the right, integrating under it, and adding the area of the unit rectangle with base x = 0 to x = 1.

Letting $w = \eta - 1$ in the above integral, one obtains

$$U = 1 + e^{z/\lambda}\int_{w=0}^{\infty} e^{-\sqrt{z^2+wa^2}}\,dw = 1 + L$$

Hence

$$\alpha < \frac{D_{P\ell}(z,\infty)}{D_{P\ell}(z,a)} < 1 + \alpha$$

where

$$\alpha = \frac{2\lambda^2}{a^2}\left[1 + \frac{z}{\lambda}\right].$$

Under the assumptions used, the average of the upper and lower bounds provides a good estimate of the value of summation, and, since the bounding functions possess positive second derivatives, this average can be shown to be a lower bound itself; i.e.,

$$\frac{D_{P\ell}(z,\infty)}{D_{P\ell}(z,a)} \geq \frac{1}{2} + \alpha$$

In actual practice, however, there often occurs a radiation "hardening effect" (i.e., an observable increase in the effective relaxation length) with increasing z. In this case the expansion of the $D_{P\ell}(z,\infty)$ in an exponential,

$D_{P\ell}(z_o,\infty)\, e^{-(z-z_o)/\lambda}$, is not adequate. Thus $D_{P\ell}(z,\infty)/D_{P\ell}(z,a)$ will frequently be larger than the value predicted by the above expression and may, in fact, exceed the estimated upper bound, $1 + \alpha$.

Disk Source to Point Transformation

One can differentiate Eq. (5) to get

$$D'_{P\ell}(z,\infty) = \sum_{\nu=0}^{\infty} \frac{z}{\sqrt{z^2 + \nu a^2}}\, D'_{P\ell}\left(\sqrt{z^2 + \nu a^2},\, a\right)$$

where the prime indicates differentiation with respect to the first argument.

Defining $B(z) = -\dfrac{D'_{P\ell}(z,a)}{2\pi z}$ and using Eq. (3), one obtains the relation

$$G(z) = \sum_{\nu=0}^{\infty} B\left(\sqrt{z^2 + \nu a^2}\right) \tag{6}$$

This last equation defines a method of determining the kernel from the data using straightforward operations. It is only applicable where a is large compared to the attenuation length of the radiation, but for those cases in which this condition is not met the disk will be a good approximation to a point source and the data will indicate G(R) directly.

Plane to Sphere Transformation

It is often of interest to calculate the intensity to be expected from a source spread uniformly over the surface of a sphere. The usual isotropic medium is assumed, and this must extend inside as well as outside the sphere. The geometry is shown in Fig. III-B-6. For this case

$$D_S(r_o,r) = 2\pi r^2 \int_{\theta=0}^{\pi} G(R) \sin\theta \, d\theta$$

where

$$R^2 = r^2 + r_o^2 - 2rr_o \cos\theta,$$

$$2R \, dR = 2rr_o \sin\theta \, d\theta.$$

Thus

$$D_S(r_o,r) = 2\pi \frac{r}{r_o} \int_{r_o-r}^{r_o+r} G(R) \, R \, dR$$

$$= \frac{r}{r_o}\left[2\pi \int_{r_o-r}^{\infty} G(r) \, R \, dR - 2\pi \int_{r_o+r}^{\infty} G(R) \, R \, dR \right]$$

$$= \frac{r}{r_o}\left[D_{P\ell}(r_o - r,\infty) - D_{P\ell}(r_o + r,\infty) \right] \tag{7}$$

If $2r >> \lambda$, the relaxation length, then the second term in the bracket will be negligible compared to the first, and the following approximate expression becomes useful:

$$D_S(r_o,r) \cong \frac{r}{r_o} \, D_{P\ell}(r_o - r,\infty) \tag{8}$$

Plane to Cylinder Transformation

There is no simple general transformation for this case, but it can be shown for most specific attenuation kernels that the relation between cylindrical and plane geometry for large attenuations (thick shields) should be approximately

$$D_C(r_o,r) \cong \sqrt{\frac{r}{r_o}} \; D_{P\ell}(r_o - r,\infty) \tag{9}$$

where

$D_C(r_o,r)$ = dose to be expected from an infinitely long cylindrical source of unit surface strength imbedded in shielding material,

r_o = distance from the axis of the cylinder to the measuring point,

r = cylinder radius,

$D_{P\ell}(r_o - r,\infty)$ = dose to be expected at a distance $r_o - r$ from an infinite plane source of unit surface strength imbedded in the same shielding material.

This relation (8) is not unreasonable, in that the cylinder is intermediate between plane and sphere, and the factor of proportionality, $\sqrt{r/r_o}$, is intermediate between unity and that for plane to sphere, Eq. (7).

Although it is possible to extend the treatment of transformations somewhat further without specifying the form of the attenuation kernel, it is usually much easier to choose some simple form which will fit at least over a limited range and to use this in the transformations. The next section demonstrates this method.

Geometry for Partially Specified Attenuation Functions

In this section advantage will be taken of the fact that the attenuation in shields is large, so that contributions from the nearest sources are dominant and crude approximations are adequate to indicate the additional contributions of more distant sources. This process is commonly used in shielding with considerable success.

Consider an isotropic source spread uniformly over a curving surface so that the strength of the source on an element of area dS is just dS. Let the nearest source point be located at the origin, the surface being tangent to the xy plane at the origin and then curving away so that the distance between the surface and the xy plane is given approximately by

$$z_1 = \frac{1}{2}\left(\frac{x^2}{a} + \frac{y^2}{b}\right) \tag{10}$$

Thus a and b are the normal curvatures of the surface, and use of Eq. (9) is a direct consequence of the assumption regarding distant sources, since it surely will not fit well except in the region near the origin.

The detector is at z, and the distance from this to the element of surface dS is R (see Fig. III-B-7). The reading on an isotropic detector is then

$$D(z) = \int_{\text{Surface}} G(R)\, dS \tag{11}$$

$$dS = dx_1\, dy_1 \sqrt{1 + \left(\frac{\partial z_1}{\partial x}\right)^2 + \left(\frac{\partial z_1}{\partial y}\right)^2}$$

$$\cong dx_1\, dy_1 \left(1 + \frac{x_1^{\,2}}{2a^2} + \frac{y_1^{\,2}}{2b^2}\right) \tag{12}$$

G(R) is now approximated by an unspecified (and therefore presumably exact) function for the kernel for the distance z, times an exponential for the extra distance (R - z).

$$G(R) \cong G(z)\, e^{-(R-z)/\lambda} \tag{13}$$

UNCLASSIFIED
DWG. 15441A

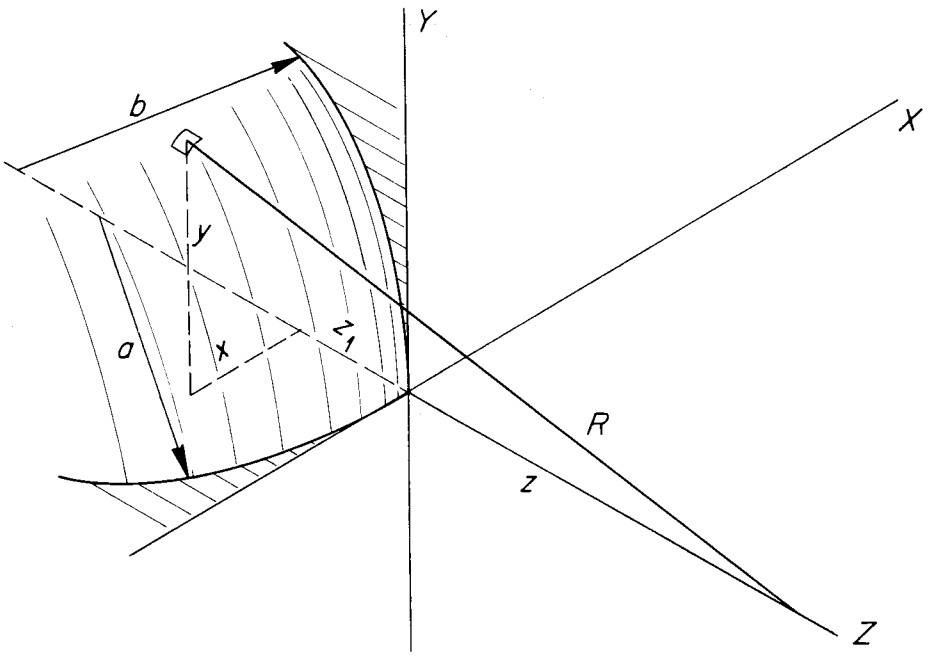

Fig. III-B-7. Quadric-Surface Source Geometry.

UNCLASSIFIED
ORNL-LR-DWG 314

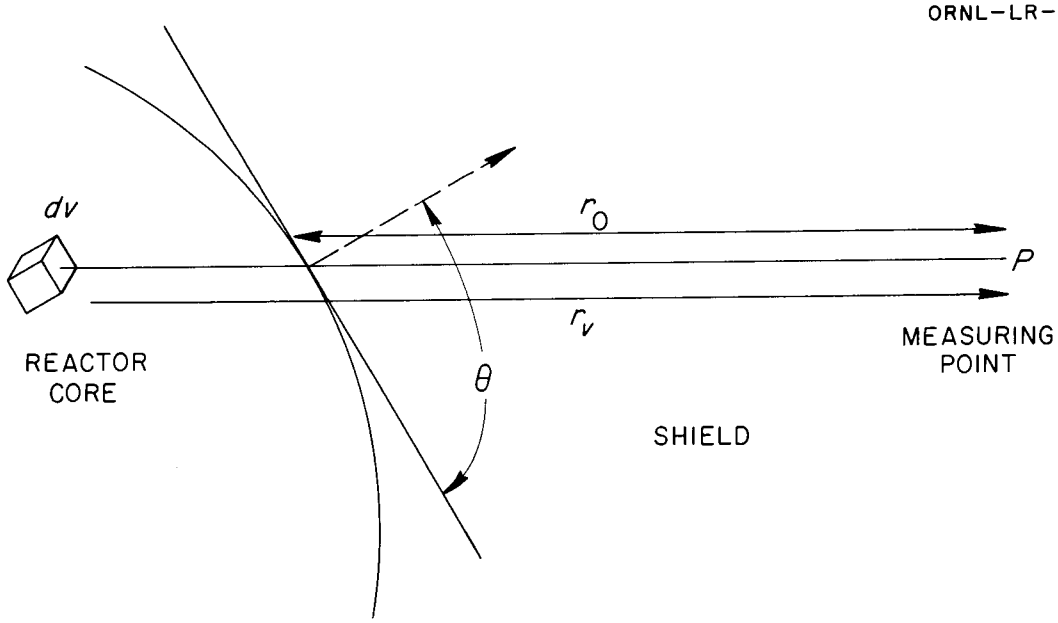

Fig. III-B-8. Volume-Source Geometry.

λ is a relaxation length, presumably one which makes Eq. (13) correct. Actually, since λ will be slowly varying, it can be taken from almost any convenient data for the proper material and source with attenuation over a distance of about z. For example, λ could be taken directly from Lid Tank data.

Up to now G(R) has always been an arbitrary displacement kernel. Equation (13) is a statement about the shape of G(R) in the neighborhood of R = z. G remains a displacement kernel.

An approximate form is now required for R in order to make Eq. (11) integrable:

$$R = \sqrt{(z_1 + z)^2 + x_1^2 + y_1^2} \tag{14}$$

On expanding and ignoring terms of the order of z_1^2, in comparison with x_1^2 and y_1^2, it is found that

$$R - z = \frac{x_1^2}{2z} + \frac{y_1^2}{2z} + \frac{x_1^2}{2a} + \frac{y_1^2}{2b} \tag{15}$$

If Eq. (15) is accepted as adequate,

$$D(z) = G(z) \int_{-\infty}^{\infty} dy_1 \int_{-\infty}^{\infty} dx_1 \, e^{-\frac{x_1^2+y_1^2}{2\lambda z} - \frac{x_1^2}{2\lambda a} - \frac{y_1^2}{2\lambda b}} \left[1 + \frac{x_1^2}{2a^2} + \frac{y_1^2}{2b^2}\right] \tag{16}$$

A cumbersome but not difficult integration yields

$$D(z) = 2\pi\, G(z) \left[\frac{1}{\left(\frac{1}{\lambda z} + \frac{1}{\lambda a}\right)^{1/2} \left(\frac{1}{\lambda z} + \frac{1}{\lambda b}\right)^{1/2}} + \frac{1}{2a^2 \left(\frac{1}{\lambda z} + \frac{1}{\lambda a}\right)^{3/2} \left(\frac{1}{\lambda z} + \frac{1}{\lambda b}\right)^{1/2}} + \frac{1}{2b^2 \left(\frac{1}{\lambda z} + \frac{1}{\lambda a}\right)^{1/2} \left(\frac{1}{\lambda z} + \frac{1}{\lambda b}\right)^{3/2}} \right] \tag{17}$$

The last two quantities in the brackets are in general much smaller than the first for a and b large compared to λ:

$$D(z) \approx 2\pi\, G(z) \left[\frac{1}{\left(\frac{1}{\lambda z} + \frac{1}{\lambda a}\right)^{1/2} \left(\frac{1}{\lambda z} + \frac{1}{\lambda b}\right)^{1/2}} \right] \tag{18}$$

for a, b $\gg \lambda$.

For a sphere a = b = r,

$$z = r_o - r$$

and

$$D_S(r_o, r) = 2\pi\, G(z)\, \lambda z\, \frac{r}{r_o} \tag{19}$$

If at this point it is recognized that

$$\frac{d}{dz} D_{P\ell}(z,\infty) = -\frac{D_{P\ell}(z,\infty)}{\lambda} \tag{20}$$

it is possible at once to confirm that Eqs. (19) and (3) agree.

For a cylinder, a $=\infty$, b = r, and z = r_o - r. By similar manipulation it is seen that Eq. (18) then confirms Eq. (9).

Comparison of Source Strengths

In order to apply the above formulas to shielding problems of interest, one must somehow replace actual volume sources by isotropic surface sources. There are a number of different possible approaches to the problem. In one approach the source is described by the radiation escaping through the surface of the reactor core. In general, this is done by determining the angular and energy distribution at every point of the surface. It will be done somewhat differently here.

It must now be assumed that the medium is sufficiently absorptive so that most of the contribution to the detector response comes from the region of the surface nearest to the detector, with regions farther away contributing

significnatly less. Further, the flux through this part of the surface is preferentially in the forward direction, i.e., toward the detector. Since the radiation in this direction is the most important, one replaces the actual angular distribution with an isotropic one whose magnitude is the same as that of the actual distribution in the forward direction. The actual distribution at more distant regions of the surface is replaced by an isotropic distribution of the same magnitude. (All this should tend to overestimate the effective source strength somewhat.) With this uniform isotropic source, the geometry transformations discussed above can be used.

In summary then, it can be said that the source density is taken to be constant and isotropic with a value equal to that at the nearest point on the surface to the detector in the direction of the detector (i.e., along the normal). This source strength is just the radiation leaking per unit area in the direction of the normal at the point and is given by

$$A \int_0^\infty e^{-x/\lambda} P(x)\, dx$$

where x is the distance in from the point along the normal, P(x) is the power density at x, A is a conversion factor from power density to radiation source density, and λ is the relaxation length in the core for radiation of the given type. The upper limit on the integral is taken to be infinite since the core will be assumed to be opaque.

This argument can be illustrated quantitatively for the geometry of Fig. III-B-8. The dose at the measuring point P is

$$D(P) = \int_{core} G(r_v)\, AP(r_v)\, dv$$

Exponential attenuation in the core will be assumed so that

$$4\pi r_v^2\, G(r_v) = e^{-r_v - r_o/\lambda}\, 4\pi r_o^2\, G(r_o)$$

From Fig. III-B-8 it is seen that the volume element is

$$dv = \frac{ds_c \cos\theta}{r_o^2}\, r_v^2\, dr_v$$

where θ is the angle of r_o with the normal to the surface and ds_c is the element of core surface. Then

$$D = \int G(r_o)\, ds_c \quad \cos\theta \int_o^\infty e^{-r_v - r_o/\lambda} \quad AP(r_v)\, dr_v$$

In the region of the surface nearest the detector, $\cos\theta \sim 1$ and the remaining factor in the expression for the effective source strength is just the leakage integral mentioned above. It is taken as constant at its maximum value. For a uniform power density it is actually constant.

From a more mathematical point of view, one might look at this type of procedure in the following way:(8) Let the angular distribution of the sources on the surface be given by $S(r)\, f(r,\theta)$ where r represents a point on the surface and θ is the angle with the local normal at r. It is assumed that the dose at a point P is

$$D(P) = \int S(r)\, f(r,\theta)\, G(R)\, dS$$

where

dS = element of surface area,

(8) After H. Goldstein, "Notes on the Transformation from Sphere to Plane Isotropic Source," NDA Memo 12-5 (Sept. 23, 1953).

R = distance from r to P,

θ = angle made by R with the normal.

The discussion above is equivalent to the statement that if G falls off sufficiently rapidly,

$$D(P) \cong S(r_o)\, f(r_o, \theta = 0) \int G(R)\, dS$$

where r_o is the surface point for which $\theta = 0$.

Just what is involved in the source approximation can be perhaps more clearly seen from an example. Suppose one wishes to compute the dose at a large distance r_o from a spherical shell of radius r, the source being constant but with an angular distribution $f(\theta)$. The total dose at P is

$$D(P) = \int G(R)\, f(\theta)\, dS$$

where now θ varies with R and is always the angle between R and the normal (see Fig. III-B-9). Then

$$D(P) = \int_0^{\pi} G(R)\, f(\theta)\, 2\pi r^2 \sin\phi\, d\phi$$

Since

$$R^2 = r^2 + r_o^2 - 2rr_o \cos\phi,$$

$$2R\, dR = 2rr_o \sin\phi\, d\phi,$$

$$D(P) = 2\pi \frac{r}{r_o} \int_{r_o - r}^{r_o + r} G(R)\, Rf(\theta)\, dR$$

UNCLASSIFIED
ORNL-LR-DWG 315

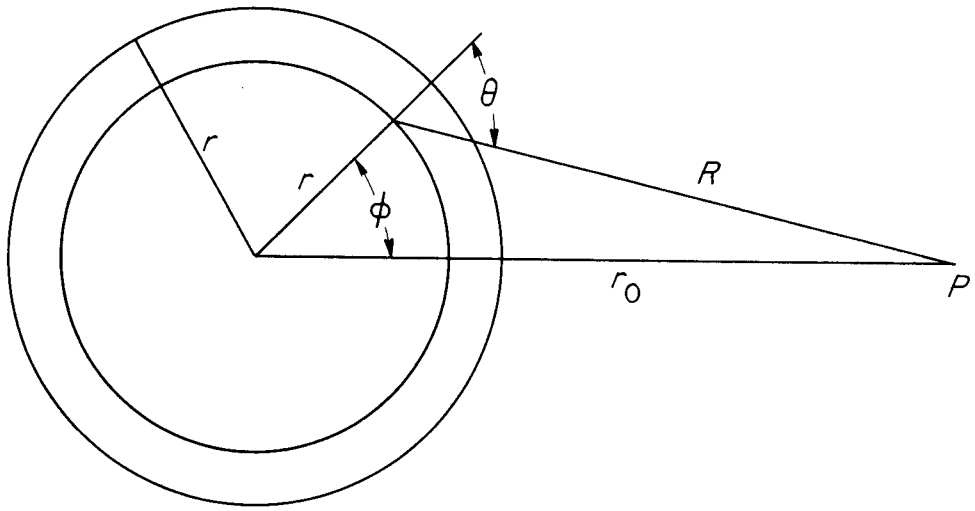

Fig. III-B-9. Geometry for Spherical Source Calculations.

UNCLASSIFIED
ORNL-LR-DWG 316

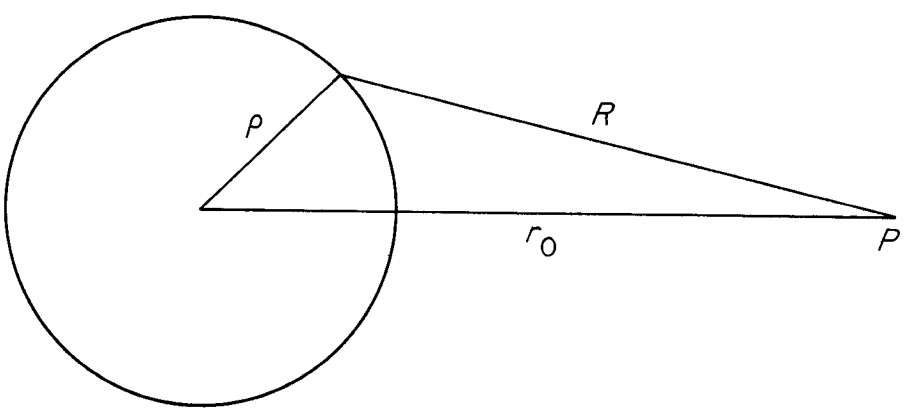

Fig. III-B-10. Geometry for Volume Source Calculations.

Now if G(R) falls off sufficiently rapidly or if $f(\theta)$ does not vary too fast near the normal direction, or both, then a good approximation to this is

$$D(P) \cong 2\pi \frac{r}{r_o} f(0) \int_{r_o - r}^{\infty} G(R)\, R\, dR$$

The dose at P from an infinite plane of source strength unity per unit area at a distance $(r_o - r)$ is

$$D_{P\ell}(P) = 2\pi \int_{r_o - r}^{\infty} G(R)\, R\, dR$$

so that

$$D(P) = \frac{r}{r_o} f(0)\, D_{P\ell}(P)$$

As a concrete example of how good this type of approximation might be in a typical case, one can compute the next approximation. Suppose that $f(\theta) = \cos\theta$. If the observation point P is far away, i.e., if $r_o >> r$, $\theta = \phi$ and

$$\cos\theta = 1 - \frac{R - (r_o - r)}{r} = 1 - \frac{z}{r}$$

where $z = R - (r_o - r)$.

It will also be assumed that

$$4\pi R^2\, G(R) = 4\pi (r_o - r)^2\, G(r_o - r)\, e^{-z/\lambda}$$

Then

$$D(P) = 2\pi \frac{r}{r_o} \int_0^{2r} \frac{(r_o - r)^2\, G(r_o - r)}{r_o - r + z}\, e^{-z/\lambda} \left(1 - \frac{z}{r}\right) dz$$

Since $z << r_o - r$,

$$D(P) \cong 2\pi \frac{r}{r_o} (r_o - R)\, G(r_o - r) \int_0^{2r} e^{-z/\lambda}(1 - \frac{z}{r})\, dz$$

In terms of the displacement kernel G, the dose is

$$D(P) \cong 2\pi \frac{r}{r_o} \lambda(r_o - r)\, G(r_o - r) \left[1 + e^{-2r/\lambda} - \frac{1 - e^{-2r/\lambda}}{r/\lambda}\right]$$

The second and third terms in the brackets are corrections for the anisotropy of the source. For $r/\lambda >> 1$, they become small. The dose from an infinite plane source is

$$D_{P\ell}(z) = 2\pi \int_z^\infty G(R)\, R\, dR = 2\pi z^2\, G(z) \int_z^\infty e^{-(R-z)/\lambda} \frac{dR}{R}$$

$$= 2\pi z^2\, G(z) \int_0^\infty e^{-x/\lambda} \frac{dx}{z + x}$$

Expanding in powers of x/z and keeping the first two terms should give a fair asymptotic series. One gets

$$D_{P\ell}(z) = 2\pi z\, G(z) \int_0^\infty e^{-x/\lambda} (1 - \frac{x}{z})\, dx = 2\pi\lambda z\, G(z)\, (1 - \frac{\lambda}{z})$$

Then to first order in r/r_o,

$$D_{sphere}(P) = \frac{r - \lambda}{r_o} D_{P\ell}(r - r_o)$$

and for $r >> \lambda$, this becomes

$$D_{sphere}(P) = \frac{r}{r_o} D_{P\ell}(r - r_o)$$

There is an alternative way of looking at the source in the case of a spherical geometry.(9) This is to consider the volume source as made up of elementary uniform isotropic surface sources and to sum over the surfaces (see Fig. III-B-10). Here

$$D(P) = 2\pi \int_0^r d\rho \, \frac{\rho}{r_o} \int_{r_o-\rho}^{r_o+\rho} G(R)\, R\, dR$$

Integrating by parts, one finds that

$$D_{SV}(P) = \frac{\pi r^2}{r_o} \int_{r_o-r}^{r_o+r} G(R)\, R\, dR - \pi \int_{r_o-r}^{r_o+r} \frac{(R - r_o)^2}{r_o} G(R)\, R\, dR$$

or

$$D_{SV}(P) = \pi \int_{r_o-r}^{r_o+r} \frac{r^2 - (R - r_o)^2}{r_o} G(R)\, R\, dR$$

Let $R = r_o - r + x$. Then

$$R\, G(R) = \frac{1}{R}(r_o - r)^2\, G(r_o - r)\, e^{-x/\lambda}$$

and

$$D_{SV}(P) = \pi \int_0^{2r} \frac{x(2r - x)}{r_o} (r_o - r)^2\, G(r_o - r) \frac{e^{-x/\lambda}}{r_o - r + x}\, dx$$

$r,\ x << r_o$, and so to first order in r/r_o,

$$D(P) = \frac{2\pi r}{r_o} (r_o - r)\, G(r_o - r) \int_0^{2r} \left(x - \frac{x^2}{2r}\right) e^{-x/\lambda}\, dx$$

$$= \frac{2\pi r}{r_o} \lambda^2 (r_o - r)\, G(r_o - r) \left[1 - \frac{\lambda}{r} + \left(1 + \frac{\lambda}{r}\right) e^{-2r/\lambda}\right]$$

(9) See E. P. Blizard, "Reactor Leakage for Shielding Calculations," CF-53-7-170 (Nov. 27, 1953).

The source with which this is to be compared is now not a plane source, but a semi-infinite volume source of unit source density. The dose at a distance z from the boundary plane is

$$D_{PV}(z) = 2\pi \int_z^\infty dx \int_0^\infty G(R)\, y\, dy = 2\pi \int_z^\infty dx \int_x^\infty G(R)\, R\, dR$$

$$D_{PV}(z) = 2\pi \int_z^\infty G(R)\, R\, dR \int_z^R dx = 2\pi \int_z^\infty G(R)\, R\, (R - z)\, dR$$

Since $R^2 G(R) \cong z^2 G(z)\, e^{-(r-z)/\lambda}$, then

$$D_{PV}(z) \cong 2\pi z^2\, G(z) \int_z^\infty e^{-(R-z)/\lambda}\, dR - 2\pi z^3\, G(z) \int_z^\infty e^{-(R-z)/\lambda}\, \frac{dR}{R}$$

$$= 2\pi\lambda z^2\, G(z) - 2\pi z^2\, G(z) \int_0^\infty e^{-x/\lambda}\, (1 - \frac{x}{z})\, dx = 2\pi\lambda^2 z\, G(z)$$

The dose from the sphere has the same form as before in terms of the dose from a (now solid) slab geometry:

$$D_{sphere}(P) = \frac{r - \lambda}{r_o}\, D_{PV}\, (r - r_o)$$

It is also true that in terms of an infinite plane source

$$D_{sphere}(P) = \lambda\, \frac{r - \lambda}{r_o}\, D_{P\ell}(r - r_o)$$

If λ is chosen to be characteristic of a plane rather than a point source, the result is valid to all orders in r/r_o and λ/r, as can be shown.[9] Differences in the definition of λ make no difference in the geometry factors to first order.

3. Assumptions Involved in the Comparison Methods

The two preceding sections (III-B-1 and 2) have described two differing comparison methods for designing shields. It must be emphasized that neither method is intended to provide an a priori procedure for designing shields without reference to bulk shielding experiments. Rather they are designed to provide a means for transferring measurements obtained with the LTSF or BSF to the particular reactor under design. Thus their principal purpose is to give an indication of how the dose outside a shield varies with changes in geometry of the core and shield. Neither technique is completely satisfactory as a result of various assumptions implicit in the methods, some of which have been mentioned briefly before. In this section these assumptions will be examined critically with a view to seeing when the two approaches are applicable, and when neither one can be used with confidence. Briefly, comparisons of neutron shields can be made without too great an assault on realistic conditions. One still does not know, however, how to compare gamma shields in some arrangements of highly dissimilar media.

Homogeneous Shield Method

The assumptions inherent in the general method for homogeneous shields are the following:

(1) Reactor and shield form an infinite homogeneous medium.

(2) Attenuation over a small distance is nearly exponential.

(3) Effective surface sources are isotropic. (This assumption is not always required; see below.)

The major assumption in the displacement kernel method is that the reactor core and shield form a homogeneous medium shielding-wise (assumption 1). This condition is met approximately for neutrons, since all neutron

shielding materials considered have roughly comparable attenuation lengths for fast neutrons. On the other hand, most shields are laminated, and the various layers can have very different gamma-ray attenuation properties.

The medium is seldom present on both sides of a plane source. This is not too serious, as it affects only the radiation scattered through large angles on the opposite side of the source from the detector and this is not expected to be very important.

In addition to the medium not being infinite, it usually cuts off just at the detector. Experimentally, though, the error introduced has been found to be small.

The attenuation over a small distance must be assumed to be exponential (assumption 2) in order to derive many of the results. This is embodied in the mathematical statement that

$$4\pi R^2\ G(R) \cong 4\pi z^2\ G(z)\ e^{-(R-z)/\lambda}$$

where R - z is not large compared to λ or z.* In general, such an expansion is reasonable for sufficiently large R and z, i.e., far from the source, as long as $(R - z)/z \ll 1$. Contributions from $R \gg z$, where the expansion may not hold, are unimportant. λ can be taken from any convenient attenuation experiments. If the expansion is valid, λ should be roughly the same for many source geometries at the same distance, even though it is defined in terms of a point source.

It can be claimed that assumptions 1 and 2 are the only assumptions inherent in the homogeneous shield method. In fact, Blizard, working with only these two restrictions, has derived expressions for comparison of the dose from a uniform spherical volume distribution and an infinite plane

* See p. 84 ff. for definitions of terms.

source.[9] Historically, however, the homogeneous method has also been taken to include the further step of replacing the core by an isotropic surface distribution. Certainly, the most widely known formulae come from this "subspecies" of the homogeneous shield technique, in which the transformations are used to derive equivalent surface sources. If this convenience is taken advantage of assumption 3 must be added.

Assumption 3 states that the effective surface sources are isotropic. As shown above, they really are not isotropic, and errors are introduced in treating them as such. In general, these errors will not be small unless

(a) The detector is far from the core, i.e., $r/r_o << 1$, where r_o is the distance of the detector from the core and r is a measure of the core radius.

(b) The core is nearly opaque to the radiation, i.e., $\lambda/r << 1$.

If these two conditions are satisfied, the necessary transformations can be derived to first order in r/r_o and λ/r. The assumption that the detector is far from the core is a useful one for primary radiation, although it is less useful for calculations of secondary radiation and heating. Most cores considered are reasonably opaque to neutrons; this assumption is less well satisfied for gammas.

The condition $\lambda/r << 1$ is a condition on the size of the core. In addition it is to be taken as a condition on the local curvature of the part of the surface nearest the detector. One must also demand that the radius of curvature in this region be large compared to λ.[10]

(10) Some of the consequences of anisotropy in the effective surface sources are described by H. Goldstein (see ref. 8).

Semianalytical Shield Method

The analytic approach described in section III-B-1 attempts to remove the restriction of a homogeneous shield. It does so, however, only by giving up the generality of the displacement kernel. To obtain usable results it is necessary to assume not only that the dose at a point due to a source at another point is a function of the straight line path between the two points, but that the dose may be described by a first-flight exponential kernel. The simplification of an exponential kernel allows an analytic attack on many problems not previously accessible. Thus it is no longer necessary to assume the detector is far from the source; reasonably accurate values can be obtained right against the core. A much wider variety of situations can thus be described than by the homogeneous method. The formulas derived in section III-B-1 also in principle assume only a monoenergetic source.

The assumptions involved in the semianalytic approach may thus be listed as follows:

(1) The dose is a function only of the straight line path between source and detector points.

(2) The dose is given by an exponential kernel.

(3) The sources are monoenergetic.

(4) Certain geometrical assumptions are made.

The last three assumptions are of much less consequence than the first. To take them in reverse order, the geometrical restrictions are for the most part trivial. Only in the case of the dose along a line perpendicular to a cylindrical core axis are they any limitation. Otherwise the approximate formulas, for all practical purposes hold, right up to the core surface.

The monoenergetic assumption really comes in implicitly when we write a σ_0 or σ as the same for all neutrons or photons no matter what their energy. In principle one could rectify the situation by replacing n_0 by a source energy distribution $n_0(E)\,dE$, with σ likewise a function of E. The dose due to source particles of energy E would be a function of E through n_0 and σ; the total dose would be found by integrating over E. Practically, such a procedure is neither feasible nor warranted by our knowledge (or lack thereof) of the source spectra. In particular, the exponential kernel for neutron penetration is justified only when it is feasible to use the removal cross section for σ. This concept implies one value to be used for all energies. Moreover, in both neutron and gamma-ray penetration it often occurs that a narrow energy band is dominant in determining the relaxation length of the entire dose.

The assumption of an exponential kernel is a more difficult one to swallow. It has already been pointed out that it may be used for neutrons only within the framework of the removal cross section concept. One may similarly try to define effective removal absorption coefficients for gamma rays by taking for σ the average slope of the total dose curve, either from experiment or from the theory of photon penetration. Nevertheless, numerous cases must arise in which one cannot be certain at what point on the curve the slope should be taken or what buildup factors are applicable, If for no other reason this assumption would seem to preclude the use of the method for a straightforward a priori analytic design of the shield.

Overshadowing these restrictions is the first assumption, implying that scattering within the shield media never causes the particle to deviate greatly from the straight line path. When the shield is homogeneous or

nearly so, the assumption is probably correct so long as the shield is reasonably thick. But when the shield layers are greatly dissimilar, it is possible that paths other than the direct line may predominate; the analytic theory then becomes suspect. And it is in just these situations that we have the greatest need for guidance on the geometrical transformations.

To try to clarify these points let us make a slightly over-simplified picture of the physical origins of the geometrical corrections. Consider first a homogeneous shield with an isotropic spherical surface source (Fig. III-B-11a). The essential difference between the dose from the sphere AB and that from the equal plane source AC is the additional distance BC that a particle must travel to reach D. In the analytic method it is again the path difference which gives rise to the geometrical correction. With a non-homogeneous shield the diagrams must be drawn differently, but the principle remains the same. For the spherical source and a two-medium shield we have Fig. III-B-11b, with Fig. III-B-11c giving a similar picture for the plane source.

Now suppose medium I is highly absorbing (e.g., lead) and medium II has a very long relaxation length in comparison (e.g., water). Only the path length through lead will then be important. The analytic method calculates the dose in each case, assuming the particle goes from B to D or C to D in a straight line. In essence the difference in dose from the two sources will be determined by the difference between BE and CF. Actually, however, the media are scattering. It is conceivable that the "shortest" actual path to reach D in the spherical case is for a photon to go radially through the lead to point E' and then be scattered so as to reach D. The radial path may be shorter than the direct ray by many mean free path lengths. Similarly

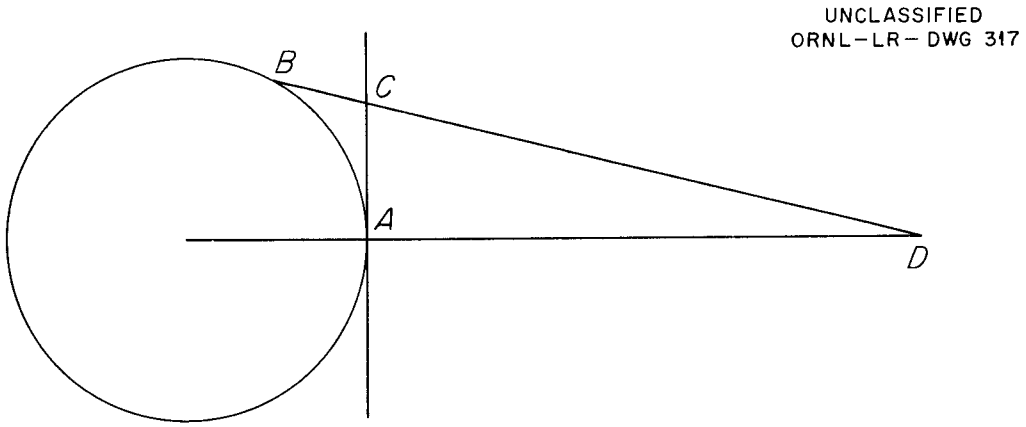

Fig. III-B-11a. Geometry for Comparison of Spherical and Plane Surface Sources.

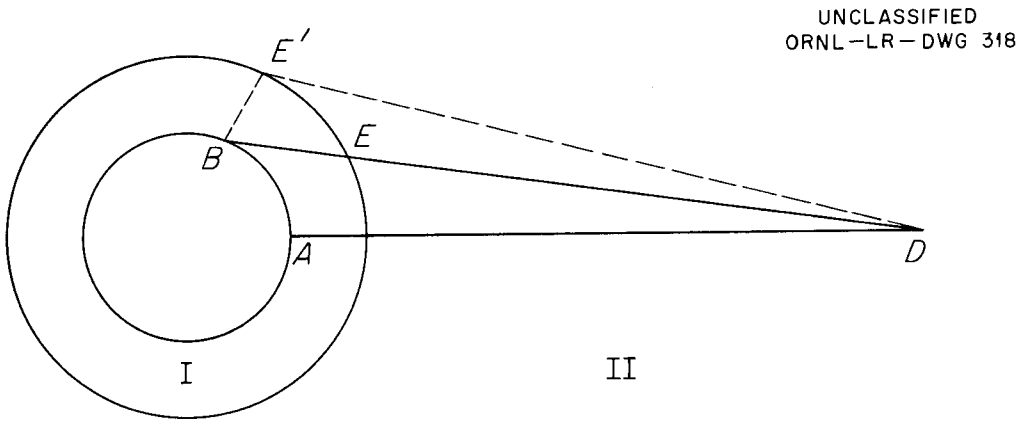

Fig. III-B-11b. Geometry for Spherical Source in Two-Medium Shield.

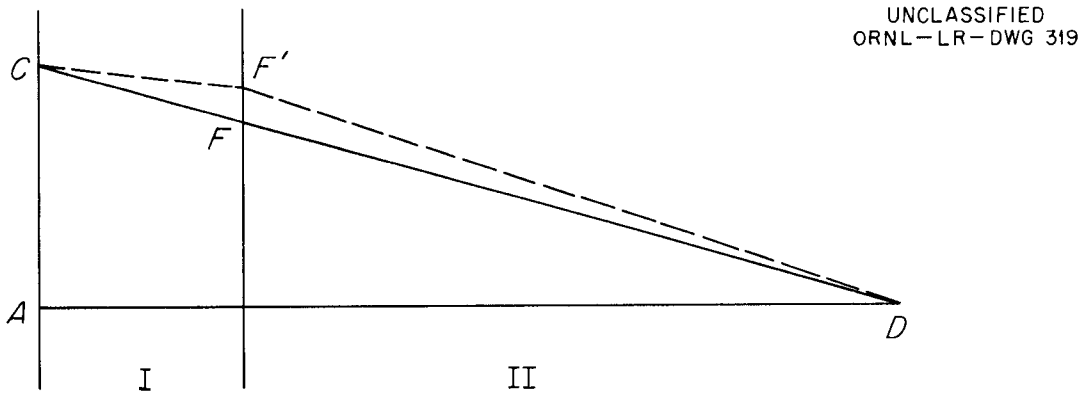

Fig. III-B-11c. Geometry for Plane Source in Two-Medium Shield.

in the plane case, CF'D may be a better approximation to the path of a penetrating particle. Where there is a possibility of substantially "short circuiting" the direct line path through scattering, the results of either method must be considered suspect.

Summary

In summary, when the shield is homogeneous, either method is valid for comparison purposes. This can be seen from the equations in section III-B-2 for the comparison between plane and spherical sources. The displacement kernel G(R) no longer appears, and the same result must therefore be obtained if G(R) is specialized to an exponential. If the shield is not homogeneous, but propagation is still essentially straight line, then the analytic method is preferable. It is also the choice, even with homogeneous media, in many geometries not easily amenable with the general displacement kernel assumption. When we deal with a badly heterogeneous shield in which scattering is important, neither approach seems valid.

No consistent scheme has been worked out to handle these refractory problems. Some day, perhaps not too far away, we shall be able to do them as rigorously as the infinite medium problem can be done. Meanwhile the best approach seems to be to consider separately the propagation from one interface to the next; the flux at each interface serves as the source for penetration through the next medium. The technique has already been applied to find the leakage from cores. In the situation illustrated in Fig. III-B-11c the procedure would be to calculate the angular distribution of the photons emerging at the boundary between mediums I and II. If medium I is thick and highly absorbing, it will be nearly radial. This new source should

then be allowed to propagate to D by, say, first single scattering in medium II and then first-flight to D. Such a calculation has not yet been carried out.

4. Recipes for the Application of the Comparison Methods

For obtaining information from the bulk shielding experiments it is useful to have concise expressions which can be used to predict shield behavior from the experimental measurements. The methods that have been developed in sections III-B-1 and 2 are useful for the purpose.

The appropriate approach to use depends on the extent to which (1) inhomogeneity of shielding properties or (2) buildup of scattered particles is unimportant. Insofar as one or the other can be neglected, the method for homogeneous shields or the semiasymptotic methods can be applied. It will be useful to subdivide the discussion according to the type of radiation under consideration. All lengths discussed in this section are in centimeters.

Fast Neutrons

In this case the method for homogeneous shields is applicable. The equivalent surface source strength of the reactor in question is taken to be

$$\sigma = \int_0^\infty P(x)\, e^{-x/\lambda}\, dx$$

where x is measured inward from the surface of the core along the normal through the point of detection and λ is the attenuation length in the core. λ is found by measuring the removal cross section $1/\lambda_i$ of each component of the core and then finding an average λ for the core by the formula

$$\lambda = \frac{\sum_i V_i}{\sum_i \frac{V_i}{\lambda_i}}$$

where the V_i's are the volume fractions of the various components. This procedure is valid if variations in the λ_i occur over distances small compared to λ.

If more than one of the components is present in a thickness greater than an attenuation length, the attenuation factor $e^{-x/\lambda}$ should be replaced by an exponential factor $e^{-\sum x_i/\lambda_i}$, where x_i is the distance the ray must travel through the ith component.

If the power density varies linearly over the first relaxation length or so in the core as

$$P(x) = A + Bx$$

then

$$\sigma = A\lambda + B\lambda^2$$

For comparison with Lid Tank data, one also needs the Hurwitz correction to the Lid Tank source. If $D_{LT}(z)$ is the reading at z cm from the source plate with a mockup in place, one needs the value of

$$D(z,\infty) \equiv \sum_{n=0}^{\infty} D_{LT}\left(\sqrt{z^2 + 1260n}\right)$$

A good approximation to this is

$$D(z,\infty) = \frac{D_{LT}(z)}{1 - e^{-630/\lambda z}}$$

where λ is the average attenuation length over the 30-cm region of the Lid Tank curve between z and z + 30 cm.

The following formulas can be used to get the dose from a reactor of a given shape at the edge or in the interior of the shield (as long as r_o or $z \gtrsim 100$ cm):

Sphere:

$$D_{SPH}(r_o) = 10^3\sigma\frac{a - \lambda}{r_o} \qquad \frac{D_{LT}(r_o - a)}{1 - e^{-630/[\lambda(r_o-a)]}}$$

Curved side of long circular cyclinder:

$$D_{CYL}(r_o) = 10^3\sigma\sqrt{\frac{a}{r_o}}\ \frac{D_{LT}(r_o - a)}{1 - e^{-630/[\lambda(r_o-a)]}}$$

for $\sqrt{(r_o - a)^2 + (h)^2} - r_o - a > \lambda$

End of cylinder:

$$D_{END}(z) = 10^3\sigma\,(1 - e^{-a^2/2\lambda z})\ \frac{D_{LT}(z)}{1 - e^{-630/\lambda z}}$$

Rectangular box:

$$D_{BOX}(z) = \frac{160\sigma A}{\lambda z}\ \frac{1}{\left(1 + \frac{b^2}{24\lambda z}\right)\left(1 + \frac{c^2}{24\lambda z}\right)}\ \frac{D_{LT}(z)}{1 - e^{-630/\lambda z}}$$

In these formulas

r_o = distance of detector from center of sphere or axis of cylinder,

a = radius of sphere or cylinder,

h = half-length of cylinder,

z = distance of detector from flat surface,

A = area of flat surface,

b,c = dimensions of face of box next to shield.

For comparison with BSF measurements, the following formulas are of use (the BSF data are assumed normalized to 1 watt):

$$D_{SPH}(r_o) = 45\sigma\lambda(a - \lambda)D_{BSF}(r_o - a)$$

$$D_{CYL}(r_o) = 45\sigma\lambda\sqrt{ar_o}\ D_{BSF}(r_o - a)$$

$$D_{END}(z) = 45\sigma\lambda z\ (1 - e^{-a^2/2\lambda z})\ D_{BSF}(z)$$

$$D_{BOX}(z) = 7.2\sigma A\ \frac{1}{\left(1 + \frac{b^2}{24\lambda z}\right)\left(1 + \frac{c^2}{24\lambda z}\right)}\ D_{BSF}(z)$$

Primary Gamma Rays

Dense High Z Material in Outside Layer. In this case the buildup is relatively small and an exponential attenuation factor will not give too great an error. The semianalytic method was used to derive the formulas in which

(1) λ is the relaxation length to be obtained from experiment or calculation[11] and is taken to be constant in each medium,

(2) λ_o is the relaxation length in the core and is derived* by dividing the measured attenuation length in water at a distance z from the core by the core density,

(3) Integrals appear in the form

$$\int_a^b dr/\lambda \text{ and } \int_a^b dr/\lambda r^2;$$

with the constant λ these integrals can be easily performed,

(4) Uniform volume production of gamma rays in the core is assumed,

(5) The shape referred to is the shape of the core; the shield is assumed to be right up against the core and to have the same shape (i.e., a slab shield against a flat end, a spherical shell around a sphere, and a hollow cylindrical shield about a cylindrical core),

(6) a is the outer radius of the core and the inner radius of the shield,

(11) See for instance H. Goldstein, J. E. Wilkins, Jr., and S. Preiser, "Interim Report on the NDA-NBS Calculations of Gamma Ray Penetration," NDA Memo 15C-20.

* This method for obtaining λ_o will be valid for all cores which contain only negligible amounts of elements of large atomic number, since iron, water, and all low Z materials can be considered to be essentially pure Compton scatterers. If heavy elements are present in appreciable amounts this approach is not adequate.

(7) b is the outer radius of the shield,

(8) r_o may be at any distance sufficiently far from the core,

(9) ℓ is the length of the reactor core,

(10) V is the volume of the reactor core.

The formulas then are:

$$D_{SPH}(r_o) = \frac{1.5\lambda_o P}{a^3} \frac{1 - e^{-(1/2)\int_a^b (a^2/\lambda r^2)dr}}{\int_a^b \frac{dr}{\lambda r^2}} D_{LT}(r_o - a)$$

$$D_{CYL}(r_o) = \frac{0.6\lambda_o P}{a} \frac{1}{1 + \frac{a^2}{6}\int_a^b \frac{dr}{\lambda r^2}} D_{LT}(r_o - a)$$

$$D_{END}(z) = \frac{2\lambda_o P z^2}{\ell a^2} \frac{1 - e^{-(1/2)(a^2/z^2)\int_a^b (dr/\lambda)}}{\int_a^b \frac{dr}{\lambda}} D_{LT}(z)$$

$$D_{BOX}(z) = \frac{\lambda_o P}{\ell} \frac{1}{\left(1 + \frac{b^2}{24z^2}\int_a^b \frac{dr}{\lambda}\right)\left(1 + \frac{c^2}{24z^2}\int_a^b \frac{dr}{\lambda}\right)} D_{LT}(z)$$

The Lid Tank dose $D_{LT}(z)$ is taken from the data normalized to 6 watts. Also,

$$D_{SPH}(r_o) = \frac{6\lambda_o P}{a^3} \frac{1 - e^{-(1/2)\int_a^b (a^2/\lambda r^2)dr}}{\int_a^b \frac{dr}{\lambda r^2}} D_{BSF}(r_o - a)$$

$$D_{CYL}(r_o) = \frac{2.5\lambda_o P}{a} \frac{1}{1 + \frac{a^2}{6}\int_a^b \frac{dr}{\lambda r^2}} D_{BSF}(r_o - a)$$

$$D_{END}(z) = 8\,\frac{\lambda_o P z_o^2}{\ell a^2}\,\frac{1 - e^{-(1/2)(a^2/z^2)\int_a^b (dr/\lambda)}}{\int_a^b \frac{dr}{\lambda}}\, D_{BSF}(z)$$

$$D_{BOX}(z) = 4\,\frac{\lambda_o P}{\ell}\,\frac{1}{\left(1 + \frac{b^2}{24z^2}\int_a^b \frac{dr}{\lambda}\right)\left(1 + \frac{c^2}{24z^2}\int_a^b \frac{dr}{\lambda}\right)}\, D_{BSF}(z)$$

In comparing these formulas with those involving D_{LT}, it should be noted that one would expect that

$$D_{LT}(z) = 4D_{BSF}(z)$$

where $D_{LT}(z)$ is normalized to 6 watts and $D_{BSF}(z)$ to 1 watt. For pure water, at least, a comparison of experimental data gives a rough confirmation of this.

<u>Low Z Material in Outside Layer</u>. In this case the buildup cannot be neglected, in general, and the shield may be far from homogeneous. The geometry corrections from plane to curved shield given by the semianalytic approach are an upper bound to the attenuation. A conservative estimate is to ignore geometry corrections altogether. The truth is somewhere in between, but where the semianalytical correction is large, one must estimate the correct answer by other means.

The geometry correction for secondary gamma rays can be found if the sources are known. In general, the correction is between that for the

primaries and unity. Each problem must be investigated separately, as no general formula is likely to be useful.

Dose away from the Reactor

The formulas in this section give the dose in the interior (for large z) or at the edge of the shield. By going back to the section on the semi-analytic method one can see for regular geometries how to find the dose at some distance outside of the shield. If the method for homogeneous shields is used it is adequate to make an inverse square correction to the dose at the edge of the shield. That is,

$$D(\rho) = \left(\frac{r_o}{\rho}\right)^2 D(r_o)$$

where $D(r_o)$ is the dose at the edge of the shield and $D(\rho)$ is the desired dose away from the shield. The distances r and ρ can be taken to be distances from the center of the core to a generally adequate degree of accuracy.

III-C. HEATING IN SHIELDS

Each time a photon or neutron makes a collision some energy is transferred to the medium and manifests itself in the resulting charged particles. Thus in elastic neutron collision the struck nucleus recoils and carries away a fraction of the energy. In gamma-ray compton scattering part of the energy is transferred to the recoil electron. Nuclear reactions resulting from the collision may also lead to energetic charged particles, e.g., fission fragments, of Li^7 and He^4 from the $B^{10}(n,\alpha)$ reaction. The range of all such charged particles in matter is almost always much less than that of the penetrating photon or neutron. Hence the charged particle loses almost all of its energy in the immediate vicinity of the collision, the energy being rapidly transformed into thermal excitation of the medium. The rate of heat production in a shield material is therefore given essentially by the volume collision density times the energy acquired per collision by charged particles. Some energy may be carried away from the collision by penetrating particles other than the incident, e.g., gamma rays from neutron capture or inelastic scattering. This energy should be considered as a new source, contributing to the heating elsewhere, not at the original collision site.

It is convenient to distinguish collisions in which the energy lost is some fraction of the incident energy from those leading to exoergic reactions where the energy released bears little relation to the incident energy (e.g., as in slow neutron fission). In the first, the "endoergic" type of collision, the volume rate at which energy is transformed into heat can be calculated as follows.

Let $N(\vec{r}, E, \Omega)$ be the particle flux of penetrating radiation at position $\vec{r}$ per unit volume at energy E per unit energy range, which is going in direction Ω

per unit solid angle. Then the collision density at $\vec{r}$ of particles having the energy E in range dE is

$$\mu(E,\vec{r})\ N_o(\vec{r},E)\ dE = \mu\ dE \int_{4\pi} N(\vec{r},E,\Omega)\ d\Omega$$

where $\mu(E,\vec{r})$ is the macroscopic linear absorption coefficient at energy E at the point $\vec{r}$. If E_a is the average energy carried off by the charged particles per collision, then the rate of heat production per unit volume due to incident particles of energy E in range dE is

$$\begin{aligned} dw &= \mu E_a N_o\ dE \\ &= \mu \frac{E_a}{E}\ I_o\ dE \end{aligned}$$

Here I_o is the energy flux, defined as EN_o. If we define a new absorption coefficient μ_a as

$$\mu_a = \frac{\mu E_a}{E}$$

then dw has the simple form

$$dw = \mu_a I_o\ dE$$

or

$$w = \int \mu_a I_o\ dE$$

The names that have been given to μ_a in the past are many. We shall call it the "energy absorption coefficient."(1)

As far as the shielding of reactors is concerned, there are only three types of gamma-ray collision processes -- photoelectric effect, pair production,

(1) Other symbols used are: "$\mu - \sigma_s$" by W. Heitler, Quantum Theory of Radiation, Oxford Univ. Press, New York, 1944, and W. S. Snyder and J. L. Powell, "Absorption of γ-Rays," ORNL-1421 (March, 1950); "True absorption" cross section by G. R. White, "X Ray Attenuation Coefficients," NBS-1003 (May 13, 1952).

and compton scattering. For gamma-ray collisions, μ_a can therefore be written as

$$\mu_a = f_1 \mu_{PE} + f_2 \mu_{PP} + \frac{\overline{E_e}}{E} \mu_c$$

where f_1 and f_2 are the fraction of incident energy lost in a photoelectric absorption and in pair production respectively, and $\overline{E_e}$ is the average recoil electron energy in compton scattering. Strictly speaking, f_1 and f_2 are less than unity. Some energy is emitted in these processes in the form of penetrating radiation, fluorescence in the case of photoelectric effect, and annihilation radiation in pair production. For most practical purposes, however, we can consider f_1 and f_2 to be unity, and μ_a can then be written as

$$\mu_a = \mu - \frac{\overline{E'}}{E} \mu_c$$

where $\overline{E'}$ now is the average energy of the scattered photon. Table III-C-1 lists μ_a for water, aluminum, iron, and lead. In this table the more exact formulation of μ_a is used to the extent of correcting the pair production and compton scattering terms for the energy carried away by bremsstrahlung. More extensive (but considerably less reliable) graphs of μ_a are given in the compilation of Powell and Snyder.(2)

For neutron elastic scattering, μ_a has the form

$$\mu_a = \frac{\overline{E_r}}{E} \mu$$

where $\overline{E_r}$ is the average recoil energy given by

$$\overline{E_r} = \frac{2EA}{(A + 1)^2} \frac{\mu_{tr}}{\mu}$$

Here A is the atomic mass of the target nucleus and μ_{tr} is the macroscopic

(2) ORNL-421, op. cit.

Table III-C-1. Energy Absorption Coefficients for Various Materials[a] (Prepared by G. R. White and I. E. Hornstein, NBS, and previously published in Reactor Handbook, Vol. 1, p. 763, June, 1953)

Energy (Mev)	μ_a, Energy Absorption Coefficient (cm^2/g)			
	H_2O	Al	Fe	Pb
0.088	0.0252	0.0445	0.312	2.46
0.10	0.0253	0.0371	0.219	2.16
0.125	0.0266	0.0307	0.123	1.55
0.15	0.0278	0.0282	0.0801	1.08
0.175	0.0289	0.0276	0.0595	0.779
0.20	0.0299	0.0275	0.0485	0.586
0.25	0.0312	0.0279	0.0390	0.358
0.30	0.0320	0.0283	0.0340	0.241
0.40	0.0328	0.0287	0.0306	0.136
0.50	0.0330	0.0287	0.0293	0.0904 (0.0901)[b]
0.60	0.0329	0.0286	0.0287 (0.0286)[b]	0.0689 (0.0684)
0.70	0.0326	0.0283	0.0280 (0.0278)	0.0566 (0.0560)
0.80	0.0321	0.0278	0.0274 (0.0272)	0.0483 (0.0477)
0.90	0.0316	0.0274	0.0268 (0.0266)	0.0431 (0.0424)
1.0	0.0311 (0.0310)[b]	0.0270 (0.0269)[b]	0.0264 (0.0261)	0.0391 (0.0384)
1.25	0.0297 (0.0296)	0.0258 (0.0257)	0.0252 (0.0248)	0.0325 (0.0317)
1.5	0.0284 (0.0283)	0.0247 (0.0246)	0.0241 (0.0237)	0.0290 (0.0280)
1.75	0.0272 (0.0271)	0.0237 (0.0236)	0.0232 (0.0227)	0.0275 (0.0260)
2.0	0.0261 (0.0260)	0.0229 (0.0227)	0.0224 (0.0219)	0.0265 (0.0248)
2.5	0.0243 (0.0241)	0.0216 (0.0213)	0.0215 (0.0209)	0.0260 (0.0238)
3.0	0.0229 (0.0227)	0.0205 (0.0201)	0.0210 (0.0203)	0.0264 (0.0238)
4.0	0.0208 (0.0204)	0.0192 (0.0188)	0.0208 (0.0198)	0.0290 (0.0253)
5.0	0.0194 (0.0189)	0.0185 (0.0180)	0.0211 (0.0198)	0.0317 (0.0272)
6.0	0.0184 (0.0178)	0.0180 (0.0174)	0.0214 (0.0200)	0.0344 (0.0287)
7.0	0.0176 (0.0170)	0.0177 (0.0171)	0.0219 (0.0203)	0.0368 (0.0298)
8.0	0.0170 (0.0163)	0.0176 (0.0169)	0.0225 (0.0206)	0.0391 (0.0309)
9.0	0.0165 (0.0158)	0.0175 (0.0168)	0.0232 (0.0209)	0.0410 (0.0319)
10.0	0.0161 (0.0154)	0.0176 (0.0167)	0.0238 (0.0213)	0.0428 (0.0328)

a Values of the fractions f were estimated as follows:

$$f_{photo} = 1 - F_K K_\alpha / h\nu$$

$$f_{scatt} = 1 - R_C - 1/h\nu \int_0^{T_{max}} p_C\,(h\nu, T)\,T\,G_{brem}\,(T)\,dT$$

$$f_{pair} = 1 - 2mc^2/h\nu - 1/h\nu \int_0^{h\nu - 2mc^2} p_p(h\nu, T^+, T^-)\left[T^+ G_{brem}(T^+) + T^- G_{brem}(T^-)\right] dT^+$$

where

K_α = energy of radiation in the K series,

F_K = fluorescent yield in K series,

R_C = average fraction of incident-photon energy retained by photon after compton scattering,

$p_C(h\nu,T)$ = probability that compton scattering yields recoil electron of energy T,

$p_p(h\nu,T^+,T^-)$ = probability that pair production yields positron of energy T^+ and electron of energy T^-,

$G_{brem}(T)$ = fraction of electron energy radiated as bremsstrahlung (from NBS Report No. 2364).

b Energy-absorption coefficients with corrections for bremsstrahlung loss are given in parentheses. The simple law of combination of absorption coefficients for a mixture of elements does not hold exactly when the effect of $G_{brem}(T)$ is appreciable.

transport cross section in the center of mass system. When the scattering is isotropic in the center of mass system, $\mu_{tr} = \mu$. So long as the scattering is more to the front than to the rear (which is almost always true) $\mu_{tr} \leq \mu$. The elastic energy absorption coefficient is thus

$$\mu_a = \frac{2A}{(A + 1)^2} \mu_{tr} \leq \frac{2A}{(A + 1)^2} \mu$$

Elastic scattering is not the only scattering process that can occur, however. Similar but more complicated expressions can be written for recoil energy in inelastic scattering, but so little is known about the details of the inelastic process that the formulas would be of little utility. Inelastic scattering, however, will occur only in the heavier elements. When A is large it can be shown, without great labor, that the average recoil energy in inelastic scattering is less than for elastic scattering for reasonable angular distributions. It is therefore safe to use the elastic scattering μ_a for the total neutron energy absorption coefficient.

In any case it should be noted that the recoil energy decreases as 1/A, so that the energy loss decreases as the element becomes heavier. We should therefore expect that most of the neutron heating will occur in the hydrogenous media which can be treated more carefully. In contrast μ_a approaches closer to μ for gamma rays as Z (and therefore A) increases. Most of the gamma-ray energy production therefore tends to occur in the heavy materials.

In addition, some heat production occurs in neutron collisions in which the neutron is captured. Since the capture cross sections are so much smaller at high energies than at thermal energies, one can neglect fast-neutron reactions almost completely and assume that captures take place only for thermal neutrons. In this case the volume rate of energy developed is given by

$$w_c = \sum_c \phi Q_c$$

where $\sum_c$ is the macroscopic absorption length for the capture process, ϕ is the thermal-neutron flux, and Q_c is the energy carried away by charged particle products of the reaction. About the only reactions of interest are

$Li^6(n,\alpha)$	$Q_c = 4.64$ Mev
$B^{10}(n,\alpha)$	$Q_c = 2.35$ Mev
$N^{14}(n,p)$	$Q_c = 0.60$ Mev

It should be noted that in the B^{10} case Q_c is less than the Q of the reaction, because most of the transitions go to an excited state in Li^7, about 450 kev above the ground level, which then decays by photon emission.

The natural units in which the formulas for w are expressed are Mev/cm^3·sec. Since these units are not yet current in engineering practice, it may be advisable to give conversion factors to more conventional units.

$$\begin{aligned} 1 \text{ Mev/cm}^3\cdot\text{sec} &= 1.60 \times 10^{-13} \text{ watts/cm}^3 \\ &= 1.51 \times 10^{-16} \text{ BTU/cm}^3\cdot\text{sec} \\ &= 8.92 \times 10^{-12} \text{ BTU/hr}\cdot\text{in.}^3 \end{aligned}$$

Knowledge of μ_a, or $\sum_c Q_c$, is however only the initial step in determining the heating. The really difficult part is in finding the energy flux spectrum I_o, or the thermal flux Φ. No simple, clear cut, procedure can be outlined for this part. Certainly were it possible to give I_o and Φ everywhere in the shield, all other major questions of shield design could be answered at the same time, and we are far from this millenium.

Two general procedures are available:

(1) Use of bulk shielding measurements to give something proportional to the heating density,

(2) Calculations of fluxes from assumed sources.

Both the gamma-ray ionization chamber and the fast-neutron dosimeter are designed to measure the rate of energy absorption in a material similar to tissue. Thus there is the possibility of using dose measurements to give information on heating. With gamma rays, for example, 1 r corresponds to 84 ergs absorbed per gram of air. Only slight numerical changes are needed for any other low Z material ($Z \lesssim 13$). Over most of the energy spectrum of interest the dominant interaction process in such materials is compton scattering. The mass absorption coefficient is then proportional to Z/A. For air the ratio is accurately 1/2, as it is for most light elements or mixtures thereof. Where hydrogen forms a substantial fraction of the molecular weight this ratio may be somewhat different. In general therefore the energy deposition per gram is related to the dose in light elements by the relation

$$w = 168 \frac{Z}{A} \quad \text{ergs/g/r}$$

For water Z/A is 0.556 and w = 93 ergs/g/r. Usually such differences are of little importance to the shield designer, and as a rough rule for light elements one can use

$$1 \text{ r/hr} = 2.4 \times 10^{-9} \text{ watts/g}$$

It must be emphasized however that this works only for light materials. For high Z elements -- including iron -- it breaks down badly giving results which are far too low. Heating in such elements depends sensitively on the spectrum of the photons, since μ_a increases so rapidly as E decreases.

Dose measurements may also be used to obtain heating due to fast neutrons in certain cases, although the process is rather more subtle than for gamma rays. The neutron dose unit, the rep, is defined as that amount of radiation for which the energy absorption is 93 ergs per gram of tissue. Now most of this energy absorption, for fast neutrons, is due to hydrogen recoils. At a guess, only

around 10% may arise from other sources. In most other hydrogenous substances -- plastics, water (practically the same as tissue), carbohydrates, and hydrides -- the hydrogen contributes about the same percentage of the total heating. A rough measure (to about 20%) of the heating in these substances is therefore given by the relation:

$$\text{Energy absorbed in ergs/g} = 93 \frac{\alpha_s}{\alpha_t} \cdot \text{dose (in rep)}$$

Here α_s is the weight fraction of H in the substance S and α_t is the corresponding value in tissue or water, equal to 1/9. For a CH_2 compound, for example, α_s is 1/7 and the energy absorption per rep is about 120 ergs/g. In terms of rate of energy absorption this formula becomes

$$w = 2.3 \times 10^{-11} \alpha_s D \text{ watts/g}$$

where D is the fast-neutron dose in mrep/hr.

When the rate of energy production is desired in a nonhydrogenous substance, the tissue dose rate can still be used to furnish, in effect, the flux needed for calculating the energy loss. The energy absorbed per unit mass of a single element per unit time can be written

$$w = \frac{\mu_a}{\rho} I_o = N_m \frac{2A}{(A+1)^2} \sigma_{tr} I_o$$

where ρ is the density, N_m is the number of atoms per unit mass and σ_{tr} is the microscopic transport cross section. In terms of number flux F_o, rather than energy flux I_o, we have

$$w = N_m \frac{2A}{(A+1)^2} \sigma_{tr} E F_o$$

In pure hydrogen this relation reduces to

$$w = N \frac{\sigma E}{2} F_o, \qquad N = \text{Avogadro's number}$$

However we have seen that in pure hydrogen w is approximately equal to 755 ergs/g·sec per rep/sec dose rate. Therefore this can be written

$$755D = N \frac{\sigma E}{2} F_o$$

where D is the dose rate in rep/sec. Actually there will be an energy spread of the neutrons and σE must be averaged over the spectrum of the neutron flux. Since σ for hydrogen is very roughly inversely proportional to E, σE is closer to being independent of E than σ is alone, which is the reason for using number rather than energy flux. Over the range of E from 700 kev to 7 Mev one can approximate $N\sigma E$ for hydrogen as 0.38 cm^2/Mev/g to within $\pm$ 30%. Accordingly, if the dose rate is known, one roughly has

$$F_o = 4 \times 10^3 D$$

and in a substance other than hydrogen

$$w = 4 \times 10^3 \, DN_m \frac{2A}{(A+1)^2} \overline{\sigma_{tr} E}$$

where D is in rep/sec, w is in ergs/g·sec, and E is in Mev. Where several elements are involved in a material, one would correspondingly write

$$w = 4 \times 10^3 \, D \sum_m N_m \frac{2A_m}{(A_m+1)^2} \overline{\sigma_{tr}(m) E}$$

What average value of $\sigma_{tr}E$ should be used must be left to the intelligence and skill of the designer in guessing what is the energy spread of the neutrons in the specific situation. As a suggestion one might use an average from 1 to 4 Mev.

Heating due to neutrons is usually less of a problem than that due to photon absorption. For most reactors the neutron energy leakage is usually less than 1 Mev/fission. On the other hand, more than 12 Mev of gamma rays are emitted per fission, and a good fraction of this leaks from the core.

Further, the heavy gamma-ray shielding materials are such efficient absorbers that all the heating occurs in a relatively small volume. The major heating problem, therefore, is usually due to gamma rays, particularly in heavy materials. In such cases direct dose measurements are usually inadequate and recourse must be had to the second method requiring calculations of the flux in the material in question.

No rigid scheme for such calculations can be given, since the actual procedure depends upon the particular problem and design. Some hints, so to speak, may be useful, however. The first step is to decide on the gamma-ray sources of importance, their locations, strengths, and energies. Among the processes giving rise to gamma rays which may have to be considered are prompt emission in the fission process, fission product radiations, neutron capture, and inelastic scattering. It should be kept in mind that the sources of interest for heating may not be the same as those dominating the external dose. For example, heating near the core may be due mostly to the primary photons, while the gamma-ray dose outside the shield may be determined mainly by the secondaries. Similarly, for questions of deep penetrations it may be proper to consider the capture gamma-ray spectrum of iron to consist mainly of an energetic 7-Mev photon. For heating near the location of the capture, the part of the spectrum below 1-2 Mev may be more important. Useful summaries of information about the sources of radiation have been published elsewhere.(3)

(3) E. P. Blizard and F. C. Maienschein, "Sources of Radiation," Reactor Handbook, Vol. 1, p. 737, Technical Information Service (June, 1953); E. P. Blizard and T. A. Welton, "The Shielding of Mobile Reactors (I)," Reactor Sci, Tech. 1, p. 15 (Dec., 1951); P. Mittelman, "Gamma Rays Resulting from Thermal Neutron Capture," NDA 10-99 (Oct. 6, 1953); E. P. Blizard, "Introduction to Shield Design," CF-51-10-70, Part I Revised (Jan, 1952), Part II Revised (Mar., 1952).

Once the nature and location of the sources are established, the next step would be to determine the flux at any given point due to some infinitesimal element of the source. Again just how this is done will depend upon the problem, e.g., on whether one wishes to treat the sources as a distribution of elementary point sources, plane sources, or shell sources. It is important in any case to include the effects of buildup of scattered radiation, even when these effects are not important for the biological dose. In the heavy materials μ_a is so large at low energies that even a small amount of highly degraded flux will contribute appreciably to the local heating. Fortunately, a fair amount of information is available on the buildup factors, and more will be available shortly. The nature of this information is summarized briefly in the following paragraph.

Consider a monoenergetic source radiating into a material. At a point $\vec{r}$ the heating is given by

$$w(\vec{r}) = \int_0^{E_0} dE\, \mu_a(E) I_0(E, \vec{r})$$

Contributing to the flux I_0 is the unscattered flux $I_0^{\,0}$, which is all at the initial energy E_0, and which may usually be calculated quite easily. The heating due to this unscattered component is

$$w^0(\vec{r}) = \mu_a(E_0) I_0^{\,0}(E_0)$$

By defining a buildup factor for energy absorption, $B_a(E_0, \vec{r})$, as

$$B_a(E_0, \vec{r}) = \frac{w(\vec{r})}{w^0(\vec{r})}$$

the heating may be written as

$$w(\vec{r}) = B_a \mu_a(E_0) I_0^{\,0}$$

All of the effects of the scattered radiation are concentrated in the buildup factor B_a. Calculations of these factors have been in progress for some time,[4] but results are not yet available.[5] However, Goldstein has suggested an approximate procedure based on the conservation of energy, which is probably adequate not too far from the source. For a point isotropic source radiating one photon of energy E_o per second into an infinite homogeneous medium, conservation of energy requires that the integral of the heating over all space just equal the energy release from the source,

$$\int w(\vec{r})\, dV = E_o$$

This may now be written as

$$4\pi\mu_a(E_o) \int_o^\infty r^2 B_a(E_o,\vec{r}) I_o^{\,o}\, dr = E_o$$

The unscattered energy flux is here

$$I_o^{\,o} = \frac{E_o e^{-\mu_o r}}{4\pi r^2}$$

so that the condition reduces to

$$\int_o^\infty B_a(E_o,x) e^{-x}\, dx = \left(\frac{\mu}{\mu_a}\right)_{E=E_o}$$

Here $x = \mu_o r$, the number of mean free path lengths in the medium. This condition is sufficient to fix one parameter in the buildup factor. There is some evidence, for example, that out to 4 to 5 mean free path lengths B_a is often a linear function of μx. If we write B_a as

(4) H. Goldstein and J. E. Wilkins, Jr. and L. V. Spencer, "Systematic Calculations of Gamma-Ray Penetration," Phys. Rev. 89, p. 1150 (1953).

(5) H. Goldstein, J. E. Wilkins, Jr., and Stanley Preiser, "Interim Report on the NDA-NBS Calculations of Gamma Ray Penetration," NDA Memo 15C-20 (Sept. 8, 1953).

$$B_a = 1 + k\mu r$$

then the conservation of energy condition gives

$$k = \left(\frac{\mu}{\mu_a}\right)_{E=E_o} - 1$$

For lead and energies of 1 Mev or lower, it seems a better approximation to take

$$B_a = 1 + k\sqrt{\mu r}$$

and then k has the value

$$k = \frac{\sqrt{\pi}}{8}\left[\left(\frac{\mu}{\mu_a}\right)_o - 1\right]$$

On the other hand with low Z materials and initial energies of 1 Mev or lower, B_a rises very rapidly, indeed almost exponentially. If we take

$$B = e^{+(\mu-\mu_a)r}$$

than the conservation equation is satisfied and the heating reduces to

$$w = \frac{\mu_a E_o e^{-\mu_a r}}{4\pi\ r^2}$$

Replacing μ by μ_a in the exponential has frequently been used in the past as an overestimate of the energy absorption. The more refined calculations show that it is best used near the source and only for substances like water at 1 Mev or lower.

Similar buildup factor approximations can easily be derived for other source geometries. For a plane monodirectional source, if scattering back of the source is neglected, then the same linear approximation holds as for a point isotropic source. With a plane isotropic source, in the linear approximation the coefficient has the value

$$k = 2\left[\left(\frac{\mu}{\mu_a}\right)_{E=E_o} - 1\right]$$

The general procedure for finding the heating in a volume V_2 due to sources in a volume V_1 (see Fig. III-C-1) can be written as

$$w = \int dE \int dV_2 \int w_{12}(E) \;\; \rho_1(E)\, dV_1$$

where w_{12} is the heating at point 2 due to a unit point source at point 1, and $\rho_1(E)$ is the source density at point 1 emitting photons of energy E in unit energy range. One can also write w_{12} as

$$w_{12} = \mu_a(2,E)B_a(r_{12},E)I_o^{\,o}(r_{12},E)$$

In practice, this type of approach is feasible only if the medium is homogeneous in both volumes, and the geometry is simple. This type of approach is described in somewhat greater detail in the Reactor Handbook.(6)

Often the situation permits some simplification in the geometry. For example, suppose it is desired to find the heating due to primary gamma rays in a reflector surrounding a spherical reactor (see Fig. III-C-2). If the thickness of the reflector is not too large compared to the core radius, the problem is practically identical with one in plane geometry shown in Fig. III-C-3. The energy and angular distribution of the equivalent plane source can be calculated from the leakage as shown in section III-B-1. For a sphere whose radius is large compared to a mean free path the angular distribution is cosine about the outward drawn normal.

With the same geometry, one is often interested in the heating in the reflector due to capture gamma rays produced in the reflector. At any given

(6) F. H. Murray, "Heat Generation in Shields," Reactor Handbook, Vol. 1, op. cit., p. 817.

UNCLASSIFIED
ORNL-LR-DWG 534

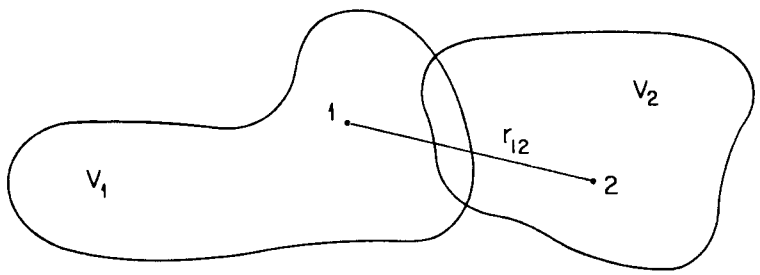

Fig. III-C-1. Geometry for Calculating Heat in V_2 Due to Sources in V_1.

UNCLASSIFIED
ORNL-LR-DWG 535

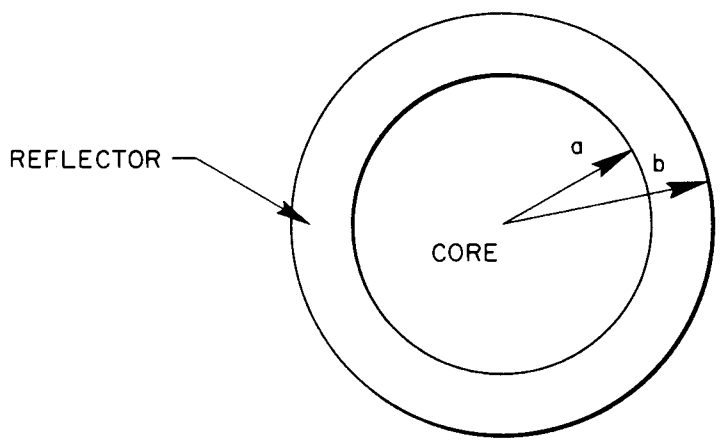

Fig. III-C-2. Reflector Heating in Spherical Geometry.

UNCLASSIFIED
ORNL-LR-DWG 536

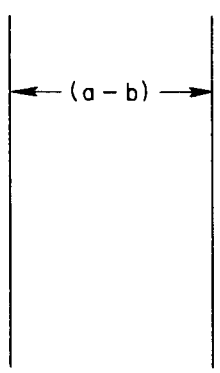

EQUIVALENT SURFACE SOURCE

Fig. III-C-3. Reflector Heating in Plane Geometry.

distance x from the inner boundary neutron captures produce a plane isotropic source of gamma rays of energy distribution

$$\sigma_a \phi(x) N(E) E$$

where σ_a is the macroscopic thermal-neutron capture cross section, ϕ is the thermal-neutron flux, and N(E) is the energy distribution of the capture gamma rays in photons per capture per unit energy range. The heating at any point in the reflector due to such an isotropic point source can be found by the techniques described above, and the total heating at a point is obtained by integrating over x. Enlund[7] has given detailed formulas for this type of problem, assuming diffusion theory for $\phi(x)$, but unfortunately neglecting buildup. A number of similar problems can be tackled in the same way, e.g., heating due to gamma rays from inelastic scattering. Here the biggest stumbling block is lack of data on the cross sections involved.

(7) H. L. F. Enlund, "Energy Absorption of Capture Gammas," CF-52-6-99 Supplement (Oct. 16, 1952).

III-D. UNFAMILIAR SHIELD MATERIALS AND THEIR EVALUATION

It has been felt for some time that major shield weight reductions can be achieved through the application of materials which are not familiar to the design engineer. By and large, aircraft shield design has been described in terms of lead, iron, and water, since these are familiar engineering materials, and since the most experience has been obtained with them in the test facilities. In the report of the 1950 Shielding Board[1] it was pointed out that some weight could be saved through the use of gasoline and certain unfamiliar materials, and since that report was published the use of various weight-saving plastics and rubbers has been considered.

Two major deterrents to the evaluation of shielding materials in 1950[1] were the paucity of empirical data and the inadequate development of shielding theory. In the case of hydrogenous neutron shields these obstacles have been overcome sufficiently so that we are now able to perform crude evaluations of various shielding materials. However, in the cases where secondary gammas are the governing consideration, such as for heavy materials near the core, adequate techniques for evaluating various materials simply have not yet been devised and little more is known about heavy materials than was reported previously.[1] Fortunately in most cases the neutron shielding comprises a half or more of the total weight of the shielding material, and this importance will increase if permissible neutron dose levels are lowered. In addition, gamma materials appreciably superior to those already available are not likely to be found.

(1) "Report of the ANP Shielding Board for the Aircraft Nuclear Propulsion Program," ANP-53 (Oct. 16, 1950).

In this section, the characteristics of a good shielding material will be considered, methods for evaluation from a shielding standpoint will be discussed, and specific materials will be considered with the resultant weight savings estimated.

1. Characteristics of a Good Shielding Material

Shielding Characteristics

The usual mechanism for shielding against high-energy neutrons is to slow them to low energies by moderation, usually with hydrogen, and finally to capture them in lithium or boron, a method which does not produce troublesome secondary gammas. It has been suggested in the past that the moderating might be carried without hydrogen to intermediate energies,(2) rather than to low energies, and resonance or intermediate capture might then be used; this possibility has not been explored in any detail, and in all of the neutron shields considered herein, hydrogen ultimately plays an important role. Blizard(3) has shown on a very simplified basis that if all elements behaved in an orderly fashion hydrogen would give the lightest shield; however, it does have the disadvantage of low cross section at high energies, so that in practice, it may sometime be desirable to deviate from the predominantly hydrogenous shield.

In degrading high-energy neutrons, production of hard inelastic gammas must be avoided as much as possible; similarly, in capturing slow neutrons, the emission of capture gammas must be suppressed.

(2) "Nuclear-Powered Flight; A Report of the Atomic Energy Commission," LEXP-1, Chap. IV-B, p. 24 (Sept. 30, 1948).
(3) E. P. Blizard, "Introduction to Shield Design," CF-51-10-70, Part I Revised, p. 29 (Jan 30, 1952).

Evaluating gamma shielding materials which are to be placed in any appreciable thickness near the core is exceedingly difficult, since it will be the secondary (neutron-induced) processes rather than the primary gammas from the core which will govern. The situation is further complicated by the fact that, especially in a spherical geometry, there is an optimum spatial distribution between the heavy and light materials which make up the shield.

Physical, Chemical, and Mechanical Considerations

The density of the material plays an important role in determining weight savings, since the greater the number of a given type of interacting electrons and nuclei that can be packed into a given volume, the lower the shield weight for a reactor of finite size.

Most of the promising materials are solids at operating conditions, but this poses very real problems in heat removal. It seems preferable to have a circulating liquid shield.

The thermodynamic properties of some interesting materials are such that they are gaseous at normal operating temperatures and pressures (ammonia and the lower alkanes, for example). In these instances, refrigeration is required. This can be accomplished with little weight penalty[4] but, despite the fact that refrigeration does not appear to be impractical, it has been viewed with anything but enthusiasm by the aircraft companies.

Radiation stability is a quality which is essential for those regions close to the core. A solid material presumably would have to exhibit appreciably higher radiation stability than a circulating liquid which would spend only part of the time in the highest intensity regions and which could be replaced after each flight.

(4) E. P. Blizard, H. L. F. Enlund, and J. H. Wyld, "Ammonia as an Aircraft Shield Component," Reactor Sci. and Technol. 2, No. 1, TID-2001, p. 79 (April, 1952).

A number of engineering questions must be considered in choosing shielding materials. Examples are: bonding (such as the problem of bonding plastic or boron to steel); penetration by structure or by control, electrical, or hydraulic lines; fabricability, especially as regards massive parts; creep (lead, for example, tends to sag under its own weight*); welding or joining; containing problems (including self-sealing liners for liquids).

Cost or availability considerations sharply limit the use of materials such as gold osmium, or some of the borohydrides, although it must be pointed out that every pound of shield weight saved results in the saving of several pounds of airplane weight, and aircraft costs of $20 to $50 per pound can be anticipated. Over and above this direct saving are the various efficiencies and lower attrition rates resulting from decreased aircraft size.

Most organic shielding materials which are attractive at room temperature expand so rapidly as they are heated that at operating temperature they become considerably less attractive, and in the case of solids such as polyethylene, the expansion presents an insurmountable mechanical problem.

Safety considerations will influence the choice of shield materials. Explosive materials cannot be considered, and there is some argument against the use of highly volatile inflammable materials. Some interesting materials, such as lithium borohydride, react violently with water; some, like water, react with the liquid metal coolants characterized by sodium; some, such as ammonia, are highly toxic; and some, like like lithium, create tritium or other radiactive hazards.

---

* This may be fairly easy to counteract by the addition of small amounts ($<1\%$) of other metals (such as tellurium, antimony, or calcium).

Other considerations may be the compatability of solid materials with liquid coolants, the thermal stability of the material, and the viscosity or heat transfer properties of both circulating fluid and solid shielding materials.

2. Methods of Evaluation

Neutrons

All fast-neutron attenuation characteristics are determined by use of removal cross sections. Since the concept of the removal cross section is elaborated upon in considerable detail elsewhere,(5) only its definition will be repeated here. The removal cross section of a given material as used herein is defined as that cross section which gives the proper dose attenuation of fast neutrons by the material, for an infinite plane isotropic fission source, when a thin slab of the material of infinite extent is placed against the source and a large thickness of water lies between the sample and the detector. Removal cross sections as determined in this manner at the ORNL Lid Tank Facility are listed in Table III-D-1. These can be plotted against atomic weight, as shown in Fig. III-D-1.

For the six heavier elements ($A > 25$) measured, a fairly smooth monotonic curve results. The removal cross section of oxygen distributed uniformly throughout water was reported by Welton and Blizard(6) as 0.8 barn. This value was deduced from Lid Tank water data, using a calculated hydrogen attenuation. Goldstein(7) suggests that Welton's hydrogen buildup factors

(5) E. P. Blizard and T. A. Welton, "The Shielding of Mobile Reactors," Reactor Sci. and Technol. 1, No. 3, TID-73, p. 15 (Dec. 1951); R. D. Albert and T. A. Welton, "A Simplified Theory of Neutron Attenuation and Its Application to Reactor Shield Design," WAPD-15 (Nov. 30, 1950).

(6) T. A. Welton and E. P. Blizard, "The Shielding of Mobile Reactors (II)," Reactor Sci. and Technol. 2, No. 2, TID-2002, p. 73 (Aug., 1952).

(7) H. Goldstein, private communication, June, 1952.

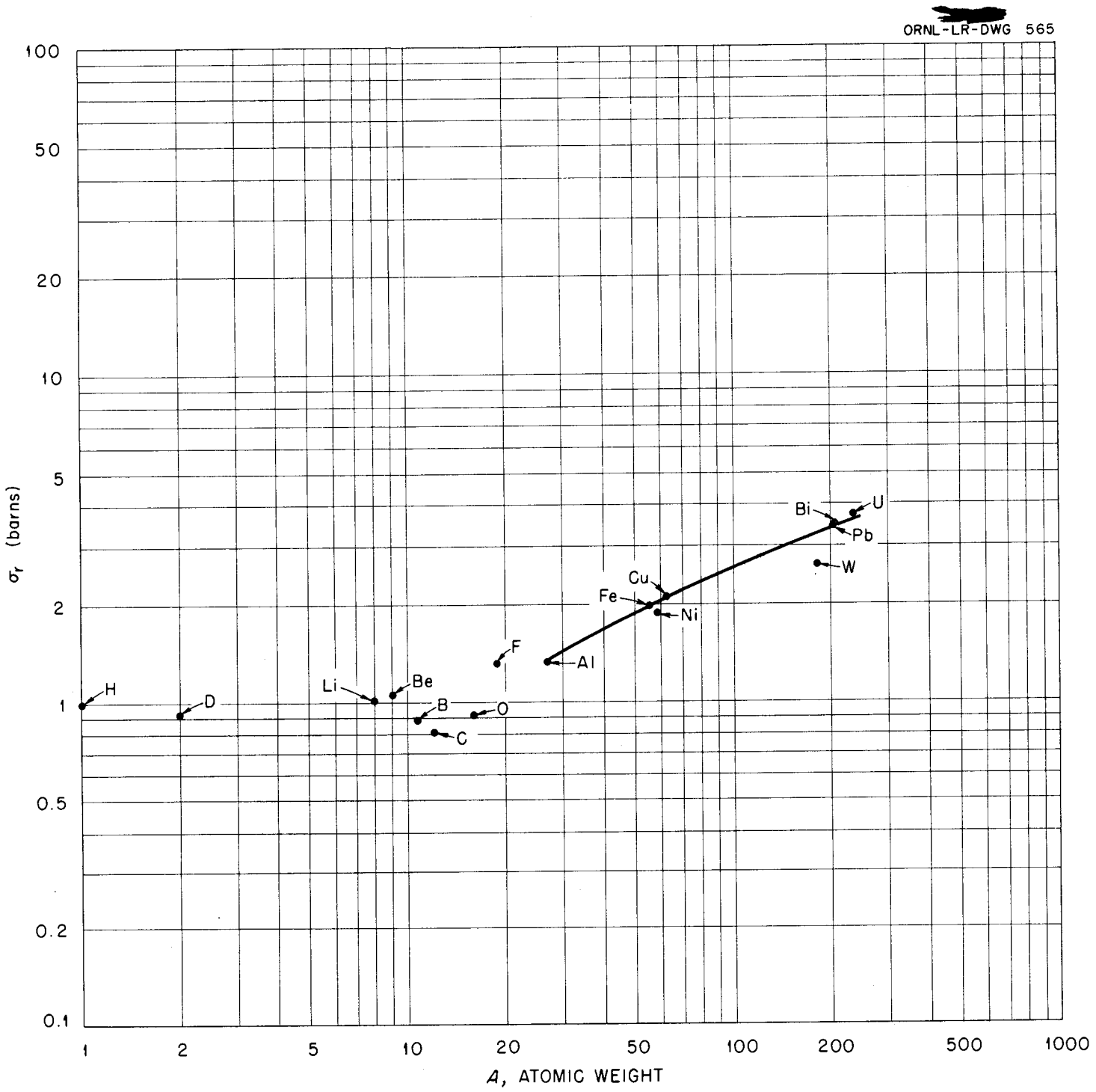

Fig. III-D-1. Fast-Neutron Removal Cross Sections vs. Atomic Weight.

Table III-D-1. Fast-Neutron Removal Cross Sections[a]

Element	σ_r(barns/atom)
H	0.98
D	0.92
Li	1.0
Be	1.05
B	0.87
C	0.80
O	0.94
F	1.31
Al	1.31
Fe	1.35
Ni	1.85
Cu	2.08
W	2.6
Bi	3.43
U	(3.71)

[a]All of these values, except that for Li, were presented at the Shielding Information Meeting, Chicago, Nov. 12 and 13, 1953.. A number of them are considered tentative.

were too low, and the effect of using Goldstein's buildup factors would be to raise the oxygen removal cross section to the neighborhood of 0.9 barn. Blizard experimentally determined the removal cross section for oxygen[8] up close to the source plate as follows: (1) the difference between the oxygen and carbon cross sections was determined by comparing experiments with H_2O and H_2C to be 0.14 cm^{-1}; (2) the carbon cross section was determined experimentally to be 0.80 barn; (3) the oxygen cross section is then 0.80 + 0.14, or 0.94 barn. The Welton and Goldstein values were for distributed oxygen while the Blizard value is for a slab of oxygen near the source; as pointed out later, there is no reason known for the two values to differ. In view of these diverse values, a legislated removal cross section for oxygen of 0.9 barn was used.

The lithium removal cross section has been taken as 1 barn. There is still considerable uncertainty connected with this value; it is derived from results of theoretical calculations performed at NDA and based on solution of the Boltzmann equation by the moments method. The results will depend on the values of the lithium total cross section used, and these are still uncertain. A value for the lithium removal cross section of 1.44 barns was obtained experimentally,[9] however, this value is considered to be very tentative.

The attenuation characteristics of a pure hydrogen shield can be calculated, and as has already been mentioned, they have been calculated by Welton. However, in order to avoid recalculating for a new oxygen cross section of 0.9 barn, the attenuation due to hydrogen only was determined by multiplying the observed water dose by $e^{\Sigma_o z}$, where Σ_o is the macroscopic

(8) "Removal Cross Sections," ANP Proj. Quar. Prog. Rep. June 10, 1953, ORNL-1556, p. 122.
(9) "Removal Cross Sections," ANP Proj. Quar. Prog. Rep. Sept. 10, 1953, ORNL-1609, p. 145.

oxygen removal cross section and z is the distance at which the reading is taken. In other words, the dose beyond a hydrogen shield is expressed as

$$D_H(t) = D_{H_2O}(t)\, e^{\Sigma_o t}$$

and, by definition of the removal cross section, if another material is added (suppose it is added interstitially) to the hydrogen shield, then

$$D(t) = D_H(t)\, e^{-\Sigma_x t}$$

where Σ_x is the macroscopic removal cross section of the added material.

Now suppose we replace a pure water spherical shield of thickness t, at some large distance from the center of which is observed a dose D(t), by a different hydrogenous medium of thickness t', containing N_i atoms of element i of cross section σ_i and N_H atoms of hydrogen per unit volume. t' is to be determined such that at the same distance as D(t) was observed, D(t') = D(t). Then

$$D(t) = D(t') = D_{H_2O}(t'')\, e^{\Sigma_o t''}\, e^{-\sum_{i=0}^{\infty}(N_i \sigma_i t')}$$

where $\sum_{i=0}^{\infty}$ indicates a sum over i, and t" is the thickness of pure water which has the same amount of hydrogen per square centimeter as the new shield will have, i.e.,

$$t'' = \frac{N_H(\text{new})t'}{N_H(H_2O)}$$

The above expression neglects the change in geometrical effects due to going from thickness t to t', but this will be a small change (see section II-B-4). D_{H_2O} is the dose observed in water, for example in the Lid Tank, corrected to a plane monodirectional source. Such a dose curve is available.[6] Fortunately, in the region of interest, the curve is almost a straight line, so

$$D(z) = ke^{-\Sigma z}$$

and the expression becomes

$$\Sigma_{H_2O}t = (\Sigma_{H_2O} - N_o\sigma_o)\frac{N_H(\text{new})}{N_H(H_2O)}\ t' + \sum_{i=o}^{\infty} N_i\sigma_i t'$$

$$= (\Sigma_{H_2O} - N_o\sigma_o)t'' + \sum_{i=o}^{\infty} N_i\sigma_i t'$$

$$= (\Sigma_{H_2O} - \Sigma_o)t'' + \sum_{i=o}^{\infty} N_i\sigma_i t'$$

In particular, if a water shield is to be replaced by a two-region shield of new materials 1 and 2,

$$\Sigma_{H_2O}t = \Sigma_1 t_1 + \Sigma_2 t_2$$

This is not quite exact, however, unless the new shield includes about as much hydrogen as the water shield with which it is compared.

Geometrical Problems. It has already been pointed out that the above method neglects the effects of curvature on the replacement of water by new materials. These effects are probably minor. Another effect which is not yet understood is the effect on the removal cross section of distributing the material throughout the shield, instead of using it as a slab placed against the source plate. It was originally thought that for geometrical reasons having to do with scattering from the material into the detector, the cross section in the distributed case should be lower than in the case with the slab against the source plate. During the session a quick look was taken at this effect, and no backing for this theory was found; indeed, it was shown, though inconclusively, that this particular geometrical effect was expected to go the other way. The only conclusions which were drawn concerning the position of the sample in the water were that the effect of varying the position of the sample is not understood and that the effect should not be large.

Additivity. Another question which arises is whether or not removal cross sections are additive. They probably are not for small water distances behind the sample, since in this case the effects of partly degraded neutrons are important. However, at larger water distances these effects are unimportant, since here only the high-energy penetration of the sample is important. At high energies important window effects would not be found, so it would be expected that removal cross sections are additive. It has been observed experimentally so far that this is the case.

Materials Heavier than Water. A neutron shielding material which is heavier than water may not have a high enough macroscopic removal cross section to outweigh the adverse effect of its higher density. Frequently it occurs that up to a certain radius, the volume effect (i.e., weight saving due to reduction in shield volume) outweighs the density effect, and use of the new material saves weight, while beyond this radius water or some other lighter material should be used. The optimum radius for the new material is found by writing the expression for the weight of the new shield in terms of the radius to which the new material is to be carried, and, holding dose outside the shield constant, differentiating the weight with respect to this radius and setting the resulting expression equal to zero. The expression below was set up by Stern,[10] using the following assumptions:

(1) The effects of gammas on the optimization were not considered, mainly for lack of time.

(2) The attenuation through a material is a function of its thickness only (i.e., no curvature or other subtle geometrical effects).

(3) Removal cross sections can be used to represent the attenuation characteristics of the materials.

(10) H. Stern, private communication.

(4) The reactor-shield geometry is spherical (see Fig. III-D-2).

(5) $t_1 = \dfrac{-b + \sqrt{b^2 - 4ac}}{2\mu_1}$ and $t_2 = \dfrac{\ln A - \mu_1 t_1}{\mu_2}$

where

$$a = \frac{1}{\mu_1^2} - \left(\frac{\mu_1 - \mu_2}{\mu_1\mu_2}\right)^2 Q,$$

$$b = 2\left[\frac{r_o}{\mu_1} + \left(r_o + \frac{\ln A}{\mu_2}\right)\left(\frac{\mu_1 - \mu_2}{\mu_1\mu_2}\right) Q\right],$$

$$c = r_o^2 - Q\left(r_o + \frac{\ln A}{\mu_2}\right),$$

$$Q = \frac{\dfrac{\mu_1 - \mu_2}{\mu_2}}{\dfrac{\rho_1 - \rho_2}{\rho^2}},$$

μ_1, μ_2 = macroscopic removal cross sections of materials 1 and 2, respectively,

ρ_1, ρ_2 = densities,

r_o = radius of the core,

A = total attenuation required ($A > 1$),

t_1 = thickness of material 1 (heavy),

t_2 = thickness of material 2 (light).

<u>The Optimum Member of an Organic Series</u>. As the molecular weight of a hydrocarbon in a given series increases, its density increases. In the hydrocarbon series of interest in shielding, the number of hydrogen atoms per carbon atom decreases with increasing molecular weight. In such series, an optimum molecular weight exists for the series. This was determined by LaMarsh[11] for the alkane series,* using the same set of assumptions listed

(11) J. LaMarsh, private communication.

* The analysis referred to the liquid alkanes only.

UNCLASSIFIED
ORNL-LR-DWG 566

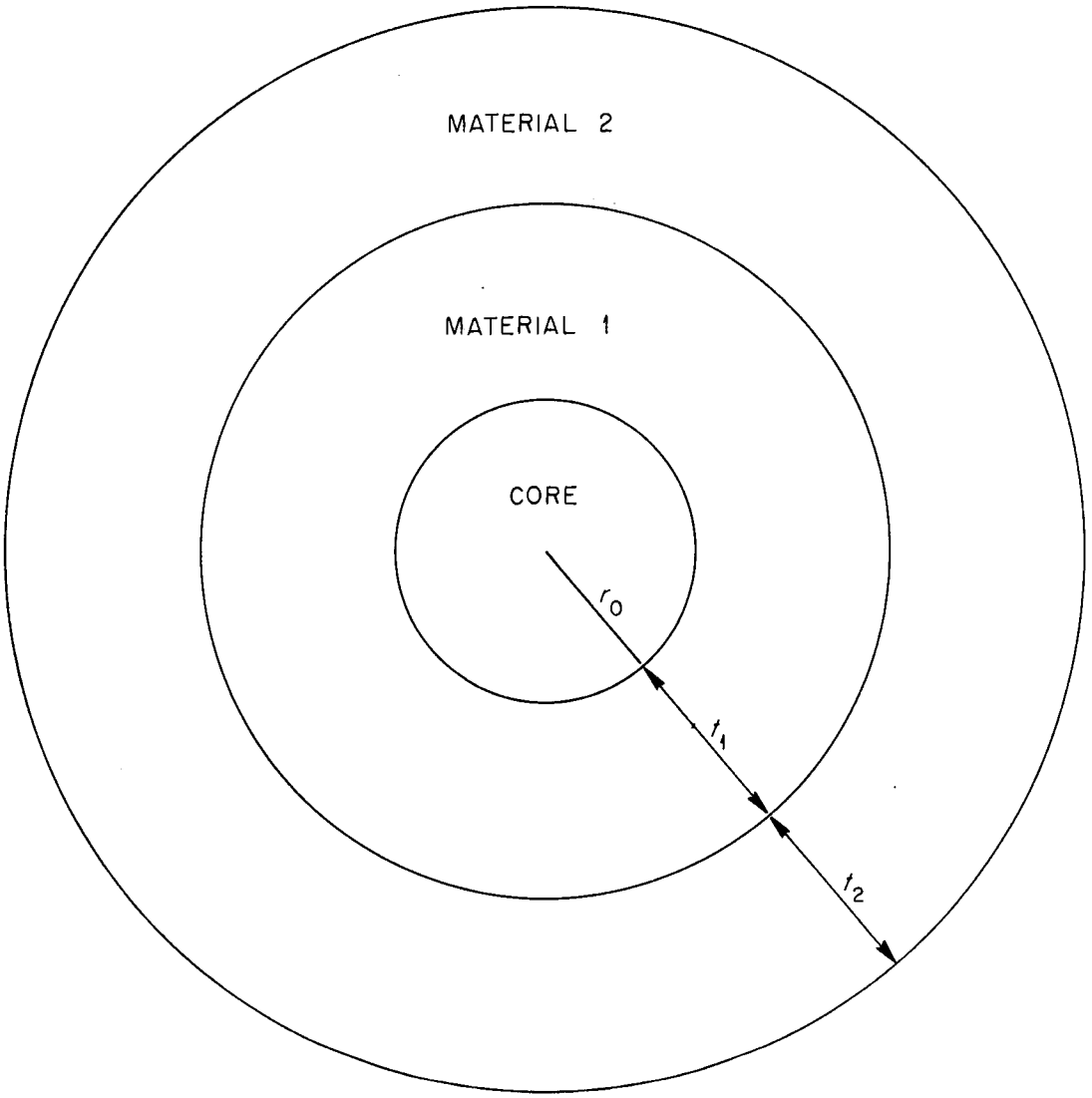

Fig. III-D-2. Geometry for Calculation of Optimum Two-Region Shield.

above. For an alkane replacing a 3 ft thick water shield surrounding a 5 ft diameter core, the optimum number of carbon atoms per molecule was found to be about 15.

Gammas

When the new neutron shielding material is lighter than the water it replaces, a loss in gamma shielding material results. For the purposes of this study, a layer consisting of 2/3 lead and 1/3 oil (CH_2, 0.8 g/cc) by volume was added outside the reactor or pressure shell to make up for the loss of gamma shielding. The condition for gammas, similar to that for neutrons (see page 148) is

$$\mu_{H_2O} t = \mu_1 t_1 + \mu_2 t_2$$

where μ_1 and μ_2 are the absorption coefficients of the lead-oil layer and of the new shielding material. Using the neutron condition and the gamma condition gives two equations in two unknowns, t_1 and t_2, from which the weight of the new shield is obtained.

For the light materials, it was deemed adequate to take effective mass absorption coefficients equal to that of water. A relaxation length of 24 cm was used for water.

For the lead, the situation is far more complicated, and any real determination of the gamma attenuation characteristics of the lead is outside the scope of a study of this kind. In one lead-water experiment, effective absorption coefficients for lead ranged from ~ 0.5 to ~ 0.25 cm^{-1},[12] depending on the neutron to gamma ratio. However, it is assumed that a certain amount

(12) C. E. Clifford, "Gamma Attenuation Behind 3.8-, 7.6-, and 11.4-cm Solid Lead Shadow Shields in Pure Water as a Function of Water Reflector Thickness," CF-52-5-163 (May 20, 1952).

of care is taken to control secondaries and that an absorption coefficient of 0.4 cm^{-1} can be conveniently attained. It was originally hoped that the weight of the added gamma shielding would be small compared to the total shield weight; unfortunately this did not turn out to be the case for the most promising materials.

For neutron shields heavier than water, time did not permit considering gammas in determining the optimum configuration, but a correction was made at the end of the calculation for the amount of lead to be removed from the sides of a "standard" crew compartment to account for the added gamma shielding at the reactor.

3. Light Hydrogenous Materials Considered for Comparison

The number of shielding materials which can be considered in seeking a weight saving is almost boundless. Figure III-D-3 presents the types which can be studied. Fortunately, by applying a few elementary principles, the number of materials to be considered in detail can be reduced to one or two dozen and a discussion of how this has been accomplished for the light materials shown in Fig. III-D-3 follows.

Water is used as the reference material, and weights of all shields using other materials are compared to it.

The light metal hydrides, specifically the hydrides of lithium and of beryllium, are of primary interest as neutron shields, not only for their hydrogen content, but also for the lithium or beryllium atoms, which are good neutron removers themselves (see page 145). Little is known about the properties of beryllium hydride, so by elimination lithium hydride becomes the representative of this group.

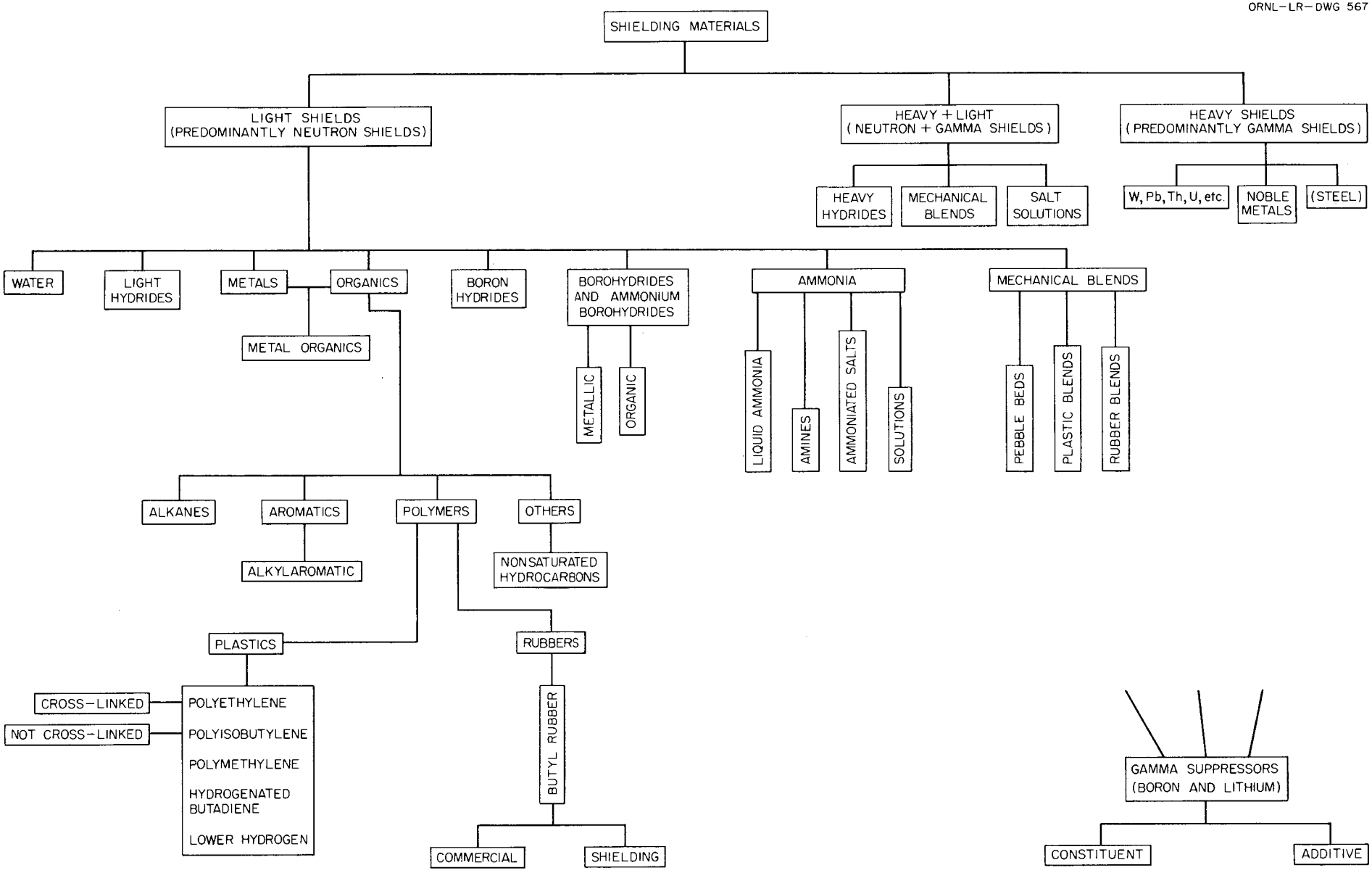

Fig. III-D-3. Types of Shielding Materials.

The light metals themselves are of interest; beryllium, for example, is used in reflector-moderated reactors as a combined reflector-shield. Beryllium is chosen as a representative of this group for comparison purposes.

The organics as a group consist of thousands of materials. For many of these the hydrogen content per unit volume compares favorably with that of water, while the density is lower. The organics with the highest hydrogen content per molecule are the alkanes, and of the alkanes, LaMarsh (see page 150) has shown that if gamma attenuation is not considered those with $\sim$15 carbon atoms have the best combination of density and hydrogen content per molecule. With gamma attenuation, this number will go up; it is assumed that $C_{20}H_{42}$ (density of 0.72 at 250°F) is a good representative of the straight chain hydrocarbons.

Through polymerization, the common plastics polyethylene and polyisobutylene are formed. These have density of 0.92 at room temperature, but their densities decrease appreciably as the temperature is increased. An unfamiliar plastic, polymethylene, has a room temperature density of 0.94, but retains almost this density at operating temperature.[13] All three of these plastics have the empirical formula $(CH_2)_x$. Shielding-type butyl rubber is cross-linked polyisobutylene, with additives totaling several weight percent. The polymers have been represented in this study by a substance having a CH_2 composition and a density of 0.92.

Interest has been expressed in the alkyl aromatics as shielding materials. They will not save as much weight as the alkanes, but they are

(13) Held, K., "Polymethylene as Shielding Material," NDA-71 (May 20, 1953).

somewhat more stable under irradiation. They are quite preferable to water in most instances because of their lower vapor pressure. Since a particular commercial mixture identified as alkylbenzene has received considerable attention it was chosen as a representative alkyl aromatic.

Another large group of shielding materials that has been suggested for study are the boron hydrides. Unfortunately, the lighter boron hydrides, which could save the most weight, are explosive or otherwise unstable. It is necessary to go to molecules containing eight or ten boron atoms before stability is reached. Decaborane is chosen as an example of the boron hydrides. Held[14] lists a number of truly exotic boron complexes but points out that little is known about any of them; while these are interesting subjects for research, consideration of them in the current study would be premature.

The borohydrides and quaternary ammonium hydrides, particularly lithium borohydride and tetramethyl ammonium borohydride (hence forth called TMB), have received considerable attention. Although these two materials are not yet practical from an engineering point of view (see page 159), they theoretically are good shielding materials and have been of considerable interest in the past. They may be more practical when used in conjunction with other materials. For these reasons they have been included on the study list.

Ammonia and its derivatives form another major group of shielding materials. The first material to be considered is liquid ammonia, refrigerated to various temperatures. A note suggesting the use of ammonia as a shielding material and indicating its practicality, appeared some time ago.[4]

---

(14) Held, K., "Shielding Materials," NDA-10-52 (March 21, 1953).

An amine is formed when one or more of the hydrogen atoms in ammonia is replaced by any of various organic radicals. Alkyl radicals give the greatest hydrogen content, but no weight saving over the simple alkanes would result unless a high density is achieved, since the amino group (NH_2) in the alkyl amine is not as useful relative to its weight as the hydrogen atom in the alkane. Since the alkyl amine densities do not appear to be higher than the corresponding alkane densities, no weight saving can be expected through their use. However, the amines might serve as coolants or solvents in other systems, and for this reason, tetraethylene pentamine, having high density, and decylamine, having a high number of hydrogens per carbon plus nitrogen, have been considered in the weight comparison.

Another system of interest is the ammonia plus borohydride solutions. Solutions with up to 70 wt. % $LiBH_4$ have been prepared. The vapor pressure of the 70% solution is understood to have been only 20 mm at room temperature. Held[14] estimates the density of this solution to be $\sim$0.63 at 150°F. This material would probably be liquid at operating conditions.

A further group of ammonia compounds are the ammoniated salts. For example, since cobalt hexamine fluoride exists,[15] why would not cobalt (or some other metal) hexamine ammonium borohydride also exist? Little is known about these materials, and therefore they have not been included in the evaluation study, but research work on them appears to be justified.*

Mechanical blends of light materials are also of interest; examples are blends of hydrides or borohydrides with plastic or rubber, or a pebble bed of lithium hydride cooled by a circulating hydrocarbon.

(15) "Handbook of Chemistry and Physics," 35th ed., Chemical Rubber Publishing Co., Cleveland, Ohio, 1953.

* Such work is currently in progress.

The heavy materials, used primarily as a gamma shield, and the heavy-plus-light materials, used primarily as a combined neutron-gamma shield, are not discussed in detail herein, since, as pointed out earlier, their evaluation depends on techniques which have not yet been adequately developed.

The most frequently considered heavy materials are uranium, thorium, tungsten, and lead. The noble metals have repeatedly been ruled out on the bases of cost and unavailability. Steel is often considered a "heavy metal" for high-temperature application. Little more can be said now about the heavy metals than was said in the report of the 1950 Shielding Board.(1)

Heavy-plus-light materials can be prepared in several ways. One is by mechanical blending, using a rubber or plastic matrix(16) or by concentric shell or pebble bed configuration. Another is by preparing water solutions of salts; for example, certain thallium salts yield solution densities up to 5.(15) Finally, the heavy hydrides (UH_3, ThH_4) can be employed.

4. Results of Comparisons

Light Hydrogenous Shields

In Table III-D-2 are listed the results of a crude comparative study of the light materials discussed in the preceding section. It was assumed that the new material replaces a water shield which is 3 ft thick and which surrounds a 5 ft core or pressure shell. Except as noted, the new material operates at about 250°F. For the light hydrogenous materials, the ρt for gammas will be lower than the original water ρt, so that a heavy layer must be added outside of the pressure shell. The heavy layer is assumed to

(16) J. W. Born, "Closure Report (on) Plastic and Elastomeric Materials as Shielding Components for Nuclear Reactors," B. F. Goodrich Co., ORO-80 (July 2, 1952).

consist of lead (2/3 by volume) and oil of density 0.8 and CH_2 composition (1/3 by volume). The gamma attenuation of this layer will depend on its thickness and upon the character of the radiation incident upon it, but because of time limitations, it was assumed for this study that lead in this location attenuates with an absorption coefficient of 0.4 cm^{-1} in all cases.

In the last column of Table III-D-2 are shown weight savings, expressed as a fraction of the weight of the water in the original shield.

A major factor which does not show up in the table (except for LiH-oil and perhaps $LiBH_4$-NH_3) is the cooling question. All of the solid materials will require cooling throughout at least part of the shield. While such cooling might be accomplished with a hydrocarbon, which can be a lighter shield than water, the full gains indicated for the best solid materials cannot in practice be realized.

Disposal of thermal neutrons was not considered quantitatively at this point, but it should not have a major effect on the weights.

From Table III-D-2 it can be concluded that lithium hydride offers about the greatest weight saving of the shielding materials considered in this group, amounting to a little over 1/4 of the weight of the water shield used for a standard. The TMB and lithium borohydride figures in the table indicate similar weight savings but are unrealistic since they include no cooling allowance; the NH_3 + $LiBH_4$ figure, 22%, is more realistic from this standpoint. In addition, neither $LiBH_4$ nor TMB is particularly attractive from an engineering standpoint. TMB decomposes[17]

(17) M. D. Banus, R. W. Bragdon, and T. R. P. Gibb, Jr., "Preparation of Quaternary Ammonium Borohydrides from Sodium and Lithium Borohydrides," J. Am. Chem. Soc. 74, 2346 (1952).

Table III-D-2. Light Hydrogenous Shields

Material	Formula	Density* (g/cc)	Removal Cross Section (cm^{-1})	Absorption Coefficient (cm^{-1})	Lead-Oil Layer		Light Layer		Fractional Weight Saving
					Thickness (ft)	Weight (lb)	Thickness (ft)	Weight (lb)	
Water	H_2O	0.94	0.091	0.0417			3.00	39,700	0
Lithium hydride	LiH	0.80	0.121	0.0333	0.194	7,800	21.6	19,800	0.30
70% Lithium hydride + 30% oil	$0.7LiH + 0.3C_{20}H_{42}$	0.78	0.112	0.0325	0.178	7,100	2.35	22,000	0.27
Plastic	$(CH_2)_x$	0.92	0.112	0.0383	0.107	4,300	2.49	27,500	0.20
Alkane oil	$C_{20}H_{42}$	0.72	0.0900	0.0300	0.117	4,700	3.07	31,100	0.098
Tetraethylene-pentamine	$C_8H_{23}N_5$	0.91	0.0983	0.0379	0.055	2,100	2.89	34,400	0.081
Decylamine	$C_{10}H_{23}N$	0.70	0.0863	0.0292	0.111	4,500	3.22	33,000	0.057
Alkylbenzene blend	$C_{18.3}H_{30.6}$	0.81	0.0893	0.0338	0.064	2,500	3.17	36,300	0.023
Decaborane	$B_{10}H_{14}$	0.94(25°C)	0.1054	0.0392	0.072	2,800	2.68	31,300	0.14
Tetramethyl ammomium borohydride	$(CH_3)_4NBH_4$	0.80	0.1142	0.0333	0.164	6,700	2.38	22,900	0.25
Lithium borohydride	$LiBH_4$	0.66	0.102	0.0275	0.198	8,000	2.55	21,500	0.25
Ammonia	NH_3	0.70(-55°F)	0.0953	0.0292	0.148	6,000	2.88	27,400	0.159
		0.60(80°F)	0.0818	0.0250	0.149	6,000	3.35	31,000	0.071
		0.50(180°F)	0.0682	0.0208	0.149	6,100	4.01	36,200	-0.065
Ammonia + lithium borohydride	$0.3NH_3 + 0.7LiBH_4$	0.63(150°F)	0.0948	0.0262	0.192	7,700	2.75	23,300	0.22

* At 250°F unless otherwise noted.

at the rate of 0.1% per hour in vacuo at 150°C,* and it is expensive ($700/lb in very small lots; production cost unknown). $LiBH_4$ is not particularly stable either. It also is expensive (~$100/lb)[18] and is a rather unpleasant material to handle. However, the ammonia solution does have attractive features, and further research on this system would seem well justified.

The CH_2 type of plastic, it is seen, saves an appreciable amount of weight, and in view of the engineering practicality of this type of material, further research and developmental work on polyethylene, cross-linked polyethylene, polymethylene, and butyl rubber, seems well justified.

Neutron Shields Heavier than Water

This class of materials is more complicated to evaluate than the lighter materials, since there is usually an optimum fraction of the shield that the new material should occupy, and for all but the lightest materials the gamma question is too important to be treated as a perturbation, as was done for the lighter-than-water condition.

An evaluation of beryllium metal was made, using methods previously described (page 140). There is some uncertainty in the removal cross section of beryllium; early experiments give 1.13 barns,[9] and a recent experiment (results not yet published) gives 1.19 barns. For this study, 1.16 barns was used.** Table III-D-3 indicates weight savings attainable through use of beryllium in the standard shield of this section.

* This might be reduced by carefully controlling impurities or by maintaining a proper atmosphere over the TMB.

(18) Mela, R., private discussion with Mr. Landolt of Metalloy Corp. re: Lithium Hydride, NDA-10-59 (Feb. 11, 1954).

** An even later figure is 1.05 barns (see page 145);use of this figure would lower the weight saving somewhat, but it was made available too late to be included in this study.

Table III-D-3. Weight Savings Gained by Using Beryllium in Standard Shield

Core (or pressure shell) diameter	5 ft
Original reactor water shield thickness	3 ft
Original reactor water shield weight	39,300 lb
Optimum thickness of beryllium	1.24 ft
Thickness of water in new reactor shield	1.17 ft
Weight of new reactor shield	34,900 lb
Weight savings with new reactor shield	4400 lb
Change in gamma dose reaching crew	-37%
Approximate weight savings for 50-250-0* crew compartment	1200 lb
Total weight savings over reactor water shield	5600 lb
Fractional weight saving	0.143

* 50 sq ft rear area, 250 sq ft side area, no shielding on front.

Larger fractional weight gains might be expected if the volume to be enclosed is smaller than the 5 ft sphere considered here, as in the RMR design. However, it should be pointed out that in practice a considerable amount of hydrogenous material must follow the beryllium to remove the partly degraded neutrons.

No time was available to search for materials in this category other than beryllium. Titanium hydride (TiH_2) was mentioned, but since the macroscopic removal cross section for TiH_2 is about equal to that of LiH, while its density is almost five times as high, there is no advantage whatsoever in using TiH_2 as a neutron shield. If it is to be used as a neutron plus

gamma shield, these evaluation methods are not advanced enough to calculate its effect. However, if combined neutron and gamma shielding is sought, it seems likely that the heavier hydrides would be more useful.

Heavy Plus Light Materials

Techniques for evaluating this type of material have not yet been developed. However, experimental information on lead-water systems is available. If a heavy plus light region attenuates neutrons and gammas to the same extent as the lead-water systems, and if the capture gamma intensity of the lead-water system can be reproduced in the new system (by boration or lithiation), then the lead-water experiments may be used to evaluate other heavy plus light systems.

For example, consider a unit shield 4 ft thick which surrounds a spherical reactor or pressure shell 5 ft in diameter. The shield consists first of a 2 ft thick lead-water region (1/3 lead by volume as in ANP-53[1]). Outside the heavy region lies 2 ft of water.

The lead-water region is to be replaced by a region consisting 70% by volume by thorium hydride—lithium hydride pellets, cooled by $C_{20}H_{42}$ oil (30% by volume) operating at 250°F. The water region is to be replaced by lithium hydride. The original shield weighed 134,000 lb and the weight of the new shield is to be determined. Here there are three conditions to meet: (1) The gamma source strength of the outside surface of the new shield is to be the same as for the lead-water shield; (2) the same for neutrons; (3) the amount of LiH in the heavy plus light layer is such that the ratio of neutrons to gammas at the outside of the new heavy layer remains the same as for the original shield. It is assumed that the heavy layer is

sufficiently lithiated that the capture gammas are no more serious than they were for lead. While the composition of the heavy layer should be varied with radius, there was not enough time to perform a calculation on this basis, and a uniform composition heavy layer was assumed; this means that the weight may be far from optimum.

The results are given in Table III-D-4, and the constants assumed are given in Table III-D-5. It is re-emphasized, for reasons already stated, that these weight estimates are exceedingly crude and should be used only as a basis for a more realistic study.

5. Conclusions

Requirements of shielding materials have been outlined, and simple methods for evaluating their shielding merits have been presented.

For the types of geometry chosen in comparing various light hydrogenous shielding materials, lithium hydride seems to offer the greatest weight saving. Further investigation of lithium hydride seems justified. A few other light materials may be of interest, but there is not enough known about them to enable proper evaluation.

Little progress seems to have been made since the report of the 1950 Shielding Board[1] in the field of heavy shielding materials. Although day-to-day interests fluctuate in ANP projects, sooner or later interest is bound to turn again to unit shields. (Indeed, it has to some extent for fireball-type shields.) It is unfortunate that so little fundamental work has been aimed at the development of this type of shield. Specifically, the following types of work should be embarked on: (1) materials research;

Table III-D-4. Unit Shield with New Materials

	Original Materials	New Materials
Core (or pressure shell) radius (ft)	2.5	2.5
Heavy layer composition (vol fraction)	1/3 Pb, 2/3 H_2O	0.3 oil ($C_{20}H_{42}$) 0.6 ThH_4 0.1 LiH
Light layer composition	Water	LiH
Heavy plus light layer thickness (ft)	2	1.770
Light layer thickness (ft)	2	1.311
Heavy plus light layer weight (lb)	86,000	85,800
Light layer weight (lb)	48,000	20,100
Total weight (lb)	134,000	105,900
Fractional weight saving		0.21

Table III-D-5. Constants Used in Unit Shield Study

Material	Density (g/cc)	Removal Cross Section (cm^{-1})	Absorption Cross Section (cm^{-1})
H_2O	1	0.0967	0.0417
ThH_4	8.3	0.156	0.32
LiH	0.8	0.121	0.0333
$C_{20}H_{42}$	0.72	0.0900	0.0300
Pb	11	0.108	0.40
1/3 Pb, 2/3 H_2O	4.4	0.100	0.161

(2) fundamental neutron and gamma studies, including the development of machine methods; (3) engineering design of shields; (4) Lid Tank experiments and analysis; and (5) irradiation studies. Only by conducting a well-directed and integrated research program of this type can the unknowns discussed in this section be resolved.

III-E. CALCULATION OF CREW COMPARTMENT DOSE*

Radiation can reach the interior of the crew compartment by four routes:

(1) Direct path from the source of radiation;

(2) Scattering from the air around the plane;

(3) Scattering from the fuselage and other structure;

(4) Scattering from the ground.

This section deals with the methods for calculating the dose in the crew compartment arriving by the first two routes. Calculations of structure and ground scattering are given in section III-G.

1. Direct Path Radiation

In almost all designs of nuclear-powered airplanes considered up to the present time direct radiation from the source is incident only upon the rear face of the crew compartment. To provide substantial attenuation of direct radiation in the sides of the crew compartment would increase the weight of the side shielding beyond economical limits. In cases where secondary radiations from the engines or heat exchangers may be incident on the sides of the crew compartment, where possible it is usually better to extend the rear face so as to "shadow" the sides than to add shielding to the sides directly. It will also be assumed, at the start, at least, that the radiation falls normally upon the rear of the crew compartment, which is taken to be composed of a layer of hydrogeneous material, similar to water, followed by a layer of lead.

For both neutrons and gamma rays the most sensible method at present of calculating the attenuation resulting from the hydrogeneous layer is to assume it to be the same as if the layer were moved back to the outer surface

---

* This section is largely taken from the corresponding Chapter 2.9 of Reactor Handbook, Vol. 1, p. 869, Technical Information Service, USAEC, (June, 1953).

of the reactor shield. That this cannot be completely correct is clear. At the crew compartment the radiation incident on the layer is normal to the surface, while the radiation entering the outer layers of the reactor shield has some angular spread. For gamma rays, where the evidence indicates photons emerge from the reactor shield nearly normally, the difference should not be important. One cannot be as sure that the procedure is valid with neutrons, but if the penetration is determined by the unscattered neutrons--which are confined closely to the radial direction--it should still be a safe method.

The heavy material layer must be treated differently. Neutron penetration is best handled by assuming exponential attenuation. However, one cannot use in this exponential the relaxation length derived from the observed removal cross section. In measuring the removal cross section a thick layer of water after the heavy material filters out the slower neutrons due to inelastic scattering. In the crew compartment shield no such filtration takes place, and the actual neutron flux penetrating the heavy material must be substantially greater than predicted by the removal cross section. Available experimental information is not adequate to determine definitely what relaxation length should be used, but a few data are suggestive. In a LTSF experiment(1) the fast-neutron attenuation through a 7-in. hemispherical shell of lead around the detector corresponded to a mean free path of about 17 cm. This figure agrees reasonably well with the rate at which thermal flux directly behind lead slabs in another LTSF experiment(2) decreased with lead thickness. It should be noted that the relaxation length is about twice as great as would be obtained from the removal cross section.

(1) J. D. Flynn and G. T. Chapman, "Attenuation by Lead of Fast Neutrons from a Fast Fission Source," ORNL-CF-53-3-166 (Mar. 10, 1953).
(2) C. E. Clifford et al., "Bulk Shielding Experiments," The Aircraft Nuclear Propulsion Project at the Oak Ridge National Laboratory, ORNL-768, p. 36 (Aug. 14, 1950).

Gamma-ray attenuation by the heavy material should be calculated more carefully, since that is the main function of this layer. A completely conservative way to treat this problem would be to assume that the gamma radiation incident on the lead is made up purely of 3-Mev photons and that the lead attenuation and buildup are characteristic of this energy since lead is most transparent to 3-Mev photons. However, the gamma flux has been attenuated prior to the lead by several mean free paths of hydrogenous material, and there is surely a large fraction of softer radiation which is more easily attenuated by the lead. To estimate the effect of the energy spread of the incident gamma rays, Mela[3] has assumed an energy distribution such as was found by Maienschein[4] for the forward emitted photons that emerge from the shadow-shielded region of a reactor shield. The attenuation of this spectrum through lead was then computed, using unpublished NDA calculations of the buildup factors in lead for plane monodirectional sources. It was found that the attenuation is nearly exponential through 15 cm of lead with a mean free path of 2.37 cm. At 15 cm there is twice as much penetration as there would be if the incident energy were 3 Mev and buildup were neglected. If the buildup factor for 3-Mev photons is included, the actual penetration is about 60% of what this most conservative assumption would predict. It therefore seems reasonable to use a mean free path of 2.37 cm, except when there is reason to believe the spectrum is concentrated at energies substantially different from 3 Mev.

No mention is made here of how to calculate the direct radiation incident on the crew compartment rear face since this is treated in section III-B.

---

(3) Private communication.

(4) F. C. Maienschein, "Gamma-Ray Spectral Measurements with the Divided Shield Mockup," Part III, CF-52-8-38 (Aug. 8, 1952);...and T. A. Love, Part IV, CF-52-11-124 (Nov. 17, 1952).

However, it should be noted that the gamma-ray current, not dose, at the outside of the crew compartment is needed. The buildup factor in lead automatically includes the conversion from current incident to dose on the inside of the crew compartment.

2. Air-Scattered Radiation

Basic Assumptions

The majority of calculations of air scattering whether of photons or neutrons involve a few basic assumptions. Some are quite well satisfied in practice, and their effects are easily calculable, while others may be of significance. This section states the assumptions usually made, and the following two sections describe the results of calculations based on these conditions, for gamma rays and neutrons respectively. The final section considers briefly the errors introduced by some of the assumptions.

The results presented in the following two sections assume the following conditions:

(1) The source is effectively a point. If the particles emitted from the reactor shield all radiate from a single point this requirement is rigorously satisfied. In an actual shield the emerging rays deviate from the radial. However, the size of the reactor is usually small compared to the average distance to the scatterer and therefore may be considered a point.

(2) The source is cylindrically symmetric about the source-receiver axis. For all currently envisaged designs this seems to be quite well satisfied.

(3) Only single scattering is involved. Since the source-receiver distance is usually a small fraction of a mean free path this assumption would seem valid. There is some experimental and theoretical evidence, however,

that the multiple scattering effects compensate almost completely for the attenuation of the particles in traveling through the air. For neutrons the calculations below therefore assume single scattering without air attenuation. In the case of gamma rays the detailed calculations do include the small effect of air attenuation, but corrections to remove air attenuation can easily be made if desired.

(4) The scattering is calculated always for sea level air densities. If the single scattering assumption is valid then the scattered dose is strictly proportional to the density, and corrections to other altitudes may be made accordingly.

(5) The crew compartment is taken as a cylindrical shell coaxial with the reactor crew axis and closed at both ends by separate plugs of uniform thickness. In calculating the separate contributions through the side, rear, and front, respectively, further geometrical idealizations are made.

For the dose through the side walls the isotropic receiver is assumed to be on the axis of a cylinder whose dimensions are small compared to the reactor-crew distance, yet so long that it subtends a solid angle of 4π at the receiver. The contribution from the rear is obtained by replacing the rear wall by an infinite plane of the same thickness; and similarly for the front wall. These assumptions tend to overestimate the dose contributed by the respective walls, but usually not significantly. Only if the actual crew compartment is more like a truncated cone than a cylinder is the error likely to be important. Further discussion of this question is given in the last section.

Gamma-Ray Scattering

Under the assumptions stipulated, the geometry of the scattering through the sides of the crew compartment can be depicted as in Fig. III-E-1.

One can always write the scattered gamma-ray dose at the receiver in the form

$$I(D) = \int_0^{\infty} S(E_o) \int_0^{\pi} N(E_o,\psi)\, f(E_o,\psi,d,D)\, d\psi\, dE_o \qquad (1)$$

where

$S(E_o)$ = energy radiated per unit time from the source per unit energy interval at the energy E_o,

ψ = angle an emergent ray makes with the source-receiver axis,

$N(E_o,\psi)/4\pi$ = fraction of radiation at E_o which is emitted at angle ψ per unit solid angle; $N(E_o,\psi)$ is unity for an isotropic source,

d = a symbol to represent the composition and thickness of the cylindrical crew shield,

D = source-receiver distance,

$\frac{2}{\sin\psi} f(E_o,\psi,d,D)$ = single-scattered dose at a distance D with a crew shield d due to a unit source emitting photons of energy E_o at angle ψ only.

While it is natural to state angular distributions in terms of radiation emitted per unit solid angle, it is more convenient numerically to give the integration as one over the angle. The conversion from solid to linear angle is then contained in the f function and accounts for the factor $2/\sin\psi$

UNCLASSIFIED
ORNL-LR-DWG 250

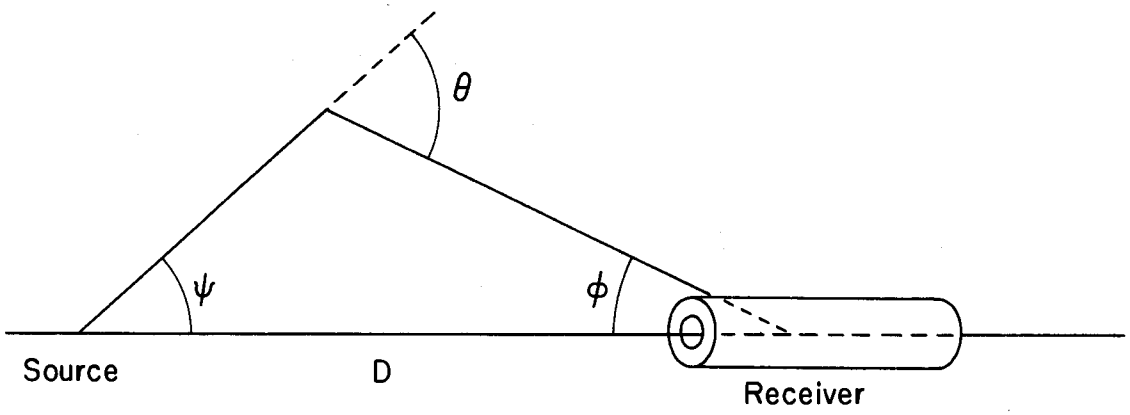

Fig. III-E-1. Geometry of Single-collision Air Scattering

occurring in the description of f. As proof of this factor note that for a source emitting photons only at an angle ψ' and energy E_o'

$$S(E_o) = \delta(E_o - E_o')$$

$$N(\psi) = \frac{2}{\sin\psi'} \delta(\psi - \psi')$$

and therefore

$$I(D) = \frac{2}{\sin\psi'} f(E_o', \psi', D)$$

as stated. All phenomena occurring after the photon leaves the source are concentrated in the function f. The remaining functions N and S are intrinsic properties of the source and its shield and will be discussed, as far as is possible, later on in this section. In turn the function f can be written as

$$f(E_o, \psi, d, D) = \frac{n}{2DF} \int_{\psi}^{\pi} A(\theta, \phi, D) \frac{E(\theta, E_o)}{E_o} \sigma(\theta, E_o) C(E_o, \theta, \phi, d) d\theta \qquad (2)$$

The new symbols used here are defined as follows:

n = volume density of electrons in air (3.88×10^{20} cm^{-3} at STP),

F = conversion factor between energy flux and dose rate, here taken as independent of energy, with a value of 5.5×10^5 $(Mev/cm^2 \cdot sec)/(r/hr)$,

θ = scattering angle,

$E(\theta, E_o)$ = energy of a photon after having been scattered from an energy E_o through angle θ

$$\frac{E}{E_o} = \frac{1}{1 + \frac{E_o}{mc^2}(1 - \cos\theta)} \qquad (3)$$

$\sigma(\theta, E_o)$ = Klein-Nishina differential scattering cross section for scattering through an angle θ at E_o; tables of $\sigma(\theta, E_o)$

are available in a Rand report,[5]

ϕ = grazing angle of incidence of the scattered gamma rays on the receiver, as measured from the source-receiver axis,

$A(\theta,\phi,D)$ = factor representing the attenuation in air and is given by

$$A(\theta,\phi,D) = \exp\left[-\frac{D}{\sin\theta}\left(\frac{\sin(\theta-\phi)}{\ell}+\frac{\sin\phi}{\ell_o}\right)\right] \qquad (4)$$

where ℓ_o and ℓ are the photon mean free path lengths in the air before and after scattering, respectively,

$C(E_o,\theta,\phi,d)$ = attenuation suffered by the scattered photons in penetrating through the shield at the receiver. For a shield consisting of several layers of thickness d_i, it is convenient to write C in the form

$$C(E_o,\theta,\phi,d) = \exp -\csc\phi\left[\sum_i (1-\epsilon_i)\mu_i(E)d_i\right] \qquad (5)$$

where $\mu_i(E)$ is the absorption coefficient through the i'th material at an energy $E(E_o,\theta)$, and $\epsilon_i(E,d_i,\phi)$ is a correction factor representing the buildup of gamma rays penetrating the shield which must at present be determined empirically.[6]

Calculations have been made[7] of the function f at a separation distance of D = 15 m for initial energies of E_o = 1.5, 3, 6 and 12 mc^2 and for shield

(5) R. Latter and H. Kahn, "Gamma-Ray Absorption Coefficients," R-170, Tables 1 and 2 (Sept. 19, 1949).

(6) For a spherical shield consisting of several layers of thicknesses $d_{1,2}$ etc., C obviously has the form $C(\theta,\phi,d) = \exp -\sum_i (1-\epsilon_i)\,\mu_i\,(E)d_i$.

The ϵ_i's for this geometry have not been determined, but should be obtained well enough from the calculated buildup factors for plane monodirectional sources; see U. Fano, "Gamma-ray Attenuation," Reactor Handbook, Vol. 1, p. 753, Technical Information Service (June, 1953).

(7) Described in detail by H. Goldstein and R. Aronson, ORNL-1179, to be published.

compositions consisting of an exterior layer of polyethylene (density 0.90 g/cc) backed by a layer of lead. The following combinations of thicknesses of the two layers were chosen.

Lead thickness (cm)	Plastic thickness (cm)		
0	0	17.5	35
0.63	0	17.5	35
1.27	0	17.5	35
2.54	0		

Some of the information required for the calculations is not known in a closed analytical form, or must be obtained empirically. Examples are the mean free path lengths in air, absorption coefficients in shield materials, etc. These were obtained from the following sources:

(1) The term representing absorption in air, $A(\theta,\phi,D)$, involves the mean free path length in air, values of which were taken from the compilation of Plesset and Cohen.(8) These differ from the figures given in the later compilation of White(9) but not enough to affect A significantly. In practice it was found that for D equal to 15 m, A is sensibly independent of ϕ for constant E_o and θ. Table III-E-1 lists such averaged values of A, denoted by $\bar{A}$, for initial energies of 1.5, 3, 6, and 12 mc^2. Replacing A by $\bar{A}$ changes the final dose by less than 5% for D = 15 m. At reactor-crew distances which are not too different from this separation, the values of $\bar{A}$ can be found from the formula

(8) M. S. Plesset and S. T. Cohen, "Scattering and Absorption of Gamma-Rays," J. Applied Phys. 22, p. 350 (1951).
(9) G. R. White, "X-Ray Attenuation Coefficients from 10 Kev to 100 Mev," National Bureau of Standards, NBS-1003 (May 13, 1952).

Table III-E-1. Values of Average Air Absorption, $\bar{A}$, for Reactor-Crew Separation of 15 m

θ	$\bar{A}$, Air Absorption Factor			
	E_o = 1.5 mc^2	E_o = 3.0 mc^2	E_o = 6.0 mc^2	E_o = 12.0 mc^2
0	0.865	0.90	0.93	0.96
10	0.865	0.895	0.93	0.96
20	0.865	0.89	0.93	0.96
30	0.858	0.88	0.92	0.947
40	0.851	0.87	0.91	0.935
60	0.837	0.86	0.90	0.918
80	0.818	0.84	0.88	0.902
100	0.812	0.84	0.88	0.887
120	0.760	0.80	0.84	0.87
140	0.649	0.70	0.75	0.82
160	0.454	0.50	0.53	0.61
180	0	0	0	0

$$\ln \overline{A}\,(D) = \frac{D}{D_o} \ln \overline{A}\,(D_o)$$

The effect of air absorption is quite small for the usual range of D, i.e., about 0.1 to 0.2 of the photon mean free path in air, provided the scattering angle is not too large. Moreover, photons which have suffered scattering through a large angle are highly degraded and do not contribute to the total dose. It seems likely, in any case, that the air attenuation is in large measure compensated by the effects of multiple scattering and should probably be omitted in future calculations.

(2) The absorption coefficients of the incident photons in the materials of the crew compartment shield were taken from the compilation of White.(9)

(3) Values of ϵ_i, representing the buildup in the crew compartment shield, were arrived at on the basis of experiments performed at NBS(10) and BNL.(11) Figures III-E-2 through III-E-10 are graphs of ϵ_i so arrived at, for each of the shield combinations listed above, as a function of photon wavelength in units of the compton wavelength, h/mc (which is the reciprocal of the energy in units of mc^2). The buildup in lead-plastic combinations was arbitrarily divided in the following manner. The factors ϵ_i for lead were taken to be independent of the thickness of the plastic layer in front. However the ϵ_i's for plastic then depend upon the lead thickness in the combination. Figures III-E-2 through III-E-4 show ϵ_i for lead layers; Figs. III-E-5 through III-E-11 give ϵ_i for 17.5 and 35 cm of plastic, for the various lead thicknesses.

(10) Partially reported by F. S. Kern et al., "Oblique Attenuation of X-Rays from Co^{60} and Ce^{137} in Polyethylene, Concrete and Lead," National Bureau of Standards, NBS-2125 (Dec. 23, 1952).
(11) Private communications from R. Schamberger.

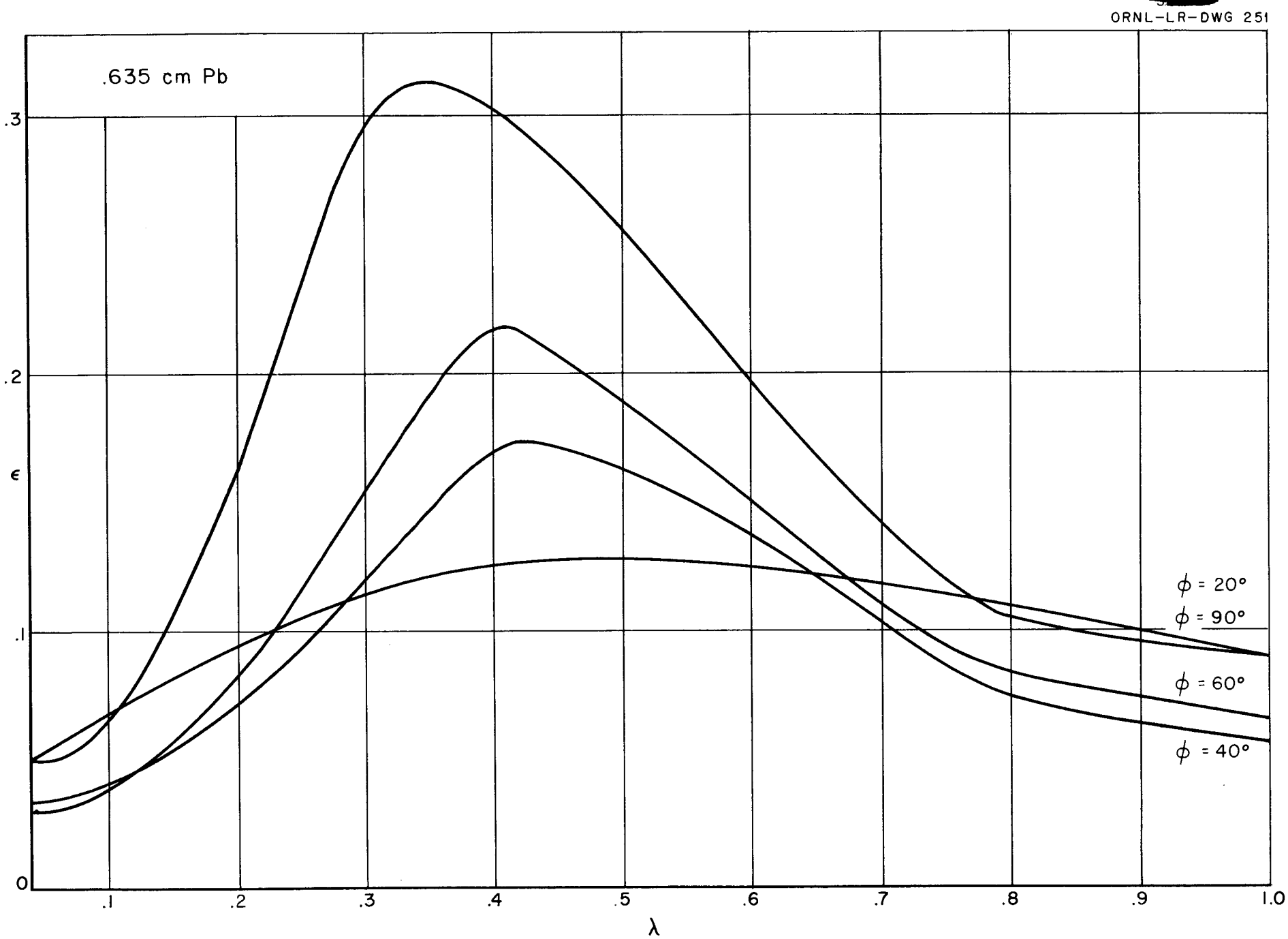

Fig. III-E-2. ε vs Wavelength (λ) in Compton Units for Several Grazing Angles of Incidence (φ) for a Lead Slab 0.635 cm Thick.

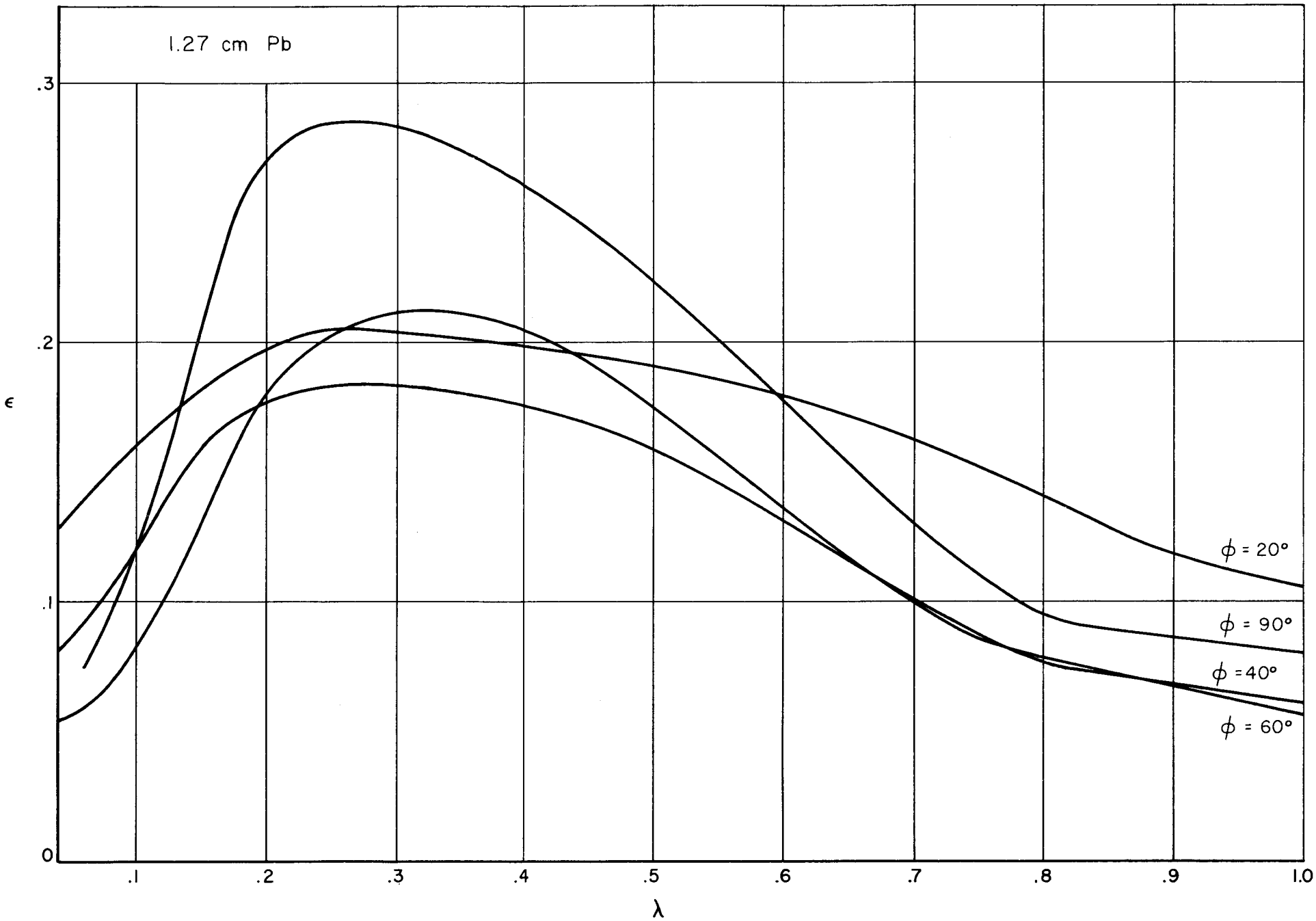

Fig. III-E-3. ε vs Wavelength (λ) in Compton Units for Several Grazing Angles of Incidence (ϕ) for a Lead Slab 1.27 cm Thick.

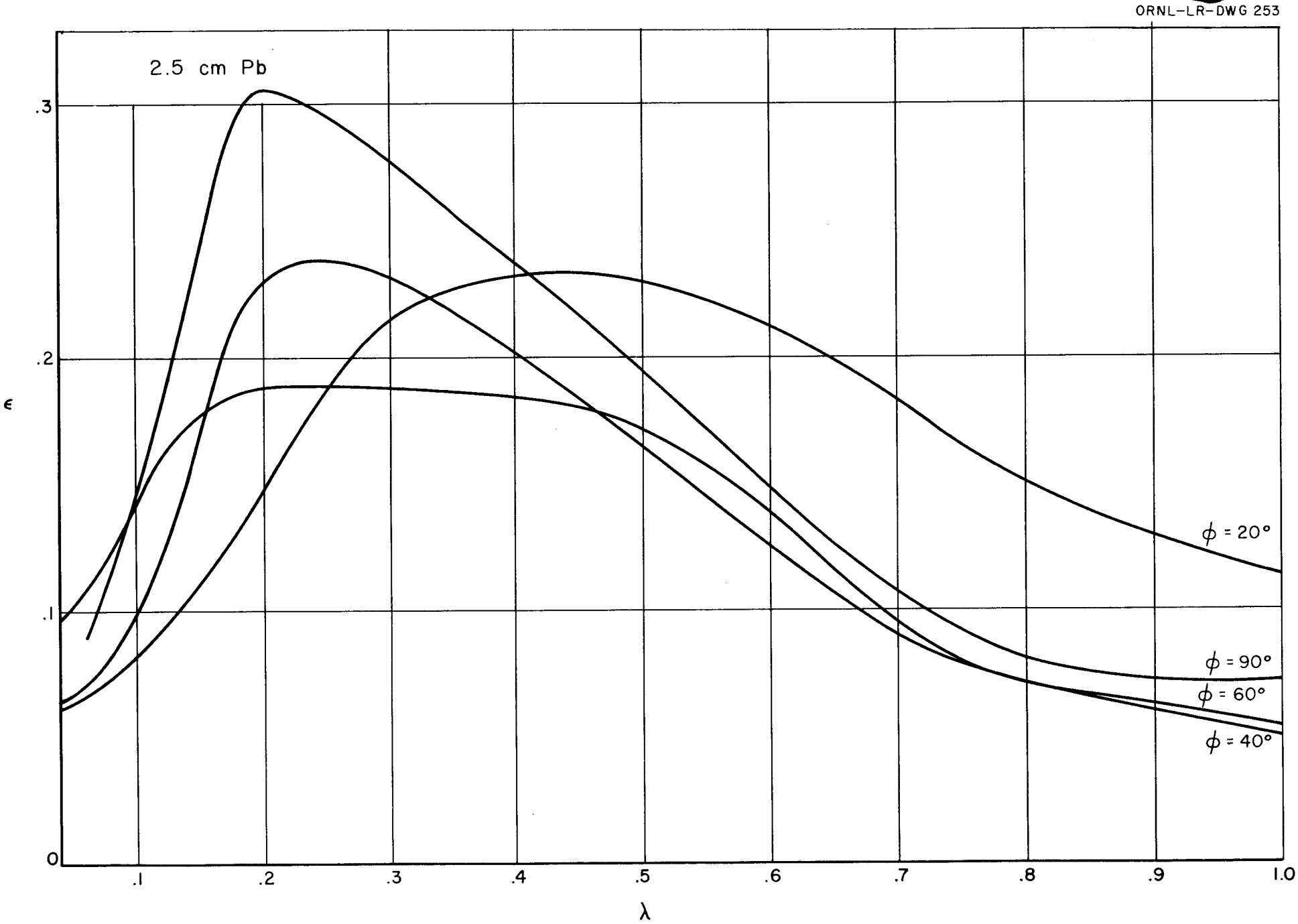

Fig. III-E-4. ε vs Wavelength (λ) in Compton Units for Several Grazing Angles of Incidence (φ) for a Lead Slab 2.54 cm Thick.

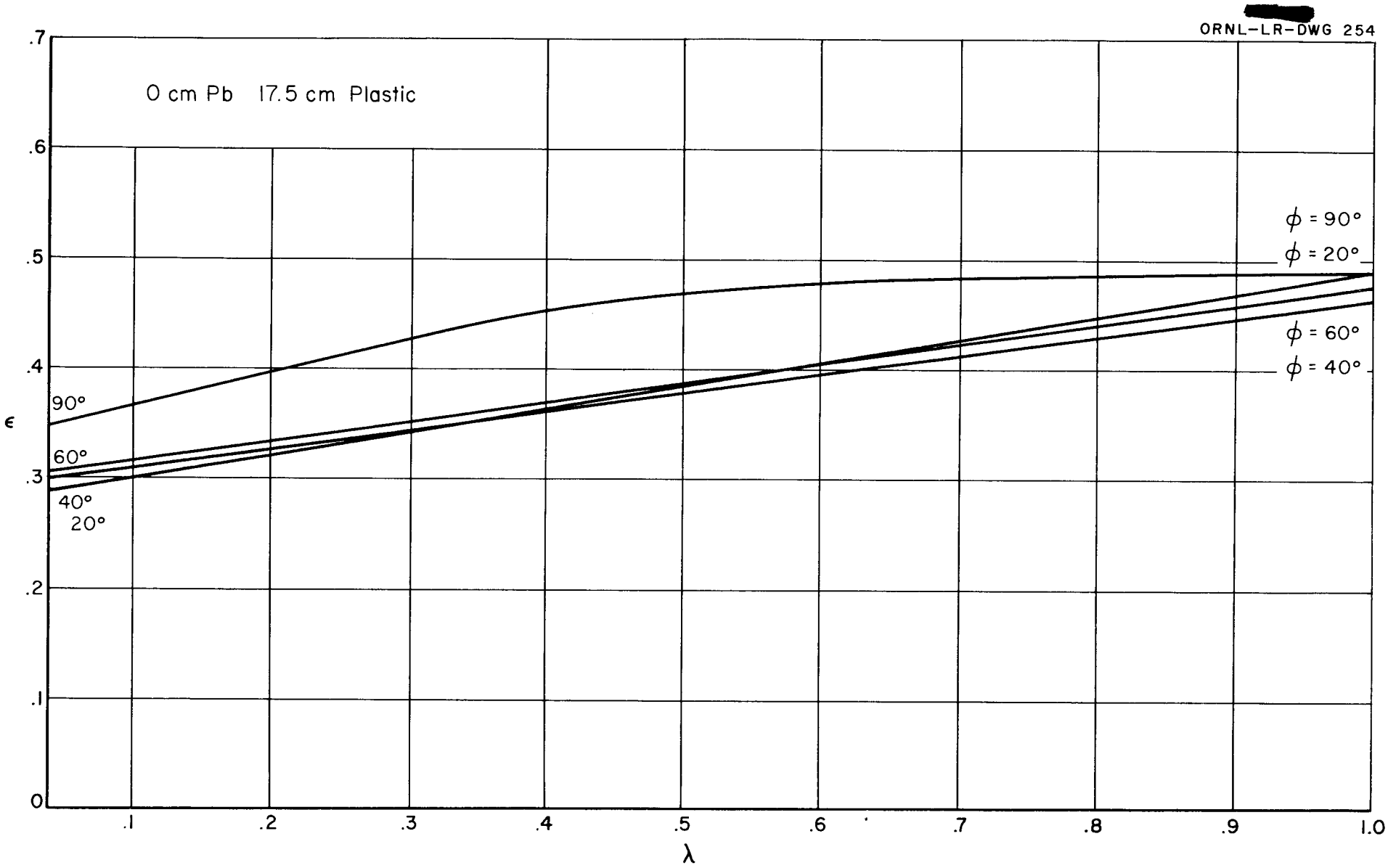

Fig. III–E–5. ϵ vs Wavelength (λ) in Compton Units for Several Grazing Angles of Incidence (ϕ) for a Plastic Slab (Density 0.90) 17.5 cm Thick.

[redacted]

ORNL-LR-DWG 255

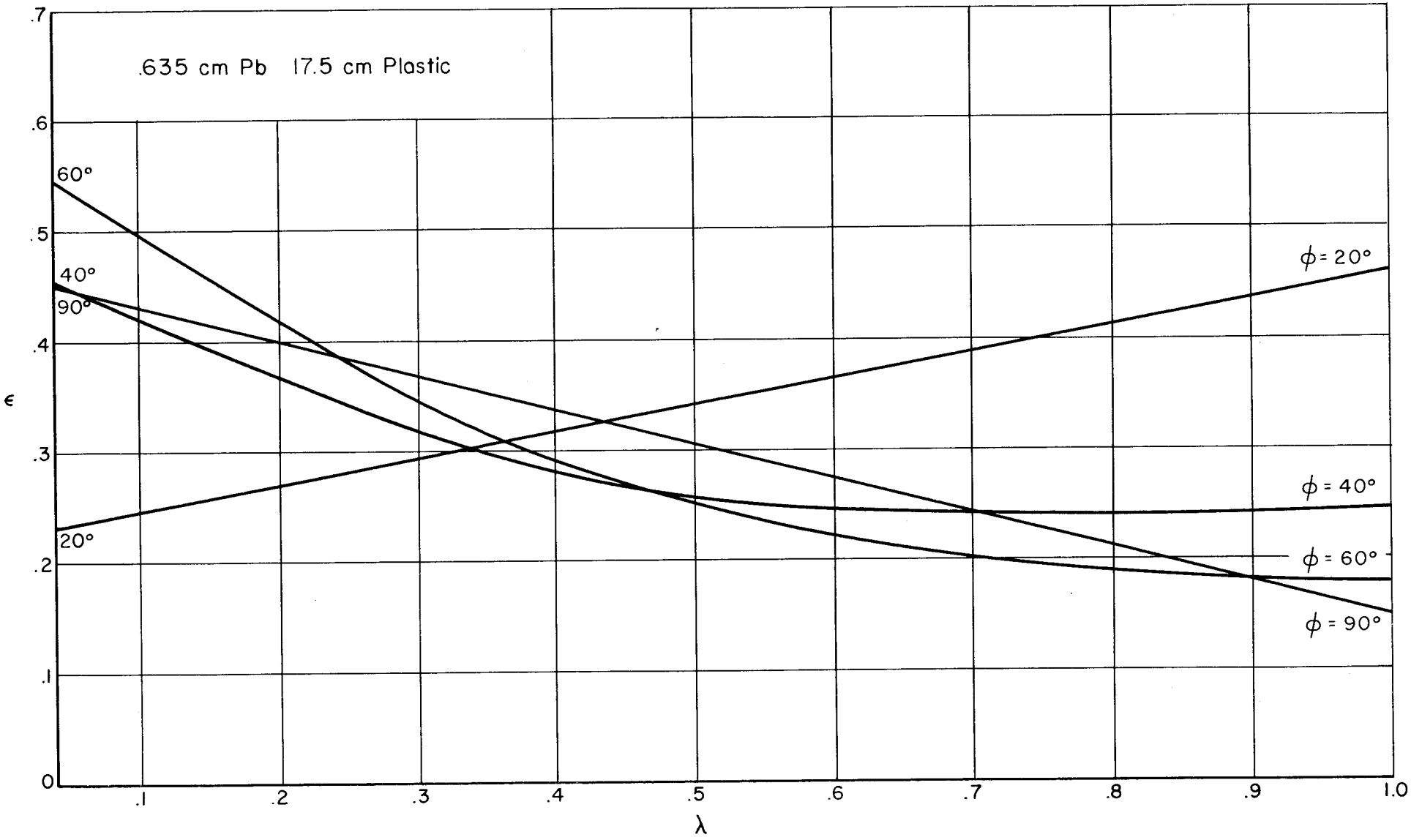

Fig. III-E-6. ϵ vs Wavelength (λ) in Compton Units for Grazing Angles of Incidence (ϕ) for a Plastic Slab (Density 0.90) 17.5 cm Thick Backed by a Lead Slab 0.635 cm Thick.

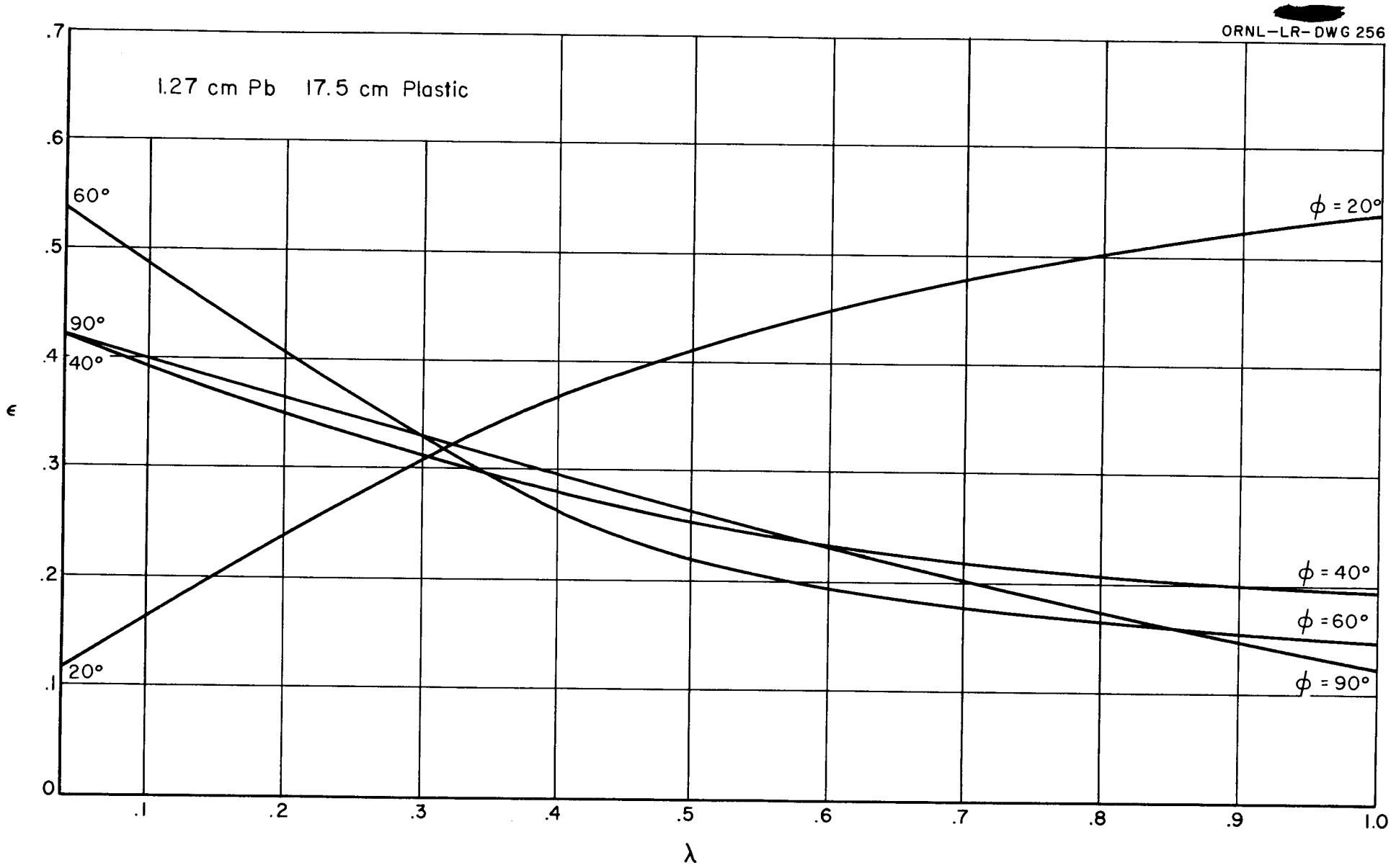

Fig. III-E-7. ε vs Wavelength (λ) in Compton Units for Several Grazing Angles of Incidence (φ) for a Plastic Slab (Density 0.90) 17.5 cm Thick Backed by a Lead Slab 1.27 cm Thick.

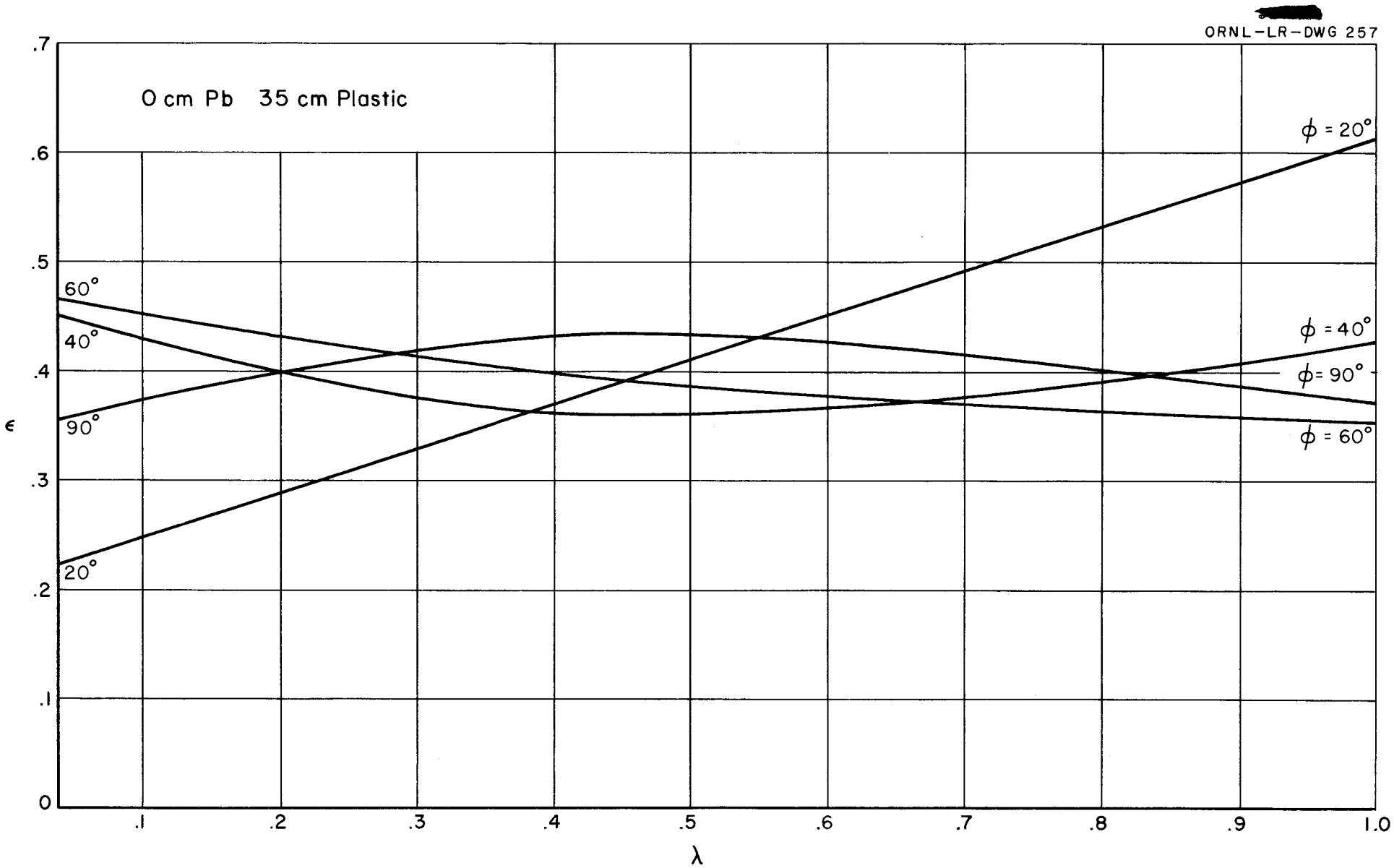

Fig.III-E-8. ϵ vs Wavelength (λ) in Compton Units for Several Grazing Angles of Incidence (ϕ) for a Plastic Slab (Density 0.90) 35 cm Thick.

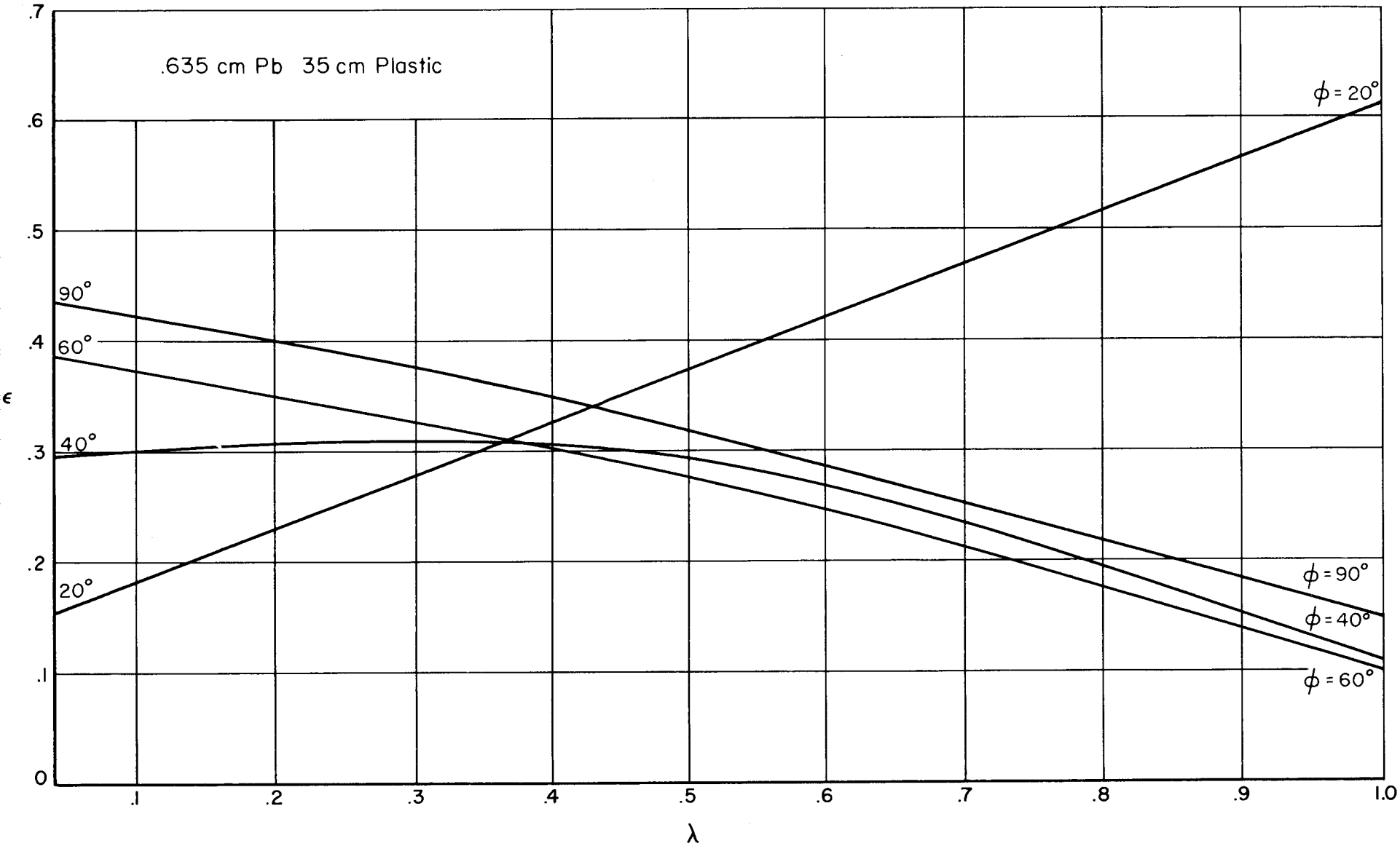

Fig. III-E-9 ϵ vs Wavelength (λ) in Compton Units for Several Grazing Angles of Incidence (ϕ) for a Plastic Slab (Density 0.90) 35 cm Thick Backed by a Lead Slab 0.635 cm Thick.

[redacted]

ORNL-LR-DWG 259

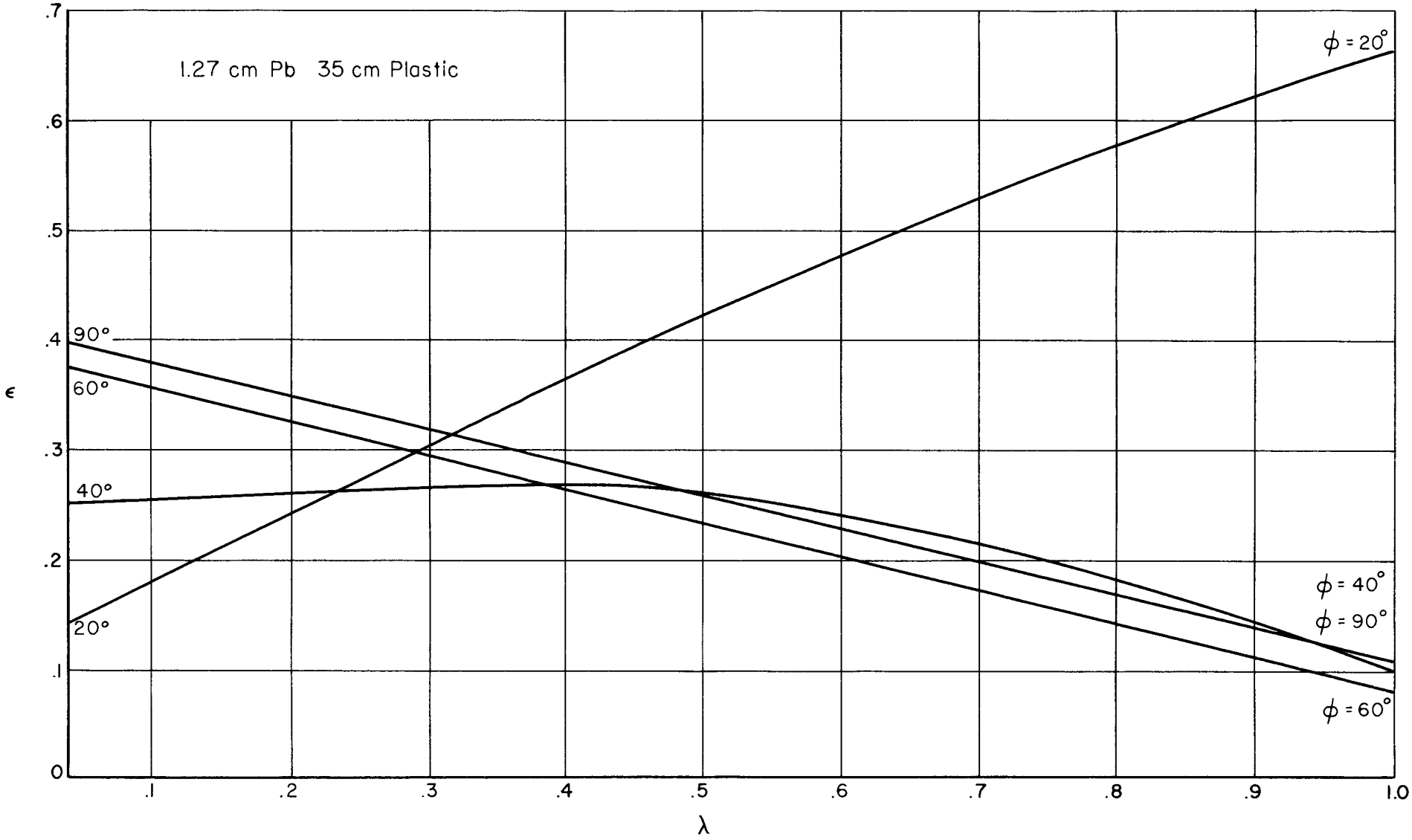

Fig. III-E-10 ϵ vs Wavelength (λ) in Compton Units for Several Grazing Angles of Incidence (ϕ) for a Plastic Slab (Density 0.90) 35 cm Thick Backed by a Lead Slab 1.27 cm Thick.

[redacted]

ORNL-LR-DWG 260

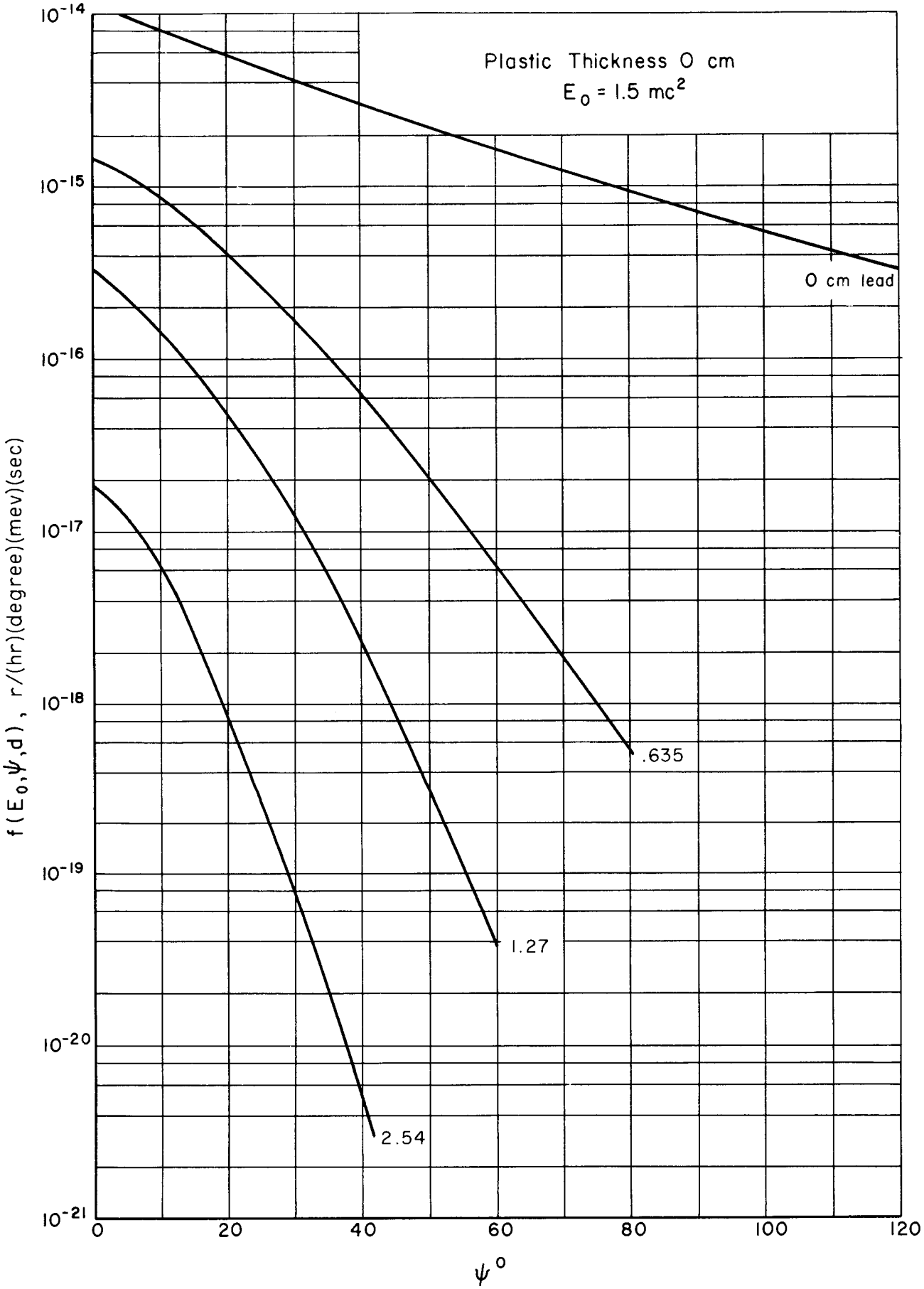

Fig. III-E-11 $f(E_0, \psi, d)$ as a Function of Emergent Angle (ψ) for Crew Compartment Side Walls.

With these input data the response function $f(\psi)$ was calculated from Eq. (2) by numerical integration. Figures III-E-11 through III-E-22 are plots of f vs. ψ for each initial energy and shield composition. For large plastic thicknesses the uncertainty in f may be more than 50%. In most instances it will be considerably less. Once the energy and angular distribution of the photons emerging from the reactor is known, the single air-scattered dose can be calculated from Eq. (1).

At the present time there is no satisfactory way of determining the energy and angular distribution for any given reactor design. With regard to the angular distribution it is current engineering practice to replace the reactor and its shield by a point isotropic source, shadowed through some range of ψ by an opaque shield (Fig. III-E-23). Under these assumptions the distribution is given by

$$\begin{aligned} N(\psi) &= 0 \qquad\qquad , \psi \leq \psi_o \\ &= \frac{2}{1 + \cos \psi_o} \quad , \psi > \psi_o \end{aligned} \qquad (6)$$

It has also been the practice to assume all the emergent photons are at one energy E_o. Under this assumption, and with an ideal shadow shield of angle ψ_o, the single-scattered dose of Eq. (1) reduces to

$$I(D,E_o) = \frac{2S(E_o)}{1 + \cos\psi_o} \int_{\psi_o}^{\pi} f\,(E_o,\psi,d,D)\, d\psi$$

where $S(E_o)$ is the total energy radiated by the <u>shielded</u> source per unit time. In terms of S_o, the total energy radiated by the <u>unshielded</u> <u>isotropic</u> source, S is given by

[redacted]

ORNL-LR-DWG 261

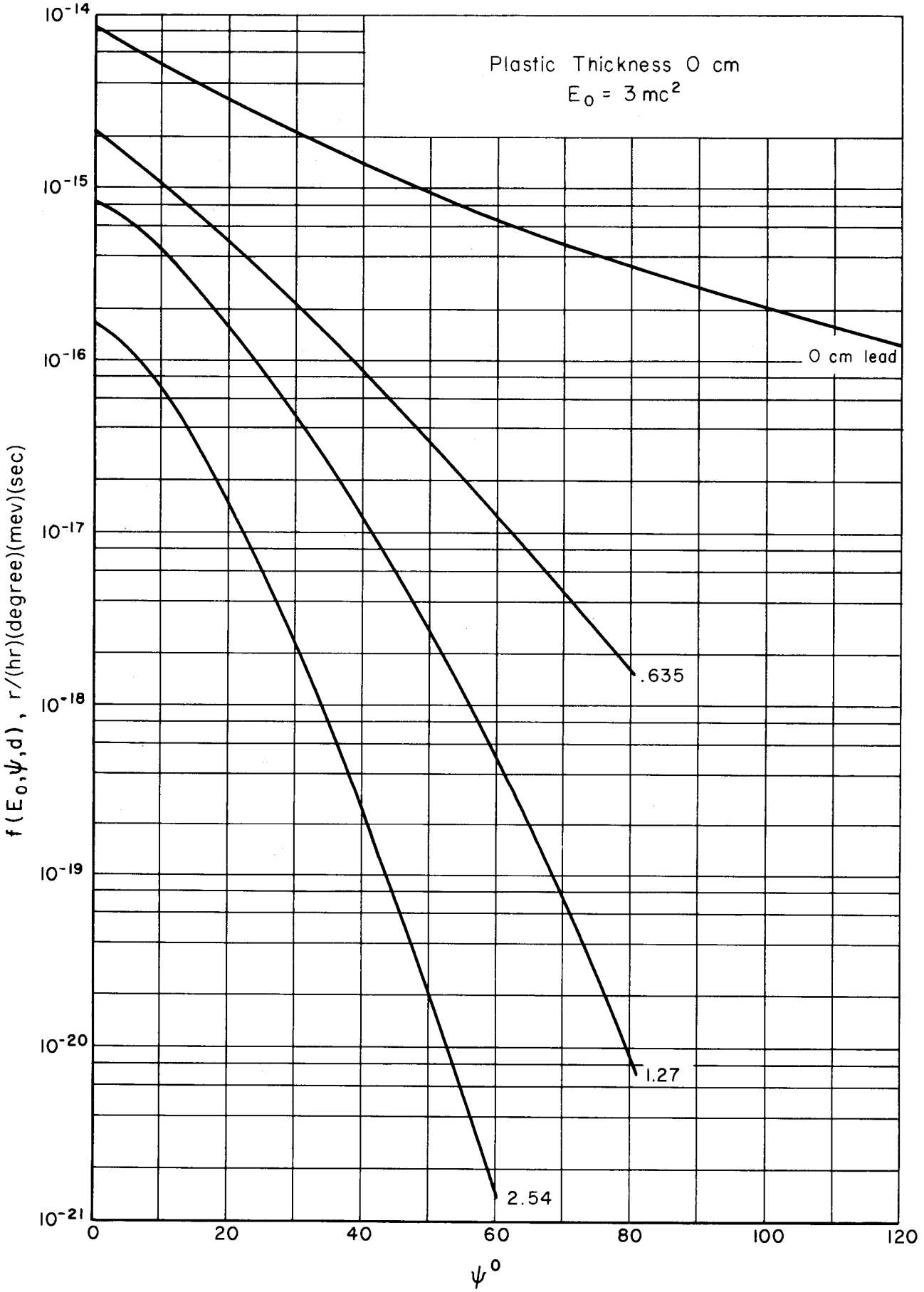

Fig. III-E-12 $f(E_0, \psi, d)$ as a Function of Emergent Angle (ψ) for Crew Compartment Side Walls.

[redacted]

ORNL-LR-DWG 262

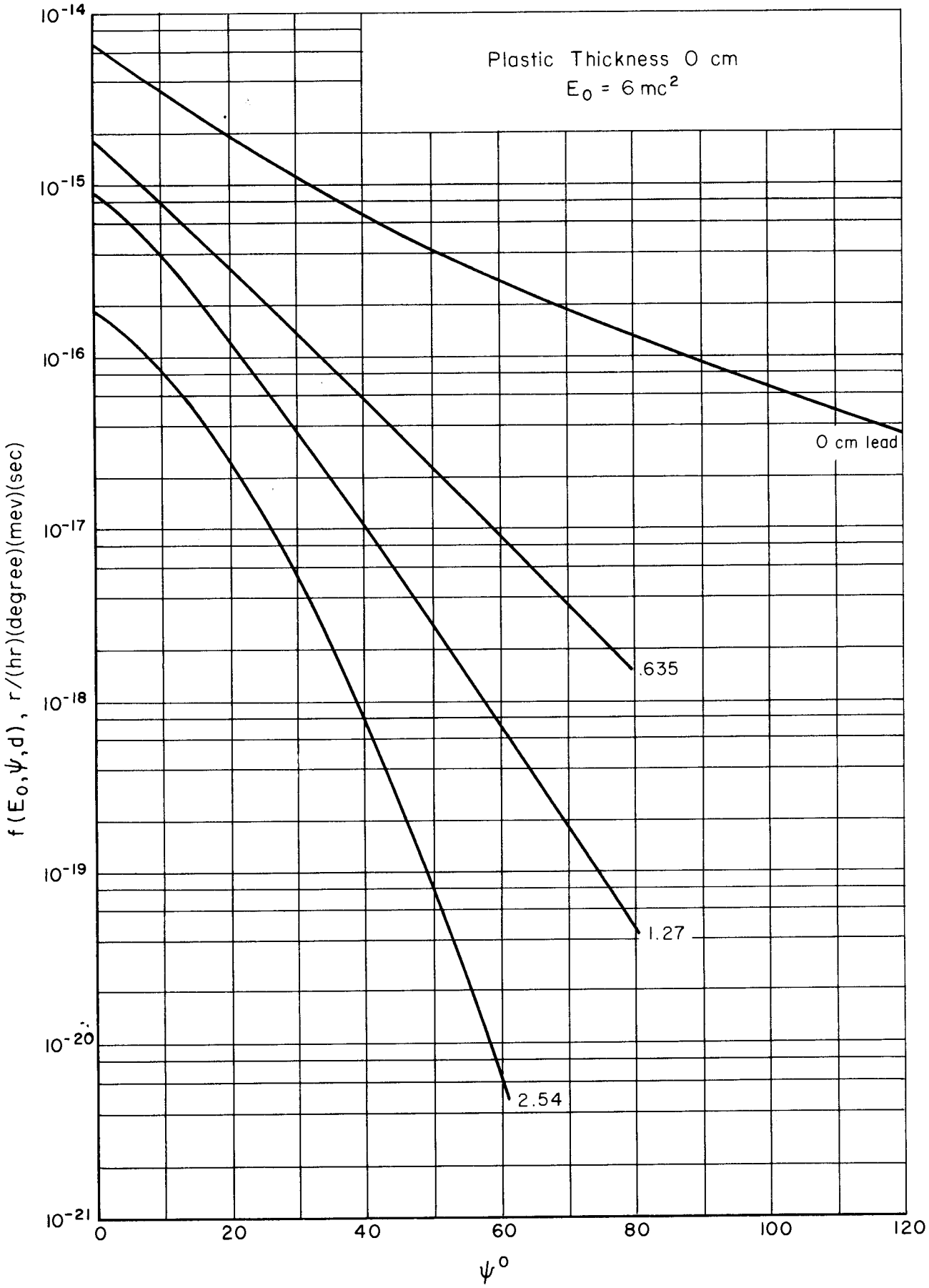

Fig. III-E-13 $f(E_0, \psi, d)$ as a Function of Emergent Angle (ψ) for Crew Compartment Side Walls.

[redacted]
ORNL-LR-DWG 263

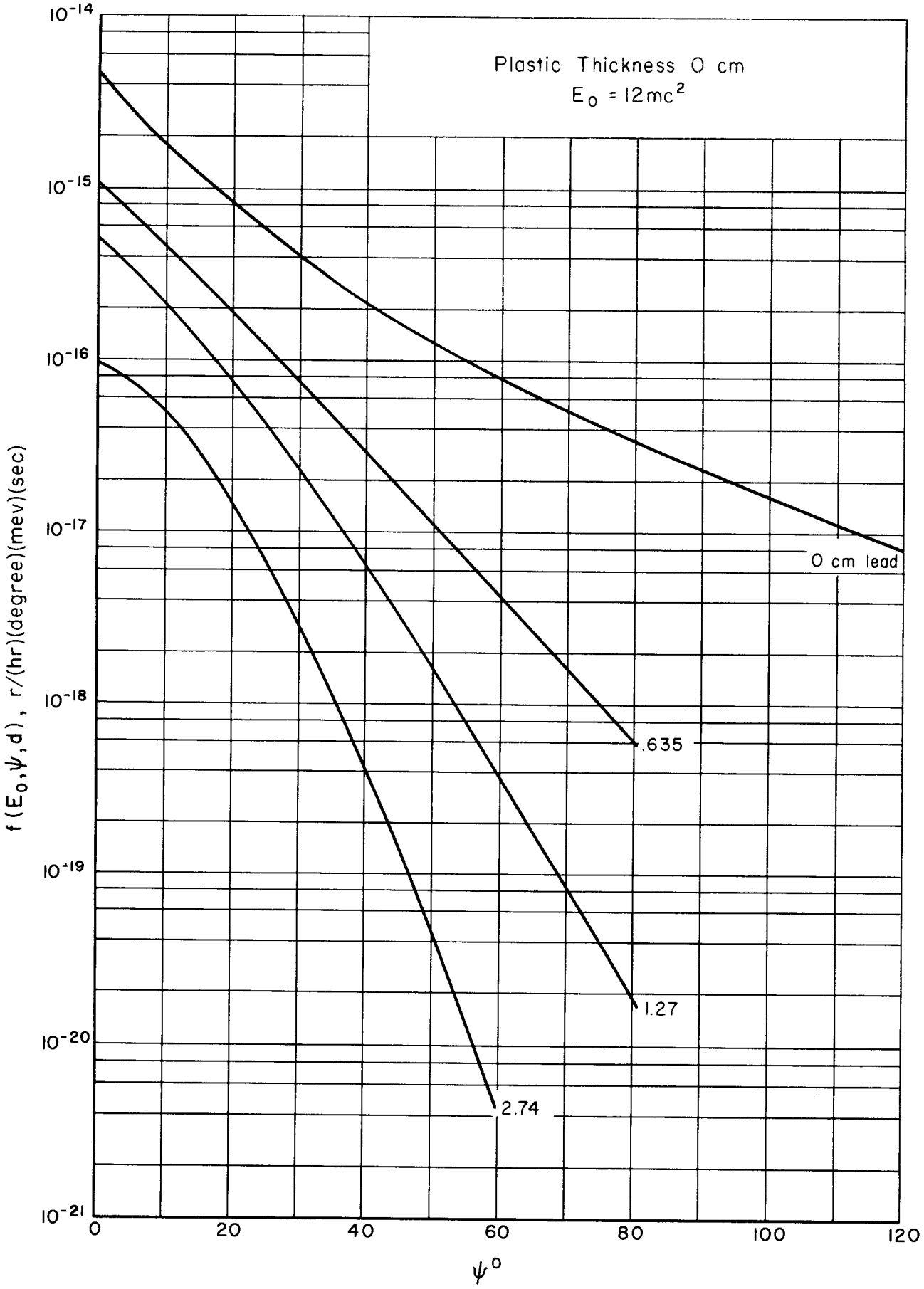

Fig. III-E-14 $f(E_0, \psi, d)$ as a Function of Emergent Angle (ψ) for Crew Compartment Side Walls.

[redacted]
ORNL-LR-DWG 264

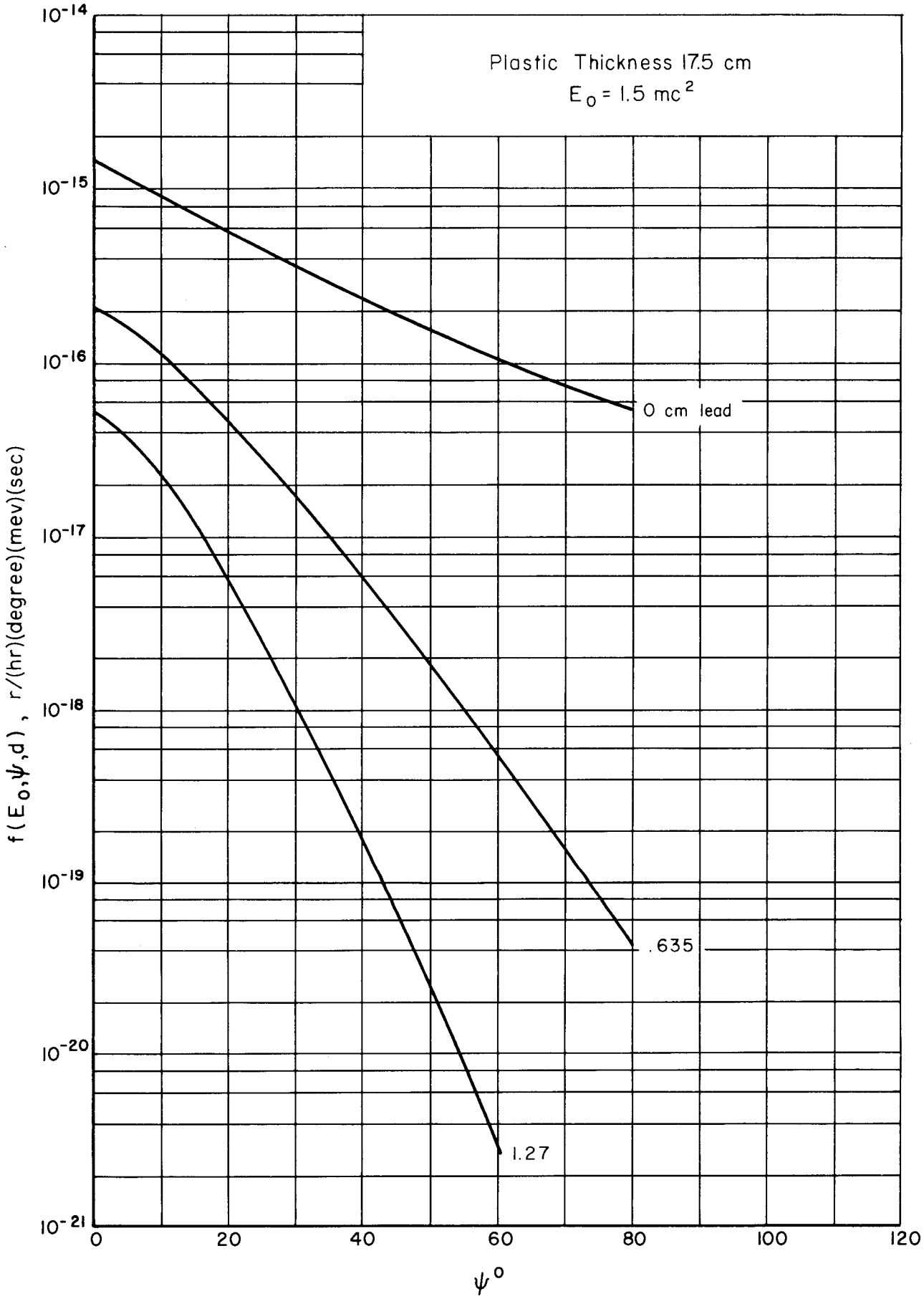

Fig. III-E-15 $f(E_0, \psi, d)$ as a Function of Emergent Angle (ψ) for Crew Compartment Side Walls.

[redacted]
ORNL-LR-DWG 265

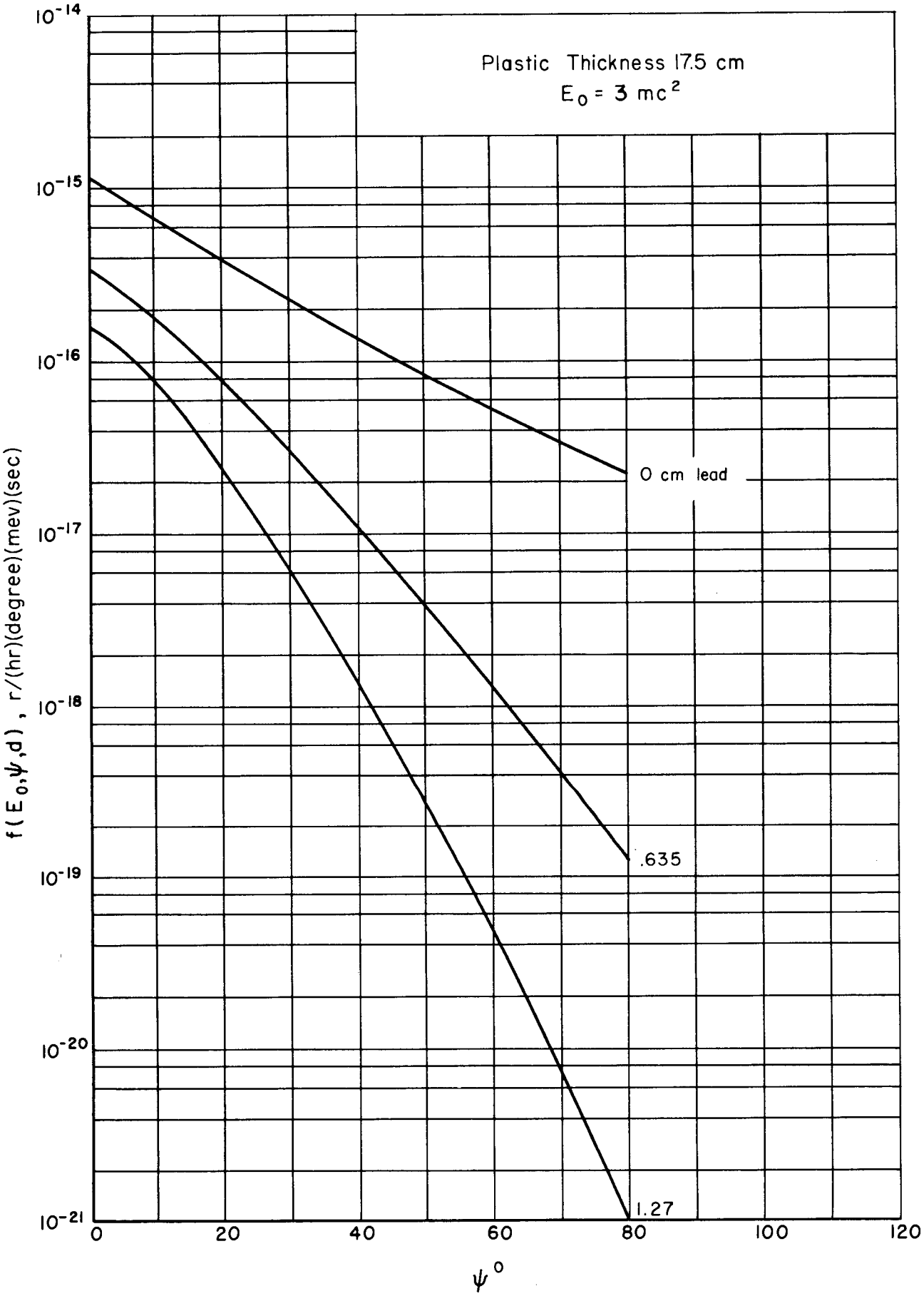

Fig. III-E-16 $f(E_0, \psi, d)$ as a Function of Emergent Angle (ψ) for Crew Compartment Side Walls.

[redacted]

ORNL-LR-DWG 266

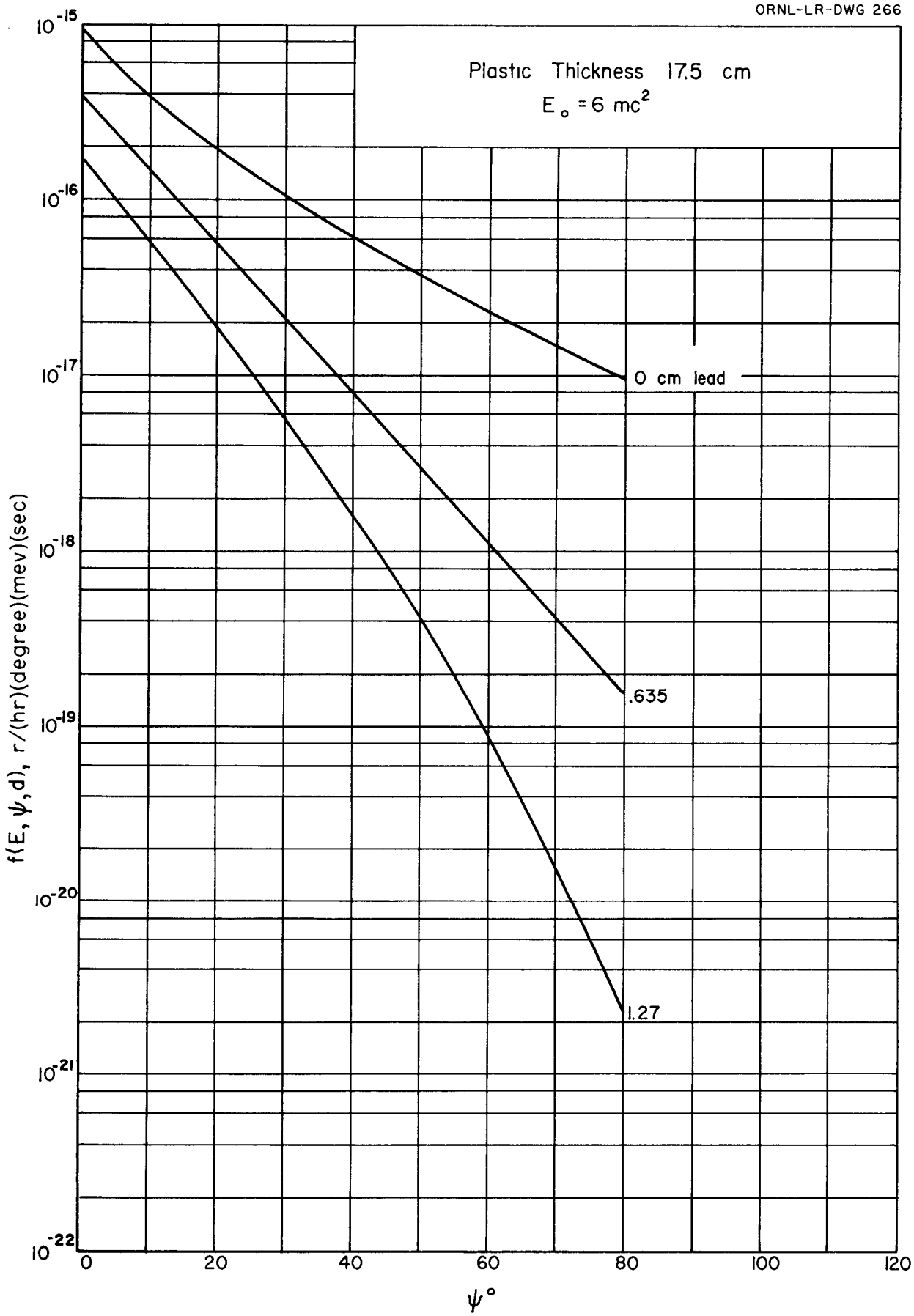

Fig. III-E-17. $f(E_0, \psi, d)$ as a Function of Emergent Angle (ψ) for Crew Compartment Side Walls.

[redacted]

ORNL-LR-DWG 267

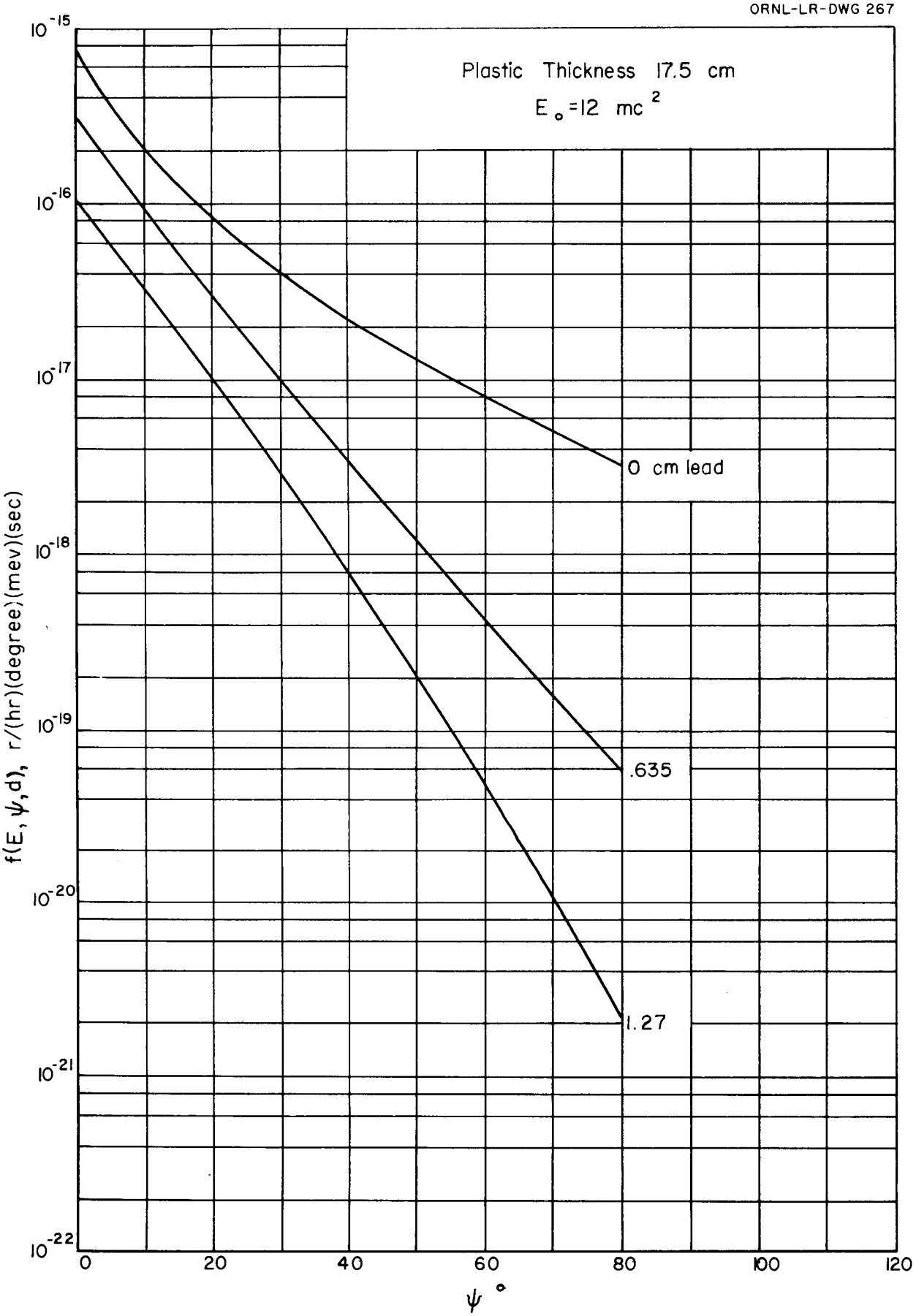

Fig. III-E-18. $f(E_0, \psi, d)$ as a Function of Emergent Angle (ψ) for Crew Compartment Side Walls.

[redacted]

ORNL-LR-DWG 268

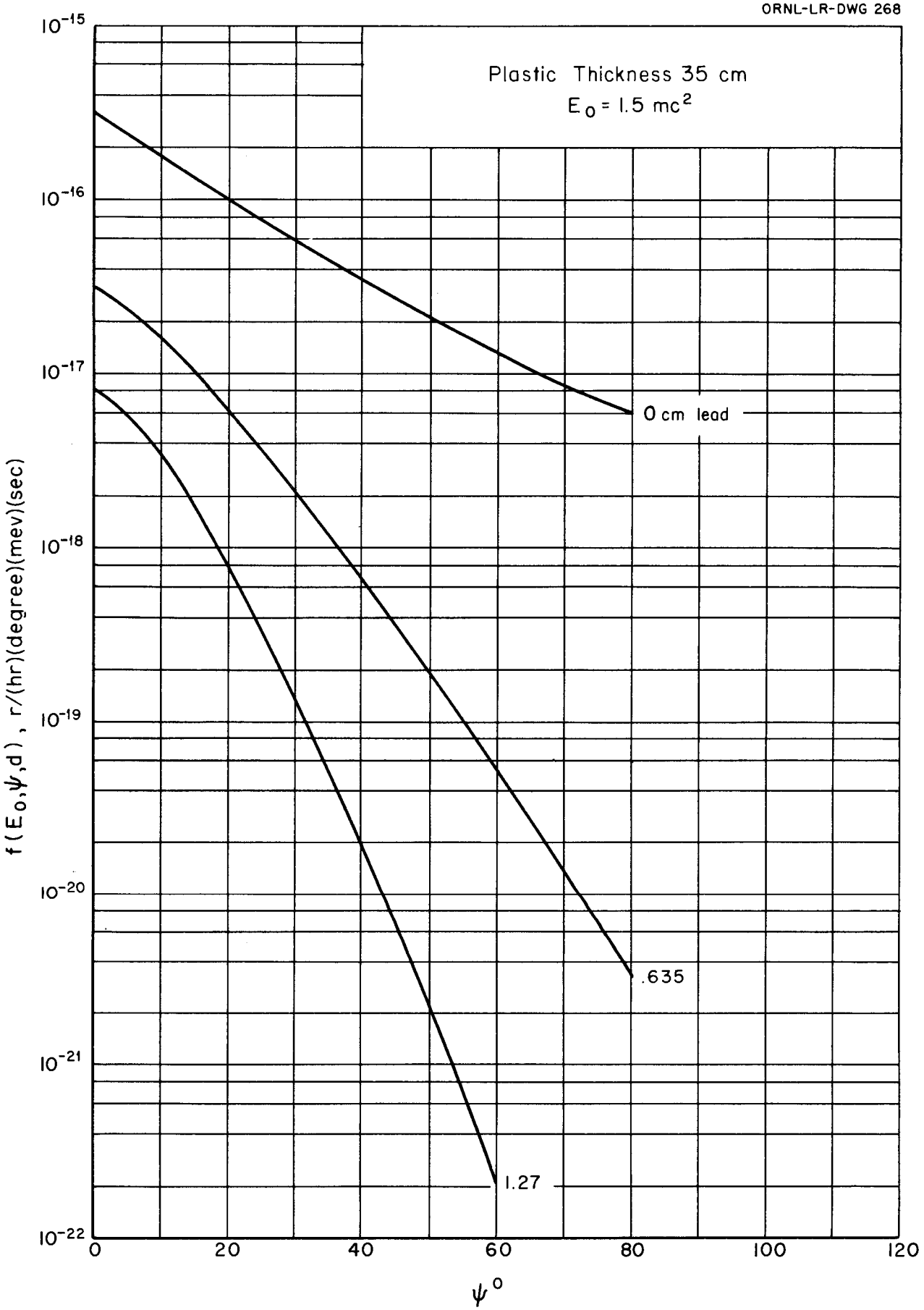

Fig. III-E-19. $f(E_0, \psi, d)$ as a Function of Emergent Angle (ψ) for Crew Compartment Side Walls.

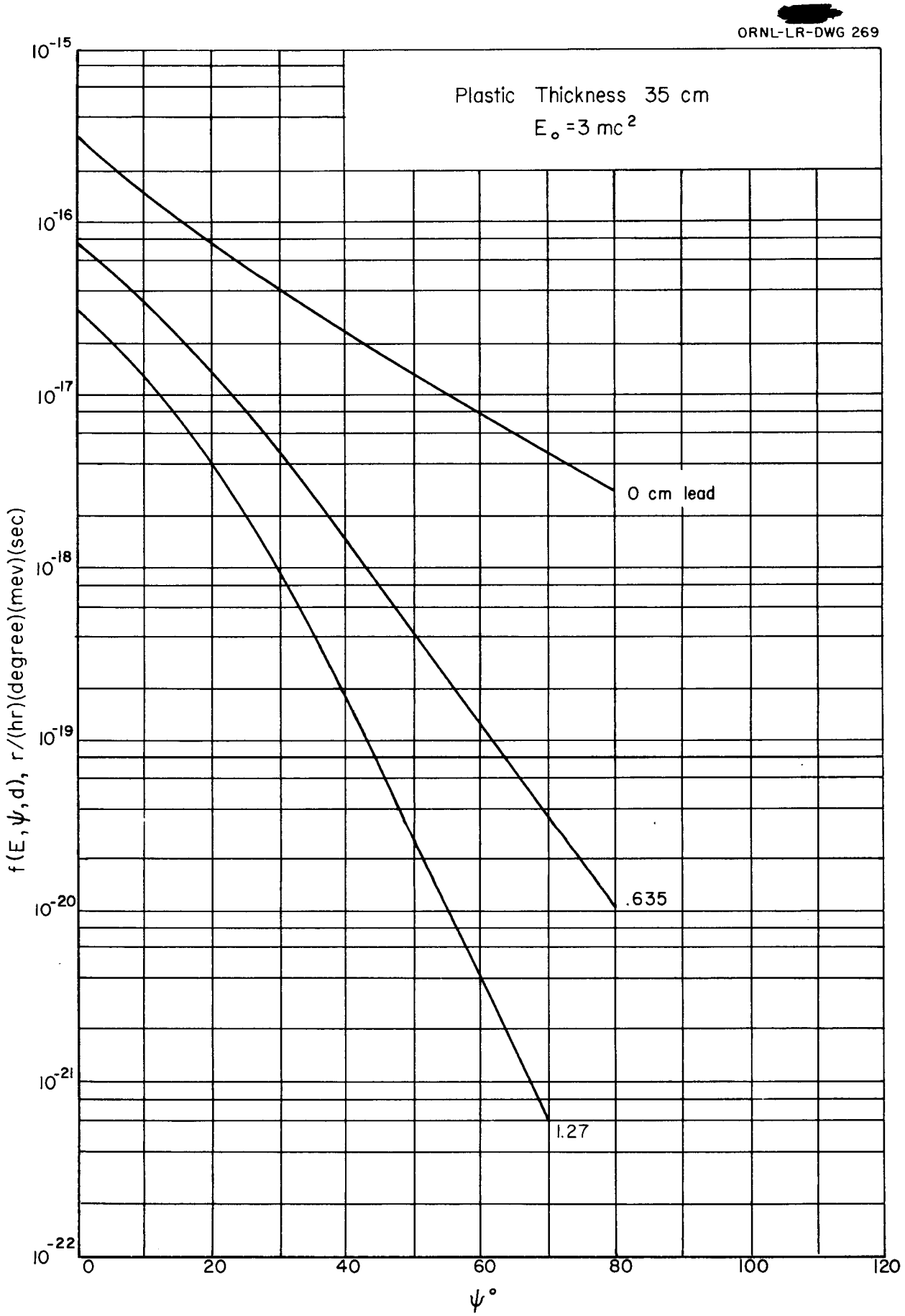

Fig. III-E-20. $f(E_0, \psi, d)$ as a Function of Emergent Angle (ψ) for Crew Compartment Side Walls.

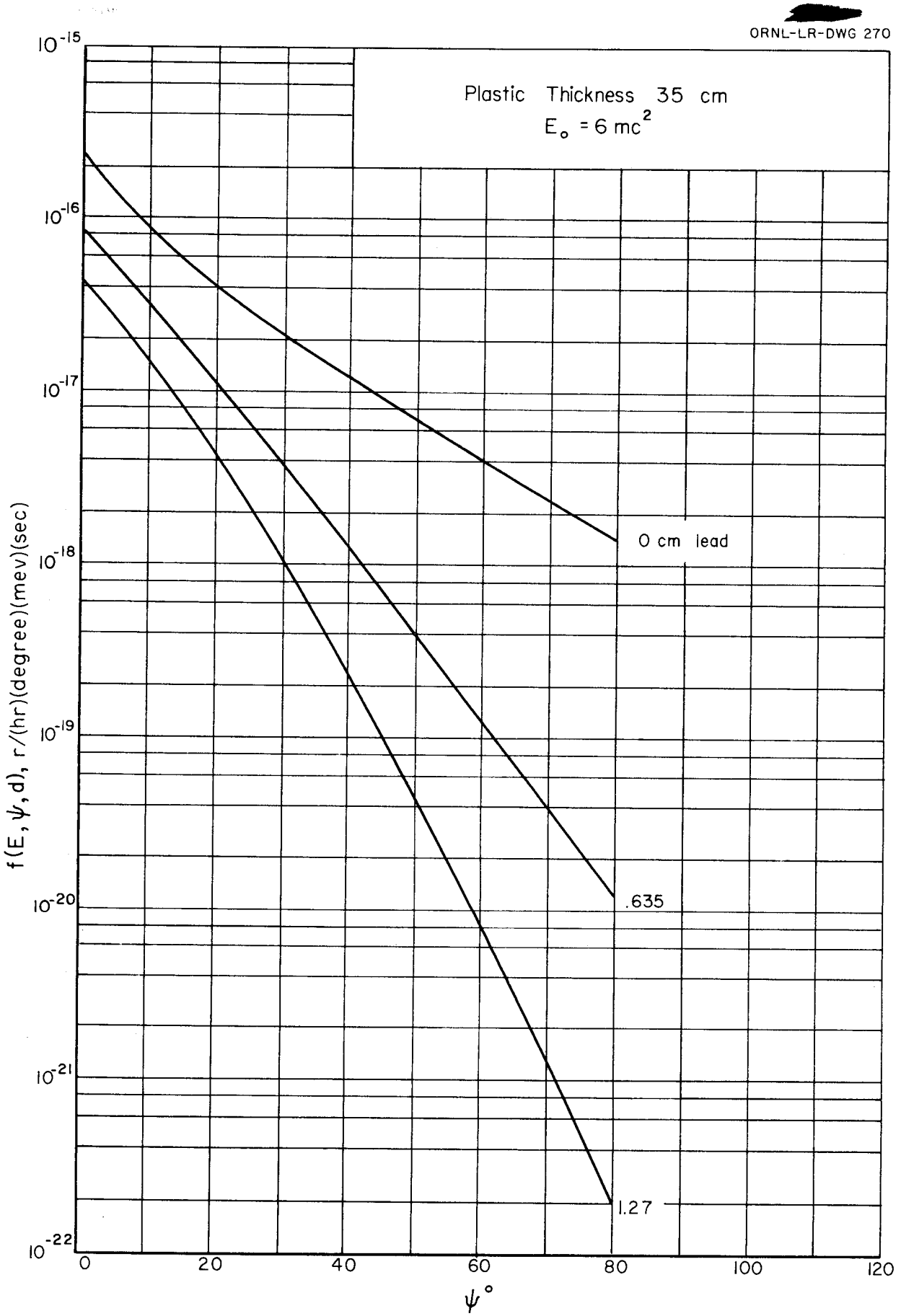

Fig. III-E-21. $f(E_0, \psi, d)$ as a Function of Emergent Angle (ψ) for Crew Compartment Side Walls.

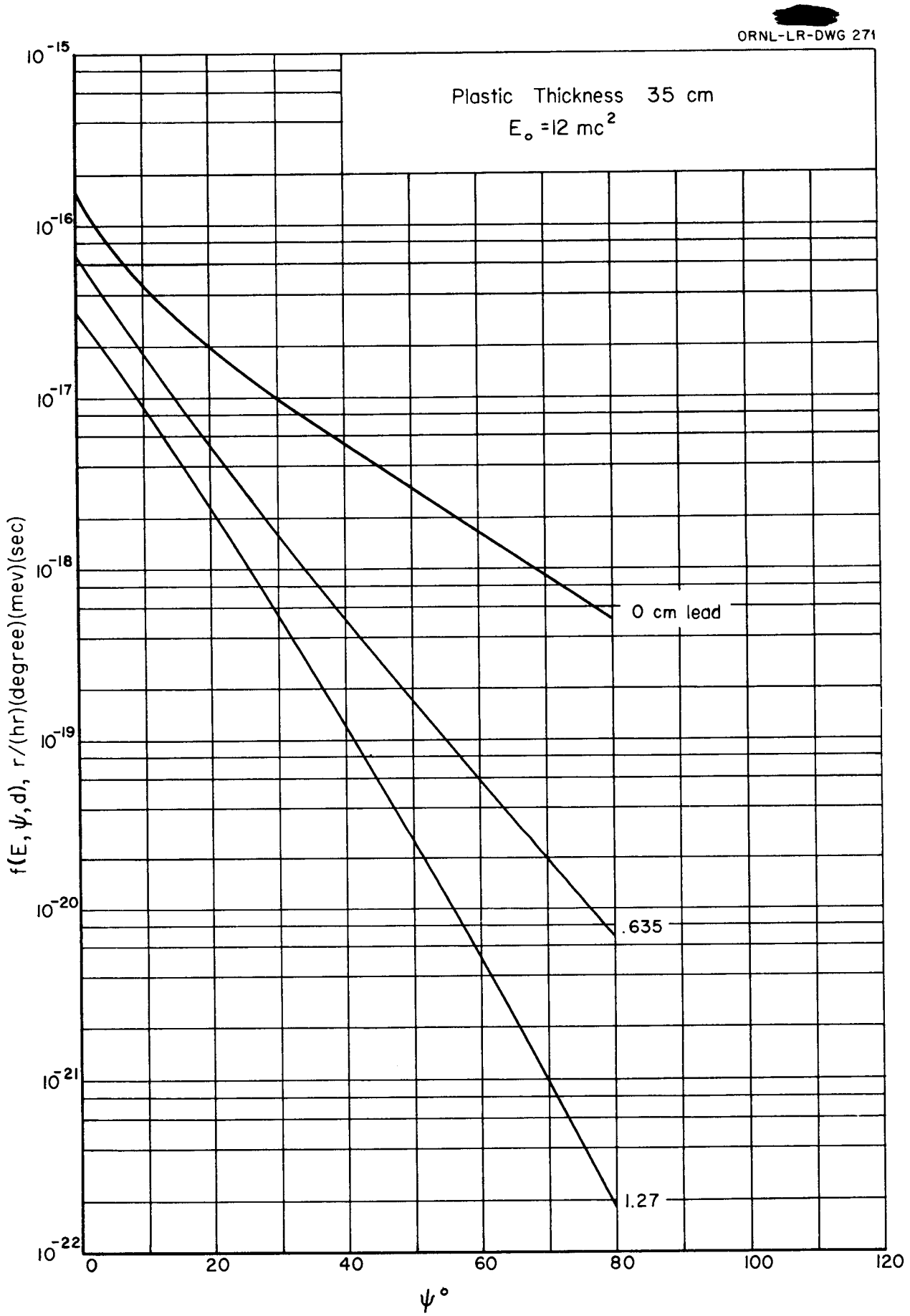

Fig. III-E-22. $f(E_0, \psi, d)$ as a Function of Emergent Angle (ψ) for Crew Compartment Side Walls.

[redacted]
ORNL-LR-DWG 272

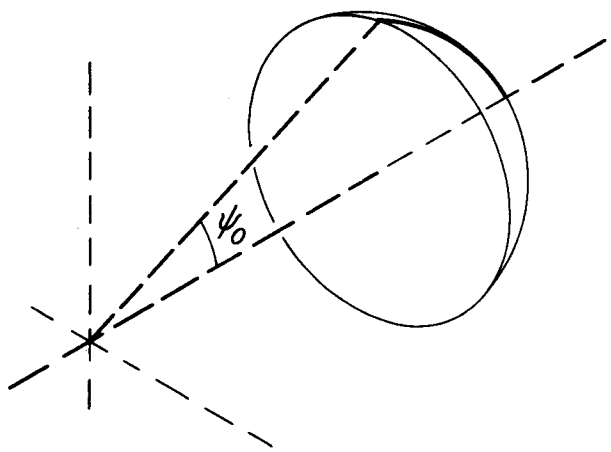

Fig. III-E-23. Ideal Shadow Shield Geometry.

$$S = \frac{1 + \cos \psi_o}{2} S_o$$

It is therefore convenient to express the scattered dose in terms of the isotropic source strength S_o, leading to the expression

$$I(D,E_o) = S_o \int_{\psi_o}^{\pi} f(E_o,\psi,d,D)\, d\psi \qquad (7)$$

As an example, Figs. III-E-24 present $I(D,E_o)/S_o$ as a function of E_o for $\psi_o = 10^o$, 20°, and 30° and for a crew shield composed of lead and plastic. At low energies the high photoelectric absorption of lead takes an increasingly large bite into the scattered dose. For thicknesses of lead which are not too great it is seen that the dose per unit energy radiated is substantially constant from 1.5 to 6 Mev. Maienschein[12] has shown that for a typical design most of the emitted energy is concentrated in this region, with a peak at about 2 to 3 Mev. The assumption of a monoenergetic source around 3 Mev is therefore reasonable for the scattered dose calculation.

It is difficult to decide for any given shadow shield what is the best choice for the equivalent ideal shield angle ψ_o. In only one specific design is the angular distribution known well enough to determine what the angle should be to give the correct answer.[13] The shadow shield in question subtended a half angle of about 60° at the center of the reactor core, with every point in the core subtended by at least 45°. The detailed calculations gave a result corresponding to an equivalent shadow shield angle closer to 60° than to 45° for an <u>unshielded receiver</u>. However these angles are much

(12) F. C. Maienschein, "Gamma-Ray Spectral Measurements with the Divided Shield Mockup," ORNL-CF-52-3-1 (March 3, 1952).
(13) F. Bly and F. C. Maienschein, "A Calculation of Gamma Radiation Reaching the ANP-53 Crew Shield," ORNL-CF-53-5-117 (May 23, 1953).

[redacted]

ORNL-LR-DWG 184

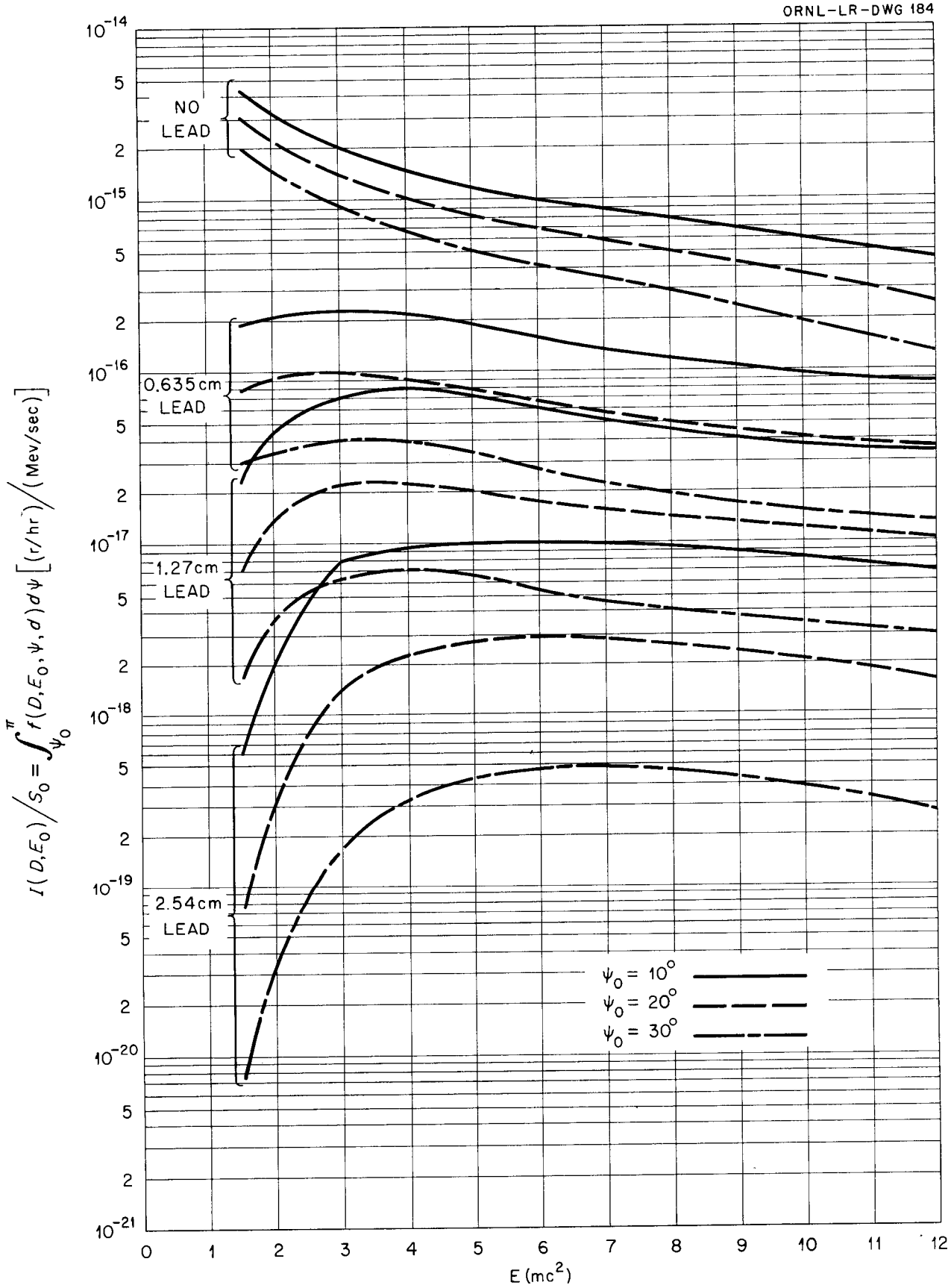

Fig. III-E-24a. Gamma-Ray Single Scattered Dose for Several Ideal Shadow Shield Angles— 0-cm Plastic Thickness.

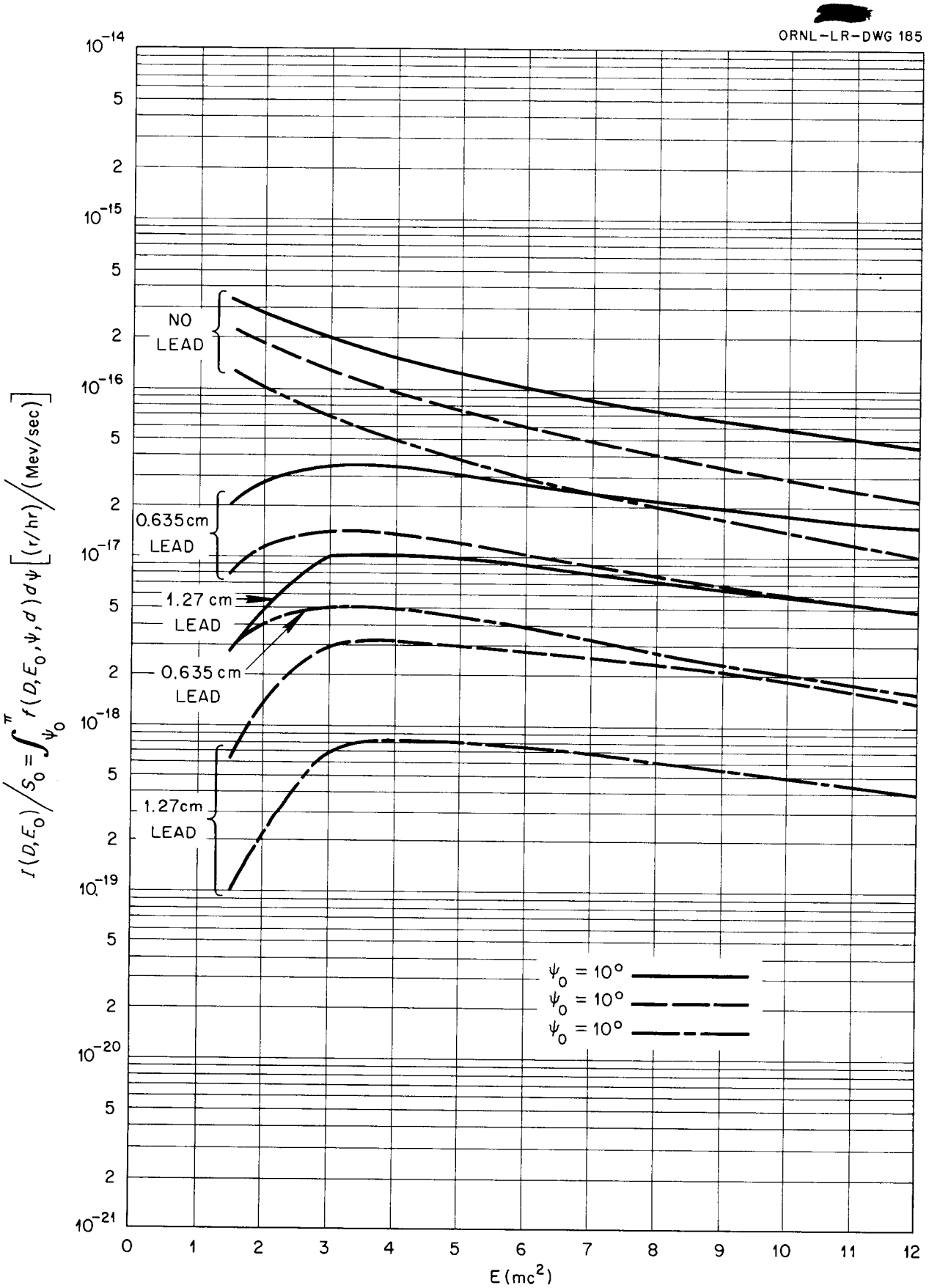

Fig. III-E-24b. Gamma-Ray Single Scattered Dose for Several Ideal Shadow Shield Angles — 17.5-cm Plastic Thickness.

[redacted]

ORNL-LR-DWG 186

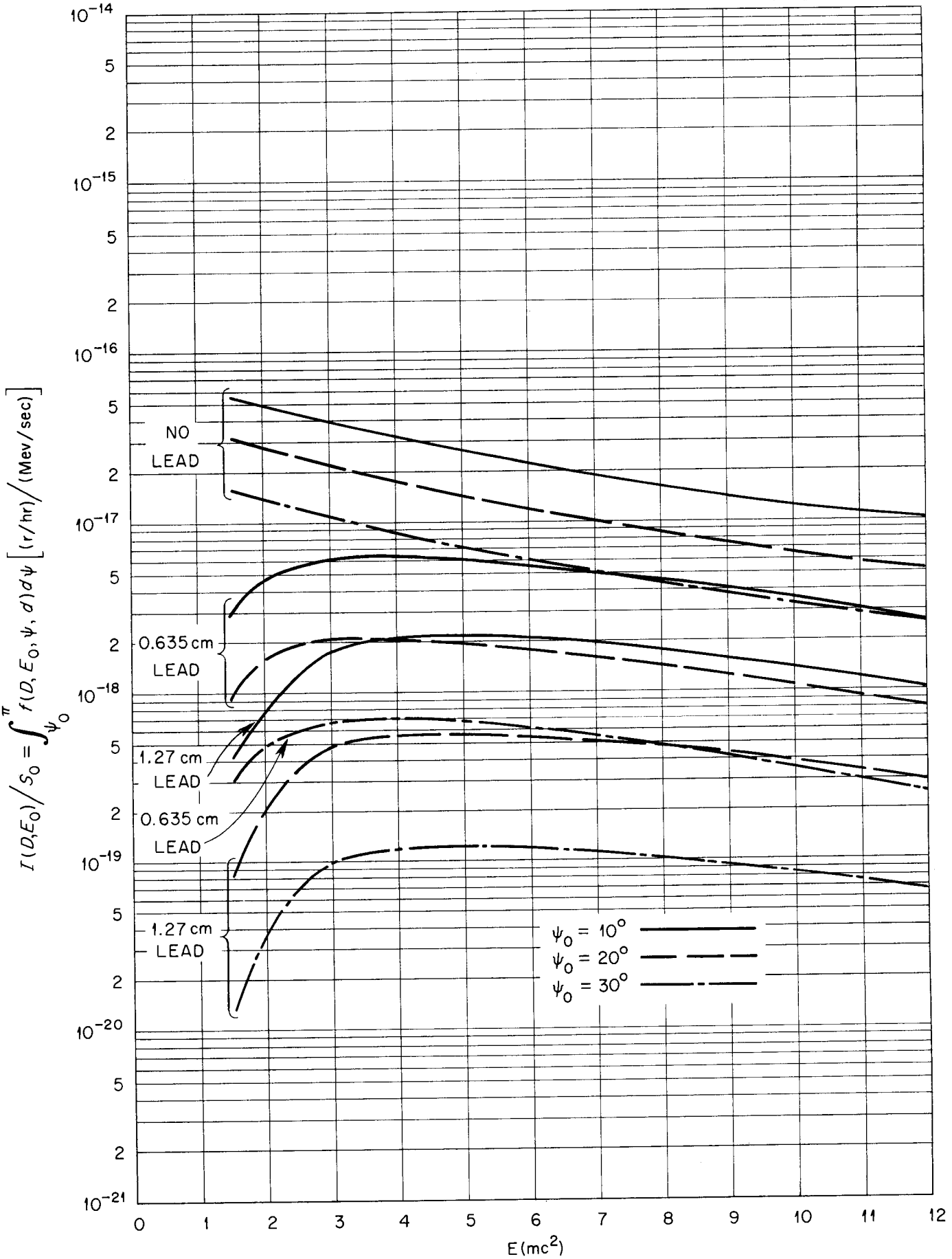

Fig III-E-24c. Gamma-Ray Single Scattered Dose for Several Ideal Shadow Shield Angles — 35-cm Plastic Thickness.

larger than are likely to be used in actual designs. Further, the effect of crew compartment shielding will be to emphasize the effect of streaming around the shadow shield, and thus reduce the effective angle. For design purposes it seems best to take a reasonably conservative value, e.g., the least angle subtended at any point in the core. This is only reasonably conservative since there may be sources of gamma radiation outside the core--capture gamma rays, circulating fuel, activated coolants, etc. Where such external sources are likely to be considerable in magnitude and volume extent, the shield should be extended, perhaps with reduced thickness.

There are other reasons for tapering the thickness of the shadow shield. At small angles the thickness is likely to be determined by the shielding requirements for the direct beam, and this is usually more than is needed for air scattering purposes. For larger angles the direct beam plays a smaller role in determining the thickness, which can probably be reduced somewhat. Also, as the angle increases, the effectiveness for air scattering of a photon emitted in the given direction decreases, and less shielding is needed. One should not go too far in the tapering, however, since scattering and streaming of the photons in the hydrogenous shield will largely upset any angular distribution calculations based on direct ray path geometries. For example, even with the large shadow shield angle of 60°, streaming around the edges of the shield contributed more to the direct beam than the straight through radiation. It clearly does not pay to make even the center of the shield too black. Either more shielding should be put on the rear of the crew compartment, or the shadow shield extended to large angles by thin "flaps."

Beyond mention of these general points it is impossible to give explicit directions as to how to design the shadow shield, or what angular distribution

should be chosen. Each reactor design is a species by itself, and the individual designer must work out his own procedures. All too often the only guidance available must be his own physical and engineering intuition.

Air attenuation has been included in the calculations. Experiments on air scattering at Convair,[14] indicate that multiple scattering may compensate for air attenuation. It might therefore be preferable to omit the A term in future calculations. However, the effect of air scattering is small if the shadow shield angle is not too large. With an unshielded receiver and isotropic source, and D = 15 m, air attenuation reduces the scattered dose by 8% at 6 Mev, 16% at 3 Mev, and 33% at 0.5 Mev. Except at the low source energy this change is too small to be important for design purposes. A shadow shield on the source increases the effect somewhat, because the average scattering angle is larger. However, shielding on the crew compartment has the opposite effect, since it favors the more penetrating scattered radiation. Check calculations indicate that the figures for air attenuation with unshielded source and detector can be taken as upper limits for reasonable designs. In fact with appreciable side shielding, at 3 Mev, 10% seems to be a more realistic assessment of air attenuation for D = 15 m.

While the results illustrated in Figs. III-E-11 through III-E-22 have been calculated for a reactor-crew separation of 15 m only, it is a relatively simple matter to adjust the values for other distances. From Eq. (2) it is seen that D enters only in the factor 1/D and in the exponential in the absorption from A. As we have seen, it is questionable whether the A term should be included at all. Hence the essential variation with D is contained in the geometrical 1/D factor. The dose at any distance D can therefore be taken as

(14) B. Leonard *et al.*, private communication.

equal to the dose at 15 m times 15/D over the region from 5 to 30 m with an error estimated to be less than $\pm$ 20%.

In addition to the air-scattered dose through the side walls of the crew compartment there will be contributions through the rear and the front walls of the compartment. At the rear wall the air scattering competes with the direct flux from the reactor and with the structure scattering, both of which are usually much larger than the air scattering term. It therefore seems worth while calculating this contribution only approximately, chiefly to satisfy oneself that it is small.

In principle, the only changes required in the formulas to calculate the rear wall air scattering is to replace C in Eq. (2) by

$$C = \exp - \left[\sum_i \mu_i d_i (1 - \epsilon_i) \sec\phi \right] \qquad \text{(Rear wall, } \phi < \pi/2)$$

and to change the upper limit in the integral in Eq. (2) to $\psi + \pi/2$ when ψ is less than $\pi/2$ (i.e., maximum angle of incidence is 90°). If one is interested in a rough upper limit one can easily approximate f. In actual shield designs the rear wall usually is quite thick to shield against the direct photons. Hence, the exponent in C is always large, and the decrease of C with ϕ is the most rapid variation of any of the functions in the integrand. An upper limit to f is given by expanding $\sec\phi$ as $(1 + \phi^2/2)$:

$$f(E_o,\psi,d,D) = \frac{n}{4DF} \sqrt{\frac{2\pi}{\sum_i \mu_i d_i (1 - \epsilon_i)}}\ \bar{A}(E_o,\psi,D)\ \frac{E(\psi)}{E_o}\ \sigma(\psi)\ \exp - \sum_i u_i d_i (1 - \epsilon_i)$$

where it should be kept in mind μ_i and ϵ_i are functions of E and therefore of ψ. To obtain some idea of the magnitude of the rear wall-scattered dose, I has been computed using this form of f for a monoenergetic point source of

12 mc^2 with ideal shadow shields of 0, 20, and 40°, respectively. Figure III-E-25 shows I/S_0 so calculated as functions of rear wall lead thickness for thicknesses of polyethylene plastic of 0, 30, and 60 cm. The initial energy of 12 mc^2 was chosen so as to have minimum absorption coefficient in lead for the scattered radiation. These thicknesses of lead and plastic exceeded the limits of the experimental data for ϵ_i. However, the penetration is nearly normal and one can therefore use the theoretical predictions as described by Fano.(15)

The dose scattered through the front wall can in principle be calculated similarly. Here ϕ must always exceed $\pi/2$ and consequently C can be written as

$$C = \exp + \left[\sum_i \mu_i d_i \, (1 - \epsilon) \sec\phi \right] \qquad \text{(front wall, } \phi > \pi/2)$$

and the integration over θ is from $\psi + \pi/2$ to π. However, it will be noticed that in order to get into the windshield the single scattering angle is at least 90° and is likely to be very much greater. Hence photons which enter the front wall after only one collision will be very low in energy, and, in addition, there will be only few of them, since the back-scattering cross section is small at high energies. This is one situation, therefore, in which it seems possible that multiply scattered photons may contribute a large share of the dose, if not actually predominate. Since it is not yet possible to calculate the multiply scattered component it is still necessary to design on the basis of a single scattering calculation, which clearly should not be too elaborate.

For initial energies of 2 Mev and higher the scattered energy and the cross section decrease only slightly for scattering angles beyond say 135°.

(15) U. Fano, "Gamma-ray Attenuation," Reactor Handbook, Vol. 1, op. cit., p. 753.

[redacted]

ORNL-LR-DWG 273

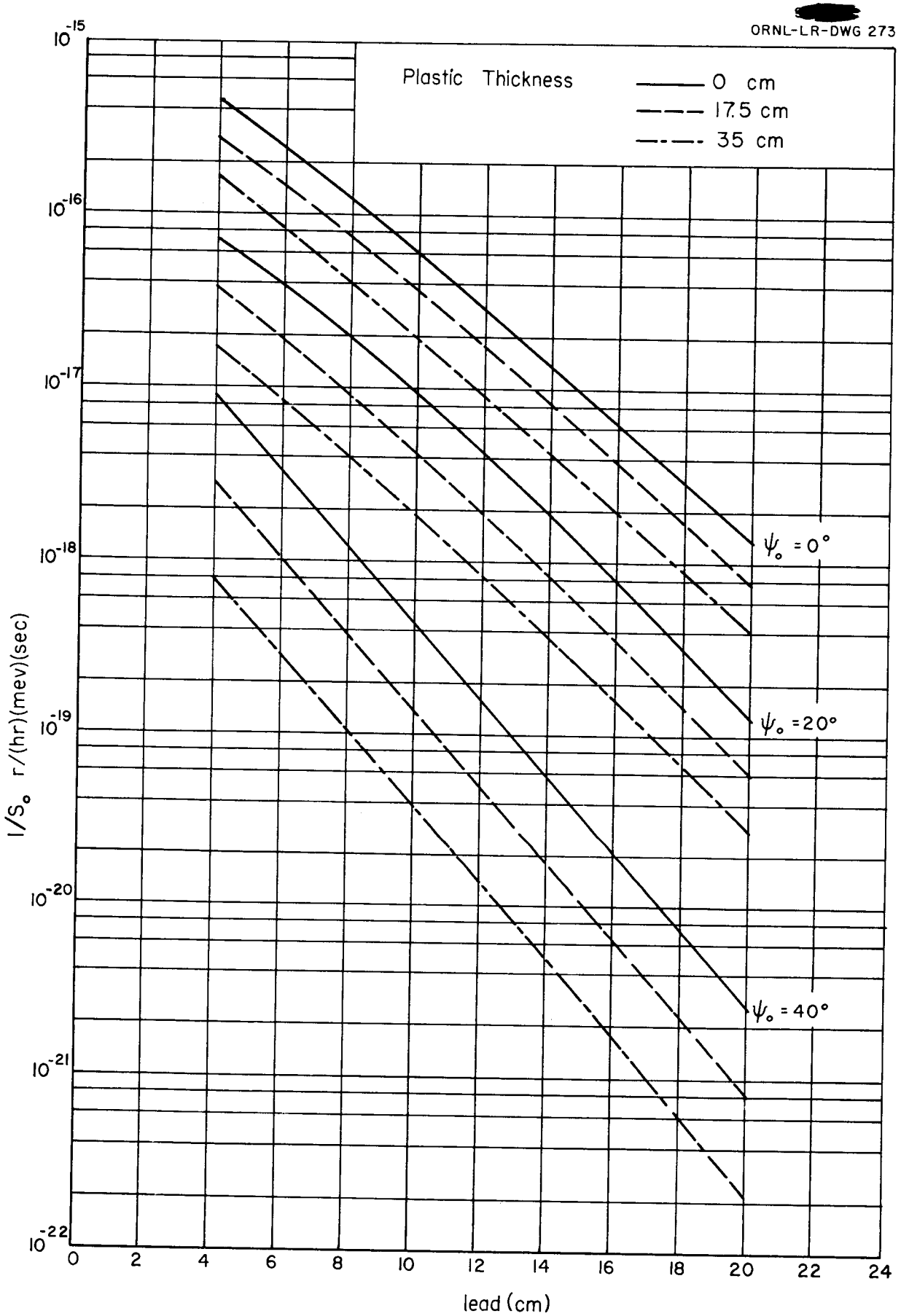

Fig. III-E-25. Gamma-Ray Single Scattered Dose Per Unit Source Strength Through Rear Face of Crew Compartment as a Function of Lead Thickness for Various Plastic Thicknesses and Ideal Shadow Shield Half Angles (ψ_0).

There is little error, therefore, in replacing $\sigma(\theta)$ by $\sigma(\pi)$. Further, the energy for scattering that is nearly backwards is practically independent of initial energy (providing it is much larger than mc^2) and has a value about $mc^2/2$ (255 kev). Also, as an attempt to include partially the effects of multiple scattering, it may be assumed that there is no absorption in air, i.e., $\bar{A} = 1$. One can then write f as

$$f(\psi,E_o,D,d) = \frac{n}{4DE_oF} mc^2 \sigma(\pi) \int_{\psi}^{\pi/2} \exp -\sum_i \mu_i d_i (1 - \epsilon_i) \sec\alpha \, d\alpha$$

where $\alpha = \pi - \phi = \pi + \psi - \theta$. It is somewhat less satisfactory to evaluate μ_i and ϵ_i at a single energy for all E_o and θ, since μ for lead is a rapidly varying function of energy in this region. However, a value of, say, 350 kev seems to be a reasonable overestimate. In that case, the integral becomes independent of E_o. In addition, for initial energies of 2 Mev or higher, $\sigma(\pi)$ can be well approximated by

$$\sigma(\pi) = \left(\frac{r_o^2}{4}\right)\left(\frac{mc^2}{E_o}\right)$$

where r_o is the classical electron radius, e^2/mc^2. If the source is assumed monoenergetic and isotropic with an ideal shadow shield, the front scattered dose is

$$I = \frac{S_o}{2D} \left(\frac{mc^2}{E_o}\right)^2 G(\psi_o,d)$$

where G is independent of initial energy and is given by

$$G(\psi_o,d) = \frac{nr_o^2}{8F} \int_{\psi_o}^{\pi/2} d\psi \int_{\psi}^{\pi/2} \exp - \sum_i \mu_i d_i (1 - \epsilon_i) \sec\alpha \, d\alpha$$

In calculating this double integral μ_i has been evaluated at 350 kev and ϵ_i has been taken as zero for the lead (since the photoelectric effect predominates), while for plastic ϵ_i has been assumed to be independent of α and has been approximated from the predictions for normal penetration. Table III-E-2 lists the values taken for ϵ at this energy as a function of plastic and lead backing thickness.

Figure III-E-26 shows $G(\psi_0,d)$ as a function of lead thickness for several thicknesses of plastic for shadow shield angles of 0, 20, and 40°.

Summarizing the gamma-ray scattering calculations, it may be stated that the dose through the side walls can be rather accurately calculated under the basic assumptions provided that the energy and angular distribution of the photons emitted from the reactor shield is known or can be estimated. Scattering through the rear and front walls cannot be calculated as closely, but the former is likely to be small compared to other effects, while the weight penalty for an error in the front wall-scattered dose is usually tolerable.

Table III-E-2. ϵ at 350 kev for a Plastic of Thickness d_1, Backed up by Lead of Thickness d_2

d_1 (cm)	ϵ_i, Slant Penetration Buildup Function			
	d_2 = 0.2 cm	d_2 = 0.4 cm	d_2 = 0.6 cm	d_2 = 0.8 cm
15	.40	.32	.27	.24
30	.36	.29	.25	.21

[redacted]

ORNL-LR-DWG 274

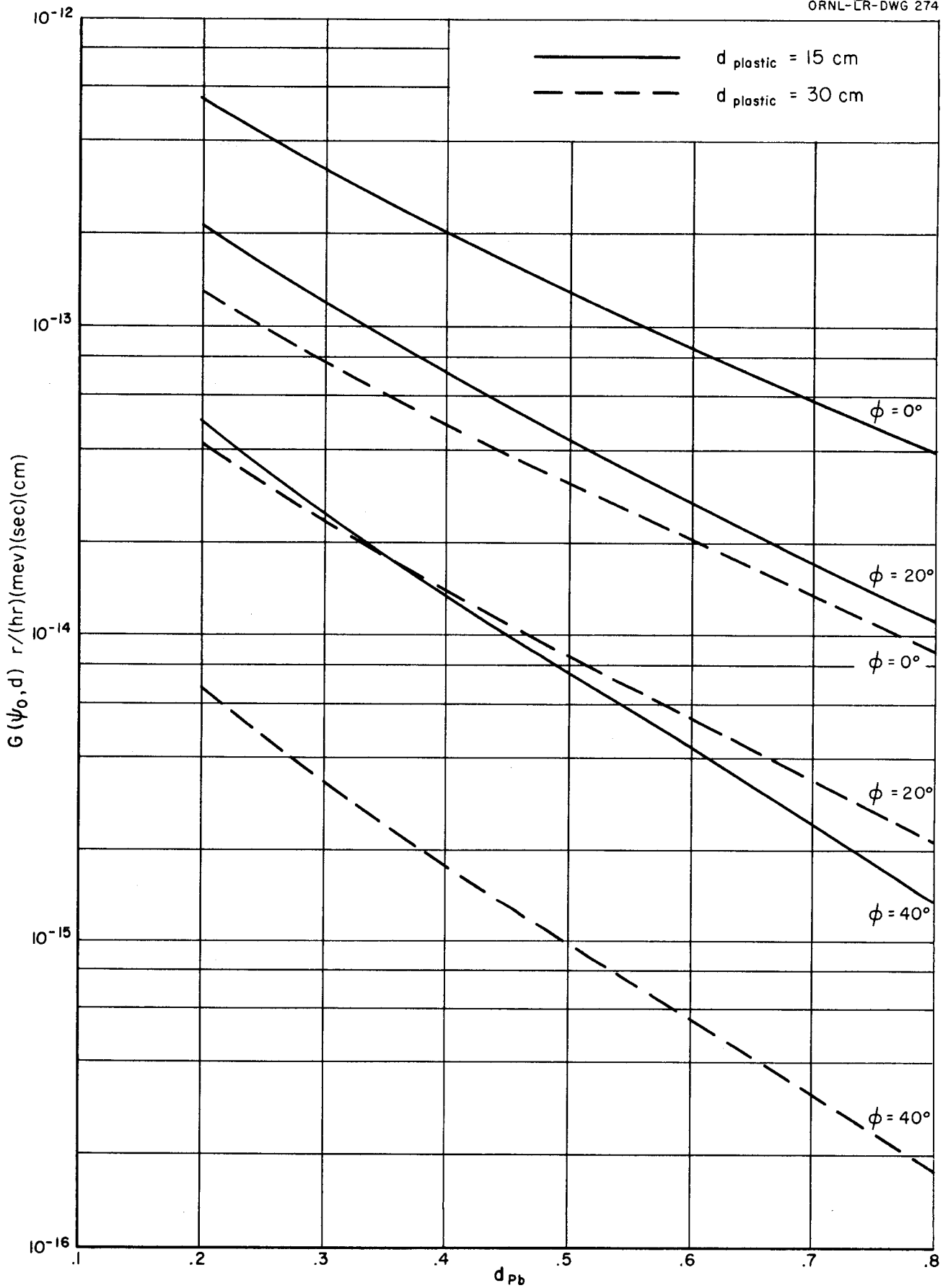

Fig. III-E-26. $G(\psi_0, d)$ for Front Wall, Single Scattered, Gamma-Ray Dose as a Function of Lead Thickness for Various Plastic Thicknesses and Ideal Shadow Shield Half Angles (ψ_0).

Neutron Scattering

Obviously, the previous formula for single gamma scattering could be taken over for neutron scattering with only a relabeling of some of the factors. However, the different manner in which neutrons interact with matter (and perhaps more important, lack of detailed knowledge of this manner) makes it convenient to rephrase the scattering equations.

Among the changed circumstances the following may be listed:

(1) Each collision in air, for practical purposes, can be taken as without loss of energy. Under any conditions a neutron colliding elastically with a nitrogen nucleus could lose no more than 25% of its energy. This is too small an energy loss to produce substantial changes in the neutron cross sections and can be neglected for a single scattering theory. It is true some absorptive collisions can occur, such as the (n,p) and(n,α) reactions in nitrogen. But even under the most optimistic considerations these do not amount to more than 0.2 barn compared to an elastic cross section of the order of 2.0 barns. The inelastic cross section, likewise, is expected to be of the same order of magnitude as the absorptive processes. It is therefore reasonable to consider the total cross section as consisting only of elastic scattering so long as, to repeat, only single scattering is considered.

(2) The total cross section for both nitrogen and oxygen varies rapidly with energy owing to the presence of many discrete scattering resonances. Almost all of these resonances are quite narrow compared to the expected energy spread of the incident neutrons. It is therefore desirable to smooth out the cross section by averaging over the resonances.

(3) The angular distribution of the scattered neutrons is at present only imperfectly known. The shape of the distribution changes rapidly across

the individual resonances so that again some average over a finite energy interval must be sought. Measurements have been made of the angular distribution for oxygen from 2 to 4.5 Mev[16] and for nitrogen from 0.8 to 2.4[17] Mev and at 14 Mev.[18] The experimental results for nitrogen at 14 Mev are in good agreement with the predictions of the statistical-continuum model of the nucleus[19] while at the lower energies there is considerably more scattering at large angles than predicted. The experimental results along with the predictions of the statistical continuum theory may be used to estimate the angular distribution for neutrons having all energies between 3 and 14 Mev.

(4) Because of the lack of energy degradation upon collision, neutrons multiply scattered in air may be more important than in the corresponding gamma-ray situation. Simon and Ritchie[20] have examined the multiply scattered contribution for an unshielded receiver, isotropic source, with isotropic and $(1 + \cos\theta)$ angular distribution. They show that multiply scattered neutron fluxes may be a large fraction of the singly scattered neutron dose even at 0.2 mean free path. As a result of these calculations, they suggest that an excellent method of correcting for multiple scattering

(16) E. Baldinger, P. Huber, and W. G. Proctor, "Streuung von schnellen Neutronen an O^{16}," Helv. Phys. Acta 25, p. 142 (1952).
(17) J. L. Fowler, C. H. Johnson, and J. R. Risser, "Angular Distribution of Neutrons Scattered from Nitrogen," Phys. Div. Quar. Prog. Rep. Sept. 20, 1952, ORNL-1415, p. 2; see also Phys. Div. Quar. Prog. Rep. Dec. 20, 1952, ORNL-1496, p. 4.
(18) T. H. Bonner, private communication.
(19) B. T. Feld, H. Feshbach, M. L. Goldberger, H. Goldstein, and V. F. Weisskopf, "Final Report of the Fast Neutron Data Project," Nuclear Development Associates, NYO-636, Section III (Jan. 31, 1951).
(20) A. Simon and R. H. Ritchie, "Background Calculations for the Proposed Tower Shielding Facility," ORNL-1273, Appendix B (Nov. 3, 1952).

is to omit the absorption item in single scattering. This practice will be followed here, although energy degradation and absorptive processes in multiple scattering weaken the conclusions in ORNL-1273[20] to some extent.

(5) Practically nothing is known about how the obliquely scattered neutrons penetrate the crew compartment side walls. Ignorance of this behavior is the largest factor in our uncertainty over the neutron-scattered dose. The most conservative practice in the past has been to assume the neutrons penetrate normally through the side walls and to take some average mean free path from the BSF measurements, in which case

$$C = e^{-\mu d}$$

(the gamma-ray shielding in the walls has a negligible neutron attenuation). A variant is to calculate the flux per unit area on the crew side walls and consider this a new flux which then penetrates normally. In this case one can write

$$C = \sin\phi \; e^{-\mu d}$$

The GE-ANP Project[21] has used another variation, introducing a buildup factor for oblique incidence which predicts greater attenuation than for normal penetration, but which it is hoped is still conservative. Experiments on oblique penetration of neutron beams are clearly called for.

The expression for the dose due to scattered neutrons is*

$$I(D) = \frac{1}{2D} \int_0^{\infty} \frac{Q(E_o)\, dE_o}{F(E_o)\, \ell(E_o)} \int_0^{\pi} N(E_o,\psi)\, d\psi \int_{\psi}^{\pi} \frac{\sigma(\theta)}{\sigma_t}\, C(E_o,\phi,d)\, d\theta$$

Since the neutron dose is more nearly proportional to number flux than

(21) "Engineering Progress Report No. 2; October 1, 1951 -- December 31, 1951," Aircraft Nuclear Propulsion Project, DC-51-12-25, p. 130 (Dec., 1951).

* Here σ_t is the total microscopic cross section, and $\ell(E_o)$ is the total mean free path in air for neutrons of energy E_o.

energy flux, it is more convenient to express the source intensity in terms of Q, the number of neutrons emitted per unit time per unit energy range, than in terms of S. $F(E_o)$ is the relationship between neutron dose and number flux as given by W. S. Snyder[22] and reported here in section III-A.

It will be shown in a later section that judicious shaping of the reactor shield, i.e., making the source anisotropic, can result in only a small reduction in the scattered dose. Therefore, if the air-scattered dose were the only consideration, there would be little advantage in departing from an isotropic source. For an isotropic source the dose is

$$I(D) = \frac{1}{2D} \int_o^\infty \frac{Q}{F\ell} dE_o \int_o^\pi \frac{\sigma(\theta)}{\sigma_t} d\theta \int_o^\theta C(E_o,\phi,d)\, d\phi$$

Further, if it is assumed that the neutrons penetrate the sides normally, in which case $C = e^{-\mu d}$, then I reduces to

$$I(D) = \frac{1}{2D} \int_o^\infty \frac{Q\, e^{-\mu d}}{F\ell} dE_o \int_o^\pi \frac{\sigma(\theta)}{\sigma_t} \theta\, d\theta = \frac{1}{2D} \int_o^\infty \frac{Q\, e^{-\mu d}}{F\ell} K\, dE_o$$

If the scattering is isotropic then

$$K = \int_o^\pi \frac{\sigma(\theta)}{\sigma_t} \theta\, d\theta = \frac{\pi}{8} = 0.392 \qquad \text{(isotropic)}$$

On the other hand if the cross section is peaked sharply forward, so that $\sigma(\theta)$ is substantially zero beyond one radian, then

$$K = \frac{1}{2\pi} = 0.159 \qquad \text{(forward scattering)}$$

(22) Forthcoming ORNL report by W. S. Snyder; for preliminary results see E. P. Blizard, "Introduction to Shield Design," ORNL-CF-51-10-70, Part II Revised (Mar. 7, 1952).

Some other examples might be mentioned:

$$K = \frac{\pi}{8}\left(1 - \frac{4}{\pi^2}\right) = 0.234, \qquad \left[\sigma(\theta) = 1 + \cos\theta\right]$$

$$K = \frac{3\pi}{16} = 0.589, \qquad \left[\sigma(\theta) = \cos^2\theta\right]$$

$$K = \frac{\pi}{8}\left(1 + \frac{4}{\pi^2}\right) = 0.550, \qquad \left[\sigma(\theta) = 1 - \cos\theta\right]$$

Incidentally, if $C = \sin\phi\ e^{-\mu d}$, then I has the same form but K is

$$K = \int_0^{\pi} \frac{\sigma(\theta)}{\sigma_t}\ (1 - \cos\theta)\ d\theta$$

For isotropic scattering K = 0.250

The foregoing treatment has been based upon the case in which penetration of the crew compartment side shield is normal to the shield. For the case in which the penetration is significantly oblique the situation changes. While no detailed study of this case has been made, experience with gamma rays indicates that the forwardness of neutron scattering should then reduce the scattered dose even more than it does in the normal incidence case.

In all of the preceding numerical discussion it has been assumed that the source is isotropic. This is not as bad an assumption as in the gamma-ray case, for there is no counterpart here of the drastic anisotropy cause by a shadow shield. Nevertheless, there is increasing tendency to "shape" the angular distribution of emerging neutrons. The following example indicates the effect such shaping may have. Let additional shielding be added to the front hemisphere of an isotropic source in such manner that the angular distribution is isotropic in the rear hemisphere and varying as $e^{(4/\pi)\psi-2}$

in the front hemisphere, so that the emergent intensity is decreased by e^2 in the forward direction. Further assume that there is normal penetration through the walls of the crew compartment. Then the scattered dose is reduced to 90% of the original value for isotropic scattering and to about 33% for the angular distribution associated with neutrons having the highest energies of interest. However, much of the penetration through the side walls is oblique. This tends to decrease the scattered dose due to neutrons emitted near the forward direction and thus reduces the savings expected from shielding of these neutrons.

The optimum shape of a reactor shield may be calculated assuming radial emission from the shield and using a spherical shield as a starting point. The result for isotropic scattering is that by optimization the scattered dose could be reduced to about 70% of the original value for the same weight. For preferentially forward scattering the shield could be reduced rather drastically at the rear and a greater weight saving would be indicated. However, the presence of structure scattering would dictate caution in this matter. Furthermore, the previously mentioned effect of oblique transmission through the crew shield and the effect of nonradial emission from the reactor shield would tend to reduce the beneficial effect of optimization. Finally, the optimum shape is a rather strong function of the angular distribution of the scattered neutrons which varies markedly for the neutron energies of importance here. In view of these facts, it is questionable whether shaping the reactor shield would result in a large saving. However, in specific designs there may be other considerations, such as the direct beam and structure scattering which would lead one to place more shielding at the front than the sides and rear of the reactor. Therefore, while the scattering

from an isotropic source will be treated in some detail, consideration will also be given to the anisotropic case.

Isotropic Source. Even with the restriction to isotropic source, the calculations still involve uncertainties in regard to

(1) Angular distribution of scattering (in the form of the quantity K),

(2) Total scattering cross section in air (affecting the values of ℓ),

(3) Energy distribution of the emitted neutrons,

(4) Transmission through the crew shield wall.

It is not possible to resolve these uncertainties without more fundamental measurements, both of microscopic data and of macroscopic parameters such as come from bulk shielding experiments. For purposes of design studies, however, a number of guesses may be made about these factors. The sections below describe how the guesses were made, and what numbers were arrived at.

(1) Assumed Values of $K = \int_0^{\pi} \theta \frac{\sigma(\theta)}{\sigma_t} d\theta$

The experimental angular distributions for oxygen and nitrogen show some preferentially forward scattering in the energy region of 2 Mev, but are otherwise nearly isotropic. Therefore, a value of 0.35 is assumed for K (slightly less than the 0.392 for isotropic scattering) from 1.0 to 2.8 Mev. Practically all of the scattering occurs at angles less than one radian for nitrogen and oxygen at 14 Mev. Therefore, K is equal to 0.16 (forward scattering) at 14 Mev. It is expected that the values of K in the intermediate energy region will be somewhat larger than those predicted by the statistical-continuum model.

(2) The Relaxation Length and Ratio of K/ℓ for Neutrons in Air

The experimental values for the total cross section of oxygen and nitrogen have been given by a number of observers.[23]

The values of K/ℓ for nitrogen, oxygen and air shown in Fig. III-E-27 were obtained ignoring the narrow resonances in the total cross section. The results for air are based on the assumption of 80% nitrogen and 20% oxygen. On the basis of the observed values the following energy dependence of K/ℓ is assumed:

$$K/\ell = 0.31 \times 10^{-4}\ \text{cm}^{-1}, \qquad E < 4\ \text{Mev}$$

$$K/\ell = 0.07 + \frac{0.95}{E}\ 10^{-4}\ \text{cm}^{-1}, \qquad E > 4\ \text{Mev}$$

(3) Energy Distribution of Emitted Neutrons

Recent calculations made by Nuclear Development Associates[24] predict that the energy distribution of neutrons leaving the reactor shield is fairly flat up to 6 Mev, falling off exponentially for higher energies. Therefore, the energy distribution of the emitted neutrons is assumed to be:

$$Q(E) = 1, \qquad E < 6\ \text{Mev}$$

$$Q(E) = e^{+0.75(6-E)}, \qquad E > 6\ \text{Mev}$$

(4) Transmission Through the Crew Shield Wall

In the discussion of the quantity K it has already been implicitly assumed that the scattered neutrons penetrate the crew compartment as if they were incident normally, i.e., C has the form $e^{-\mu d}$. (The relaxation length $\lambda = 1/\mu$ need not be the same as for normal penetration.) This assumption stems

(23) J. H. Coon, E. R. Graves, and H. H. Barschall, "Total Cross Sections for 14-Mev Neutrons," Phys. Rev. 88, p. 562 (1952); N. Nereson and S. Darden, "Average Neutron Total Cross Sections in the 3- to 12-Mev Region," Phys. Rev. 89, p. 775 (1953); C. K. Bockelman, D. W. Miller, R. K. Adair, and H. H. Barschall, "Total Cross Sections of Light Nuclei for p, T-Neutrons," Phys. Rev. 84, p. 69 (1951); C. H. Johnson, H. B. Willard, J. K. Bair, and J. D. Kington, "Total Cross Sections of N^{14}, Ge, Se, Cd, and Hg," Phys. Div. Prog. Rep. June 20, 1952, ORNL-1365, p. 1.

(24) H. Goldstein, private communication.

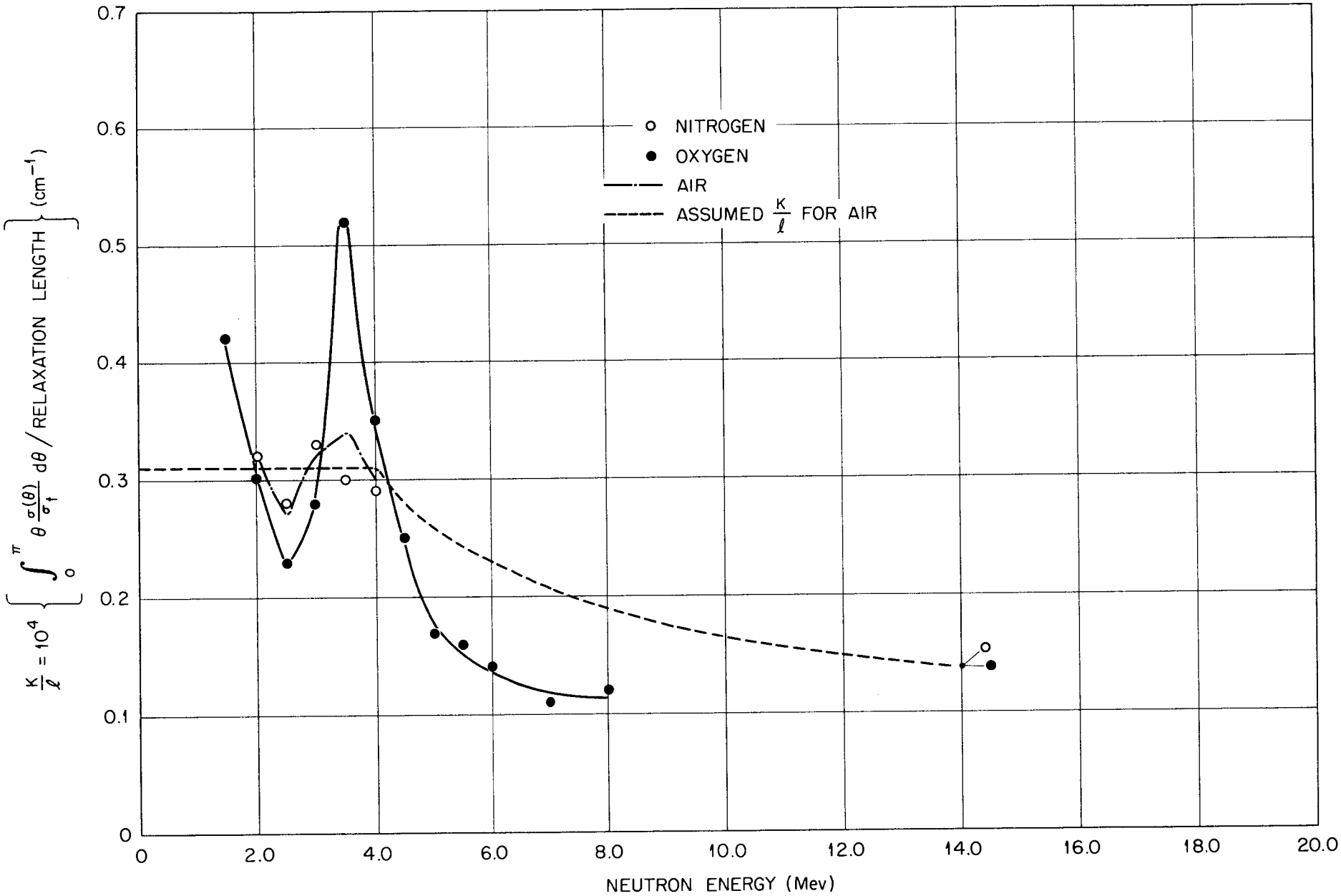

Fig. III-E-27. $\frac{K}{\ell}$ vs. Neutron Energy.

only partly from ignorance of what does actually happen. It is in part suggested by the results of the "skyshine" experiment,[25] where it was found that for the scattering geometry involved, the neutrons incident on water were attenuated exponentially with a relaxation length of somewhat less than 5 cm. This value is much smaller than the corresponding figure ($\sim$8 cm) for the outer edge of the reactor shield. It might seem, therefore, that considerable weight could be saved by moving a large amount of neutron shielding to the crew compartment. However, it must be emphasized that it is not known why the observed relaxation length is so much smaller than 8 cm. Under the circumstances it is felt unwise to split the neutron shield drastically solely on the basis of this figure. A suggested upper limit for the thickness of plastic shielding on the crew compartment is around 40 cm. For a plastic crew shield wall, use of a relaxation length of 4.5 cm on the side should be conservative since the N_H for plastic is about 20% higher than that for water. The dose in the crew compartment due to scattered neutrons may be expressed in terms of the parameters D, the separation distance, and d, the thickness of the crew shield wall:

$$I(D) = \frac{1}{2DF} \int_0^\infty \frac{Q\, e^{-\mu d}\, K}{\ell} \, dE_o$$

Since F is essentially constant for the energy range of the neutrons leaving the reactor shield and μ is constant,

$$I(D) = \frac{e^{-\mu d}}{2DF} \int_0^\infty \frac{QK}{\ell} \, dE_o$$

(25) H. E. Hungerford, "The Skyshine Experiments at the Bulk Shielding Facility," ORNL-1611.

and

$$I(D) = \frac{\overline{\left(\frac{K}{\ell}\right)} e^{-\mu d}}{2DF} \int_0^\infty Q \, dE_o$$

where

$$\overline{\left(\frac{K}{\ell}\right)} = \frac{\int_0^\infty QK/\ell \, dE_o}{\int_0^\infty Q \, dE_o}$$

$$\overline{\left(\frac{K}{\ell}\right)} = 2.7 \times 10^{-5} \text{ cm}^{-1}$$

The integral

$$I_u(D) = \frac{1}{4\pi D^2 F} \int_0^\infty Q \, dE_o$$

is the unscattered dose at the crew compartment associated with the radiation emitted from the source. Therefore

$$I(D) = 2\pi(2.7 \times 10^{-5}) e^{-d/4.5} \, D \quad I_u(D)$$

It should be remembered that the calculation is for a cylinder infinitely long. The actual shield is more closely approximated by a finite cylinder with front and rear walls. On the one hand the finite length of the cylinder reduces the air scattering through the side, but there will now be contributions due to the front and rear. If the attenuation of the neutrons through the front and rear were the same as through the side walls, the two effects, under the scattering assumptions made, would exactly compensate. In the

rear there is likely to be considerably more shielding than on the sides, in order to attenuate the direct beam properly. However, one would expect that the relaxation length in the rear shielding would be more characteristic of normal incidence than for the side, i.e., should be closer to 8 cm in water, as compared to 5 cm. Hence if the thickness of rear shielding is at least 8/5 of the side thickness the neutron dose through the rear and sides would not be greater than the infinite cylinder result given above.

For the effect of the front wall, however, the infinite cylinder calculation may not always be conservative, since it is often necessary to have less shielding in front than on the sides. One might expect that the relaxation length in the front wall would be somewhat less than in the sides because of the obliquity difference. A 10% decrease in thickness in the front wall compared to the side might therefore not increase the scattered dose above the infinite cylinder value. If any greater difference in thickness is planned it would be advisable to calculate the dose through the side and front separately.

The dose through the front wall is obviously largest at a point at the front of the crew compartment. For such a point and with the assumption of isotropic scattering, it can be shown that 3/4 of the scattered radiation is incident on the sides and 1/4 incident on the front. The total scattered dose reaching the point can therefore be written as

$$I(D) = \left(\frac{3}{4} \quad e^{-d_1/4.5} + \frac{1}{4} \quad e^{-d_2/4.5}\right) 2\pi \ (2.7 \times 10^{-5}) D \ I_u(D)$$

where d_1 and d_2 are the thicknesses of the sides and front walls, respectively, and the relaxation length (in plastic) is the same in both cases.

Anisotropic Source. In this case, the preceding equations for the scattered dose are of course invalid and one must revert to the general expression. If one assumes isotropic scattering, which is certainly conservative, the expression becomes

$$I(D) = \frac{e^{-\mu d}}{2D} \int_0^\infty \frac{Q\, dE_o}{F\ell} \int_0^\pi \frac{N(E_o,\psi)(\pi - \psi)}{4\pi}\, d\psi$$

where μ is the same as defined before. The dose at the crew compartment due to the direct beam is

$$I_u(D) = \int_0^\infty \frac{QN(E_o,0)}{4\pi D^2 F}\, dE_o$$

Therefore

$$I(D) = \frac{D\, I_u(D)\, e^{-\mu d}}{2(\bar{\ell})} \int_0^\pi \frac{N(\psi)(\pi - \psi)}{N(0)}\, d\psi$$

where $(\bar{\ell})$ is a mean value of the relaxation length for neutrons in air (100 m) and it has been assumed that the angular distribution of the neutrons leaving the reactor shield is independent of the energy. The ratio $N(\psi)/N(0)$ is the angular distribution of the neutrons emitted from the reactor shield normalized to unity in the forward direction.

The considerations concerning the relative thicknesses on the side and ends of the crew compartment are changed only slightly when there is more shielding at the front of the reactor. It remains true that if the ratio of the rear wall thickness to the side wall thickness is not less than 8/5, the calculated dose for the infinite cylinder may be used but the thickness of

the front wall may be reduced somewhat. This is due to the fact that only neutrons emitted from the reactor at angles of less than $\pi/2$ contribute to the singly scattered dose at the front wall. However, it must be remembered that multiple scattering may limit the amount of shielding material that can be removed from the front face.

The thickness of heavy material placed on the sides of the crew compartment is never large enough to attenuate neutrons appreciably. The conservative practice of neglecting the heavy material should therefore be followed.

Validity of Basic Assumptions

Point Source. There does not seem to be any detailed discussion of the effect of deviations from a point source. It should be remarked that the average distance to the point of first scattering is much less than a mean free path. In the gamma-ray situation most of the dose comes from the rays incident at around 45° or less to the crew shield side with relatively small scattering angles. Such photons cannot have been scattered at a distance more than D away from the reactor, and D/2 is more likely. However, this distance should be compared not with the reactor shield dimensions so much as with those of a smaller volume inside from which the particles may be said to originate. This is more like the core volume that the shield volume. Intuitively it seems that the assumption is adequately satisfied.

Cylindrical Symmetry. There seems to be little question as to the validity of this assumption in practice. If $N(\psi)$ were also a function of an azimuthal angle β the only formal difference would be to replace the integral over ψ by an integral over ψ and β multiplied by $\pi/2$.

Single Scattering. Some discussion of this assumption has been given above in considering gamma-ray scattering through the front wall and neutron scattering in general. One would expect that under normal circumstances the multiple scattering of gamma rays, when D is less than a few tenths of a mean free path, should be small compared to the single scattering. Unlike neutrons, photons will be rapidly degraded by the air scattering, and multiply scattered photons should not contribute much to the energy flux. So far as is known, no detailed examination has been made of the multiple scattering at these short distances for anisotropic source and receiver. By some qualitative arguments Trice[26] has come to the conclusion that the second scattering of gamma rays should be negligible. It is possible to obtain an overestimate of the second scattering for an isotropic source,[27] and this too seems small compared to the first scattering.

On the other hand, there are a number of situations in which it is difficult for a particle to reach the receiver by single scattering. This has been indicated already in the case of the front wall dose. Examination of the curves of $f(\psi)$ shown in Figs. III-E-11 through III-E-22 indicates that with any appreciable lead shielding on the crew compartment side very few gamma rays emitted at more than 40° or so with the reactor axis contribute to the singly scattered dose, while the contribution from the rear reactor hemisphere is negligible. This behavior has had some influence on shield design. For example, it would appear that an ideal shadow shield of 45° aperture would eliminate almost all of the air scattering, or that it is

(26) J. B. Trice, "The Importance of Twice Scattered Gamma Rays Arriving at the Crew Position of a Nuclear Powered Aircraft," NEPA-1297 (Feb. 27, 1950).

(27) H. Goldstein and R. Aronson, ORNL-1179 (to be published).

permissible to have huge emergent fluxes of gamma rays or neutrons provided they are pointed rearward. A word of caution in such extreme designs seems desirable. Where single scattering has been eliminated or is highly improbable, one should first look at second and higher order scatterings before concluding that the total scattered dose is negligible. Further theoretical (and experimental) examination of multiply scattered particles in such geometries is greatly needed.

Sea Level Air Density. This assumption is a conservative one, and its removal is trivial when necessary. It should be noted incidentally that water in gaseous or condensed form does not contribute to the scattering to any appreciable extent. The state of the water is obviously irrelevant; what matters chiefly is the mass of substance present. By way of comparison a dry cubic meter of air at STP weighs about 1.3 kg. Under the same conditions the saturated water vapor in air weighs only about 10 g/m^3. A heavy rain in contrast weighs only about 1 g/m^3, while a heavy sea fog may weigh two of three times as much. In all cases this is a negligible amount of matter compared to the air itself. It is conceivable that in a sand or dust storm the suspended material might reach a density comparable to that of air, but it is extremely unlikely. The heaviest density recorded -- inside a grain elevator -- was still only 1 kg/m^3.

Crew Compartment Geometry. The calculations described above have assumed detailed geometrical conditions for the crew compartment. Three aspects of these may be discussed separately:

(1) In calculating the dose through each surface it is considered infinite in extent. This is clearly an overestimate. For example, for a point A just behind the rear wall (Fig. III-E-28) a particle penetrating

[redacted]
ORNL-LR-DWG 276

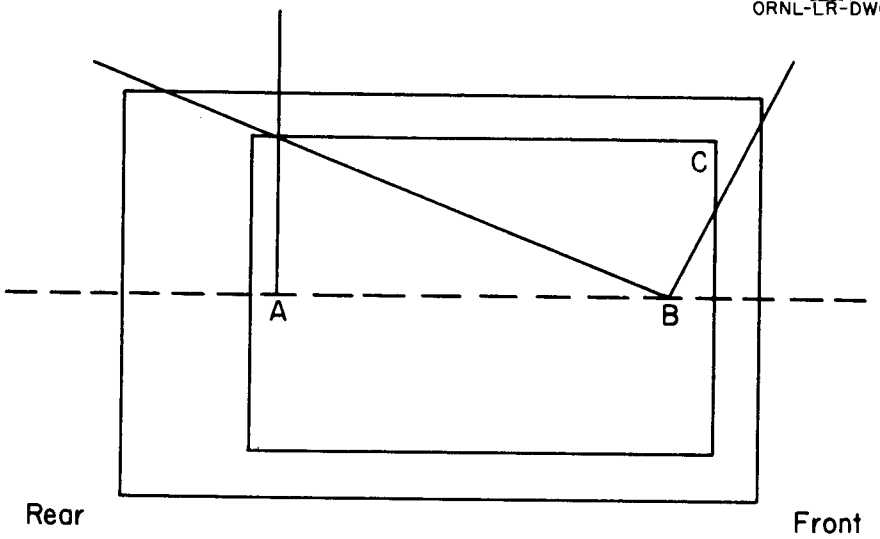

Fig. III-E-28. Variation of Scattered Dose in Various Locations of Crew Compartment.

[redacted]
ORNL-LR-DWG 277

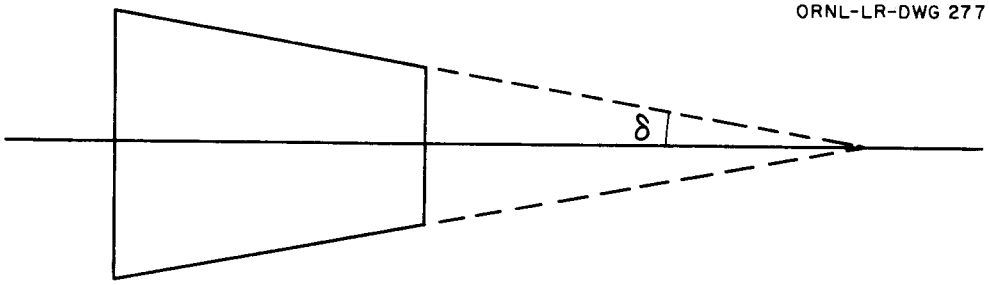

Fig. III-E-29. Geometry of a Crew Compartment in the Shape of a Truncated Cone.

[redacted]
ORNL-LR-DWG 278

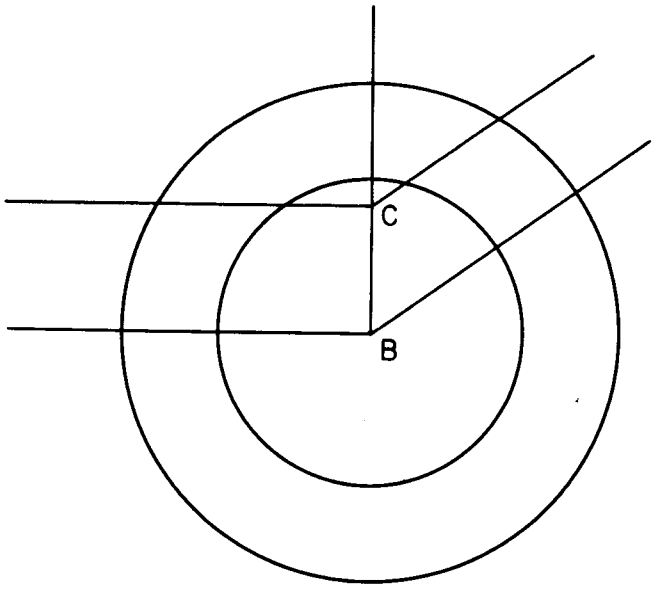

through the side must, to the first order, be incident at angles of 90° or greater. However, at the position B where the side and front dose is greatest the overestimate is obviously not very great, and it seems desirable therefore to retain this assumption.

(2) The crew compartment is assumed cylindrical. There seems to be some advantage to having it rather in the shape of a truncated cone, as shown in Fig. III-E-29. The improvement might be shown by examining the case of a monoenergetic isotropic source with an ideal shadow shield of angle ψ_o. In that case, with a cylindrical shield the side-scattered dose is proportional to

$$I \propto \int_{\psi_o}^{\pi} \bar{A}(\theta) \frac{E(\theta)}{E_o} \sigma(\theta)\, d\theta \int_{o}^{\theta-\psi_o} C(\theta,\phi,d)\, d\phi$$

With a conical shield of half-angle δ one would write instead

$$I \propto \int_{\psi_o+\delta}^{\pi} \bar{A}(\theta) \frac{E(\theta)}{E_o} \sigma(\theta)\, d\theta \int_{\delta}^{\theta-\psi_o} C(\theta,\phi-\delta,d)\, d\phi$$

Changing to an integration variable $\phi' = \phi - \delta$, this can be written

$$I \propto \int_{\psi_o+\delta}^{\pi} \bar{A}(\theta) \frac{E(\theta)}{E_o} \sigma(\theta)\, d\theta \int_{o}^{\theta-(\psi_o+\delta)} C(\theta,\phi',d)\, d\phi'$$

Thus sloping the crew compartment walls by an angle δ is equivalent to increasing the ideal shadow shield angle by the same amount.

(3) The receiver is assumed to be on the axis of the crew compartment. Off the axis, say at position C (Figs. III-E-28 through III-E-30) the scattered dose may be expected to be less than at the center, since some of

rays must now penetrate a greater thickness of shield, as shown in Fig. III-E-30. The assumption therefore appears to be conservative. A rough calculation indicates it does not result in a large overestimate even for a point like C, and it thus seems wise to retain the assumption.

III-F. RADIATIONS DUE TO FISSION PRODUCTS

1. Activation of Coolants from Delayed Neutrons

This problem has not been solved for general cases, but specific calculations applicable to the RMR are given in section IV-C.

2. Gamma Rays from Fission Decay Products

There is very little data available on the spectrum of gamma rays from the fission decay products as a function of time beginning at zero time and extending out to several hours. It was decided that a useful treatment of these gammas, of adequate accuracy as far as reactor shielding is concerned, might be obtained by taking the steady-state spectrum of the prompt plus the decay gammas and subtracting the prompt spectrum.

The spectrum from a slug in the Los Alamos water boiler was published by J. W. Motz[1] and can be approximated by

$$\text{Gamma counts/fission/Mev} = Ae^{-1.28E} \qquad (1)$$

where

A = constant,

E = energy (Mev).

Motz has estimated that the gammas are

(1) 45% decay gammas,

(2) 45% prompt gammas,

(3) 10% capture gammas in U^{235}.

If it is assumed that the 10% due to uranium capture can be subtracted from the total with the same slope as the total then Eq. (1) will also represent the

(1) J. W. Motz, "Gamma-Ray Spectra of the Los Alamos Reactors," Phys. Rev. 86, 753 (1952).

decay plus prompt gammas with the constant A having a different value.

F. C. Maienschein[2] has pointed out that the best guess for the prompt gamma spectrum as a result of preliminary data is exponential and can be represented approximately by:

$$\text{gamma counts/fission/Mev} = Be^{-1.43E}$$

where

B = constant,

E = energy (Mev).

If the energy of the prompt and decay gammas per fission are each taken to be 5.5 Mev and the spectrum is converted to an energy probability function, then

$$5.5 \text{ Mev} = \int_0^\infty EBe^{-1.43E}\, dE = 1/2 \int_0^\infty EAe^{1.28E}\, dE \qquad (2)$$

This gives

B = 11.25,

A = 18.0,

or

Total gammas/fission/Mev = $18.0e^{-1.28E}$,

Prompt gammas/fission/Mev = $11.25e^{-1.43E}$.

As mentioned before, it is now to be assumed that the decay gammas are just the difference between the total and the prompt, or

$$\text{Decays} = 18.0\, e^{-1.28E} - 11.25\, e^{-1.43E} \qquad (3)$$

A least squares approximation for this difference fitted in the region of interest is

$$\text{Decays} \approx 7.4\, e^{-1.16E} \qquad (4)$$

(2) Private communication.

If the energy of decay gammas between any energies is desired, this function can then be converted to an energy probability function by multiplying by energy and then integrating between the energies in question.

III-G. STRUCTURE AND GROUND SCATTERING*

The purpose of this section is to give methods of calculating the structurally scattered and ground scattered radiation at the crew compartment. In estimating this scattering, where time permits, it is always desirable to make an exact calculation, using known cross sections.

The scattering of neutrons and gamma rays from the aircraft structure into a receiver on the airplane may in some cases be many times larger than the air scattering. The scatter may be caused by equipment in the airplane, or by fuselage, wings, tail, engines, etc. This problem is inherently more complex than the air scatter problem because of the variety of scattering assemblies, and because of the greater possibility of multiple scatter in these assemblies. Calculation of the penetration by the scattered radiation of a shield around the receiver is also more difficult than the air scattering itself because of the unknown spectrum of the scattered radiation. The use of the pessimistic but simplifying assumption that penetration is always normal to the shield and the use of the Lid Tank relaxation lengths for shield attenuation are expedient engineering practices. (Lid Tank relaxation lengths are average relaxation lengths of the observed dose.)

There are two approximate methods conveniently available for the calculation of scattering from structures: (1) the single scattering method, with or without attenuation and buildup factors, and (2) the albedo method. The single scattering method is applicable where scattering occurs from members whose thickness is small compared to the mean free path of the radiation in the material. The albedo method is applicable where scattering

* Much of this section is taken from Chap. 2.9 of Reactor Handbook, Vol. 1, p. 869, Technical Information Service, USAEC (June, 1953).

occurs from members whose thickness is large compared to the mean free path in the material. Thus, the two methods are complementary and essentially bracket all cases in which one is interested.

The calculation of ground scattering is made using the albedo method.

The methods of calculating structure and ground scattering will be presented in detail together with some examples.

1. Single Scatter Method for Thin Structural Members

The method of calculating single scattering by a thin member, of thickness t and area dA, neglecting air attenuation is, roughly,

$$\left(\begin{array}{l}\text{No. of particles}\\ \text{scattered to}\\ \text{receiver per sec}\\ \text{per unit area at}\\ \text{the receiver}\end{array}\right) = \left(\frac{\text{No. of particles emitted}}{\text{sec steradian}}\right) \cdot \left(\begin{array}{l}\text{solid angle}\\ \text{subtended}\\ \text{at the source}\\ \text{by dA}\end{array}\right) \cdot \left(\frac{\text{probability of scattering in receiver direction}}{\text{cm steradian}}\right)$$

$$\cdot \left(\begin{array}{l}\text{cm of thickness}\\ \text{over which}\\ \text{scattering can}\\ \text{occur}\end{array}\right) \cdot \left(\begin{array}{l}\text{solid angle sub-}\\ \text{tended at the}\\ \text{scattering point}\\ \text{by unit area of}\\ \text{the receiver}\end{array}\right) \cdot \left(\begin{array}{l}\text{shield}\\ \text{attenuation}\end{array}\right)$$

This method will be illustrated by a calculation of single scatter from the fuselage of an aircraft. The fuselage thickness is small compared to the mean free path in the material. As a result, the single scatter method applies.

To obtain an overestimate of the scatter from the fuselage of an aircraft which contains a monoenergetic isotropic source, we suppose that the source S is centrally located in a long, thin cylindrical shell of radius a, thickness t, density ρ, and mass per unit length m, as shown in Fig. III-G-1. The receiver R is also assumed to be on the axis of the

[redacted]

ORNL-LR-DWG 537

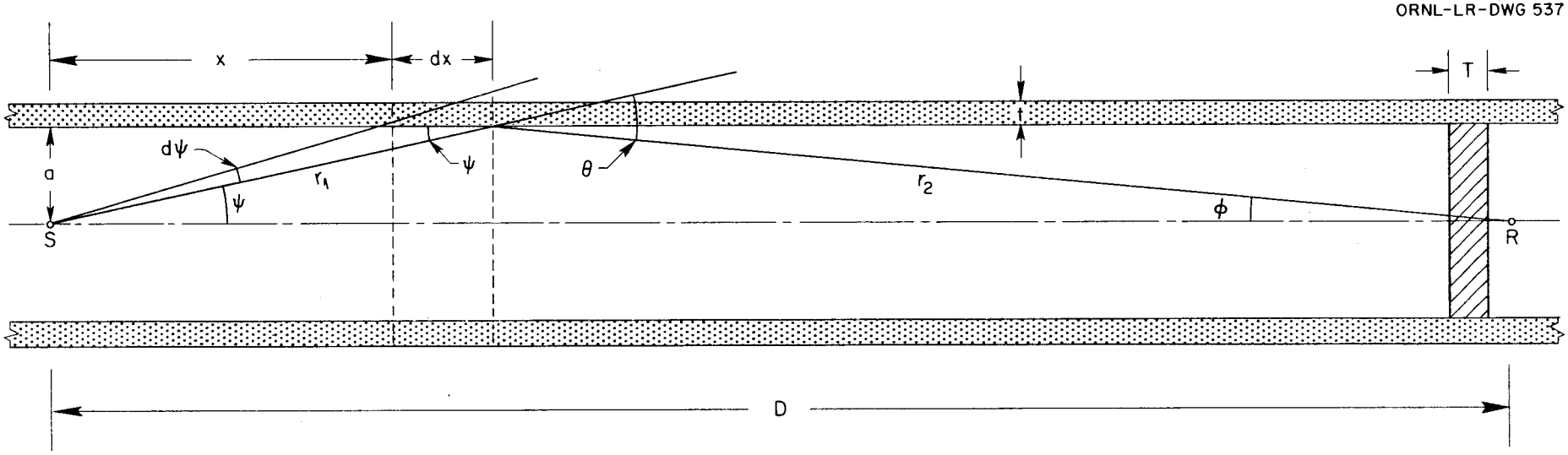

Fig. III-G-1. Source and Receiver in Aircraft Fuselage.

fuselage, at a distance D from the source. Air attenuation will be neglected since the mean free path in air of both neutrons and gamma rays is much larger than any practical separation distance D. Let the macroscopic differential scattering cross section of neutrons or gamma rays of energy E_o, scattering through angle θ in the fuselage material, be $\sigma(\theta,E_o)$ cm^{-1} $steradian^{-1}$. Then the number of particles leaving S which scatter in the fuselage at a distance between x and x + dx from the source, and which enter the receiver, per unit area at R, is

$$I_{ss}(D) = N_o(\psi) \frac{dA \cancel{\sin\psi}}{r_1^2} \sigma(\theta,E_o) \frac{t}{\cancel{\sin\psi}} \frac{1}{r_2^2} e^{-\mu(E)T \sec\phi} \qquad (1)$$

where

$N_o(\psi)$ = number of gamma quanta, or neutrons, emitted by the source per second per unit solid angle, at the angle ψ to the axis,

$dA \sin\psi/r_1^2$ = solid angle subtended at the source by fuselage area element dA,

$dA = 2\pi a\, dx$ = fuselage area element of length dx,

$\sigma(\theta,E_o)$ = probability of a particle of energy E_o scattering through θ in cm^{-1} $steradian^{-1}$,

$t/\sin\psi$ = slant distance in fuselage skin,

$1/r_2^2$ = solid angle at the scattering point subtended by unit area at the receiver at distance r_2,

$e^{-\mu(E)T \sec\phi}$ = attenuation of a slab shield of thickness T placed in front of the receiver,

$\mu(E)$ = attenuation coefficient of the slab shield at R,

$E = E(\theta, E_o)$ = energy of the radiation after scattering through angle θ, where E_o is the energy before scattering.

The quantity $N_o(\psi)$ is assumed to be cylindrically symmetric, or, over the cone ψ constant, $N_o(\psi)$ is a constant. From Eq. (1),

$$(dA \sin\psi)\left(\frac{t}{\sin\psi}\right) = t\ dA = t(2\pi a\ dx) = \frac{m}{\rho}\ dx$$

where

$$x = a \cot\psi$$

$$dx = -a \csc^2\psi\ d\psi,$$

so that

$$t\ dA = \frac{m}{\rho}\ (-a \csc^2\psi\ d\psi).$$

Consequently, the flux, or number of particles per second per unit area, at the receiver, given by Eq. (1) becomes

$$I_{ss}(D) = N_o(\psi)\ \frac{1}{r_1^2}\ \sigma(\theta, E_o)\ \frac{m}{\rho}\ (-a \csc^2\psi\ d\psi)\ \frac{1}{r_2^2}\ e^{-\mu(E)T \sec\phi} \qquad (2)$$

It is assumed that the source is monoenergetic with energy E_o as mentioned. This may be easily generalized to the case where the source emits a spectrum of energies. The exponential term may be readily modified to take account of a composite slab shield at the receiver.

Since $a = r_1 \sin\psi = r_2 \sin\phi$, then $\csc^2\psi = r_1^2/a^2$ and $1/r_2^2 = \sin^2\phi/a^2$, so that the singly scattered dose I_{ss} at the receiver R is given by

$$I_{ss}(D) = \frac{m}{a^3\rho} \int_{\tan^{-1}a/D}^{\pi} N_o(\psi)\ \sigma(\theta, E_o)\ \sin^2\phi\ e^{-\mu(E)T \sec\phi}\ G(E)\ d\psi \qquad (3)$$

for a very long cylinder, where G(E) is the conversion factor between flux and dose. For gamma rays, 1 r = 2 x 10^9 1-Mev gamma rays per cm^2. Thus, for gamma rays $G(E) = E(\theta, E_o)F$, where $F = 5.0 \times 10^{-10}$ r/(Mev/cm^2). For neutrons, G is taken to be a function of E_o only, since one may neglect, approximately and conservatively, the change in neutron energy on scattering. The values of G, for neutrons, as a function of E_o are given in Table III-A-5.

To get I_{ss}, the singly scattered dose for gamma rays, one must evaluate Eq. (3) numerically.

To get $I_{ss}^{(n)}$, the singly scattered dose for neutrons, one may assume isotropic scattering as a first approximation. An effective removal cross section $\sum_r$ can be used. The effective removal cross section is defined as that cross section which makes simple exponential attenuation apply. A more detailed discussion of the nature of the effective removal cross section has been given by Blizard and Welton.(1) The effective removal cross section $\sum_r$ is a measure of the scattering with the strong forward peak subtracted out, and $\sigma(\theta) = \sum_r/4\pi$. The limiting case of the isotropic source may be examined easily if it is assumed that the crew shield penetration is normal, and further, if the lower limit of integration of Eq. (3) is set equal to zero. Then

$$I_{ss}^{(n)} = \frac{m}{a^3\rho}\,\frac{N_o}{4\pi}\,\frac{\sum_r}{4\pi}\,G\,e^{-\mu T}\int_0^{\pi}\sin^2\phi\,d\psi = \frac{mN_oG\,\sum_r e^{-\mu T}}{8\pi a\rho\,(4a^2 + D^2)} \qquad (4)$$

where N_o is the total emission of the source $\left[N_o(\psi) = N_o/4\pi\right]$.

(1) E. P. Blizard and T. A. Welton, "The Shielding of Mobile Reactors, (Part I)," Reactor Science and Technology, Vol. I, No. 3, p. 15 (Dec. 1951).

A numerical example will be given for the B-36 airplane. The reactor-crew separation distance is 65 ft. The radius of the fuselage is 6 ft. The mass of the fuselage per foot is m = 200 lb/ft, including ribs, etc. The ratio Σ_r/ρ, in the more convenient units of cm^2/lb, is 16.8 cm^2/lb.

Omitting G and $e^{-\mu T}$, one has

$$I = \frac{m\left(\frac{\Sigma_r}{\rho}\right) N_o}{8\pi a(4a^2 + D^2)} = \frac{200(16.8)N_o}{8\pi(6)\left[4(6^2) + (65)^2\right]} \cdot \frac{1}{(30.5)^4} = 5.91 \times 10^{-9}\ N_o \tag{5}$$

The air scattering is $I_{air} = 1.2 \times 10^{-9}\ N_o$ neutrons/(cm^2/sec) for a reactor-crew separation distance of 65 ft.(2) The ratio of fuselage scattering to air scattering is thus $I/I_{air} = 4.9$ for neutrons.

The fuselage skin is 0.1 cm thick. If only the fuselage skin is considered than m = 20 lb/ft and $I/I_{air} = 0.49$ for neutrons. I_{air} is here taken for convenience as the "standard value" of Simon and Ritchie.(2) This represents a corrected version of the case in which source scattering and detection are all isotropic. Corrections are for forwardness of air scattering, air attenuation to and from the scattering point, and for the geometry of a crew shield in which half of the scattered out beam is shadowed out.

The effective value of m lies somewhere between 20 and 200 lb/ft. One would expect the results for I/I_{air} to lie somewhere between 0.49 and 4.9. The value 4.9 is very certainly thought to be an upper limit since self-shielding has been neglected, and the loading of the fuselage with gear will probably reduce the scattering from the fuselage.

The results for gamma rays are about the same as for neutrons given above.

(2) A. Simon and R. H. Ritchie, "Background Calculations for the Proposed Tower Shielding Facility," ORNL-1273 (Oct. 15, 1952).

2. Albedo Method for Thick Structural Members

The wings of an aircraft may be many mean free paths in thickness owing to the presence of fuel, fuel tanks, and other equipment. The albedo approximation is clearly indicated here.

The albedo may be defined as the ratio of the reradiated flux to the incident flux, and it can be measured experimentally. The reradiated flux may be assumed to emerge from the reflecting surface with either an isotropic distribution or a cosine distribution about the normal to the surface.

Typical values for the albedo for neutrons and gammas[3] are:

	Neutron Albedo	Gamma-Ray Albedo
Concrete	$\alpha_n = 0.12$	$\alpha_\gamma = 0.04$
Water	$\alpha_n = 0.08$	

These values were determined using a fast-neutron dosimeter and a gamma ionization chamber and are therefore neutron and gamma-ray dose albedos. To compute the dose in an unshielded crew box, one has only to add up the dose reflected from the surfaces present. To account for crew shield attenuation one must decide upon the attenuation coefficient appropriate to the reflected radiation. In the case of either gammas or neutrons one may conservatively neglect energy degradation of the scattered beam, though this may be very pessimistic. Particularly in the case where gammas are scattered from a surface and the bulk of the scattering is through large angles, energy degradation will be large and the radiation incident upon the shield will be much more strongly attenuated than the above would show. In the absence of

(3) H. E. Hungerford, "Some Ground Scattering Experiments Performed at the Bulk Shielding Facility," CF-52-4-99 (April 16, 1952).

information about the scattered spectrum, however, neglect of energy degradation is clearly indicated and is of course conservative.

Wing Scatter. An estimate of the wing-scattered contribution may be obtained by assuming that the source is a sphere of radius r_1 where $r_1 << D$. Half the sphere is assumed to extend above the wing (see Fig. III-G-2). It is assumed that the radiation emerges from the spherical source with a cosine distribution about the normal, and may scatter on one surface of the wing and into the receiver at R. It is further assumed that the source is isotropic and has a total emission of N_o. The width W of the wing is taken to be much smaller than D, the source-receiver spacing, so that the scattering surface may be considered to be concentrated on the Z axis. The wing is assumed to be rectangular with length L and area b per unit length.

It is shown by Blizard and Welton[1] that for cosine emergent radiation, the flux at a point on the wing a distance z from the origin is given by

$$\Phi_{cos} = \frac{N_o r_1}{6\pi^2 z^3} \quad \text{if} \quad z \geq 2r_1 \tag{7}$$

For simplicity this expression will be used for the whole range of z thereby underestimating the scatter somewhat. An overestimate may be obtained by multiplying this formula by a factor of two. The dose reaching the crew is then

$$I = \frac{(2)(2)e^{-\mu T} G N_o r_1 \alpha b}{6\pi^2} \cdot \int_{r_1}^{L} \frac{dz}{z^3} \frac{1}{2\pi(D^2 + z^2)} \tag{8}$$

assuming isotropic reradiation with albedo α, which is certainly an overestimate. The factor $2\pi(D^2 + z^2)$ is the area of a hemisphere over which the reradiated flux is spread, and α is the albedo. Thus, one has

[redacted]
DWG. 17850A

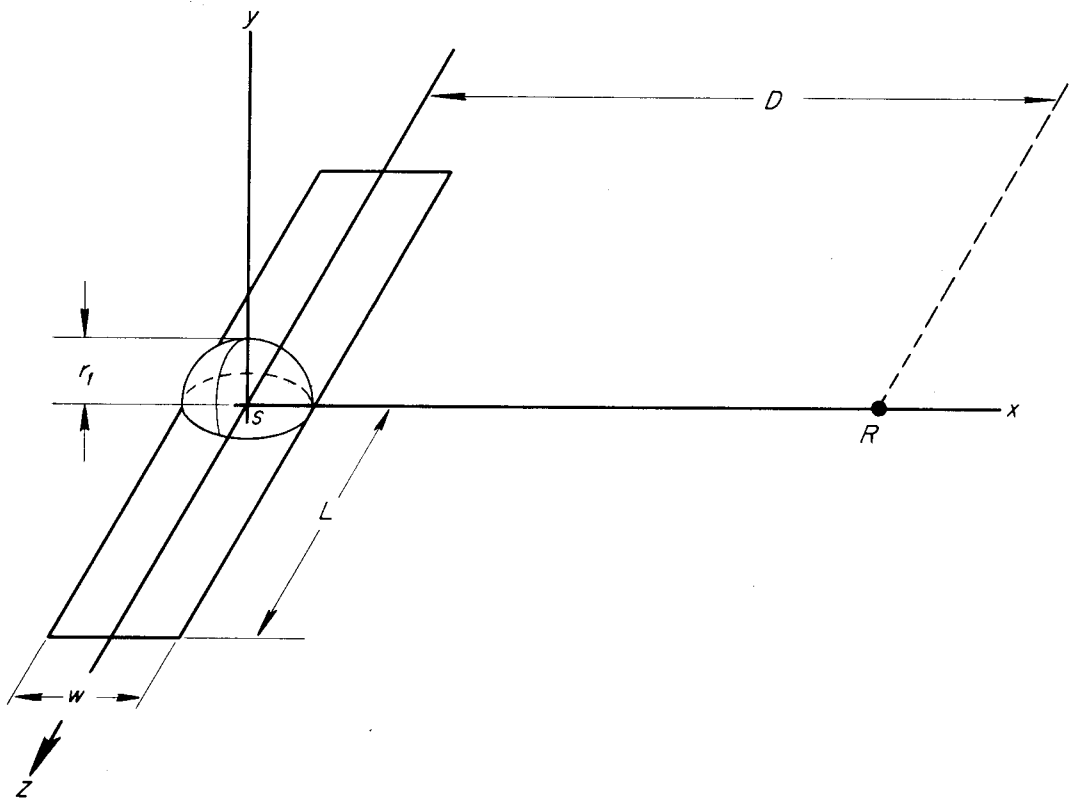

Fig. III-G-2. Albedo Scatter from Wings.

$$I = \frac{1}{6\pi^3} e^{-\mu T} GN_o r_1 b\alpha \left[\frac{1}{D^2}\left(\frac{1}{r_1^2} - \frac{1}{L^2}\right) + \frac{1}{D^4} \ln\left(\frac{r_1^2}{L^2} \quad \frac{D^2 + L^2}{D^2 + r_1^2}\right)\right] \qquad (9)$$

Normal penetration of the crew box has been assumed.

The calculations given by Blizard and Welton[1] are for a tapered, rather than a rectangular shaped, wing. If

$r_1 = 6$ ft,

$b = 20$ ft^2/ft,

$\alpha = 0.12$,

$D = 65$ ft,

$L = 115$ ft,

then, omitting G and $e^{-\mu T}$, one has, after converting to centimeters, $I = 5.26 \times 10^{-10}$ N_o neutrons/(cm^2/sec). The air scattering is $I_{air} = 1.2 \times 10^{-9}$ N_o neutrons/(cm^2/sec), so that $I/I_{air} = 0.438$, or the wing scattering is 43.8 percent of the air scattering.

In general, for albedo scatter of neutrons from a wing section of area dA, with the receiver not on the fuselage axis,

$$dI = 2\left(\frac{N_o r_1}{6\pi^2 z^3}\right) \frac{\alpha}{2\pi r^2} \, dA$$

where z is the distance from S to dA and r is the distance from dA to R.

<u>Tail Scatter</u>. A simple calculation based on isotropic radiation will be given. For the B-36 airplane, the projected area of the vertical tail assembly, as seen from the reactor, is approximately 49 ft^2. The leading edge is approximately 124 ft from the crew compartment and 59 ft from the reactor. As a result,

$$I = \frac{1}{4\pi(59)^2} \cdot \frac{49\alpha}{2\pi(124)^2} \cdot \frac{1}{(30.5)^2} N_o = 1.49 \times 10^{-12} N_o \text{ neutrons}/(\text{cm}^2/\text{sec}) \tag{10}$$

where $\alpha = 0.12$. The ratio of this to the air scattering is

$$I/I_{air} = 0.00124, \text{ or } 0.12\%$$

If we take the effectiveness of rearward neutrons for air scattering to be only 1/20 of that of the forward neutrons, to cover the case in which most of the neutrons are emitted in the rearward direction, the effective radiation from the tail at the crew compartment is still only

$$I/I_{air} = 20(0.12) = 2.4\% \text{ of the air scattering.}$$

Engine Scatter. In the B-36, the six reciprocating engines bulge below the wings with a projected area at the reactor of approximately $A = 70\ \text{ft}^2$ per pair, at distances of $r_1 = 17$, $r_2 = 37$ and $r_3 = 46$ ft from the outside of the reactor. Using an albedo calculation, the number of neutrons scattered to the crew is then

$$\frac{I}{N_o} = \frac{1}{4\pi r_1^2}\left[\frac{A\alpha}{2\pi(r_1^2 + D^2)}\right] + \frac{1}{4\pi r_2^2}\left[\frac{A\alpha}{2\pi(r_2^2 + D^2)}\right] + \frac{1}{4\pi r_3^2}\left[\frac{A\alpha}{2\pi(r_3^2 + D^2)}\right] \tag{11}$$

where the reactor-crew separation distance, D, is 65 ft. Using $\alpha = 0.12$, one has

$$I = 1.11 \times 10^{-10} N_o, \text{ and } I/I_{air} = 0.093 \text{ or } 9.3\% \text{ of the air scattering.}$$

3. Ground Scattering

The basic problem which will be considered here is the following: An isotropically emitting, monoenergetic, source S of gamma rays or neutrons is located a distance h above the ground (see Fig. III-G-3). The receiver R

[redacted]
DWG. 17851A

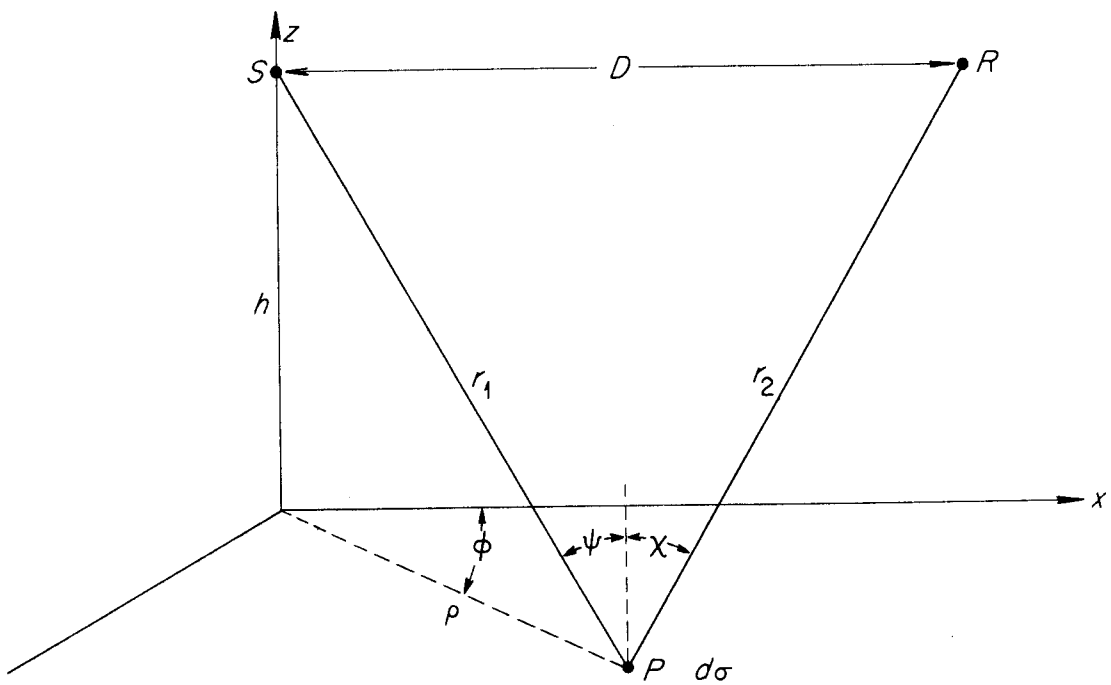

Fig. III-G-3. Geometry of Ground Scattering (Dwg. 17850 in Reactor Handbook).

is located a distance D from the source and is in the same horizontal plane. The assumption is made that h and D are both small compared to the air attenuation length so that both attenuation and buildup of radiation may be neglected. Generalization to the case of an anisotropic polyenergetic source is straightforward. Again, normal penetration of the crew shield is assumed.

Referring to Fig. III-G-3, one sees that the normal uncollided flux of particles incident upon an element of ground $d\sigma$ at a point P having coordinates (ρ,ϕ) is

$$d\Phi = \frac{N_o}{4\pi r_1^2} \cos\psi \; d\sigma = \frac{N_o h}{4\pi r_1^3} \; d\sigma \tag{12}$$

for a total source strength of N_o. If α is the albedo, the dose at the receiver is

$$dI = \frac{N_o h}{4\pi r_1^3} \; \frac{\alpha}{2\pi r_2^2} \left\{ \begin{matrix} 1 \\ 2 \cos\xi \end{matrix} \right\} G e^{-\mu T} \, d\sigma \tag{13}$$

where the choice of either isotropic or cosine reradiation has been indicated.

The coefficient 2 before $\cos\xi$ is a normalization factor from

$$1 = \int_0^{\pi/2} \frac{\beta \cos\theta}{\cancel{2\pi} \cancel{r^2}} \left(\cancel{2\pi} \cancel{r} \sin\theta\right) \cancel{r} d\theta = \beta/2$$

so that $\beta = 2$ for an albedo calculation.

The total dose at the receiver R is obtained by integrating over all ground elements $d\sigma$, so that

$$I\begin{Bmatrix}\text{isotropic}\\ \text{cosine}\end{Bmatrix} = \frac{Ge^{-\mu T}N_o h\alpha}{8\pi^2}\iint \frac{d\sigma}{r_1^3 r_2^2}\begin{Bmatrix}1\\ 2\,\dfrac{h}{r_2}\end{Bmatrix} \tag{14}$$

Expressing the variables in plane polar coordinates, one finds, after some manipulation[2,4]

$$I_{\text{isotropic}} = \left(\frac{Ge^{-\mu T}N_o h\alpha}{8\pi^2}\right)\cdot\frac{2\pi}{h^3}\int_0^1 \frac{x^2dx}{\left[1 - 2k^2x^2 + k^2(4 + k^2)x^4\right]^{1/2}} \tag{15}$$

and

$$I_{\text{cosine}} = \frac{Ge^{-\mu T}N_o\alpha}{\pi^2h^2}\int_0^\infty \frac{\rho\, d\rho\, E\,(C,\ \pi/2)}{(1 + \rho^2)^{3/2}\left[1 + (\rho + k)^2\right]^{1/2}\left[1 + (\rho - k)^2\right]} \tag{16}$$

where

E = complete elliptic integral of the second kind,

$k = D/h$,

$C = \sqrt{\dfrac{4k\rho}{1 + (\rho + k)^2}}$.

The quantities

$$\left(\frac{8\pi^2h^2}{Ge^{-\mu T}N_o\alpha}\right) I_{\text{isotropic}} \quad \text{and} \quad \left(\frac{8\pi^2h^2}{Ge^{-\mu T}N_o\alpha}\right) I_{\text{cosine}}$$

are plotted in Fig. III-G-4 as functions of D/h.

<u>Example</u>: In the B-36 airplane D = 65 ft and h = 12 ft, so that D/h = 5.4. Omitting G and $e^{-\mu T}$ and using $\alpha = 0.12$ for neutrons, one has

$$\left(\frac{8\pi^2h^2}{N_o\alpha}\right) I_{\text{isotropic}} = 0.27$$

(4) M. S. Plesset, "Scattering of Gamma Rays and Neutrons," Douglas Aircraft Company, Inc., Project Rand, RAD-196 (Aug., 1947).

[redacted]

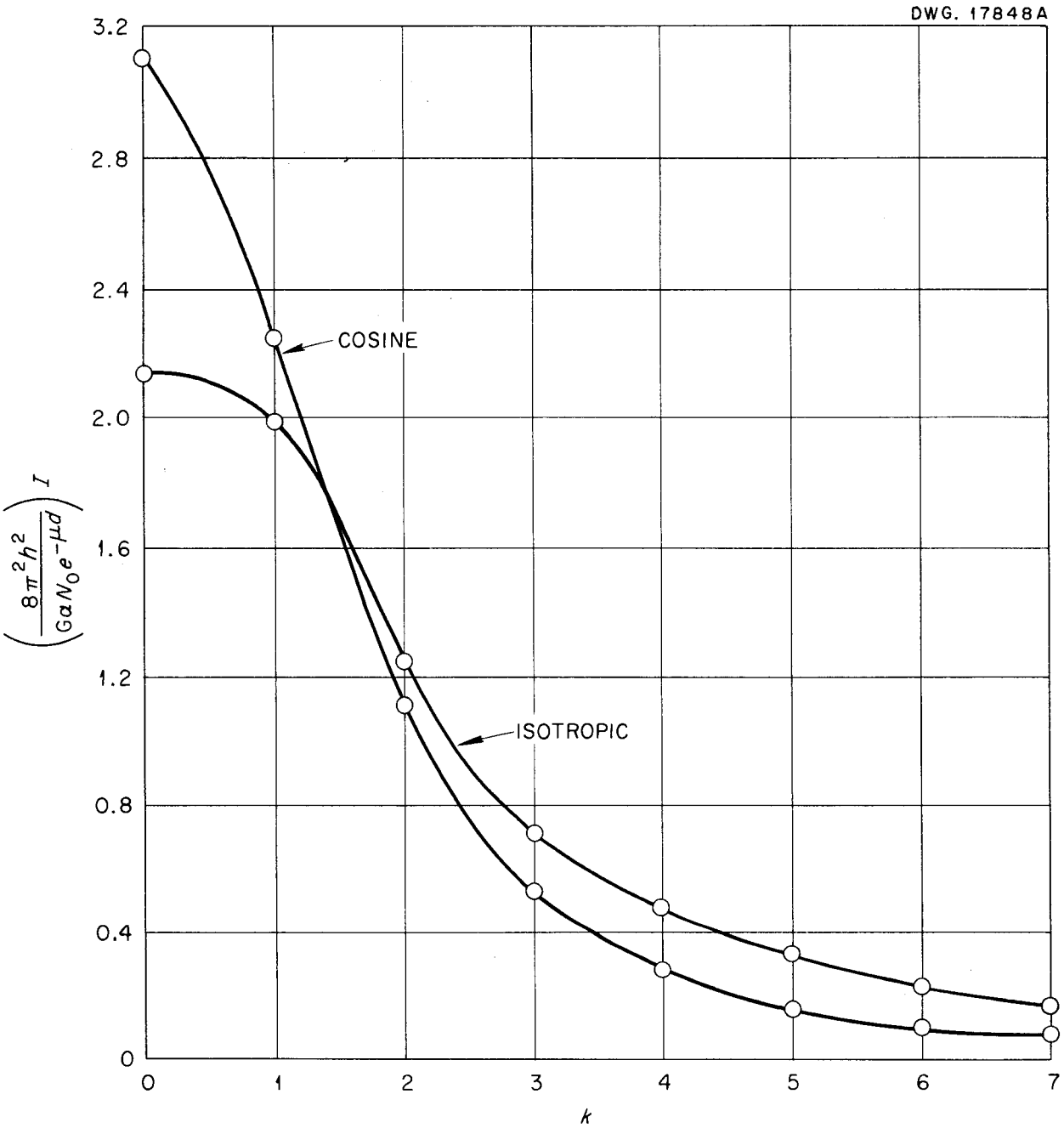

Fig. III-G-4. Dose from Ground-Scattered Neutrons or Gamma Rays.

so that

$$I_{isotropic} = \frac{0.27(0.12)N_o}{8\pi^2(12)^2(30.5)^2} = 3.07 \times 10^{-9}\ N_o \text{ neutrons/(cm}^2\text{/sec)}$$

For air scattered neutrons

$$I_{air} = 1.2 \times 10^{-9} \text{ neutrons/(cm}^2\text{/sec)}$$

so that

$$\frac{I_{isotropic}}{I_{air}} = 2.56 \text{ or } 256\% \text{ of air scattering.}$$

Similarly,

$$\left(\frac{8\pi^2h^2}{N_o\alpha}\right) I_{cosine} = 0.12$$

so that

$$I_{cosine} = 1.37 \times 10^{-9}\ N_o \text{ neutrons/(cm}^2\text{/sec)}$$

and

$$\frac{I_{cosine}}{I_{air}} = 1.14 \text{ or } 114\% \text{ of air scattering.}$$

More elaborate calculations which take into account air scattering and attenuation of the flux along the paths r_1 and r_2 may be found.[2]

III-H. DUCTS AND INTERNAL VOIDS IN SHIELDS*

The principal experimental investigations of ducts up to this time have been concerned with the effects of air ducts and voids on gamma-ray and neutron transmission in water. Many experiments on the attenuation of fast neutrons by long thin air ducts in water(1) can be understood on the basis of a phenomenological theory. This theory is presented below and is followed by a brief summary of the effect of internal voids on neutron attenuations.

The effect of ducts and voids on the attenuation of gamma rays is also discussed.

The reader should be cautioned that the theory of ducts and voids in shields is still in an embryonic stage and no completely satisfactory theory is yet at hand. It is to be hoped that careful experiments on ducts with the use of a dosimeter as the detecting instrument will clear up many of the present difficulties, such as the anomalously high "effective albedos" required in the phenomenological theory presented below. Such a program is planned at Oak Ridge. Extensive experiments on gamma-ray attenuation are being conducted at Brookhaven.

1. Attenuation of Neutrons by Air Ducts in Shields (Theory)

The attenuation of neutrons by a long thin cylindrical duct can be calculated by an albedo approach. It is assumed that the walls of the duct reradiate neutrons with an intensity proportional to the flux incident upon the wall. The constant of proportionality is the albedo, and it is assumed that the reradiation is partly isotropic and partly cosine distribution about

(1) C. E. Clifford et al. These experiments have not been published in a single report; however, they have been reported in various ORNL quarterly reports over the period from 1949 to 1952.

* Previously published in Chapter 2.6 in the Reactor Handbook, Vol. 1, p. 811, Technical Information Service, USAEC, (June, 1953).

the normal to the wall. If the reradiated flux into a unit solid angle $d\Omega$ is written

$$\frac{dF}{d\Omega} = \frac{A + 2B\cos\theta}{2\pi} \alpha' F_{inc} \tag{1}$$

where

F_{inc} = flux incident on wall,

α' = albedo of wall,

and since by conservation of neutrons there follows

$$A + B = 1$$

it can be shown[2] that the total flux at the end of a long thin duct of length ℓ and radius δ is given by

$$F = \frac{N_o}{2\pi\ell^2} \left(1 + \frac{A\alpha'}{1 - \alpha'} + \frac{4B\delta\alpha'}{\ell(1 - \alpha')}\right) \tag{2}$$

Here, N_o is the total (isotropic) source strength at the mouth of the duct. The first term represents the uncollided (non wall-scattered) flux.

The fast-neutron albedos for water and concrete have been measured at the Bulk Shielding Facility at ORNL.[3] It was found that the albedos for both were of the order of 0.1. This result, coupled with the fact that A and B are less than or equal to unity, allows one to neglect all but the first term to a reasonable approximation. Hence, the flux at the mouth of a straight duct is caused by just the uncollided neutrons to within a few percent:

$$F = \frac{N_o}{2\pi\ell^2} \tag{3}$$

An interesting by-product of this result is the prediction that one should

(2) A. Simon and C. E. Clifford, "The Attenuation of Neutrons by Air Ducts in Shields, Part I, Theory," ORNL-1217 (Nov. 28, 1952).
(3) H. E. Hungerford, "Some Ground Scattering Experiments Performed at the Bulk Shielding Facility," ORNL-CF-52-4-99 (April 16, 1952).

be able to collimate a source of fast neutrons without greatly distorting the spectrum.

The effect of a single bend in a duct can be calculated by making a simple assumption. The flux entering the region of the bend, as shown in the previous paragraph, is just the uncollided flux arriving from the source. This dose of neutrons is completely absorbed in the walls of the bend, and as a result, a reradiated flux leaves the walls with a source strength proportional to the albedo of the medium. The exact effect of the complicated scatterings at the corner is unknown; however, it will be assumed that the reradiated flux is emitted uniformly from a region of area A_t in the vicinity of the bend and with an angular distribution given by

$$\frac{dF}{d\Omega} = \frac{\alpha' D}{A_t} \quad \frac{A + 2B\cos\theta}{2\pi}$$

where

D = total uncollided neutron dose entering the region of the bend,

α' = albedo of the walls.

By conservation of neutrons,

$$A + B = 1$$

On the basis of this assumption, the total dose at the end of a duct consisting of two long thin straight sections of lengths ℓ_1 and ℓ_2 (both of radius δ) joined at an angle θ can be shown[2] to be

$$F = N_o\left(\frac{\delta^2}{2\ell_1^2}\right)\left(\frac{\alpha\delta^2}{2\ell_2^2\sin\theta}\right)(A + 2B\sin\theta) \qquad (5)$$

Here

N_o = total (isotropic) source strength at the mouth of the duct,

α = "effective albedo," a constant which is proportional to the actual albedo of the walls.

The factor $1/\sin\theta$ arises from the fact that the region of wall at the bend which is visible from the end of the duct is approximately proportional to this quantity. Figure III-H-1 illustrates this point.

Equation (5) may be generalized to cover the broad case of n + 1 straight sections of length ℓ_i (i = 1, 2, ..., n + 1) joined at angles given by $\theta_{i,i+1}$ where the subscripts denote the angle between the appropriate straight sections. The result is

$$D = N_o \left(\frac{\delta^2}{2\ell_1^2}\right) \left[\frac{\alpha\delta^2(A + 2B \sin\theta_{1,2})}{2\ell_2^2 \sin\theta_{1,2}}\right] \cdots \left[\frac{\alpha\delta^2(A + 2B \sin\theta_{n,n+1})}{2\ell_{n+1}^2 \sin\theta_{n,n+1}}\right] \tag{6}$$

In the special case of equal lengths of straight sections with equal bends, this becomes

$$D = N_o \left(\frac{\delta^2}{2\ell^2}\right) \left(\frac{\alpha\delta^2}{2\ell^2 \sin\theta}\right)^n (A + 2B \sin\theta)^n \tag{7}$$

or, since A + B = 1,

$$D = N_o \left(\frac{\delta^2}{2\ell^2}\right) \left(\frac{\alpha\delta^2}{2\ell^2 \sin\theta}\right)^n \left[1 - B\,(1 - 2 \sin\theta)\right]^n \tag{8}$$

It should be noted that Eq. (8) is not valid for angles that are so small that neutrons can go directly from one mouth of the duct to the other. In addition, the formula breaks down at angles small enough so that a large section of the wall of the bend ($>A_t$) can be seen from the end of the next leg. In this region of θ, the predicted dose should be an overestimate of the measured effect.

The constants α and B in Eq. (8) are to be determined from experiment. Their values depend on the nature of the source spectrum used as well as the

ORNL-LR-DWG 548

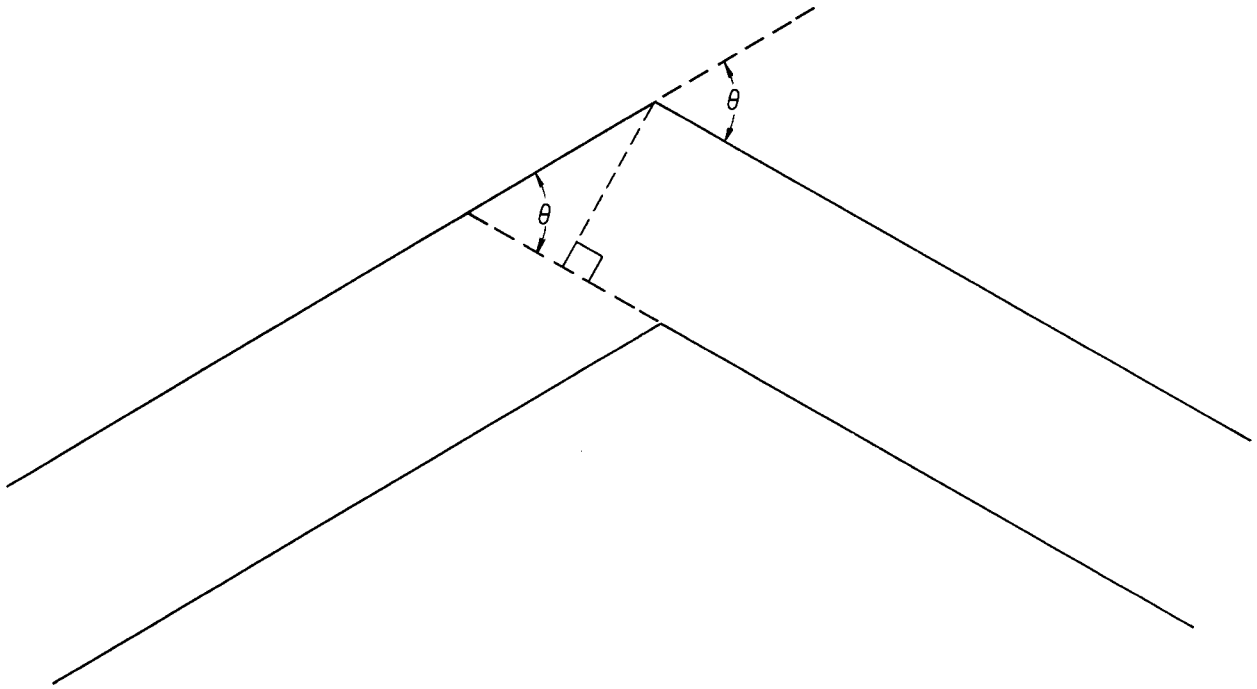

Fig. III-H-1. Dependence of Visible Wall Region at a Bend on the Angle of Bend.

type of detector. For the experiments at the Lid Tank and Thermal Column at ORNL the neutrons from a fission source were detected by means of a BF_3 counter positioned at a water-equivalent of 10, 20 or 30 cm behind the mouth of the duct. These results can be fitted by taking $B \cong 0$ (i.e., pure isotropic reradiation by the walls of the duct). The value of α depends on the counter position and is listed in Table III-H-1.

Table III-H-1. "Effective Albedo" Determined by BF_3 Measurements

Water-Equivalent Distance Between Counter and Duct (cm)	α
10	2.4
20	1.0
30	0.56

The large values of α that are needed are undoubtedly the result of using a BF_3 detector. Such a detector heavily weights the contribution of those neutrons which can be thermalized in 10, 20, or 30 cm of water. On the other hand, the measured albedos of water and concrete[3] were obtained by use of a dosimeter. It is quite probable that the wall albedos for lower-energy neutrons are considerably higher than those for the fast flux. The decrease in the value of α as the water-equivalent distance increases is in line with this picture.

It is to be expected that future experiments on duct attenuation using a dosimeter as a detector will give lower values of α.

2. Effect of Internal Voids on Neutron Attenuation

A simplified analysis of the effect of internal voids in shields on neutron transmission has been given by Tonks.[4] A method of estimating the effect of areas of weaker shielding is developed which is applicable to voids of many shapes. The result is given in terms of the excess attenuation over that which would be attained with a uniform shield having the minimum thickness found in the neighborhood of the void. This "minimal ray" technique should not be used if streaming through ducts exists. However, if the duct has been made sufficiently tortuous so that direct streaming is negligible compared to the general void effect (sometimes called "reduced density" effect), then this technique may prove to be of value.

The design of patches to compensate for internal voids has been considered by Bouricius.[5]

A diffusion theoretical treatment of the propagation of neutrons in an empty duct has been given by Whitcombe[6] and later by Roe.[7] It is not clear to what extent these treatments are applicable to fast neutrons.

(4) L. Tonks, "Enhancement of Leakage by Internal Voids in a Shield," KAPL-107 (Jan. 17, 1949).
(5) W. G. Bouricius, "Void Theory of Ducts," NEPA-1536 (Aug. 24, 1950).
(6) D. W. Whitcombe, "A Diffusion Solution for the Cylindrical Ducting Problem of Infinite Geometry," ORNL-668 (April 19, 1950).
(7) G. M. Roe, "The Penetration of Neutrons through an Empty Cylindrical Duct in a Shield," KAPL-712 (Mar. 29, 1952).

3. Attenuation of Gamma Rays by Air Ducts and Voids

The albedos for the reflection of Co^{60} gamma rays (~1.3 Mev) by concrete have been measured at the ORNL Bulk Shielding Facility.(3) By using a 50-cc standard 10^{12} ion chamber, the albedo was found to be 0.04. As a result, it may be expected that the neutron attenuation theory is applicable to gamma rays insofar as the effect of a long thin straight duct is concerned. That is, the attenuation should be geometrical. The effect of a bend on gamma attenuation is likely to be quite different from that for neutrons.

Large-scale measurements on the effect of voids on gamma-ray attenuation in water have been performed at Brookhaven.(8) The experiments have been interpreted by Kouts(9) on the basis of a two-group perturbation treatment using the integral form of the transport theory.

(8) W. W. Pratt and H. J. Kouts, "Leakage of Gamma Radiation Through Spherical and Cylindrical Voids," BNL Log No. C-6456 (Aug. 25, 1952).
(9) H. J. Kouts, "Theory of Flux Perturbations by Voids in Shields," BNL Log No. C-6459 (Sept. 15, 1952).

III-I. INTERACTION OF SHIELD WEIGHTS AND AIRCRAFT PERFORMANCE

1. Airplane and Shield Design Relationships

The performance requirements of the shield of a nuclear-powered airplane are dictated by the design specifications of the airplane. The manufacturer must show that the airplane he proposes will meet the customer's performance specifications (flight, ground handling, service and repair requirements) and payload specifications (type, weight, loading, handling facilities, etc.).

To meet the required specifications, the components of the airplane must be harmoniously designed so that each will operate in such a way that the entire airplane will perform its functions satisfactorily. The shielding must be considered as a component comparable to the power plant, wing, fuselage equipment, control surfaces, landing gear, and other systems in the airplane. This does not mean that these various parts of the plane are of equal importance, but each has its particular function and all the components must work together to produce an integrated product that will perform the functions for which it was designed.

The requirements of the shielding in an airplane are dependent on several variables which are related to the functions or performance of the airplane.

Allowed Crew Doses

The dose rate and dose to which the flight crews and ground personnel may be subjected have a very large influence on the configuration of the airplane. The magnitude of the dose rate and dose will be specified by the purchaser on the basis of medical research and the advice of physicians and biologists. The airplane designer can only show the manner in which dose rate and dose affect the configuration of the airplane.

Table III-I-1 shows a typical variation in the configuration of an airplane designed to deliver a 20,000-lb payload at high subsonic speeds at sea level. The effect of crew dose rate on aircraft gross weight and required reactor power output for a series of airplanes designed to the same performance and payload specifications is apparent. There are large differences in the cost of such airplanes and the value of decreased dose rate may therefore be determined on the basis of decreased biological hazards, increased flying time of crews, and decrease in the number of crews required. For bomber-type aircraft consideration might be given to the use of removable shield material which could be installed in training airplanes to reduce the dose rate and dose received by crews in training. Training of crews will probably be accomplished largely in flight and other training simulators and in chemically powered airplanes of similar design. A minimum of flight time will be required in the nuclear airplane.

Table III-I-1. Variation of Airplane Weight and Reactor Power with Allowed Dose Rate*

Allowed Crew Dose Rate (r/hr)	Gross Weight (lb)	Reactor Power (megawatts)	Shield Weight (lb)
0.01	730,000	910	245,000
0.10	400,000	500	137,000
1.0	265,000	331	80,000
2.0	224,000	280	65,000

* For airplane with 20,000 lb payload and high subsonic speeds at sea level.

Location of Sources

The location of the sources of radiation in an airplane is important. For instance, if the secondary heat transfer medium becomes activated the entire power plant system might be a radiation source. In other situations just the primary fluid system becomes a radiation source. These sources should be located in the airplane so that their contribution to the crew compartment dose is minimized.

Location of Sensitive Areas

The airplane designer must give consideration to the location of regions that require shielding. Their distances from the radiation sources should be made as large as is consistent with other limitations, and their surface areas should be kept as small as possible. The crew compartment, for example, should obviously be as small as possible if it is to be shielded. The airplane must be balanced, i.e., the center of gravity and the aerodynamic center of the mean aerodynamic chord must be in proper relative location for satisfactory stability and control of the airplane. The engines must be so located that satisfactory air inlet conditions are provided. The configuration and location of major components of the airplane will also affect the general aerodynamic characteristics of the airplane.

There are other sensitive regions of an airplane which must be considered. Personnel and cargo carriers will have large surface areas to be protected from radiation damage so that they present exceptional shield design problems. Compartments for equipment that may be damaged by radiation may be installed outside the crew compartment provided that this is compatible with servicing requirements. Consideration must be given to the provision for cooling facilities for the reactor and shield. These cooling provisions not only

affect the shield configuration but introduce such problems as dynamic radiator drag and power for auxiliary blowers.

The shield configurations used in airplanes will be the best compromise of the combination of the factors mentioned above and the required degree of shielding.

Effect of Altitude

The reduction in air density with altitude affects the airplane configurations as well as the shielding. The air-scattered radiation is approximately proportional to air density so that the optimum shield configuration changes with altitude. Table III-I-2 shows the variation in crew compartment dose rate for a typical bomber configuration. The assumption was made that the dose was the result of radiations which were 20% direct and 80% scattered. The dose rates at various altitudes as a function of sea level dose is shown in Table III-I-2.

Table III-I-2. Dose Rate Variation with Altitude

Dose Rate (rem/hr)		
Sea Level	20,000 ft	35,000 ft
0.10	0.065	0.045
1.00	0.65	0.45
2.00	1.3	0.90

The variation in the configuration of three typical bomber-type airplanes with altitude for a given payload flying at constant speed with a constant dose rate is shown in Table III-I-3.

Table III-I-3. Variation of Airplane Weight and Reactor Power with Design Altitude
Constant speed and dose rate

Altitude (ft)	Gross Weight (lb)	Shield Weight (lb)	Reactor Power (megawatts)
Sea level	224,000	65,000	280
20,000	153,000	38,000	81
35,000	149,000	38,200	83

The values given in this table are for an all-nuclear airplane (without chemical fuel augmentation) and the reduction in shield weight includes the effect of reduced reactor power and the reduction of air density with altitude. This relationship is shown graphically in Fig. III-I-1.

Chemical Augmentation of Power

An all-nuclear airplane may not be as effective as an airplane with power chemically augmented for take-off and high-speed flight. The reactor power of a four-engine airplane of this type would be determined by that required for operation at a safe altitude with one engine inoperative. Table III-I-3 shows an airplane designed for sea level operation with a ratio of gross weight to reactor power (W/R) equal to 224,000/280 = 800. The airplane designed for operation at an altitude of 20,000 ft would require the same effective value of W/R ratio for satisfactory sea level performance. The W/R ratio for the data given in the table is 1890. This value would have to

[redacted]

ORNL-LR-DWG 444

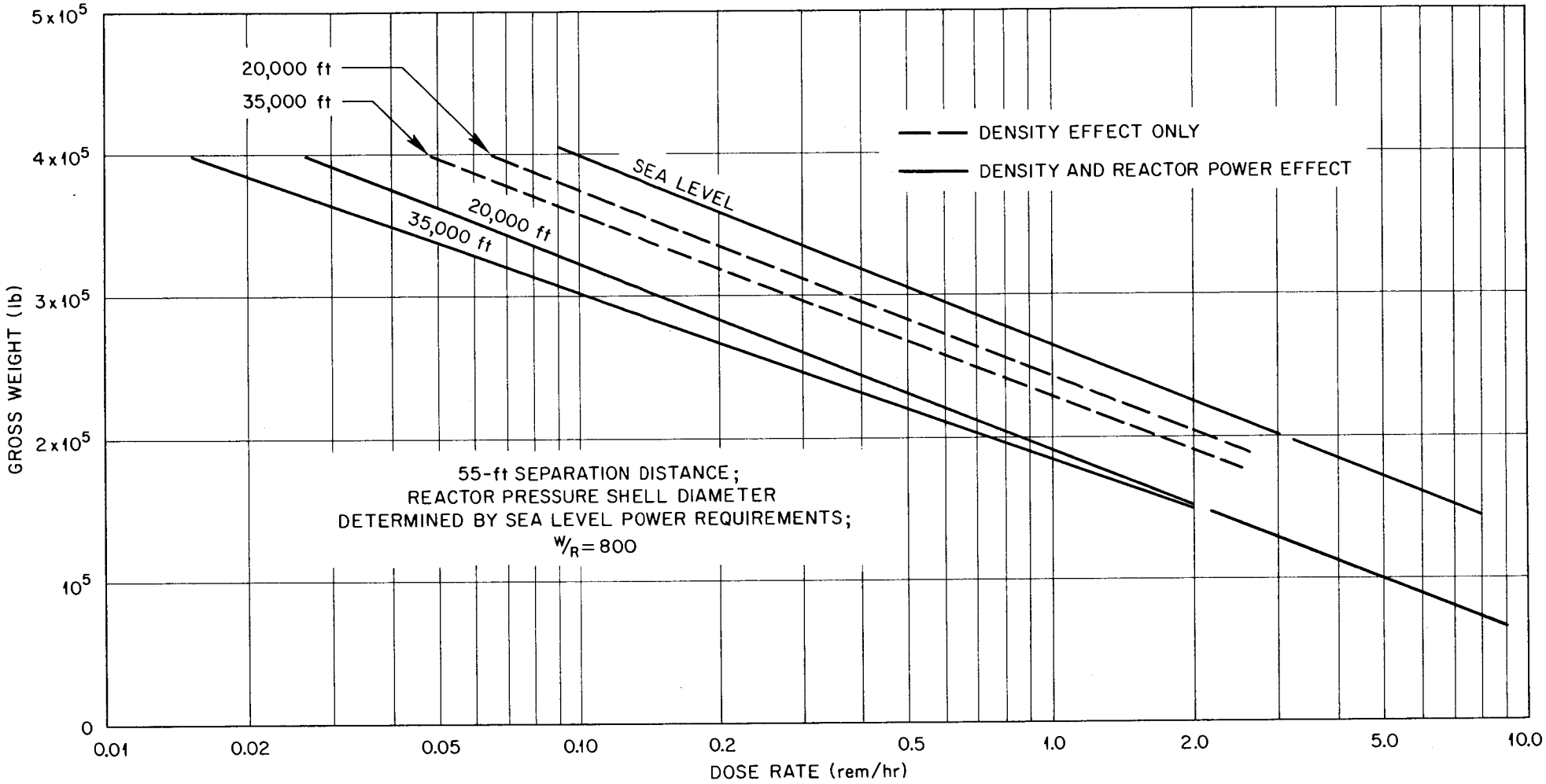

Fig. III-I-1. Variation in Gross Weight of Bomber-type Airplane (Divided Shield) with Altitude.

be reduced by the addition of thrust from chemical power so that an "effective" W/R ratio of 800 would be available. The fuel used in the chemically augmented type of airplane might be used as shielding material. For example, if the reserve fuel were located in a tank directly aft of the crew compartment, it would be effective as a shielding material until it was consumed. This would only occur in an emergency and then toward the end of the flight so that exposure time to the increased radiation would be of short duration compared with the relatively long time during which beneficial effects were being realized.

2. Effects of Shield Weight on Airplane Configuration

The weight of the shielding material required in a nuclear-powered airplane to give tolerable radiation dose rates is such a large percentage of the gross weight that it has a great influence on the airplane's configuration. Since the weight of the airplane affects the configuration and performance to such a large extent, great effort must be exerted to minimize the shield weight. The following discussion shows how the weight of the airplane is affected by variations of the shield weight.

Let the gross weight of the airplane be expressed by the following equation:

$$W = W_S + W_E + W_{PP} + W_U \tag{1}$$

where

W = gross weight,

W_S = structure weight,

W_E = equipment weight,

W_{PP} = power plant weight

= engine weight + shielding weight,

W_U = useful load

= payload + fixed useful load.

The variation of the structural weight depends on the type of aircraft; i.e.,

$$W_S = 0.20W \text{ to } 0.40W$$

For bomber-type aircraft or aircraft with relatively small payloads, the structure might be 20% of the gross weight. For cargo-type airplanes with relatively large payloads, the percentage is higher. Fast aircraft have higher percentage structural weights than slower aircraft.

Let us assume that a low-altitude high subsonic speed aircraft with a relatively small payload will have a structural weight of 25% of the gross weight so that

$$W_S = 0.25W \tag{2}$$

The equipment weight may be expressed in two parts, one a constant and the other dependent on the gross weight. The equipment weight for the aircraft being considered may be expressed by the following equation

$$W_E = 0.02W + 10{,}000 \tag{3}$$

where the constant accounts for crew provisions, instruments and other items not dependent on gross weight. The variable term accounts for controls and other items dependent on the airplane's gross weight.

The power plant weight, W_{PP}, is composed of engine weight and shielding weight. Since the engine weight is related to the power rating of the reactor, it may be expressed by

$$W_{eng} = 250\ R$$

where R is the reactor heat in megawatts. The shielding weight is dependent on the type of shield (unit or divided), reactor power rating, crew compartment and reactor separation distance, crew compartment size, and permissible dose rates both in the crew compartment and in the vicinity of the reactor at reduced power with the airplane on the ground. The shielding weight for a particular airplane configuration may be expressed by

$$W_{sh} = W_o + K_{sh}R$$

where W_o is a part of the shield weight which is independent of reactor power and K_{sh} is the rate of increase of shield weight with reactor power. Let us assume that the shield weight for the airplane being considered here may be expressed by

$$W_{sh} = 90{,}000 + 100R$$

Therefore, the total power plant weight is

$$W_{PP} = 350R + 90{,}000 \tag{4}$$

The useful load is composed of the payload and the fixed useful load. The fixed useful load includes bomb racks, missile launchers and other loads that are carried for the complete mission. Let the useful load be expressed by

$$W_U = W_{pl} + 2000 \tag{5}$$

Adding Eqs. (2) through (5), we obtain the obtain the following expression for the gross weight of the airplane:

$$W = (0.25W) + (0.02W + 10{,}000) + (350R + 90{,}000) + (W_{pl} + 2000)$$

$$= \frac{102{,}000 + W_{pl}}{0.73 - 350R/W} \tag{6}$$

The term R/W is related to the performance of the airplane.

Let the airplane considered here be required to have a speed of 595 knots (Mach. = 0.90) at sea level and a payload of 20,000 lb. Assume the following variables which are reasonable for this type of aircraft and the power plant used:

$$L/D = 6$$

$$T/R = 150$$

where L/D is the lift drag ratio of the airplane at 595 knots at sea level for

a wing loading of 100 psf. T/R is the thrust per megawatt of reactor power at 595 knots at sea level.

$$L/D = W/T$$

$$W/R = W/T \times T/R$$

$$= 6 \times 150$$

$$= 900$$

The gross weight of this airplane will then be

$$W = \frac{102{,}000 + 20{,}000}{0.73 - 350\left(\frac{1}{900}\right)}$$

$$= \frac{122{,}000}{0.341}$$

$$= 358{,}000 \text{ lb}$$

If 1 lb of shield weight is added to the airplane, the gross weight of the airplane will be increased as follows:

$$W + \Delta W = \frac{122{,}000 + 1}{0.341}$$

$$\Delta W = \frac{1}{0.341} = 2.93 \text{ lb}$$

This effect of shield weight in the gross weight of the airplane will be different for a different type of airplane or for different values in the basic assumptions. For example, suppose that the structural weight is 30% of the gross weight instead of 25%. The gross weight increase per pound of shield weight increase will then be:

$$\Delta W = \frac{1}{0.341 - 0.05} = \frac{1}{0.291} = 3.44 \text{ lb}$$

If the percentage were 20% instead of 25% the change in gross weight per pound of shield weight would be

$$\Delta W = \frac{1}{0.341 + 0.05} = \frac{1}{0.391} = 2.56 \text{ lb}$$

A change in power plant weight, i.e., letting W_{eng} = 300R instead of 250R, as a function of reactor power will change the gross weight as follows:

$$W = \frac{122{,}000}{0.730 - 400(1/900)} = \frac{122{,}000}{0.730 - 0.445}$$

$$= \frac{122{,}000}{0.285} = 428{,}000 \text{ lb}$$

With this variation in engine weight with reactor power, a pound of shield weight increase will add 3.51 lb to the gross weight of the airplane.

The performance of the airplane will affect the manner in which shield weight increases add to the gross weight of the airplane. If the L/D of the airplane were increased to 20 and the value of T/R were unchanged, then the value of W/R would be increased to 3000. The gross weight would thus be:

$$W = \frac{122{,}000}{0.730 - 350\left(\frac{1}{3000}\right)} = \frac{122{,}000}{0.730 - 0.117}$$

$$= \frac{122{,}000}{0.613} = 200{,}000 \text{ lb}$$

The reactor power of the 358,000-lb airplane with a W/R ratio of 900 would be 398 megawatts. For the 200,000-lb airplane with a W/R ratio of 3000, the reactor power required would only be 67 megawatts.

The performance of the airplane therefore has a tremendous effect on the required reactor power. The weight and reactor power comparison shown above for W/R = 900 and W/R = 3000 are for cruising conditions only. The provision of sufficient power for satisfactory take-off, climb after take-off with landing gear and flaps extended, and satisfactory performance at partial

power, will require a lower W/R ratio than the value of 3000 shown above.

The effect of shielding on the performance of an airplane is shown in Figs. III-I-2 through III-I-5. Figure III-I-2 shows the effect of crew compartment dose rate on the gross weight of the airplane. The airplane used here for the illustration of performance changes is a high subsonic speed low-altitude bomber with a power rating of 400 megawatts and a wing area of 3000 ft^2. Since dose rate is such an important variable in the design of a nuclear airplane, it was used to show how performance changes with gross weight on the basis of equivalent dose ratio. Figures III-I-3 through III-I-5 respectively show the rate of climb and ceiling, the take-off distance, and the single engine performance as a function of crew compartment dose.

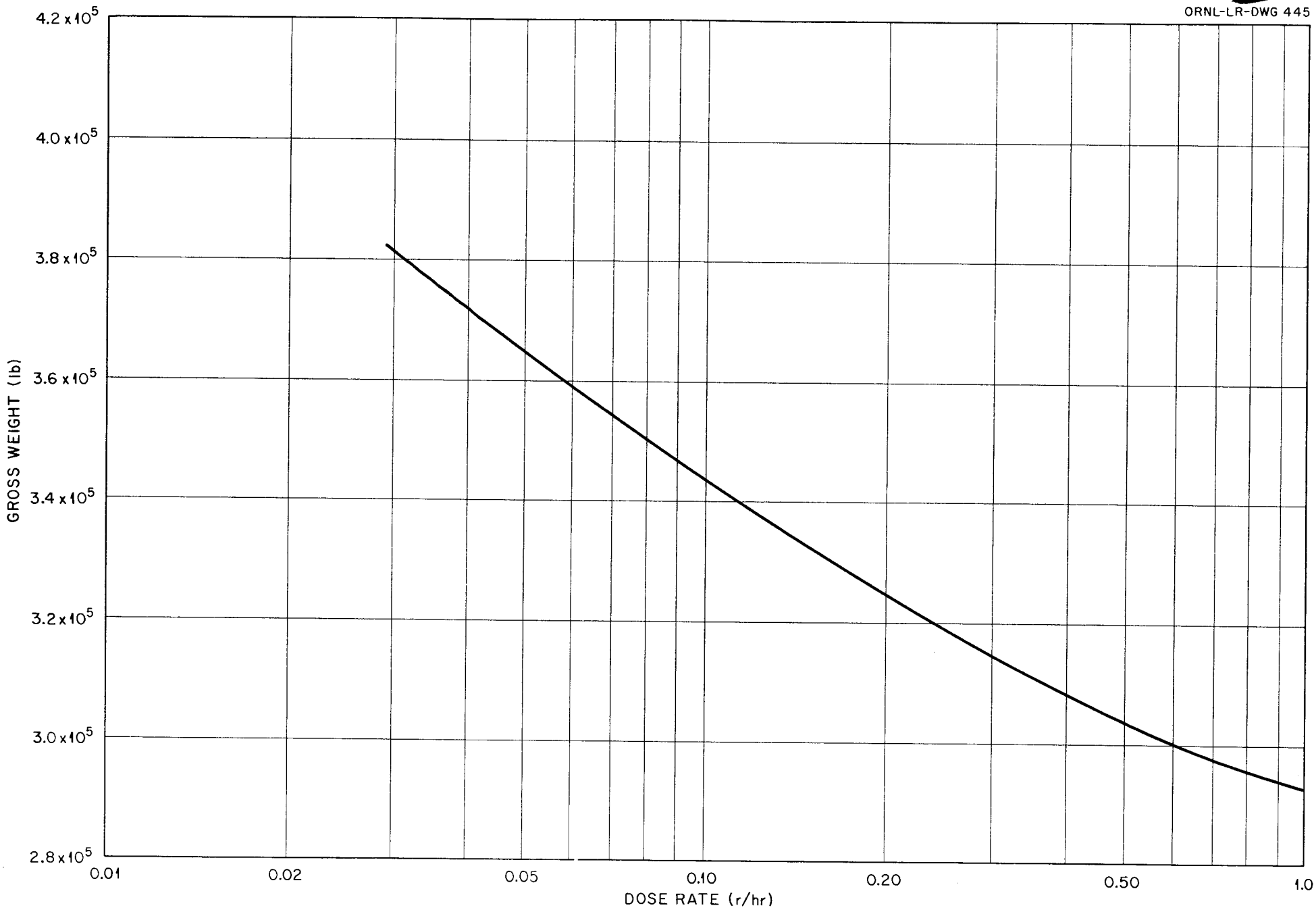

Fig. III-I-2. Variation in Gross Weight of Bomber-type Airplane with Crew Compartment Dose Rate.

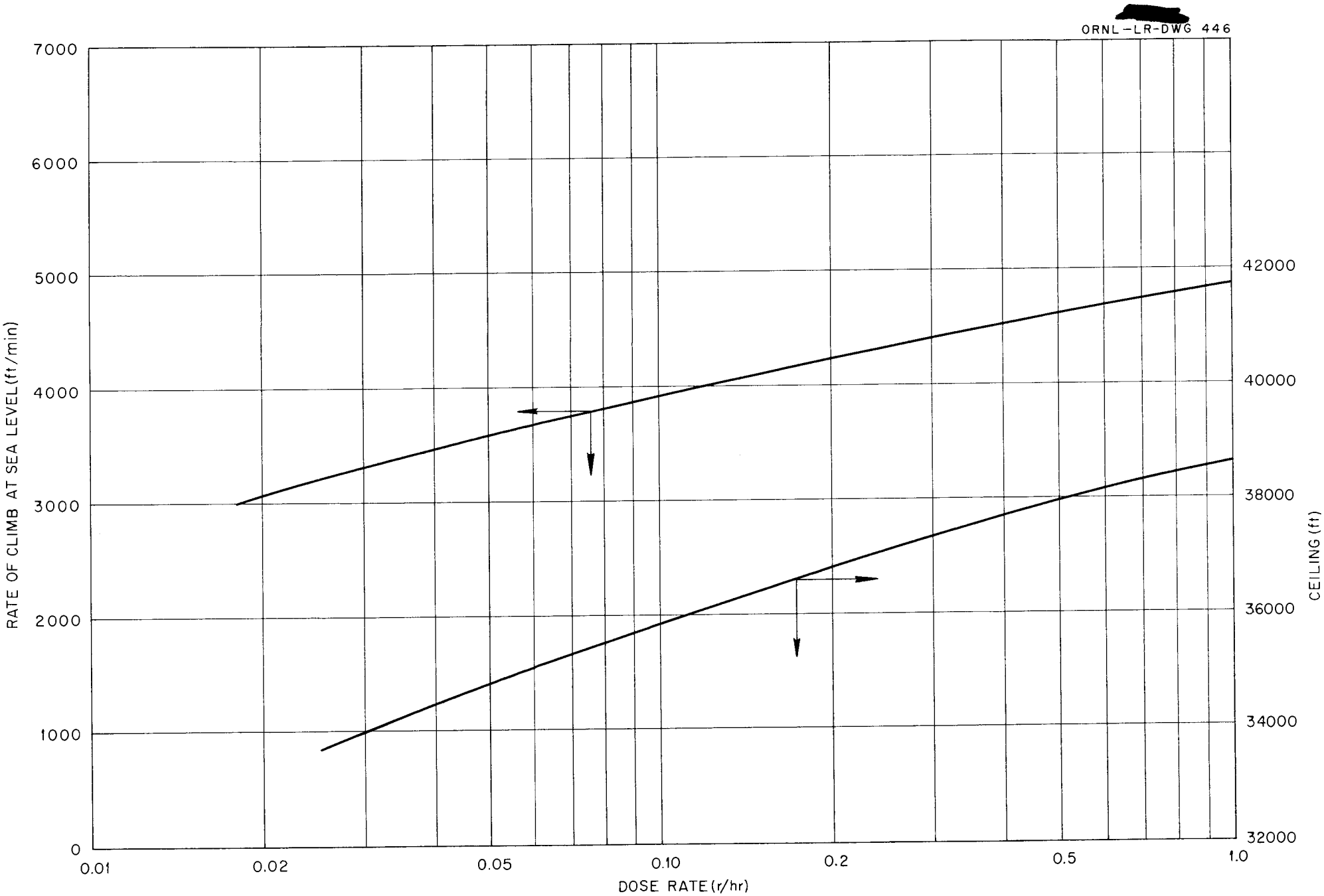

Fig. III-I-3. Variation in Rate of Climb and Ceiling of Bomber-type Airplane with Crew Compartment Dose Rate.

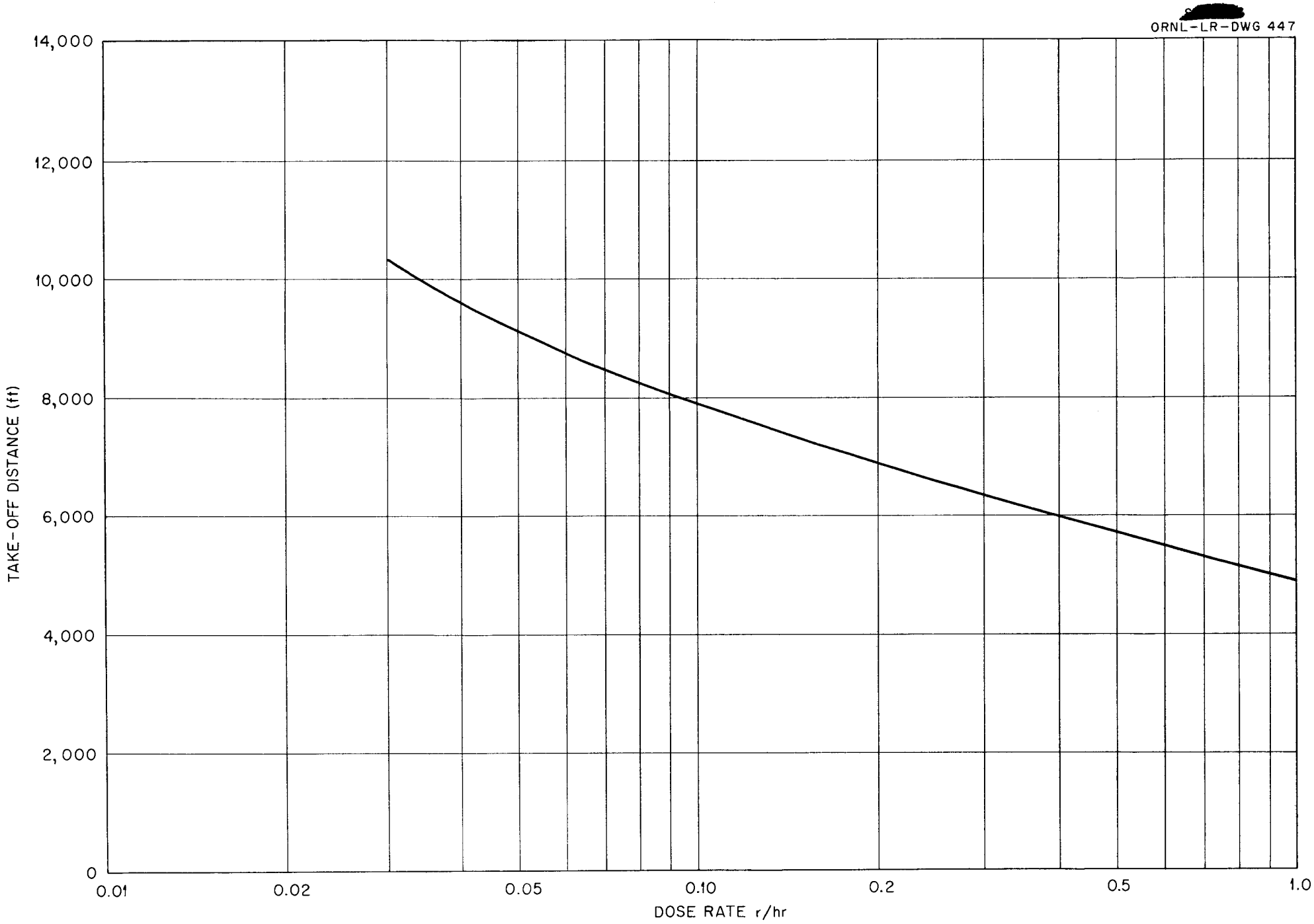

Fig. III-I-4. Variation in Take-off Distance of Bomber-type Airplane with Crew Compartment Dose Rate.

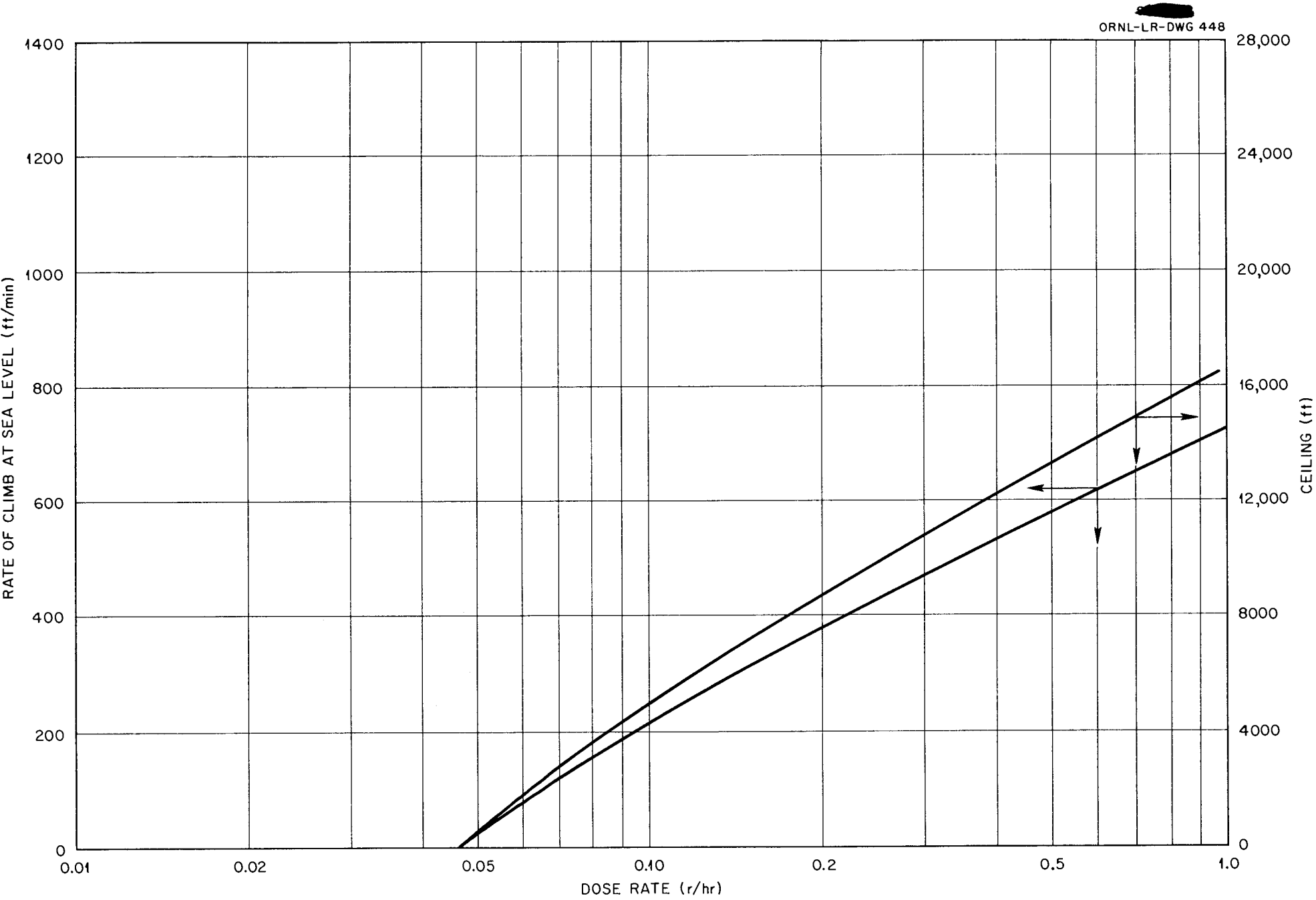

Fig. III-I-5. Variation in Single Engine Performance of Bomber-type Airplane with Crew Compartment Dose Rate.

III-J. GROUND HANDLING OF AIRCRAFT WITH UNIT AND DIVIDED SHIELDS

The nuclear-powered aircraft presents a servicing problem which is unique. The complexity of the problem is affected directly by the type of shielding which is employed around the reactor, and the type and degree of shielding will be determined by the basic form of the reactor and by the design requirements of the aircraft.

First, the permissible dose of radiation must be established for the crews which are to perform the service operations. There is no reason to believe, at present, that this will be other than the current laboratory rate of 0.30 rem/week. It is quite possible that this may be interpreted as a 3.9-rem limit for a 13-week period, allowing a worker to receive a large dose rate for a short time. In addition, an emergency and lifetime dose of 100 rem may be permitted under certain exceptional circumstances.

The shields to be discussed range from the unit (1 to 5 rem/hr at 50 ft) to the highly divided types ($\sim 10^5$ rem/hr at 50 ft). In practice, it is doubtful if the 1- to 5-rem shield will be used in the early high-speed nuclear-powered aircraft. It is more probable that, owing to weight and size limitations, shields will be in the 50- to 100-rem/hr range for the cycles with which the unit or semiunit shield may be employed.

Owing to the nature of the direct air cycle reactor, its shield will be rather highly divided and will probably give a dose of the order of 10^5 rem/hr at 50 ft from the reactor at full power, outside of the crew compartment. It is quite possible to provide unit shields with the supercritical water and the reflector-moderated reactor cycles, but, as stated before, it is considered unlikely that their shields will give less than 50 to 100 rem/hr outside of the crew shields in a supersonic aircraft.

The latter two cycles offer the additional advantage of being susceptible to ground shield augmentation by replacement of shield fluids with denser materials when proximity to the power plant is required. Since many air ducts penetrate the shield of the air cycle reactor, shield augmentation is not sufficiently effective to be attractive.* The ground handling problems associated with the air cycle are therefore of much greater magnitude than those of the other two cycles.

If it is assumed that the SCWR power plant gives 100-rem (at 50 ft, full power) or less, then within 1 hr after shutdown following an extended flight, with shield augmentation the ground crew may approach within 20 ft of the reactor for about 30 min without exceeding the weekly laboratory dose. After 24 hr have elapsed, a man may spend this period of time at 10 ft from the reactor. If the circumstances warrant, it may be desirable to use the 13-week dose rates, increasing the work time in the high radiation field but reducing the frequency of such exposures.

In the case of the RMR cycle, comparable or lower dose rates may be obtained by augmentation and drainage of the highly active fuel into buried tanks. Adoption of such procedures might make possible extended work near to the surface of the reactor itself, although, because of great handling and contamination problems, such techniques would probably not be employed after each flight.

The dose rates to be expected for the various types of reactors without augmentation is included on Fig. III-J-1.

Servicing of the direct air cycle power plant will require extensive portable shielding since it will be impossible to approach the reactor, even

* This conclusion was not shared unanimously by all Session members.

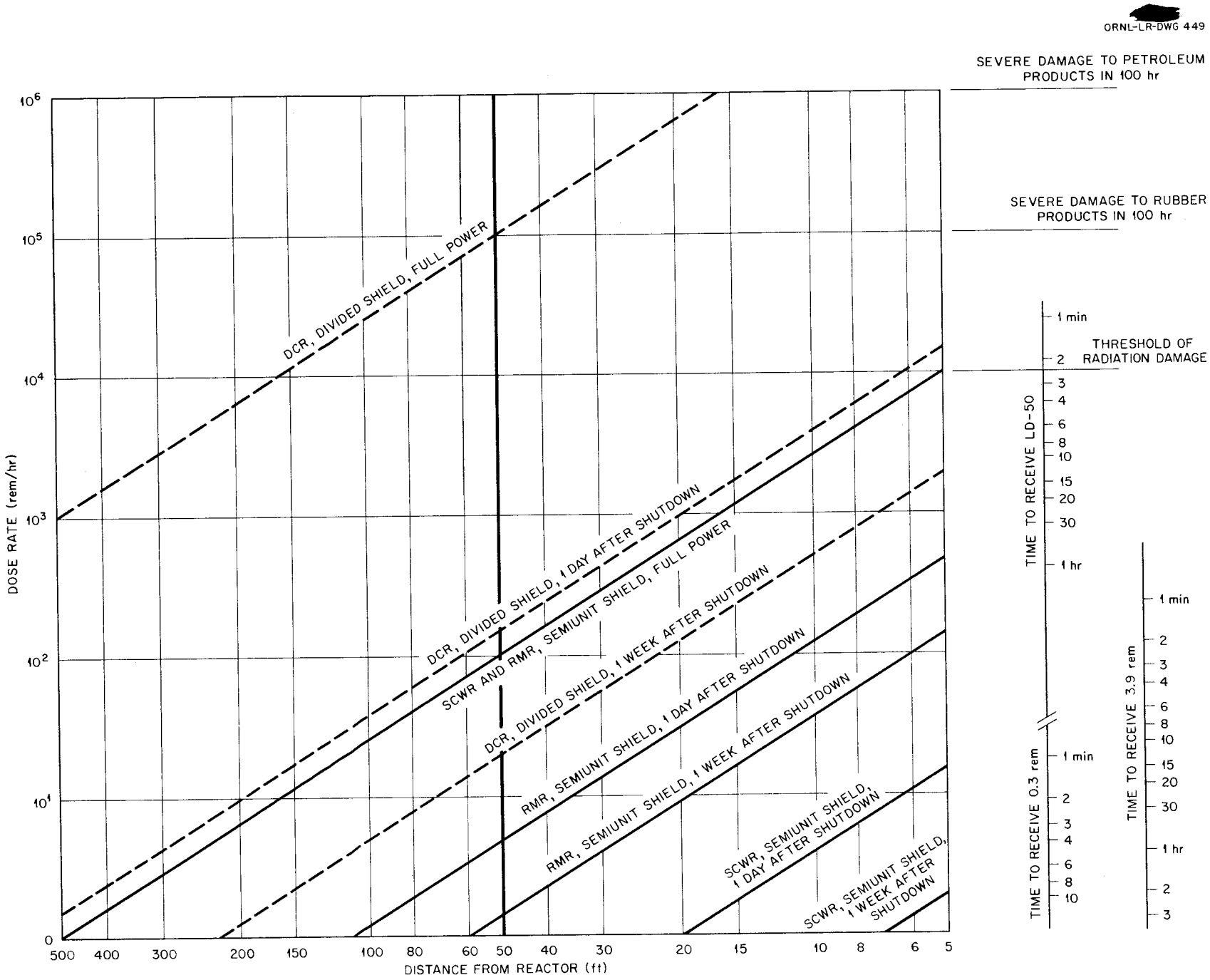

Fig. III-J-1. Radiation Levels after Shutdown, Unaugmented Shields.

10 days after shutdown, without it. Since it is assumed that there will be routine inspections and maintenance to be performed after each flight, this auxiliary equipment must be provided.

The initial step toward a solution would be to rotate work crews from a large reservoir of personnel so that individuals could work to the 3.9-rem dose rate. This implies a reserve in the neighborhood of 50 men per aircraft if it is assumed that each plane makes one flight per week and four men are required to service engines following each flight. For servicing of the engines, manipulators and shielded vehicles would be required. It is possible that for aircraft servicing, the reactor or entire power unit could be lowered into a pit beneath the aircraft, thus reducing the radiation intensity.

The highly divided shield with air ducts adds considerable difficulty to the servicing of aircraft and engine components through secondary activation by neutrons escaping via the ducts. Parts containing even trace amounts of cobalt, for example, will probably have to be handled remotely in a hot shop if close to the reactor. In the RMR and SCW power plants, the contamination exterior to the reactor will be confined to the fluid passages. These may be readily flushed clean to a low activity level and probably worked on directly. Engine and aircraft parts should not be seriously activated.

A third way in which shielding affects ground handling is indirect but important nevertheless. Crashes must be anticipated in the operation of any aircraft and evacuation of the crew from a wrecked aircraft must be considered.

It is obvious that the closer the design approaches a unit shield, the less is the protection inside the crew shield in the event of reactor shield rupture. In the case of the 10-rem/hr shield it becomes problematical whether

the crew could be saved from this type of accident. It also becomes apparent that with the unit shield more protection for the shield itself is important.

The crew inside the heavy capsule associated with the divided shield could very probably be saved if the crash were accessible to salvage vehicles. In this instance, the capsule would be removed from the aircraft and hauled to a safe location. The heavy shielding would provide vital time for the salvage operation.

Finally, the shielding of the aircraft will affect the over-all layout of the base itself. The divided shield will require much greater separation distances because of more intense radiation fields and because of activated particles discharged into the atmosphere. The buildings generally will be more heavily shielded than those in a service area for the RMR or SCW powered aircraft.

It should also be pointed out that the amount of maintenance work required on the airplane will depend in part on the degree of division of the shield. Since the most radiation-resistant synthetic rubbers and plastics shrink and become very brittle after an integrated hard gamma flux of about 5×10^{15} photons/cm^2 (i.e., a total gamma dose of 5×10^6 r), all plastic and rubber O-rings, hoses, gaskets, electrical insulation, tires, etc. would require replacement after 5 hr at 10^6 r, 50 hr at 10^5 r, or 500 hr at 10^4 r. Since much of this material would have to be closer than 50 ft from the reactor, it appears that the extremely divided shields would require either the elimination of organic materials from the airplane or else a large amount of special maintenance.

To summarize then, it will be seen that the ground handling of the nuclear-powered aircraft is strongly influenced by the dividedness of the

reactor shield. With the highly divided shield, manpower, portable shielding, portable manipulators, and base area requirements are considerably increased over those of the unit or semiunit shield. Hazards to ground personnel are greater with the divided shield but are less to flight crews.

IV. APPLICATION OF SHIELD DESIGN METHODS TO THE REFLECTOR-MODERATED REACTOR

IV. APPLICATION OF SHIELD DESIGN METHODS TO THE REFLECTOR-MODERATED REACTOR

A fairly complete series of shield designs has been made for the reflector-moderated reactor and is presented here partly to show the methods which are applicable to this type of reactor and partly to show the effects on shield weight of such variables as the degree of division of the shielding between the reactor and the crew. The material covered includes the ORNL Lid Tank tests on which the design work was based, the detail design procedure for the reactor shield, calculations of the dose expected from gamma activity in the heat exchanger and of the delayed neutron activation of sodium in the heat exchanger, the crew shield design procedure, and tables and curves presenting the results.

IV-A. SUMMARY OF THE LID TANK TESTS

The shield designs covered in this portion of the report have been based on an extensive set of shielding experiments carried out in the ORNL Lid Tank. Approximately eighty configurations were run, each differing from the others in the thickness and composition of the moderator-reflector, the heat exchanger, pressure shell, gamma shield, or hydrogenous regions. Two major sets of tests were run. In the first the beryllium reflector region was simulated with an 11.5 in. thick tank filled with beryllium pellets (to give an effective density of 1.23) followed by a solid beryllium slab 3.6 in. thick borrowed from the spare part supplies of the MTR. In the second set of tests an 11.8 in. and then a 15.4 in. thick beryllium reflector region were simulated with beryllium blocks borrowed from the Critical Experiment Facility. In both instances several different thicknesses of heat exchanger were employed. For each of the configurations a series of lead thicknesses was tested. Additional experiments carried out with some of the more interesting configurations included the substitution of nickel, Inconel, or copper for iron in the pressure shell region. Both tungsten carbide and metallic uranium were tested in place of lead and transformer oil was substituted for water. Data on the activation of sodium in the heat exchanger region were obtained for different thicknesses of the beryllium, boron, and heat exchanger regions. The results of these tests can be summarized as follows:

(1) The thickness of the beryllium reflector region should be about 12 in. to minimize over-all reactor shield weight and still remain consistent with core reactivity requirements.

(2) The thickness of the heat exchanger region has relatively little effect on neutron and gamma dose curves plotted as a function of distance from the source plate.

(3) The thickness of the lead layer over the range covered (0 to 7.5 in.) had practically no effect on the neutron attenuation curve well out in the shield.

(4) Beryllium is more effective than water on a thickness basis for neutron attenuation. This can be seen from Fig. IV-A-1 by comparison of the dashed line for pure water and the solid line representing the data with part of the water replaced by beryllium.

(5) A 0.13 in. thick layer of B^{10} (ρ = 2.1 g/cc) is as effective as a 1 in. thick layer of B_4C (ρ = 1.95 g/cc) in depressing the thermal-neutron flux. Hence, a reduction in the shield radius can be achieved by using B^{10} in place of B_4C on both sides of the heat exchanger.

(6) While separating the lead region into layers with borated hydrogenous material between the layers gives some reduction in gamma dose for a given thickness of lead, the full-scale shield design is simplified structurally by placing all of the lead together just outside the pressure shell. While lumping the lead in this fashion increases the lead thickness required, keeping its radius to a minimum largely compensates for this so that very nearly minimum over-all shield weights can be obtained in this manner. For lead thicknesses greater than about 6 in., however, the reduction in attenuating efficiency is

[redacted]

ORNL-LR-DWG 546

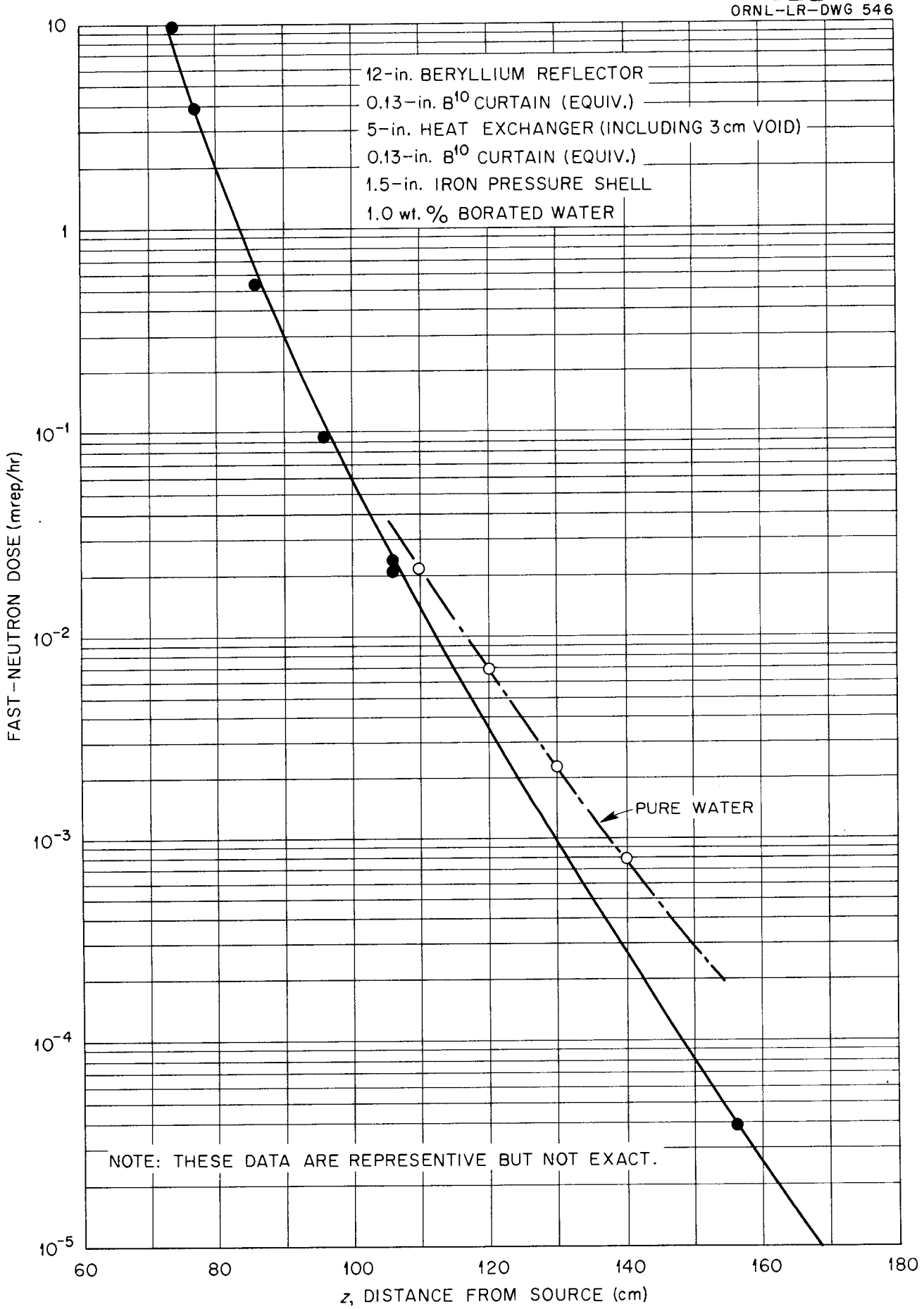

Fig. IV-A-1. Fast-Neutron Dose Beyond Typical Mockup of Reflector-Moderated Reactor and Shield.

so great that the weight penalties become significant (see Fig. IV-A-2).

(7) Transformer oil is as effective as water on a volumetric basis for attenuating the neutron flux. Since its density is about 0.87, an appreciable saving of shield weight can be obtained through its use provided it can be borated to a few percent by weight by addition of some compound such as borine triamine, $B_3N_3H_6$, B.P. = 53°C, or trimethyl borate, $B(OCH_3)_3$, B.P. = 65°C. Some of this weight saving is offset by the fact that the thickness of the lead layer must be increased because the attenuation of the gamma flux is not as great in the oil.

[redacted]

ORNL-LR-DWG 547

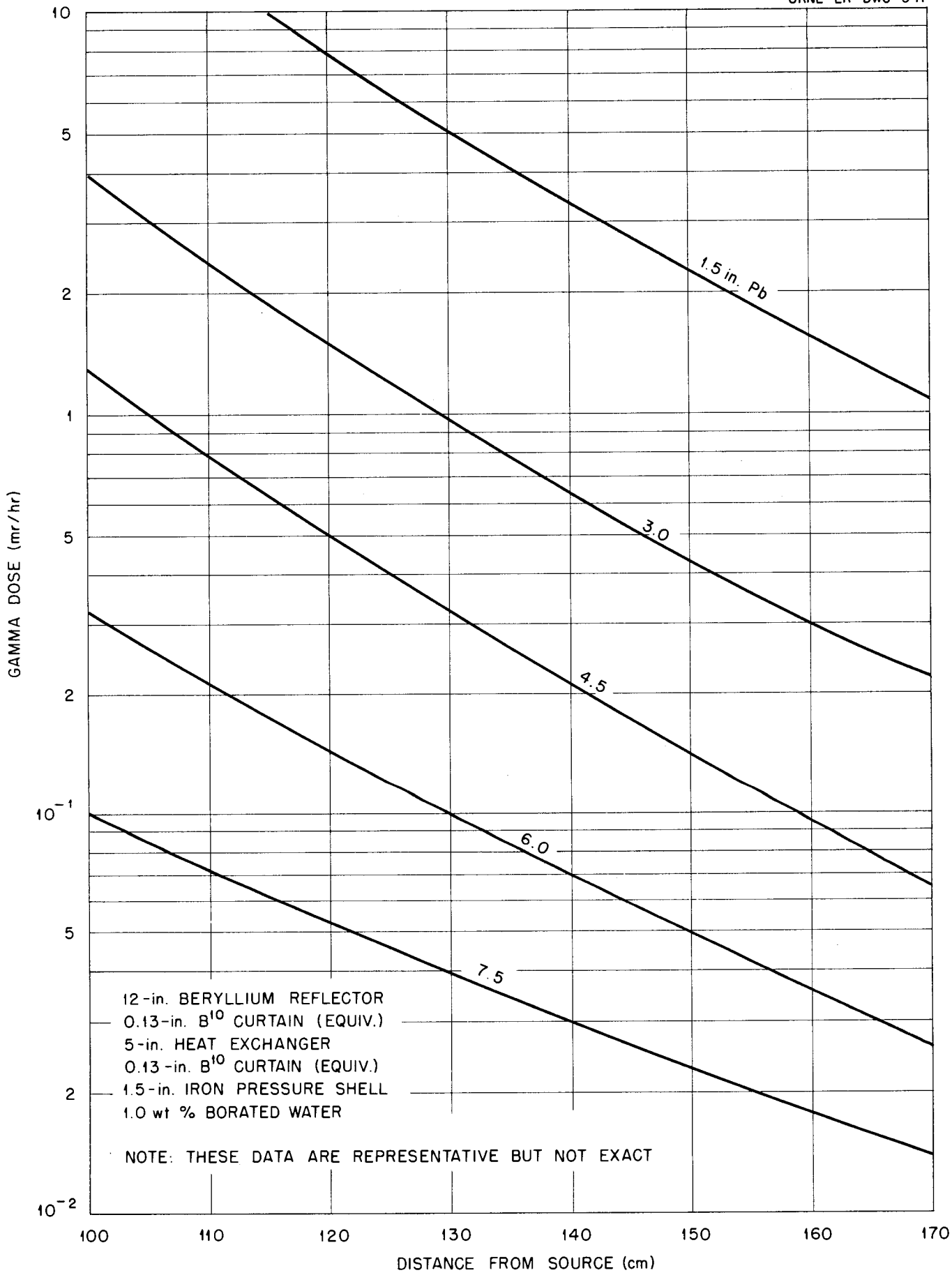

Fig. IV-A-2. Gamma-Ray Dose Beyond Typical Mockups of Reflector-Moderated Reactor and Shield.

IV-B. DESIGN PROCEDURE FOR THE REACTOR SHIELD

Where possible the shield design is achieved by a scaling up of bulk shielding measurements, in this case those from the ORNL Lid Tank. The direct (not air-scattered) dose from neutrons and gamma rays in the core, including secondary gamma rays from core-born neutrons, can thus be determined more or less directly from the Lid Tank tests. This will be described first; other components such as delayed neutrons and gamma rays produced in the heat exchanger will be treated in a subsequent section.

1. Scale-up of Lid Tank Measurements

In the Lid Tank tests a disk fission source was used directly against a slab mockup of the actual reflector, heat exchanger, and shield. The dose was then measured as a function of thickness of the outer water layer, the shield thickness being chosen subsequently to give an appropriate dose level.

There are two steps to scaling up the data to the full-power reactor case:

(1) A correction (transformation) must be made to compensate for the difference in geometry of the two situations.

(2) The source strength must be scaled up.

Because the reactor represents a distribution of sources, the geometry is inseparable from the source scale-up, and these two steps will be treated together.

The general procedure will be to transform the Lid Tank disk source data to that of an infinite plane source, to go from this to the dose to be expected with a spherical array of sources such as is approximated by the RMR core, and finally to allow by simple inverse distance squared attenuation for the fact that the crew will be remote from the reactor shield surface.

The disk to infinite plane transformation is the Hurwitz transformation described on page 301. For the present purposes the approximate form will be used.

$$D_{Pl}(z,\infty) \cong \left[\frac{1}{2} + \frac{2\lambda^2}{a^2}\left(\frac{z}{\lambda} + 1\right)\right] D_{Pl}(z,a) \qquad (1)$$

where

$D_{Pl}(z,a)$ = Lid Tank data normalized to unit source strength per unit area,

$D_{Pl}(z,\infty)$ = dose for infinite plane source of unit strength per unit area,

a = Lid Tank source radius (35.56 cm),

z = distance from source to detector,

λ = relaxation length for the dose in the region of z.

The dose from a spherical surface source was shown on page 91 to be related to that from an infinite plane source, both having the same specific source strength, as follows:

$$D_S(r_o,r) = \frac{rS}{r_o}\left[D_{Pl}(r_o - r,\infty) - D_{Pl}(r_o + r,\infty)\right] \qquad (2)$$

where

r = spherical surface source radius,

r_o = radial distance from sphere center to detector,

S = source strength on the sphere; that on the plane is unity.

If this r/r_o correction is to be used then some simple assumption must be made about the equivalent surface source strength which the actual core represents. If the fission rate were constant throughout the whole sphere and r/λ is greater than about 2, then the source strength would be

$$S_1 = p_o\lambda_c \qquad (3)$$

where

p_o = fission rate per unit volume in the core,

λ_c = relaxation length of the radiation (neutron or gamma) in the core.

Since, however, the inner sphere is inert, the source which would have been attributed to it, attenuated by the annular fuel region, must be subtracted. Thus a second, and presumably better, form is

$$S_2 = p_o\lambda_c \left[1 - e^{-(r_2-r_1)/\lambda_c}\right] \tag{4}$$

In this case, as in the previous formula, p_o should be the total power divided by the annular volume. S_2 reduces to S_1 when $r_1 = 0$ for $\lambda_c << r_2$.

A third, and still better, treatment is obtained by integrating over infinitesimal spherical shell sources within the core. In this case it is possible to take account of the radial variation in power density.

Using the expression for the relation between the dose from a plane and from a spherical shell, it can be seen that the dose from a shielded spherical volume array of sources (see Fig. IV-B-1a) is related to that from a shielded infinite plane surface source as follows:

$$D_{SV}(r_o,r_2) = \int_o^{r_2} \frac{r}{r_o} \left[D_{Pl}(r_o - r,\infty) - D_{Pl}(r_o + r,\infty)\right] p(r)\, dr \tag{5}$$

where

r_2 = outer radius of the source array (core),

$D_{Pl}(r_o \pm r,\infty)$ = corresponding dose to be expected at distance $r_o \pm r$ from a unit strength surface source on an infinite plane,

$p(r)$ = source density, assumed to be a function only of the radial distance r.

UNCLASSIFIED
ORNL-LR-DWG 418

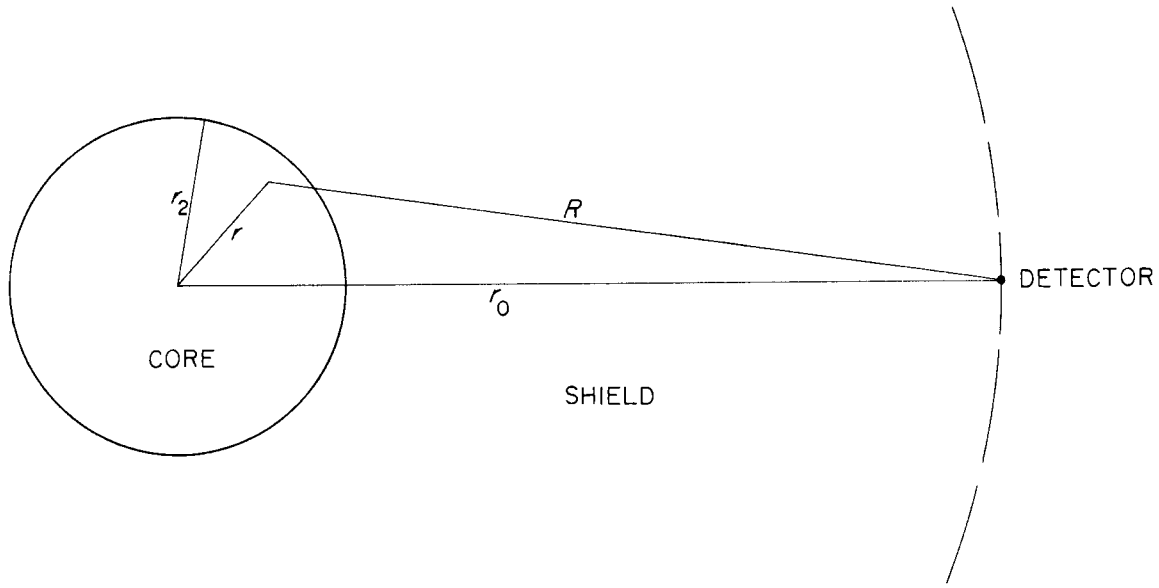

Fig. IV-B-1a. Geometry for Shielded Spherical Volume Array of Sources.

UNCLASSIFIED
ORNL-LR-DWG 419

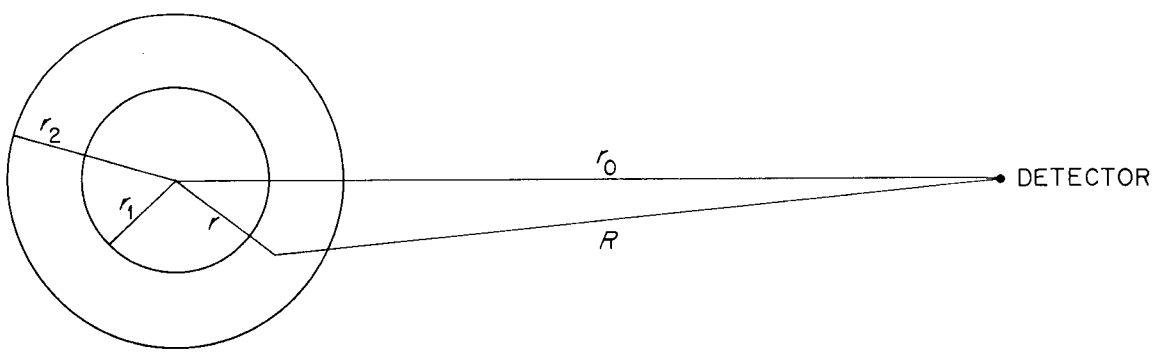

Fig. IV-B-1b. Geometry for Spherical Annular Array of Sources.

For an array of sources between two radii r_1 and r_2 (Fig. IV-B-1b) the corresponding dose is

$$D_{SV}(r_o,r_2,r_1) = \int_{r_1}^{r_2} \frac{r}{r_o} \left[D_{Pl}(r_o - r,\infty) - D_{Pl}(r_o + r,\infty) \right] p(r)\, dr \qquad (6)$$

If the two "plane doses" can be expanded in exponentials about the argument; that is, if

$$D_{Pl}(r_o \pm r,\infty) = D_{Pl}(r_o \pm r_2,\infty)\, e^{\pm (r_2-r)/\lambda} \qquad (7)$$

where λ is the relaxation length of the infinite plane source attenuation function, then

$$D_{SV}(r_o,r_2,r_1) = 2D_{Pl}(r_o - r_2,\infty) \frac{e^{-r_2/\lambda}}{r_o} \int_{r_1}^{r_2} rp(r) \sinh\left(\frac{r}{\lambda}\right) dr \qquad (8)$$

While this equation could be used in its present form it will here be tied in with the simpler methods by utilizing it to obtain the equivalent surface source strength. To do this, Eqs. (2) and (8) are compared. If in Eq. (2) the spherical source were of strength S_3, whereas the plane source had unit strength, the equation would read

$$D_{SV}(r_o,r) = S_3 \frac{r}{r_o} \left[D_{Pl}(r_o - r,\infty) - D_{Pl}(r_o + r,\infty) \right] \qquad (2a)$$

Equating this dose to that obtained by Eq. (8) and making use of the approximation Eq. (7), it is seen that

$$S_3 = \frac{\operatorname{csch} \frac{r_2}{\lambda}}{r_2} \int_{r_1}^{r_2} \sinh\left(\frac{r}{\lambda}\right) p(r)\, r\, dr \qquad (9)$$

The fission rate distribution used for all reactors was the distribution determined for ANP reactor No. 129 by multigroup reactor calculations. It was assumed that the ratio of the fission rate at the inner and outer surfaces of the fuel annulus to the minimum was constant for all core radii. The distribution is given by:

$p(r) = p_o \cosh \alpha(c - r)$, α and c being determined by the conditions

$p(r_1) = 1.5p_o$

$p(r_2) = 3.0p_o$

The ratio of the radii of the fuel annulus was assumed constant and equal to 0.67. The neutron relaxation length (λ) for the core was calculated for a number of possible fluoride fuels using measured or estimated effective removal cross sections. A value of 10 cm was taken as a reasonable average because the variation from one fuel to another was small.

The source S_3 was evaluated for the range of core diameters of interest and the results are plotted in Fig. IV-B-2. It is very interesting to compare the results of the evaluation of Eq. (9) with those based on a simplified approach. The effective source divided by the total power for both situations is given in Table IV-B-1 and Fig. IV-B-2 for a range of core diameters. The error incurred by neglected the space variation in fission rate is quite small.

It is now possible to write in a single equation the relation between dose as measured in the Lid Tank and that to be expected with the shielded RMR. If the latter is then set at the tolerable dose--it may be necessary to specify neutrons and gamma rays separately--then the appropriate Lid Tank dose measurement is specified. The shield thickness for which this dose is measured is that required for the RMR.

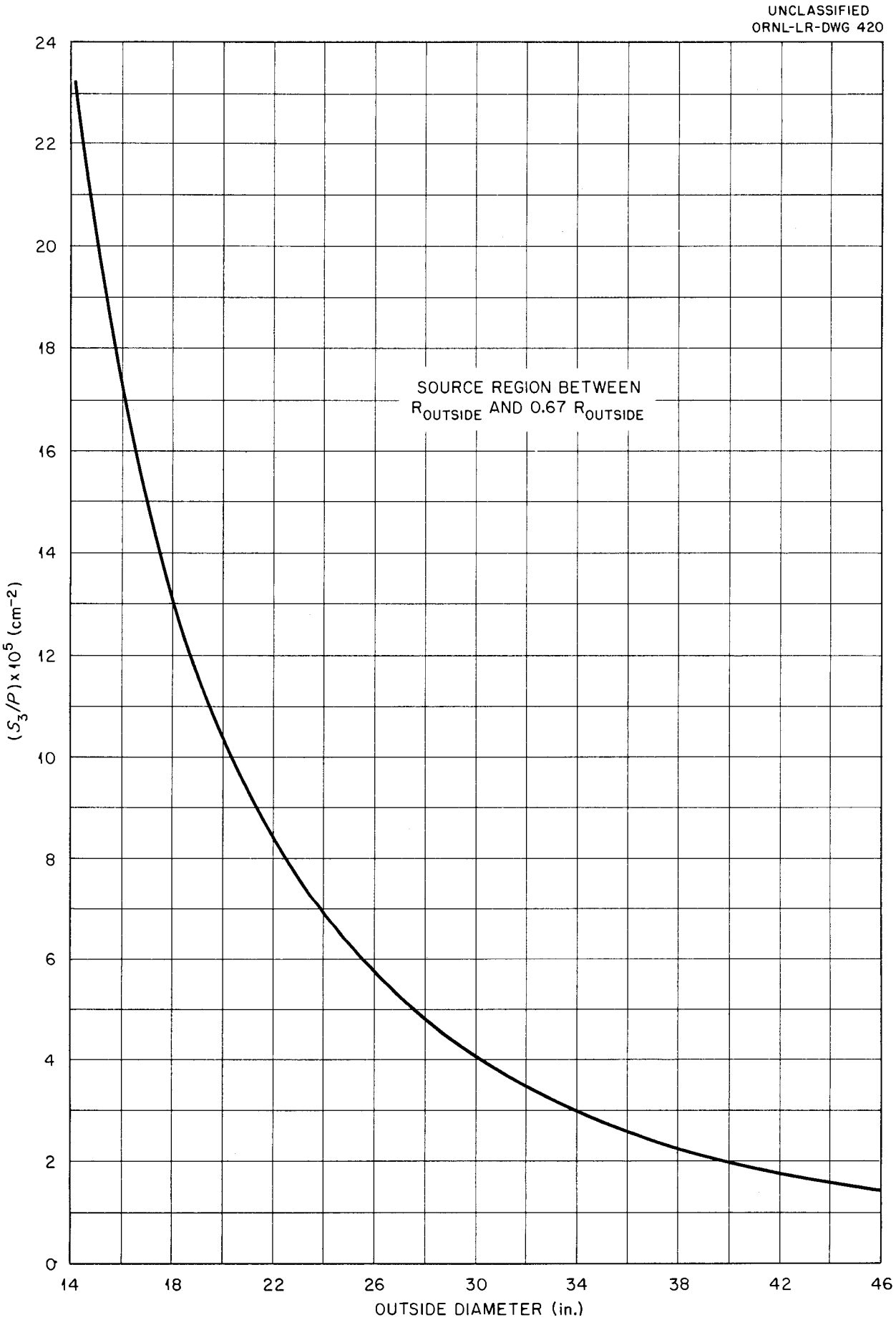

Fig. IV-B-2. Variation of Equivalent Surface Source with Core Size.

Table IV-B-1. Equivalent RMR Surface Source Strengths for Various Core Diameters

Core Diameter (in.)	S_3 $\left[\frac{(\text{watts/cm}^2) \times 10^{-5}}{\text{watt of reactor power}}\right]$	S_2 $\left[\frac{(\text{watts/cm}^2) \times 10^{-5}}{\text{watt of reactor power}}\right]$	$\frac{S_2}{S_3}$
14.3	22.9	25.6	1.12
18	13.2	15.1	1.14
22.7	7.8	8.76	1.12
28.5	4.6	5.02	1.08
36	2.66	2.78	1.04
45.3	1.52	1.52	1.00

$$\frac{(\text{Lid Tank dose})}{(\text{RMR design dose at 50 ft})} = \left(\frac{50\text{ ft}}{\text{Shield outer radius}}\right)^2 \left(\frac{\text{Lid Tank surface source}}{\text{Equivalent RMR surface source}}\right) \left(\frac{\text{Shield outer radius}}{\text{Core radius}}\right) \left(\frac{1}{\frac{1}{2} + \frac{2\lambda z + 2\lambda^2}{a^2}}\right) \tag{10}$$

where the terms on the right-hand side are, in order:

(1) Correction for remote crew position compared to Lid Tank detector which was at shield surface,

(2) Scale-up factor for source strengths,

(3) Geometrical factor as required by Eq. (2),

(4) Correction from Lid Tank disk to infinite plane source, as given in Eq. (1).

It is of course the solution of Eq. (10) that gives the shield specification, and the process of doing so is now described.

The first term needs no explanation, except the observations that inverse square attenuation is conservative for this case and that the shield outer radius is not immediately available for substitution in the equation. Regarding the latter, a trial and error solution is necessary since the Lid dose varies about exponentially with distance, making Eq. (10) a transcendental equation. Of course the shield outer radius is just the sum of core radius and shield thickness as obtained in the Lid Tank.

The second term scales up the surface source strengths. For the Lid Tank source the area is taken as 3970 cm^2, the power 6 watts, and a self-absorption factor 0.6. Thus the Lid Tank source strength is

$$S_{LT} = \frac{6 \times 0.6}{3970} = 9.04 \times 10^{-4} \text{ watts/cm}^2$$

Note that in the earlier chapters a factor A is sometimes inserted in the expressions relating dose and power to obtain one in terms of the other. This factor is not used here since, in the present "comparison method," it would occur in both numerator and denominator and hence would cancel. The RMR equivalent source strength has been discussed already.

The third term is self-explanatory.

The fourth term, the Hurwitz correction, is not clear cut. The question of the relaxation length λ requires some discussion. For neutrons it is proper to use the relaxation length observed in the Lid Tank, about 7.5 cm in this case. For gamma rays the case is not quite so simple. If the gamma rays observed at the shield periphery are core gamma rays, then the λ to use is that for gamma rays in the shield. If the gamma rays are secondary gamma

rays, produced in the shield by neutrons, then the situation is not so clear. The Hurwitz transformation does not apply to nonhomogeneous shields, but it can be used with reasonable assurance for the cases in which most of the radiation penetrates normal to the different shield layers. In this case a reasonable relaxation length to be used is that which would be observed if, as the detector is moved from the source, the intervening layers are expanded so that their thicknesses keep in the same ratios to one another. This, of course, does not happen in the experiments, but instead the water layer is increased alone. The RMR shield tests show that for the case in which the lead is all placed close to the heat exchanger most of the gamma rays observed are produced by neutrons in the outer layers of lead. The exact Hurwitz correction for this case is quite complicated. Accordingly, the neutron relaxation length, 7.5 cm, is used for both neutrons and gamma rays in the Hurwitz factor. This is not conservative or well-founded in theory, but the shield weight is not very sensitive to this factor in any case. Thus, if the gamma-ray relaxation length were used, which would increase the factor, a smaller effective z would be used, for the distance from secondary source to the detector would be less. The net result would be very little change in the factor.

2. Sample Shield Design Calculation

A sample calculation can now be made using Eq. (10) which is solved by a trial-and-error method. First an estimate of the total thickness of shielding required must be made and then the resulting equivalent Lid Tank dose can be calculated and used in conjunction with Fig. IV-A-1 to determine the total shield thickness actually required. Fortunately, convergence is very rapid

so that even if the first estimate is poor the second will probably prove satisfactory. Figure IV-A-2 can then be used to determine the lead layer thickness.

For this calculation the following conditions are assumed:

Reactor power	200 megawatts
Core diameter	18 in.
(core radius = 22.9 cm)	
Beryllium reflector	12 in. thick
Dose at 50 ft	10 rem/hr
Dose in neutrons	1/8 of total
Dose in gammas	7/8 of total

In the first trial, z, the distance from the source, is assumed to be 125 cm.

$$(\text{LT Dose})_{\text{Total}} = (10 \text{ rem/hr}) \left(\frac{1520}{148}\right)^2 \left[\frac{9.04 \times 10^{-4}}{(13.24 \times 10^{-5})(2 \times 10^{8})}\right] \left(\frac{148}{22.9}\right)$$

$$\times \left[\frac{1}{\frac{1}{2} + \frac{(2)(7.5)(125) + 2(7.5)^2}{(35.6)^2}}\right]$$

$$= 0.113 \times 10^{-3} \text{ rem/hr}$$

The gamma dose then is

$$(\text{LT Dose})_{\gamma} = 9.89 \times 10^{-5} \text{ rem/hr} = 9.89 \times 10^{-2} \text{ mr/hr}$$

and the neutron dose is

$$(\text{LT Dose})_{n} = \frac{0.113 \times 10^{-3}}{8} = 1.41 \times 10^{-2} \text{ mrem/hr} = 1.41 \times 10^{-3} \text{ mrep/hr}$$

(The RBE of fast neutrons is taken to be 10.) An examination of Fig. IV-A-1 indicates that the Lid Tank dose is higher at z = 125 cm than the allowed dose, hence more shielding is required. In a second trial assume z = 130 cm:

$$(\text{LT Dose})_n = 1.33 \times 10^{-3} \text{ mrep/hr}$$

Again referring to Fig. IV-A-1, it can be seen that the allowed dose is higher than the actual dose at 130 cm (9.8×10^{-4} mrep/hr). The thickness of the shield can then be determined by interpolation to be approximately 128 cm.

The thickness of lead is now determined directly from Fig. IV-A-2. The ordinate is fixed by the allowable gamma dose, and the abscissa is the shield thickness just determined. For this example the lead thickness required is 5.6 in.

A series of charts was prepared to facilitate the shield design work. Equation (10) is a little awkward to work with because so many numbers are involved, and because without the charts solutions must be obtained by trial and error. The Lid Tank data in Figs. IV-A-1 and IV-A-2 were used to prepare the charts given in Fig. IV-B-3. This was calculated from Eq. (10) for the ranges of variables expected in the design work. In using these charts the dose level desired at full power for unprotected personnel 50 ft from the center of the reactor is selected first. This dose should be divided by the power in megawatts, e.g.,

$$\frac{10 \text{ r/hr}}{200 \text{ megawatts}} = 0.05 \text{ (r/hr)/megawatt}$$

The intercept of the curve for this latter value in Fig. IV-B-3 with the proper core diameter curve (e.g., 18 in.) then specifies both the total thickness of shielding required (128 cm) and the ratio of dose in the Lid Tank to full-scale dose (10 r/hr) for the particular power, reactor core diameter, and full-scale reactor tolerance dose specified. Once the total shield thickness has been established, the thickness and the weight of the

ORNL-LR-DWG 421

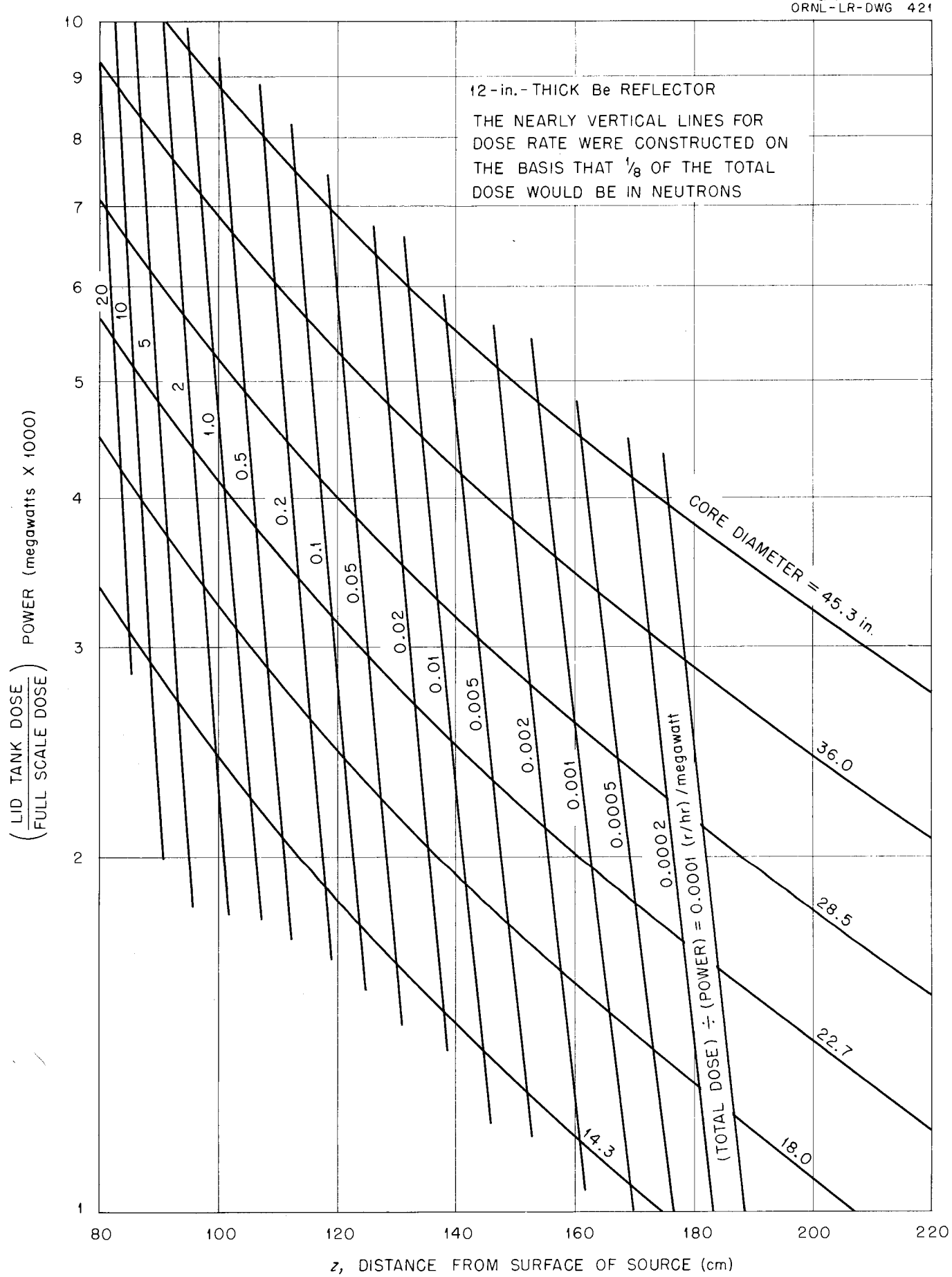

Fig. IV-B-3. Neutron Shield Design Chart for Reflector-Moderated Reactors.

lead layer can be determined from Figs. IV-B-4 and IV-B-5, respectively.

Once the total thickness of the shield and the thickness of the lead layer have been determined, calculation of the shield weight is relatively simple. The weight of the lead region can be determined very quickly using Fig. IV-B-4. The weight of the reactor-heat exchanger-pressure shell assembly for a consistent series of designs has been tabulated for a fairly wide range of reactor core diameters and reactor power outputs in Table IV-B-2. A "basic spherical shield" weight can then be obtained by adding the weight of the reactor assembly to the weights of the lead and water regions. Three additional weights must then be added. The first is an allowance for any additional lead that must be added to compensate for the fission product decay gammas coming from the intermediate heat exchanger. This may require the addition of a few tenths of an inch to the thickness of the lead layer. The second is an allowance for the patches required to compensate for leaks through the shielding represented by the fuel passages through the beryllium reflector, the NaK passages through the lead region, and the dome housing the pump-expansion tank assembly at the top of the reactor. The third is an allowance for shield structure. Previous detail design studies have indicated that the weight of structure required to integrate the reactor and shield into a satisfactory assembly can be taken as a flat 2°/o of the so-called "basic spherical shield" weight. It is to be noted that this fraction is quite low by comparison with the usual designs for other cycles. This is because the weight of the difficult-to-support water region is only about 30% of the total shield weight. The weight of the complete reactor shield assembly can then be obtained by adding these three items to the weight of the basic spherical shield. The weight of the crew shield, if one is used, can then be added to give the total weight of reactor and shielding.

[redacted]

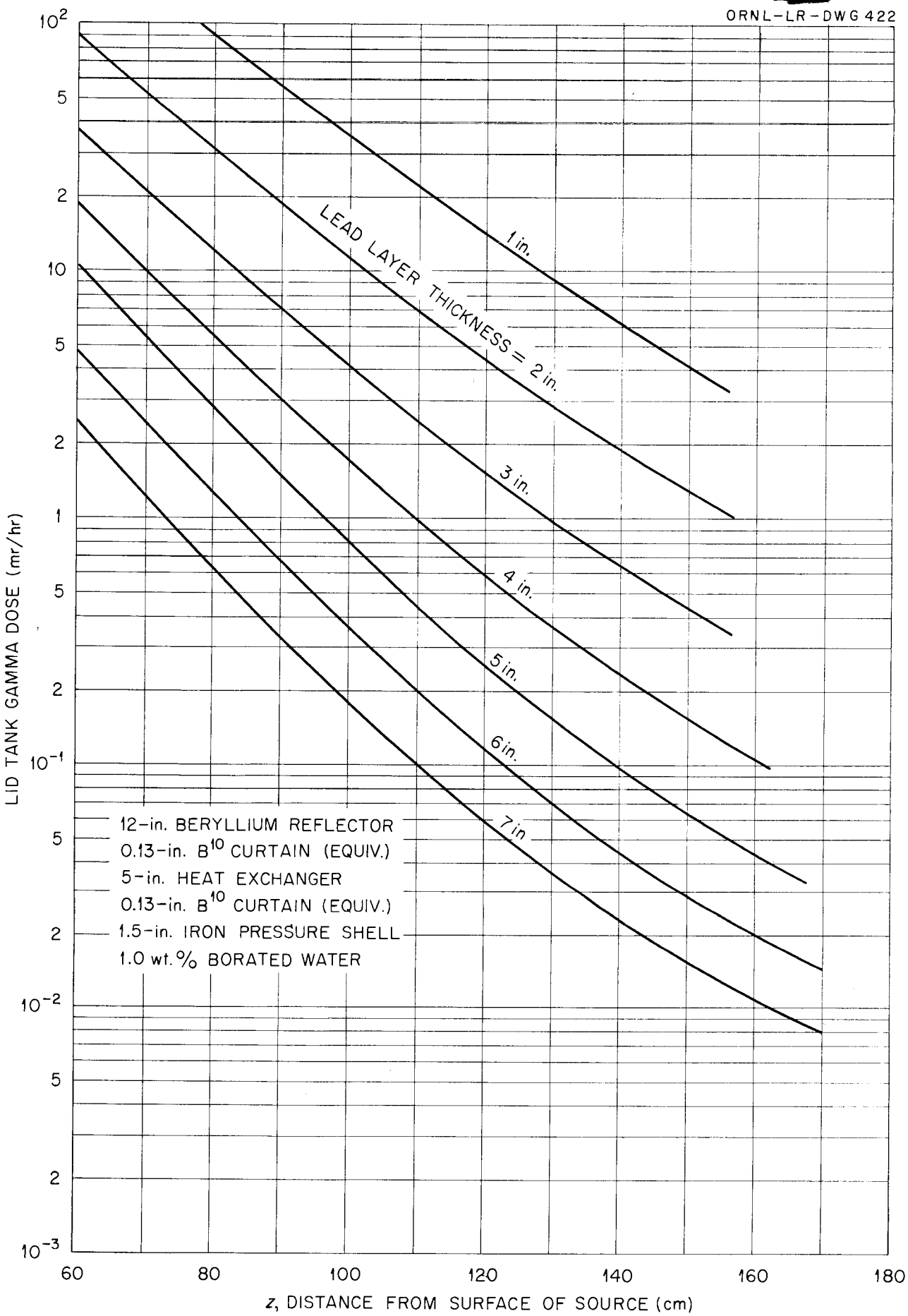

Fig. IV-B-4. Gamma Shield Design Chart for Reflector-Moderated Reactor.

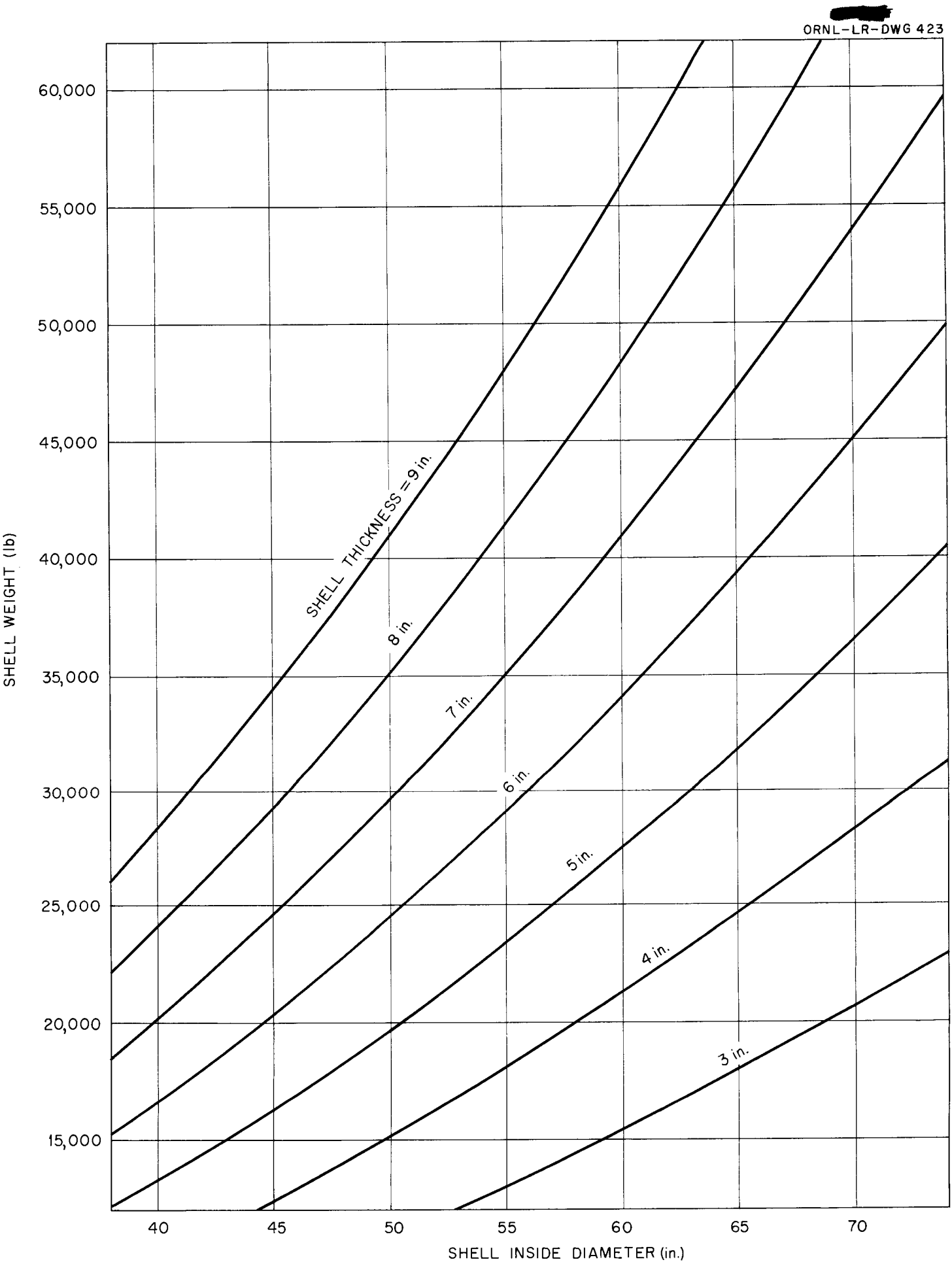

Fig. IV-B-5. Weights of Spherical Shells of Lead for RMR-Shield.

TABLE IV-B-2. WEIGHTS OF REACTOR-HEAT EXCHANGER-PRESSURE SHELL ASSEMBLIES FOR RMR

12 in. Thick Beryllium Reflector; 0.13 in. of B^{10} Inside and Outside Heat Exchanger; Constant Heat Exchanger Power Density

CORE DIAMETER (in.)	REACTOR POWER (megawatts)	SPHERE INSIDE HEAT EXCHANGER, ρ = 1.84 g/cc (115 lb/ft^3)			HEAT EXCHANGER, ρ= 3.15 g/cc (197 lb/ft^3)					OUTER B^{10} LAYER, ρ = 2.1 g/cc (131 lb/ft^3)			PRESSURE SHELL ρ = 8.5 g/cc (530 lb/ft^3)			TOTAL WEIGHT (lb)
		OD (in.)	Volume (ft^3)	Weight (lb)	Thickness (in.)	OD (in.)	Volume (ft^3)	Δ Volume[a] (ft^3)	Weight (lb)	OD (in.)	Δ Volume[a] (ft^3)	Weight (lb)	OD (in.)	Δ Volume[a] (ft^3)	Weight (lb)	
14.3	25	38.5	17.24	1,970	0.85	40.20	19.98	2.74	540	40.40	0.29	38	43.40	4.80	2,540	5,088
	50	38.5	17.24	1,970	1.80	42.10	22.72	5.48	1,080	42.30	0.32	42	45.30	5.20	2,760	5,852
	100	38.5	17.24	1,970	3.35	45.2	28.19	10.95	2,150	45.4	0.44	58	48.4	6.08	3,220	7,398
	200	38.5	17.24	1,970	6	50.5	39.14	21.9	4,300	50.7	0.45	59	53.7	7.7	4,080	10,400
18	25	42.2	22.74	2,610	0.7	43.6	25.48	2.74	540	43.8	0.33	43	46.8	5.52	2,920	6,100
	50	42.2	22.74	2,610	1.6	45.3	28.2	5.48	1,075	45.5	0.37	48	48.5	6.0	3,180	7,000
	75	42.2	22.74	2,610	2.27	46.75	30.95	8.21	1,610	46.95	0.37	48	49.95	6.40	3,390	7,658
	100	42.2	22.74	2,610	3.0	48.1	33.7	10.95	2,150	48.3	0.40	52	51.3	6.6	3,500	8,300
	200	42.2	22.74	2,610	5.3	52.8	44.64	21.9	4,300	53.0	0.49	64	56.0	8.4	4,450	11,400
22.7	100	46.9	31.2	3,590	2.5	51.8	42.2	10.95	2,150	52.0	0.47	62	55.0	7.7	4,080	9,900
	200	46.9	31.2	3,590	4.55	56	53.1	21.9	4,300	56.2	0.55	72	59.2	9.5	5,030	13,000
	400	46.9	31.2	3,590	7.95	62.8	75.0	43.8	8,600	63.0	0.71	93	66.0	11.7	6,200	18,500
28.5	200	52.7	44.2	5,090	3.75	60.2	66.1	21.9	4,300	60.4	0.64	84	63.4	10.9	5,780	15,300
	400	52.7	44.2	5,090	6.75	66.2	88.0	43.8	8,600	66.4	0.78	102	69.4	12.6	6,680	20,500
	800	52.7	44.2	5,090	11.4	75.5	131.8	87.6	17,300	75.7	1.15	151	78.7	16.65	8,820	31,360
36	200	60.2	66.07	7,600	3	66.2	88.0	21.9	4,300	66.4	0.78	102	69.4	12.6	6,680	18,700
	400	60.2	66.07	7,600	4.9	70	103.9	43.8	8,600	70.2	0.87	114	73.2	16.7	8,850	25,200
45.3	200	69.5	101.7	11,680	2.35	74.2	123.6	21.9	4,300	74.4	0.98	128	77.4	16.3	8,640	24,800

[a] Volume using outside diameter less volume using inside diameter.

IV-C. DOSE FROM GAMMA ACTIVITY IN HEAT EXCHANGER

The fission products in the heat exchanger region constitute a source of gamma radiation that is not included in the results of the Lid Tank tests. Hence to obtain the total gamma-ray dose from a reactor-shield configuration the dose due to the decay gammas from the fuel in the heat exchanger must be calculated and added to the dose determined from Lid Tank data.

Two independent methods were used to evaluate this source of radiation. The first method involved the use of an effective infinite surface source with heterogeneous shielding and conversion of the result to a spherical system with a simple radius ratio. This procedure was used for all shield configurations because it was somewhat easier to apply than the second method and yielded conservative yet quite reasonable results when compared with the second method.

The second method, the Simon-Ascoli procedure derived in section III-B, was used as a spot check on the results of the other method. The Simon-Ascoli formula considers the curvature effect of the heterogeneous shield in a precise fashion although the attenuation is limited to simple forms, hence the results obtained using this method were taken as correct. A check was made on the smallest reactor calculated where curvature effects of the source region and shield would be most significant, on the largest reactor where the agreement should be best, and on an intermediate case. The results of the calculations by the two methods are given in Table IV-C-1. While the percentage difference between the two methods is as large as 23% in the first case, the difference in the total dose from the reactor is indeed small as one can see from the figures in the last column of the table.

Table IV-C-1. Comparison of Methods Used to Evaluate Dose from Fission Products

Core Diam. (in.)	Reactor Power (megawatts)	HE Dose at 50 ft (r/hr)		$\frac{\text{LT Dose (6 r/hr) + HE Dose (Method 1)}}{\text{LT Dose (6 r/hr) + HE Dose (Method 2)}}$
		Method 1	Method 2	
14.3	25	1.74	1.40	1.05
22.7	200	2.44	2.08	1.04
45.3	800	2.22	2.01	1.03

Method 1

The first method can be outlined readily in some detail. An effective spherical surface source is needed for the volume-distributed sources in the heat exchanger annulus. Hence Eq. (9) in the preceding section (IV-B) is directly applicable, the limits of integration being changed to the internal and external radii of the heat exchanger, and p(r) changed to the gamma-ray source per unit volume which is independent of the radius in the annulus. The assumption made in obtaining Eq. (9), namely that the relaxation length for the material contained inside of the external radius is constant, is still quite reasonable. A relaxation length of 9.09 cm for gamma rays in the material in the heat exchanger was taken for the entire region. The gamma-ray source per unit volume of the total heat exchanger region is a function of the core diameter and power level. The saturated activity of the fission products per unit volume of the heat exchanger region may be taken as

$$p_o = p' \frac{V_{fHE}}{V_{HE}}$$

$$p' = K \overline{p(r)} \frac{V_{fc}}{V_{fc} + V_{fHE}}$$

where

p' = saturated activity of fission products per unit fuel volume,

$\overline{p(r)}$ = average fission rate in the core per unit volume,

V_{fc} = fuel volume in the core,

V_{fHE} = fuel volume in the heat exchanger,

V_{HE} = volume of the heat exchanger,

K = constant relating fissions to penetrating gamma rays.

It is required that the transit time of the fuel in the system be small compared to the half-lives of the fission products for the above expressions to be valid. The transit time of the fuel through the core alone is of the order of 0.1 sec which is short compared to the half-lives of the fission products of interest. Hence

$$p_o = p' \frac{V_{fHE}}{V_{HE}} = Cxf = \frac{P(\text{watts})}{V_{HE}(\text{cc})} \times 3.0 \times 10^{10} \frac{\text{fissions}}{\text{sec-watt}} \times \Gamma(\gamma) \frac{\text{photons}}{\text{fissions}} \times f \tag{1}$$

where

P = total reactor power,

f = fraction of fuel in the heat exchanger,

C = constant (power extracted per unit volume of the heat exchanger is constant).

The spectrum of the decay gammas emitted by the fission products (see section III-F) is taken to be

$$N(\gamma) = 7.4\, e^{-1.16E} \frac{\text{photons}}{\text{Mev} \cdot \text{fission}} \tag{2}$$

If there is a reasonable amount of lead shielding employed, only that part of the spectrum above 2.5 Mev need be considered. A conservative assumption consistent with Eq. (2) is that the photons are of 3 Mev and that there are

0.40 of them per fission. Thus

$$\Gamma(\gamma) = \frac{0.40 \text{ photons}}{\text{fission}} \tag{3}$$

The attenuation through a shield from an infinite plane isotropic source, assuming a one collision theory, is

$$D(x) = \frac{S}{2} \int_1^{\infty} \frac{e^{-\xi \sum_{i=0}^{x} \mu_i t_i}}{\xi} d\xi \tag{4}$$

where

S = isotropic source strength per unit area,

μ_i = absorption coefficient of ith lamina in the shield,

t_i = thickness of ith lamina,

$\sum_{i=0}^{x}$ indicates sum over all laminae between the source and the point of observation.

The dose at x from Eq. (4) was modified to account for compton collisions by multiplying it by a buildup factor. The buildup factor was taken from the NDA tables[1] based on the radial number of mean free paths through Inconel, lead, and water. The sum* of the individual buildups was used to multiply the dose calculated from Eq. (4).

The dose from the heat exchanger gammas at the surface of the shield was then calculated by substituting in Eq. (2) of section IV-B, approximating for the second bracketed term as in Eq. (7) of the same section.

(1) H. Goldstein, J. E. Wilkins, Stanley Preiser, "Interim Report on the NDA-NBS Calculations of Gamma Ray Penetration," NDA Memo 15C-20 (Sept. 8, 1953).

* The sum is not necessarily the best approximation to the buildup factor for several different layers. No firm rules have yet been established on this point.

In designing the shields presented in the following pages the shield was first designed on the basis of Lid Tank data assuming that the gammas from the core (including secondary gammas) constituted some particular percentage of the total gamma dose. The dose from the fission products in the heat exchanger was then calculated for the shield thus specified. The sum of the doses from core and core-released neutrons, as determined from the Lid Tank data and those calculated to come from the heat exchanger was then determined and the lead thickness was readjusted to make the total gamma dose equal the design dose. In most cases the initial estimates were sufficiently accurate that the change in lead thickness required was less than 0.2 in.

Method 2

The Simon-Ascoli method is presented in section III-B-1. Suffice it to say that the dose calculated using this method was modified by multiplying it by a buildup factor. For any given reactor the same buildup factor was used in each method. While Method 1 is illustrated in a sample calculation given below, Method 2 can be evaluated with the aid of Sakamoto's table (Table III-B-1 in this report).

Sample Calculation Illustrating Method 1

The gamma dose from the heat exchanger region, 50 ft from the center of the reactor, can be written as (see Eqs. (7), (2a), and (9) in section IV-B)

$$D(\text{at } 50 \text{ ft}) = \left(\frac{b}{1520}\right)^2 \frac{r_2}{b} S_3 D_{P1}(b - r_2, \varphi) \left[1 - e^{-\frac{2r_2}{\lambda_s}}\right] \qquad (5)$$

where

$\left(\frac{b}{1520}\right)^2$ = factor to convert the dose at the shield surface (radius b) to that at 50 ft from the center of the system,

$$S_3 = p_o \frac{\operatorname{csch}\left(\frac{r_2}{\lambda_s}\right)}{r_2} \int_{r_1}^{r_2} \sinh \frac{r}{\lambda_s} r \, dr$$

$$\cong p_o \lambda_s \left\{ \left[1 - e^{-\mu_s [r_2 - r_1]}\right] \left(\frac{r_1}{r_2}\right) + \frac{e^{-\mu_s [r_2 - r_1]} - 1}{\mu_s r_2} \right\}$$

for the range of r_2 and r_1 of interest, or

= $p_o \lambda_s F$, where F is the factor appearing in braces,

$\mu_s = 1/\lambda_s$

= absorption coefficient in the source region,

p_o = average source density throughout the entire heat exchanger volume,

$p_o \lambda_s = \lambda_s C_f$,

$$C = \frac{P(\text{watts})}{V_{HE}(\text{cm}^3)} \times 3.1 \times 10^{10} \frac{\text{fissions}}{\text{sec watt}} \times \Gamma(\gamma) \frac{\text{photons}}{\text{fissions}}$$

$\lambda_s C$ = 3.63×10^3 photons/cm^2.sec,

f = fraction of fuel in the heat exchanger,

P = total reactor power,

V_{HE} = volume of the heat exchanger,

$\Gamma(\gamma)$ = 0.40 photons/fission,

$$D_{Pl}(b - r_2, \infty) = \frac{BF}{2} \int_1^{\infty} \frac{e^{-\xi \sum_{i=0}^{b-r_2} \mu_i t_i}}{\xi} d\xi = \frac{E_1\left(\sum_{i=0}^{b-r_2} \mu_i t_i\right) (BF)}{2},$$

BF = buildup factor (function of $\sum_{i=0}^{b-r_2} \mu_i t_i$),

$E_1(\ )$ = exponential integral of the first kind,

$$1 - e^{-\frac{2r_2}{\lambda}} \cong 1$$

Equation (5) can then be written

$$D(\text{at } 50 \text{ ft}) = \frac{br_2}{(1520)^2} \frac{(3.63 \times 10^{13})\ Ff}{(2.3 \times 10^5)} \frac{BF}{2} E_1\left(\sum_{i=0}^{b-r_2} \mu_i t_i\right)$$

$$= (34.24)\ (br_2)\ (BF)\ E_1\left(\sum_{i=0}^{b-r_2} \mu_i t_i\right) fF \qquad (6)$$

where

2.3×10^5 photons/cm^2.sec = 1 r/hr (3 Mev).

Other values assumed for this calculation are:

$\mu_{Inconel}$ = 0.2975 (All absorption coefficients are taken at 3 Mev.)

μ_{Pb} = 0.463

μ_{H_2O} = 0.0400

$\mu t_{Inconel}$ = 1.209

B_F = buildup in Inconel + buildup in Pb + buildup in H_2O

The results of calculations using Method 1 are given in Table IV-C-2.

Plots were made of the buildup factors[1] for iron, lead, and water. The number of relaxation lengths in each material was noted and the buildup factor read from the curves. The thickness of each material was computed from the data given in Table IV-I-2 for 10 rem/hr at 50 ft.

Table IV-C-2. Calculations Used in Method 1

Core Diameter (in.)	Power (megawatts)	$\mu t_{Inconel}$	$BF_{Inconel}$	μt_{Pb}	BF_{Pb}	μt_{H_2O}	BF_{H_2O}
14.3	25	1.209	1.65	5.53	3.05	2.48	2.78
22.7	200	1.209	1.65	7.11	3.78	2.46	2.77
45.3	800	1.209	1.65	7.76	4.10	2.45	2.75

Core Diameter (in.)	Power (megawatts)	$\sum_{i=0}^{b-r_2} \mu_i t_i$	$\sum_{i=0}^{3} BF$	$E_1(\Sigma \mu t)$
14.3	25	9.220	7.5	9.77×10^{-6}
22.7	200	10.8	8.20	1.76×10^{-6}
45.3	800	11.4	8.50	0.89×10^{-6}

Core Diameter (in.)	Power (megawatts)	f	F	br_2	Gamma Dose at 50 ft (r/hr)
14.3	25	0.50	0.208	6,660	1.74
22.7	200	0.67	0.674	10,900	2.44
45.3	800	0.50	0.838	20,400	2.22

IV-D. DELAYED NEUTRON ACTIVATION OF SODIUM IN THE HEAT EXCHANGER*

The activation of sodium in the NaK secondary coolant in the RMR is expected to be an important source of gamma radiation at the crew. Since the NaK goes directly to the engines which are essentially unshielded the Na^{24} formed during flight may contribute a significant dose to the crew and, more important, will constitute a serious ground handling problem.

The object of this section of the report is to present a method of calculating sodium activation which has the advantage of simplicity and ease of calculation and which contains all the parameters of the system so that comparisons between various designs may be made expeditiously. The reliability of the method is felt to be good. It is recognized that one of the biggest uncertainties in any calculation of this effect is the lack of knowledge concerning the activation cross section of sodium. For this reason elaborate calculations of the many multigroup type seem somewhat out of order until more data on the sodium cross section become available.

For the purposes of this approach, the region of the shield in the neighborhood of the heat exchanger may be assumed to have plane geometry and to consist of three regions (see Fig. IV-D-1) reading outward from the region of the core:

(1) The beryllium reflector.

(2) The heat exchanger proper, assumed to consist of a homogeneous mixture of fuel, NaK, inconel piping and structural members. On either side of the HE is a curtain of enriched boron.

---

* Editors' Note: Subsequent to the time of preparation of this section it has been pointed out in private communications from NDA that most of the sodium activation for a heavily poisoned heat exchanger will be due to the 3.4-kev resonance. This shift in the significant activation neutron energy has rendered the treatment given here inapplicable to the activation of sodium coolants. The section has been left unchanged, however, since it does illustrate the problems encountered in activation calculations, especially for 1/v absorbers. It should be noted that measurements are contemplated at the LTSF in the near future which should yield experimental values for the activation in the ORNL RMR.

[redacted]
ORNL-LR-DWG 538

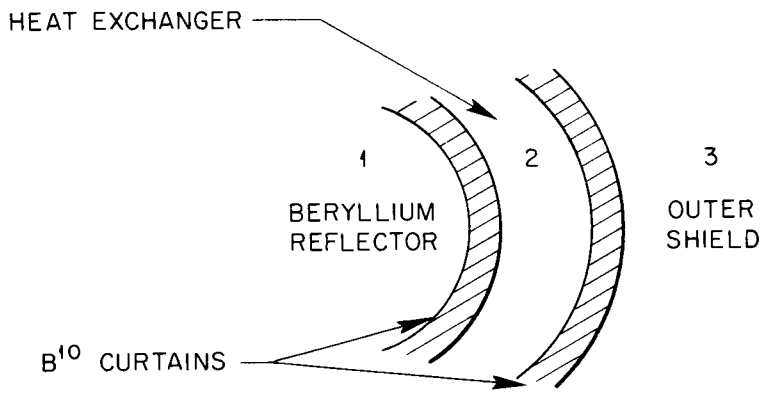

Fig. IV-D-1. Geometry of RMR-Shield in Heat Exchanger Region.

[redacted]
ORNL-LR-DWG 539

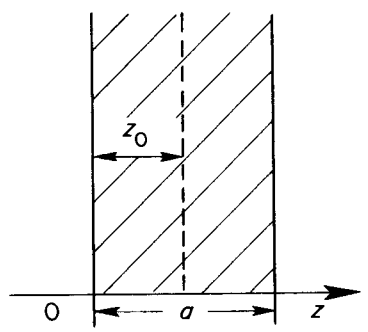

Fig. IV-D-2. Geometry of Heat Exchanger Region with Black Boundaries.

[redacted]
ORNL-LR-DWG 540

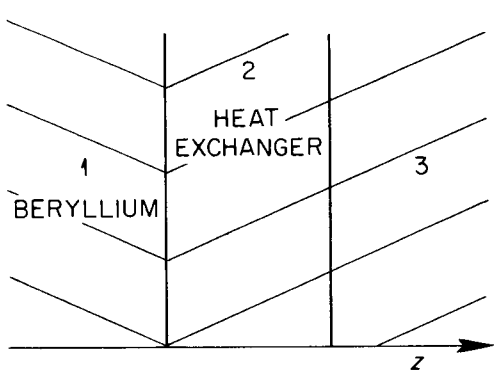

Fig. IV-D-3. Geometry of RMR Unloaded Heat Exchanger Region with Transparent Curtain.

(3) The outer region, which consists mainly of heavy material, i.e., reactor pressure shell, thermal insulation lead shielding, and borated water.

Insofar as neutrons born in the heat exchanger are concerned this region is poorly moderating. It will be assumed for convenience that the neutron transport properties of region (3) are the same as those of region (2). That this is a reasonably good assumption is easily seen.

Since the geometry of this problem is relatively simple the possibility of applying Fermi age theory comes to mind. It turns out that it may indeed be used if some reasonable approximations are made. The first of these approximations is that the delayed neutrons emitted in the heat exchanger are monoenergetic at, say, 0.5 Mev. The measured spectrum consists of five groups with 93% of the neutrons lying in four groups having energies from 420 to 620 kev. The other approximations used will be discussed as they arise.

The effect of adding boron to the heat exchanger in distributed form for the purpose of reducing the flux and resulting activation there is an important consideration.

1. Heat Exchanger with Black Boundaries

The first case to be discussed is that in which the boron curtain on either side of the heat exchanger is so thick that it is black to all neutrons born within. Though this is not true for the RMR designs considered at present this case is of interest in that it may be solved exactly within the framework of Fermi age theory. Further, the solution will be used later.

Let the origin of the z coordinate be coincident with the left edge of the heat exchanger (see Fig. IV-D-2). The equation for the slowing down density X_2, in the heat exchanger, may be written

$$\frac{\partial X_2}{\partial z^2} = \frac{\partial X_2}{\partial \tau_2} + 3\Sigma_a(u)\Sigma_s(a)\left[1 - \bar{\mu}\right] X_2(z,\tau_2) - \delta(z - z_o)\,\delta(\tau_2) \qquad (1)$$

where

$$\tau = \int_0^y \frac{du}{3\xi\Sigma_s^2 (1 - \bar{\mu})} ,$$

$u = \ln \frac{E_o}{E}$, where E_o is the source energy,

ξ = average logarithmic energy decrement = $\frac{2}{A + 2/3}$ if $A > 10$,

Σ_s = macroscopic scattering cross section,

Σ_a = macroscopic absorption cross section,

$\bar{\mu}$ = average cosine of scattering angle = $2/3A$,

A = atomic weight of scatterer.

ψ_o, the flux integrated over all angles, is related to X by the equation

$$\psi_o(z_1 u) = \frac{1}{\xi\Sigma_s(u)} \quad X\left[z, \tau(u)\right] \tag{2}$$

The solution of this partial differential equation which vanishes at the extrapolated boundaries is known. The flux may be written for a unit delta source at z_o as

$$\psi_o(z,u) = \frac{e^{-\int_0^u \frac{\Sigma_a(u)}{\xi\Sigma_s(a)} du}}{\xi\Sigma_s} \quad \frac{2}{b} \sum_{n=1}^{\infty} e^{-(n^2\pi^2/b^2)\tau(u)} \sin \frac{n\pi}{b} (z + 0.7\lambda_t)$$

$$\times \sin \frac{n\pi}{b} (z_o + 0.7\lambda_t) \tag{3}$$

where

a = thickness of heat exchanger,

λ_t = average transport mean free path,

$b = a + 1.4\lambda_t$.

The absorption term in the partial differential equation has been accounted for by a multiplicative factor

$$e^{-\int_0^u \frac{\Sigma_a(u)}{\xi\Sigma_s(u)} du}$$

Wigner has shown that the denominator of the exponent should contain the factor $(1 + \Sigma_a/\Sigma_s)$ if strong but narrow resonance absorptions occur.

To obtain the activation of the heat exchanger one distributes sources uniformly throughout the region of thickness a to give a volume density S_o neutrons/cm^3·sec. If the activation cross section of sodium is $\Sigma_{Na}(u)$, the total saturated activation Λ per unit area of the heat exchanger is

$$\Lambda = S_o \int_0^a dz \int_0^a dz_o \int_0^{u_{th}} du\, \Sigma_a(u)\, \psi(z,z_o,u)$$

$$= \frac{8bS_o}{\pi^2} \int_0^{u_{th}} du\, \frac{\Sigma_{Na}(u)}{\xi\Sigma_s(u)}\, e^{-\int_0^u \frac{\Sigma_a}{\xi\Sigma_s} du} \sum_{n=1}^{\infty} \frac{e^{-\frac{n^2\pi^2}{b^2}\tau(u)}}{n^2} \cos^2 \frac{0.7\lambda_t + n\pi}{b} \tag{4}$$

This neglects diffusion at thermal energy, which is justifiable for even the thickest heat exchanger considered in RMR design.

The series is clearly rapidly convergent if τ/b^2 is large over most of the range of u as is the case here.

2. Heat Exchanger with Gray Boundaries

Since a thickness of about 4 cm of enriched boron is necessary to make the heat exchanger boundaries really black at the source energy one must consider the transmission of the boundary as a function of energy.

To simplify this difficult situation as much as possible one supposes that the boundaries are perfectly transparent in the lethargy region

$0 \leq u \leq u_o$ and perfectly black when $u \geq u_o$. One takes u_o, somewhat arbitrarily, to be that lethargy (measured from $u = 0$ corresponding to 0.5 Mev) at which the B^{10} curtain is a half mean free path for absorption.

It will be shown that the result is insensitive to the exact choice of u_o and that this procedure is, therefore, a plausible one. The "cutoff" lethargy u_o is a design parameter of the heat exchanger system.

3. Unloaded* Heat Exchanger for Transparent Curtain ($u \leq u_o$)

Consider now the lethargy region $0 \leq u < u_o$ in which one assumes the B^{10} curtain to be transparent. It is assumed that there is no B^{10} loading in the heat exchanger so that the effect of absorption upon the flux is negligible. The age equations in this two-medium problem (see Fig. IV-D-3) read

$$\frac{\partial^2 X_2}{\partial z^2} = \frac{\partial X_2}{\partial \tau_2} - \delta(z - z_o)\,\delta(\tau_2)$$
$$\frac{\partial^2 X_1}{\partial z^2} = \frac{\partial X_1}{\partial \tau_1} \tag{5}$$

for a plane delta source at $z = z_o$. The boundary conditions are the usual ones of continuity of flux and current at the boundary, i.e.,

$$\frac{1}{\xi_2 \Sigma_{s2}} X_2 \left[0, u(\tau_2)\right] = \frac{1}{\xi_1 \Sigma_{s1}} X_1 \left[0, u(\tau_2)\right]$$
$$\frac{1}{\xi_2 \Sigma_{s2}^2 (1 - \bar{\mu}_2)} \frac{\partial}{\partial z} X_2 \left[0, u(\tau_2)\right] = \frac{1}{\xi_1 \Sigma_{s1} (1 - \bar{\mu}_1)} \frac{\partial}{\partial z} X_1 \left[0, u(\tau_1)\right] \tag{6}$$

If one assumes that $\Sigma_{s1}(u)$ and $\Sigma_{s2}(u)$ vary arbitrarily but in such a manner that their ratio is always constant, the boundary conditions may be written

* No boron added to head exchanger region.

$$X_2\left[0,u(\tau_2)\right] = \sqrt{D\delta}\; X_1\left[0,u(\tau_1)\right]$$
$$\frac{\partial}{\partial z} X_2\left[0,u(\tau_2)\right] = D\frac{\partial}{\partial z} X_1\left[0,u(\tau_1)\right] \tag{7}$$

where

$$D = \frac{\xi_2 \sum_{s2}^{2} (1 - \bar{\mu}_2)}{\xi_1 \sum_{s1}^{2} (1 - \bar{\mu}_1)}, \qquad \delta = \frac{\xi_2}{\xi_1}\,\frac{(1 - \bar{\mu}_1)}{(1 - \bar{\mu}_2)} \tag{8}$$

Then $\tau_1 = D\tau_2$ and the differential equations read

$$\frac{\partial^2 X_2}{\partial z^2} = \frac{\partial X_2}{\partial \tau_2} - \delta(z - z_o)\,\delta(\tau_2)$$
$$\frac{\partial X_1}{\partial z^2} = \frac{1}{D}\,\frac{\partial X_1}{\partial \tau_2} \tag{9}$$

The solution in medium 2 is

$$X_2 = \frac{1}{\sqrt{4\pi\tau_2}}\left[e^{-(z-z_o)^2/4\tau_2} + \frac{\sqrt{\delta} - 1}{\sqrt{\delta} + 1}\, e^{-(z+z_o)^2/4\tau_2} \right] \tag{10}$$

If one now distributes sources uniformly throughout the region and calculates the activation per unit area of heat exchanger for a source density S_o in the heat exchanger, one finds

$$\Lambda_1 = S_o \int_0^a dz \int_0^a dz_o \int_0^{u_o} du\; \frac{\sum_{Na}(u)}{\xi_2 \sum_{s2}(u)}\; X_2(z,u)$$
$$= S_o \int_0^{u_o} \frac{du}{\xi_2 \sum_{s2}} \left\{ a - \frac{\sqrt{\tau}}{1 + \sqrt{\delta}} \left[(1 - \sqrt{\delta})\,\mathrm{ierfc}\,\frac{a}{\sqrt{\tau}} - 4\,\mathrm{ierfc}\,\frac{a}{2\sqrt{\tau}} + \frac{3 + \sqrt{\delta}}{\sqrt{\pi}} \right] \right\} \tag{11}$$

where

$$\text{ierfc}(x) = \frac{2}{\sqrt{\pi}} \int_x^{\infty} dx' \int_{x'}^{\infty} d\beta e^{-\beta^2}. \quad (1)$$

A plot of ierfc(x) is given in Fig. IV-D-4. The subscript on τ_2 has been dropped.

4. Unloaded Heat Exchanger for Black Curtain ($u \geq u_o$)

One now considers that the source for the slowing down process in the region $u > u_o$ is just the slowing down density at $u = u_o$ given by Eq. (10). It is assumed that the age corresponding to u_o is so large that one may use the asymptotic value of Eq. (10). Then the new source at u_o has a volume density of

$$\tilde{S}_o = S_o \cdot \frac{a\sqrt{\delta}}{(1+\sqrt{\delta})\sqrt{\pi\tau_o}} \quad (12)$$

so that the aging process for $u > u_o$ gives the activation

$$\Lambda_2 = \frac{8b\tilde{S}_o}{\pi^2} \int_{u_o}^{u_{th}} du \frac{\Sigma_{Na}}{\xi\Sigma_s} e^{-\int_{u_o}^{u} \frac{\Sigma_a}{\xi\Sigma_s} du} \sum_{n=1}^{\infty} \frac{e^{-\frac{n^2\pi^2}{b^2}\left[\tau(u)-\tau_o\right]}}{n^2} \cos^2\left(\frac{0.7\lambda + n\pi}{b}\right) \quad (13)$$

or, by changing variables from u to $u' = u - u_o$,

(1) Hartree, Mem. Proc. Manchester Lit. and Phil. Soc. 80, 85 (1935).

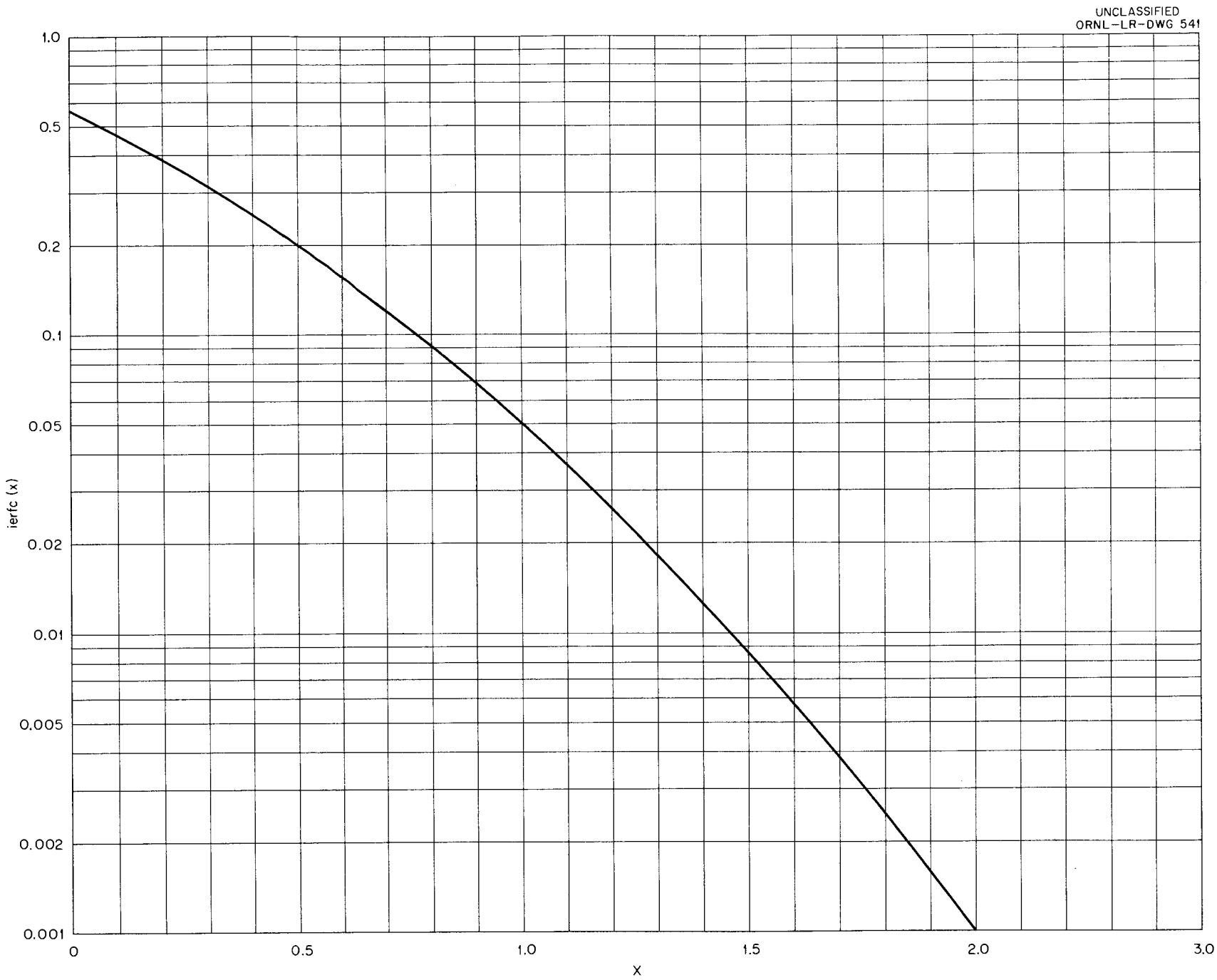

Fig. IV-D-4. ierfc $(x) = \frac{2}{\sqrt{\pi}} \int_{x}^{\infty} dx' \int_{x'}^{\infty} d\beta e^{-\beta^2}$ vs. x.

$$\Lambda_2 = \frac{8abS_o\sqrt{\delta}}{\pi^2(1+\sqrt{\delta})\sqrt{\pi\tau_o}} \int_o^{u_{th}-u_o} du' \; \frac{\Sigma_{Na}(u')}{\xi\Sigma_s(u')} \, e^{-\int_o^{u'} \frac{\Sigma_a(u'')}{\xi\Sigma_s(u'')} du''}$$

$$\times \sum_{n=1}^{\infty} \frac{1}{n^2} \, e^{-\frac{n^2\pi^2}{b^2}\tau(u')} \cos^2\left(\frac{0.7\lambda + n\pi}{b}\right) \qquad (14)$$

At this point one may observe that $\tau_o = \tau(u_o)$ enters only under the square root sign, indicating a weak dependence of $\Lambda_1 + \Lambda_2$ upon the exact choice of u_o.

The determination of the activation due to delayed neutrons in an unloaded heat exchanger then resolves into simple numerical integrations. The infinite series in Eq. (14) is rapidly converging due to the presence of an n^2 term in both the exponent and denominator. In addition, τ/b^2 is large over most of the range of integration for even the thickest heat exchanger considered.

5. Loaded Heat Exchanger for Transparent Curtain $(u < u_o)$

The solution of the age equation in a single medium with absorption is simple because the absorption effect appears in a multiplicative exponential function, leaving the form of the variation of X with τ unaffected, merely changing its magnitude. When more than one medium is involved, the effect of absorption cannot be factored out in this manner except in the trivial case where $\Sigma_a/\xi\Sigma_s$ is the same in the two media.

The case in which the function $\int_o^u \Sigma_a/\xi\Sigma_s \, du$ bears a linear relation to τ may be treated easily, but even this involves some rather cumbersome series expansions for the ranges τ both small and large.

Instead, a combination multigroup-age calculation may be carried out. One defines the cutoff lethargy u_o as before, but supposes that aging and

absorption are accomplished with all cross sections constant for $u < u_o$. The fictitious fast absorption then results in new sources in the lethargy range $u > u_o$ which may again be calculated by the more exact age theory.

This procedure is increasingly better as the boron loading in the heat exchanger is increased, because a greater part of the absorption occurs close to the source energy E_o. Actually, for heavy loading considered in the example worked out below, this assumption should be a good one.

The problem now involves three media for $u < u_o$. The flux equations in the three media are

$$\frac{d^2\phi_1}{dz^2} - k_1^2\phi_1 = 0$$

$$\frac{d^2\phi_2}{dz^2} - k_2^2\phi_2 = -\frac{3}{\lambda t}\,\delta(z - z_o) \qquad (15)$$

$$\frac{d^2\phi_3}{dz^2} - k_3^2\phi_3 = 0$$

where

$$k_i = \sqrt{3\left(\overline{\Sigma}_{tri}\,\overline{\Sigma}_{ai} + \overline{\Sigma}_{tri}\,\frac{\xi_i\,\overline{\Sigma}_{si}}{u_o}\right)}$$

and one uses the assumption that ξ and $\overline{\Sigma}_s$ in the media 2 and 3 are identical. Employing the usual conditions of continuity of current and flux at the two boundaries, one solves for the flux ϕ_2. Distributing sources uniformly through the region $0 < z < a$, and integrating over the whole heat exchanger, one finds

$$\Lambda_1 = \frac{3S_o \overline{\Sigma}_{Na}}{2k_1^3 \lambda_{ti}} \left[2ak_1 - 2(1 - e^{-k_1 a}) - (1 - e^{k_1 a}) \times \right.$$

$$\frac{\mathcal{H}_1(\mathcal{H}_3 + \mathcal{H}_2 - 2\mathcal{H}_1) \sinh k_1 a + (2\mathcal{H}_2\mathcal{H}_3 - \mathcal{H}_1\mathcal{H}_2 - \mathcal{H}_1\mathcal{H}_3)}{(\mathcal{H}_2\mathcal{H}_3 + \mathcal{H}_1^2) \sinh k_1 a + \mathcal{H}_1 (\mathcal{H}_2 + \mathcal{H}_3) \cosh k_1 a} - - -$$

$$\left. - - - \frac{\cosh k_1 a + \mathcal{H}_1 (\mathcal{H}_2 + \mathcal{H}_2) - 2\mathcal{H}_2\mathcal{H}_3}{} \right] \qquad (16)$$

where

$$\mathcal{H}_i = k_i / \Sigma_{ti}.$$

Average values for the cross sections are appropriate here and are indicated by bars over the symbols.

6. Loaded Heat Exchanger for Black Curtain $(u > u_o)$

The source for the slowing process in this lethargy region is approximately

$$\tilde{S}_o = \frac{\Lambda_1}{a\overline{\Sigma}_{Na}} \cdot \frac{\overline{\xi \Sigma_s}}{u_o} \qquad (17)$$

where it has been assumed that the flux distribution across the heat exchanger is uniform at the lethargy u_o.

The activation for $u > u_o$ is then given by Eq. (13).

7. Sample Calculations

The foregoing treatment is now illustrated for a specific reflector-moderated reactor with heat exchanger contents as follows:

Fuel (ρ = 3.15 g/cc) 30 vol. %

Composition of fuel: 46 mole % ZrF_4
50 mole % NaF
4 mole % UF_4

Inconel (ρ = 8.5 g/cc) 30 vol. %

NaK (ρ = 0.736 g/cc) 40 vol. %

Composition of NaK: 56 wt % Na
44 wt % K

The fuel fractions for various core diameters and a constant heat exchanger power density are given in Table IV-D-1. The thickness of the B^{10} curtains (ρ = 2.13 g/cc) is 0.135 in., and the density of the beryllium reflector is 1.86 g/cc.

Cross Sections and Age

The quantities which are important in the calculation are $\xi\Sigma_s$, $\Sigma_{tr} = (1 - \bar{\mu})\Sigma_s$ and Σ_a. Let the number of the ith kind of atom present per cm^3 of the heat exchanger be N_i. Then

$$\Sigma_i = \sigma_i N_i$$

The age τ may be written

$$\tau = \int_0^u \frac{du}{3\overline{\xi\Sigma_s}\ \overline{\Sigma_{tr}}}$$

where bars over the symbols indicate an average over the elements present in the mixture. The proper averages are

$$\overline{\xi\Sigma_s} = \sum_i \xi_i \Sigma_{si} = \Sigma_i \xi_i \sigma_{si} N_i$$

$$\overline{\Sigma_{tr}} = \sum_i N_i \sigma_{si} (1 - \bar{\mu}_i)$$

$$\overline{\Sigma_a} = \sum_i N_i \sigma_{ai}$$

The indicated integrations were carried out using the trapezoidal rule. A plot of the age in the heat exchanger and in the Be is given in Fig. IV-D-5. The assumption that $\tau_i = D\tau_2$ is seen to be a good one.

The quantity δ is given by

$$\delta = \frac{\bar{\xi}_2}{(1 - \bar{\mu}_2)} \cdot \frac{\overline{1 - \mu_1}}{\bar{\xi}_1} = \frac{\overline{\xi_2 \Sigma_{s2}}}{\overline{\Sigma_{2tr}}} \quad \frac{\overline{\Sigma_{1tr}}}{\overline{\xi\Sigma_s}}$$

where average values have been used and indicated. Since δ varies somewhat with energy, an average over the range $0 \leq u \leq u_o$ was taken. It varies only slightly, however, and since only $\sqrt{\delta}$ appears in the answer, it will not greatly affect the result. The quantity $\sqrt{\delta}$ was taken to be 0.485 in this example. u_o was taken as 5.

In Fig. IV-D-6 are plotted the quantities $\overline{\Sigma_{tr}}$ and $\overline{\xi\Sigma_s}$ for the heat exchanger. The quantity $\int_5^u \frac{\Sigma_a(u')}{\xi\Sigma_s(u')} du'$ which appears in the evaluation of of Eq. (14) is plotted in Fig. IV-D-7.

<u>Sodium Activation Cross Section</u>. As mentioned before, a major uncertainty in any activation calculation is the value of σ(activation) for Na^{23}.

Hughes[2] reports a value of 0.29 mb for the fission spectrum of neutrons. Reese and Abernathy[3] found a value of 0.26 $\pm$ 0.05 mb using

(2) Hughes, Spatz and Goldstein, Phys. Rev. 75, 1781 (1949).
(3) Reese and Abernathy, "The (n,γ) Cross Section for Na^{23} at 500-600 Kev," CF-53-8-22 (Aug. 4, 1953).

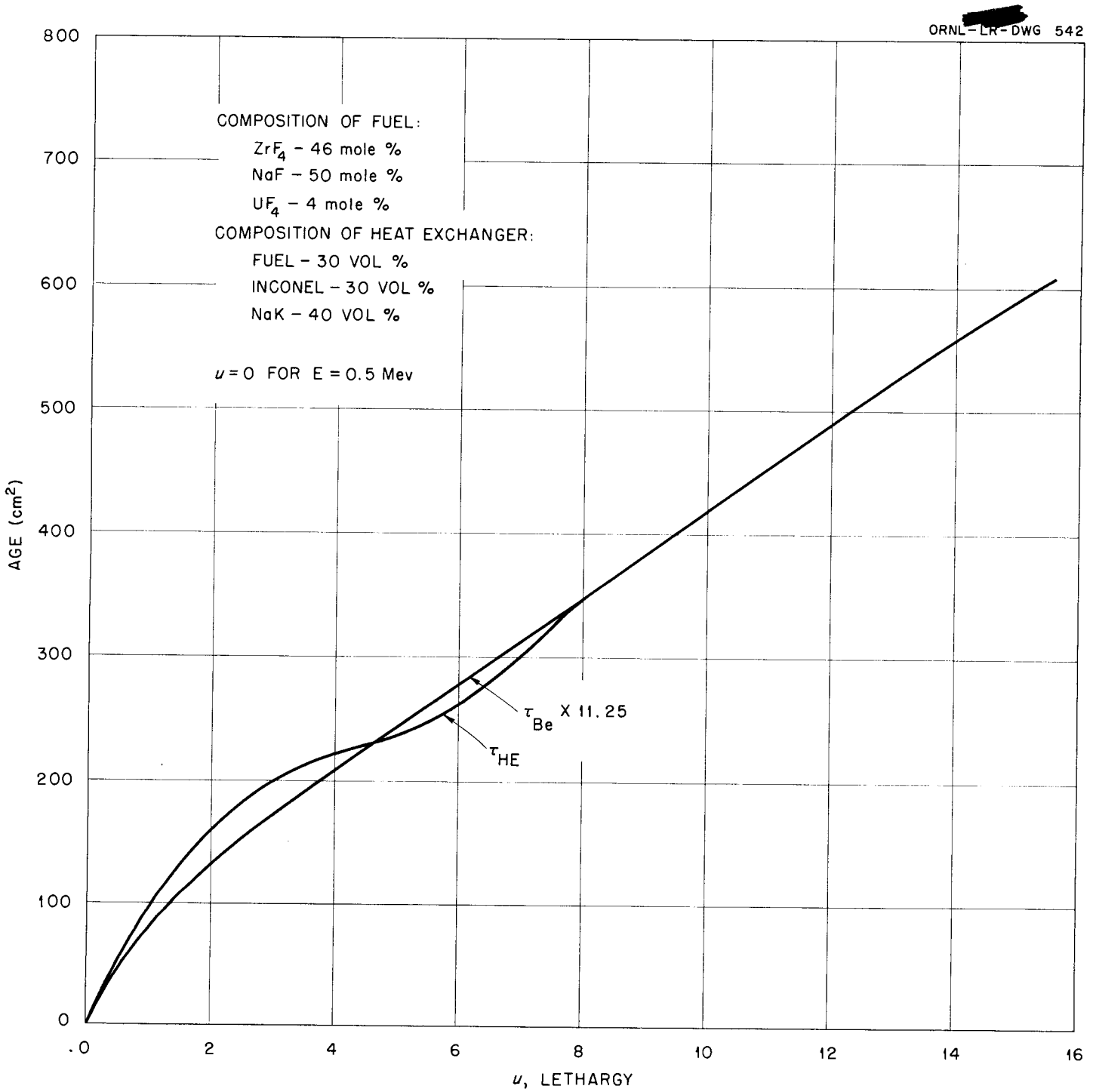

Fig. IV-D-5. Age in Heat Exchanger and Beryllium vs. Lethargy.

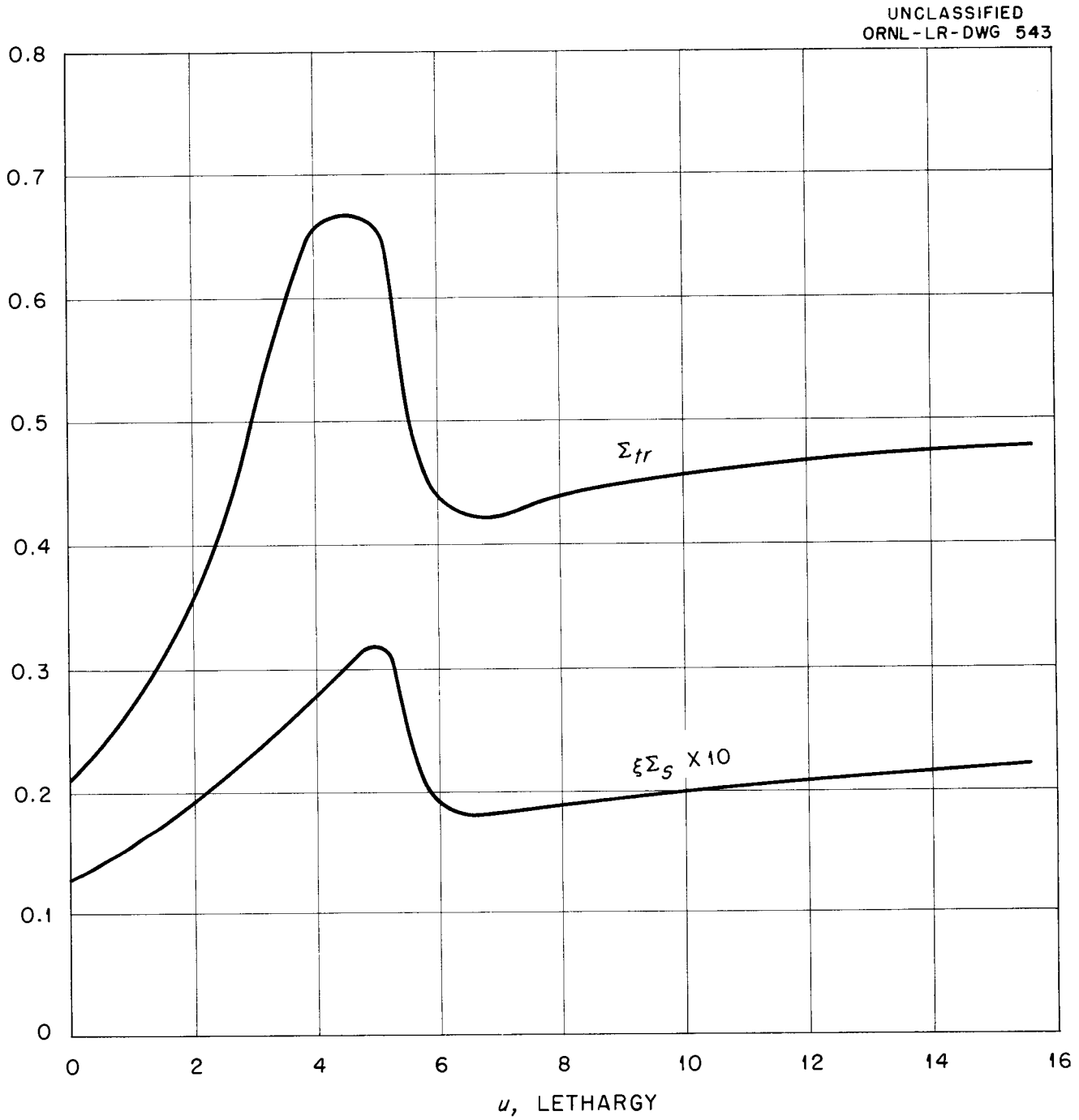

Fig. IV-D-6. Σ_{tr} and $\xi\Sigma_s$ in Heat Exchanger vs. Lethargy.

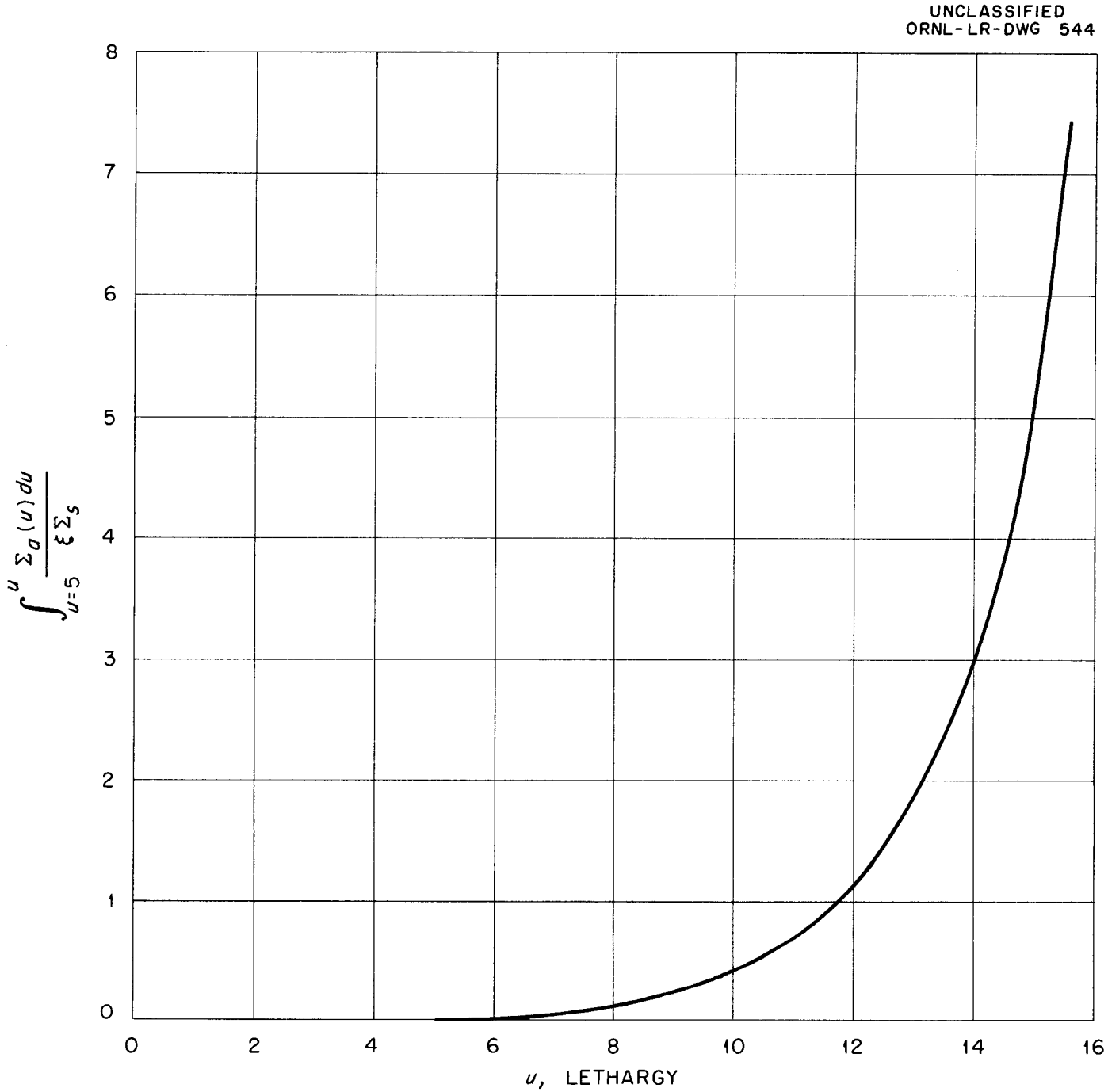

Fig. IV-D-7. $\int_{u=5}^{u} \frac{\Sigma_a(u)\,du}{\xi\Sigma_s}$ for Heat Exchanger (Unloaded).

neutrons with an energy spread from approximately 0.5 to 0.6 Mev.

The cross section assumed in this calculation was constant at 0.29 mb from 0.5 Mev down to 0.071 Mev. From this point downward in energy a 1/v variation was taken.

Activation of Sodium in Unloaded Heat Exchanger

Equations (11) and (14) were evaluated by numerical integration giving the following values:

a (in.)	$\Lambda_1(a)/S_o$	$\Lambda_2(a)/S_o$
1	8.396×10^{-5}	-
2	2.742×10^{-4}	2.32×10^{-5}
4	9.788×10^{-4}	2.64×10^{-4}
6	2.085×10^{-3}	1.41×10^{-3}
8	3.581×10^{-3}	4.93×10^{-3}
10	5.434×10^{-3}	1.46×10^{-2}

where Λ is the activation of the sodium in the NaK per unit area (of the shell) of the heat exchanger.

If it is assumed that the reactor power is 200 megawatts and the core diameter is 22.7 in., the total number of delayed neutrons born in the heat exchanger is

$$S_o = \text{Power in watts} \times 3.1 \times 10^{10} \frac{\text{fissions}}{\text{sec-watts}} \times 2.5 \frac{\text{neutrons}}{\text{fission}} \times$$

$$\times\ 0.0073 \frac{\text{delayed neutrons}}{\text{neutron}} \times \text{fuel fraction in HE}$$

$$= (2 \times 10^8)(3.1 \times 10^{10})(2.5)(0.0073)(0.67)$$

$$S_o = 7.4 \times 10^{16} \text{ neutrons/sec}$$

Since the transit time of the circulating fuel is short compared with the average half-life of the delayed neutrons, it is a good approximation to use just the fraction of the fuel in the heat exchanger (see Table IV-D-1) to obtain the delayed neutrons born there.

If A is the average area of the heat exchanger shell, and a is the thickness of the shell, Total activation = ΛA

But the total source strength, S_{ot}, in the heat exchanger is related to the source density S_o by

$$S_{ot} = S_o Aa$$

Then

$$Aa = \text{total activation} = \Lambda S_{ot}/aS_o$$

$$= 1.68 \times 10^{-3} \times \frac{7.4 \times 10^{16}}{11.7}$$

$$= 1.06 \times 10^{13} \text{ Na activations/sec}$$

In order to gain some idea of the dose rate this activation will give at the crew the following assumptions were made:

(1) 20-hr mission (no residual activity),

(2) 20% of NaK in intermediate heat exchanger,

(3) 10% of NaK deep in shield ducts,

(4) 50% self-absorption in external circuit,

(5) Activation of potassium is negligible as compared to sodium.

Thus at time t the activity of Na^{24} would be

$$\text{Activity} = A_o(1 - e^{-\lambda t})$$

The activity at the end of 20 hr of full-power operation at 200 megawatts is

$$\text{Activity} = 1.06 \times 10^{13} \left(1 - e^{-(.693 \times 20)/14.9}\right) = 6.43 \times 10^{12} \text{ decays/sec}$$

Each decay results in two gamma rays of energy 2.76 and 1.38 Mev, respectively. The dose 50 ft from the engine due to the 2.76-Mev gamma ray is

$$D_{50\ ft} = 6.43\times10^{12}\ (\text{gammas/decay}) \times 0.7 \begin{pmatrix}\text{NaK fraction}\\ \text{in external}\\ \text{circuit}\end{pmatrix}$$

$$\times\ 0.5 \begin{pmatrix}\text{self-absorption}\\ \text{in external}\\ \text{circuit}\end{pmatrix} \times \frac{1}{2.4\times10^{5}} \left(\frac{\text{r/hr}}{\text{2.76-Mev gammas/cm}^2\text{/sec}}\right)$$

$$\frac{1}{4\pi(1520)^2} = 0.325\ \text{r/hr}$$

The dose due to the 1.38-Mev gamma ray is 0.19 r/hr, and the total dose 50 ft from the engines is 0.515 r/hr. Figure IV-D-8 shows the effect of power output on activation of sodium by delayed neutrons for the external circuit.

Activation of Sodium in Loaded Heat Exchanger

The activation of the loaded heat exchanger was calculated using Eqs. (16) and (17). A loading of 20% by volume of enriched boron was assumed. The average cross sections $\overline{\Sigma}_a$ and $\overline{\Sigma}_{tr}$ appearing in the definition of k_i after Eq. (15) were found by weighting with the function $\frac{1}{\xi\Sigma_s(u)\sqrt{\tau(u)}}$. This quantity is proportional to the variation of the flux with u at points close to the source in the unloaded heat exchanger. Such a choice of a weighting function, though not strictly correct, appears plausible. The average quantity $\overline{\xi\Sigma_s\Sigma_{tr}}$ was found from

$$\frac{1}{\overline{3\Sigma_s\ \Sigma_{tr}}} = \frac{1}{u_o}\int_o^{u_o} \frac{du}{3\ \xi\Sigma_s\ \Sigma_{tr}} = \tau/u_o$$

The activation Λ_1 was found to be $0.19 \times 10^{-3}\ S_o$. Λ_2 was negligible compared with Λ_1. The activation was then 1.85×10^{12} Na atoms/sec with enriched boron replacing 20% of the volume of the heat exchanger.

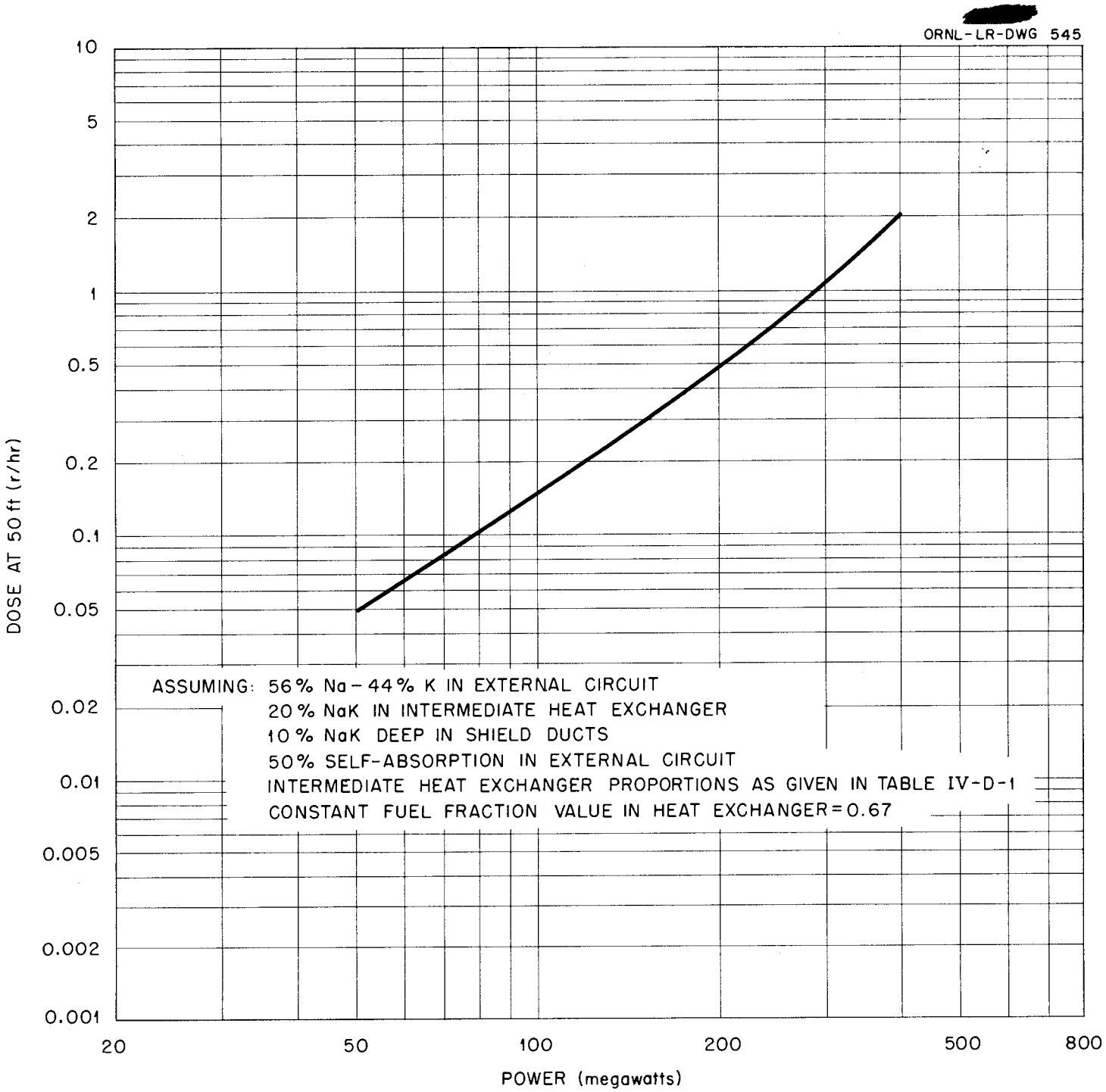

Fig. IV-D-8. Effect of Reactor Power Output on the Activation of Sodium by Delayed Neutrons for the External Circuit.

Table IV-D-1. Fuel Fractions for Various Core Diameters and Constant Heat Exchanger Power Density

Core Diameter (in.)	Reactor Power (megawatts)	Heat Exchanger Thickness (in.)	Volume of Fuel in Core (ft^3)	Volume of Fuel in Heat Exchanger (ft^3)	Fuel Fraction in Heat Exchanger
14.3	50	1.8	0.625	1.25	0.67
	100	3.3	0.625	2.5	0.80
	200	6.0	0.625	5	0.89
18	50	1.6	1.25	1.25	0.50
	100	3.0	1.25	25	0.67
	200	5.3	1.25	5	0.80
22.7	100	2.5	2.5	2.5	0.50
	200	4.6	2.5	5	0.67
	400	7.9	2.5	10	0.80
28.5	200	3.7	5	5	0.50
	400	6.7	5	10	0.67
36	200	3.0	10	5	0.33
	400	4.9	10	10	0.50

IV-E. SHIELD PATCHES

The design of shield patches to correct for radiation leakage through ducts and other shield penetrations is inherently somewhat empirical. While further test data will be required for a final detailed shield design, enough information is at hand to permit a fair estimate of the extra weight that will be entailed. Allowances must be made for three major sets of apertures in the shield. The first is that presented by the fuel ducts passing through the moderator to and from the core. The second is the irregularity represented by the expansion tank dome at the top of the reactor. The third is the set of holes in the lead region required for the secondary fluid ducts.

Experiments made at ORNL with the critical assembly for an 18-in. core have shown that there is no neutron channeling out through the fuel ducts penetrating the moderator region but that the fast-neutron flux as measured with a U^{238} counter was 40 times as high at the ends as at the sides of the reactor. When the outer ends of the fuel ducts were lined with boral sheets to a depth of 4 in. the fast-neutron flux at the ends dropped to six times the flux at the sides. This would indicate that the total thickness of neutron shielding material at the ends should be increased by about 15 cm, or 6 in.,if an increased radiation level at the top and bottom of the shield is to be avoided. The extra weight of hydrogenous shield required would be only about 600 lb, depending on the shield size, duct size, etc.

Gamma leakage through these ducts presents no problem, but an extra layer of 0.25 in. of B^{10} would probably be required just outside the

pressure shell to inhibit secondary gamma production. This point will require further tests for clarification.

The header tank and pump region at the top of the reactor constitutes a layer of about the same composition as the intermediate heat exchanger but has an effective shielding material thickness from 2 to 4 in. greater. Unfortunately, it interposes a void and requires a sizeable bulge in the lead layer, both of which increase the shield weight.

The NaK ducts through the shield will probably have little effect on the neutron attenuation because they will not introduce much effective void. However, they will permit considerable channeling of gammas through the lead layer. This channeling can be most easily taken care of by placing lead patches in the form of sleeves around the NaK ducts just outside of the lead layer. These sleeves could be tapered in thickness from root to tip to make the most effective use of material.

The total weight of the patches required was estimated as carefully as possible for about a dozen representative configurations and interpolated and cross-plotted in Figs. IV-E-1 and IV-E-2. This greatly facilitated the main design work.

[redacted]

ORNL-LR-DWG 432

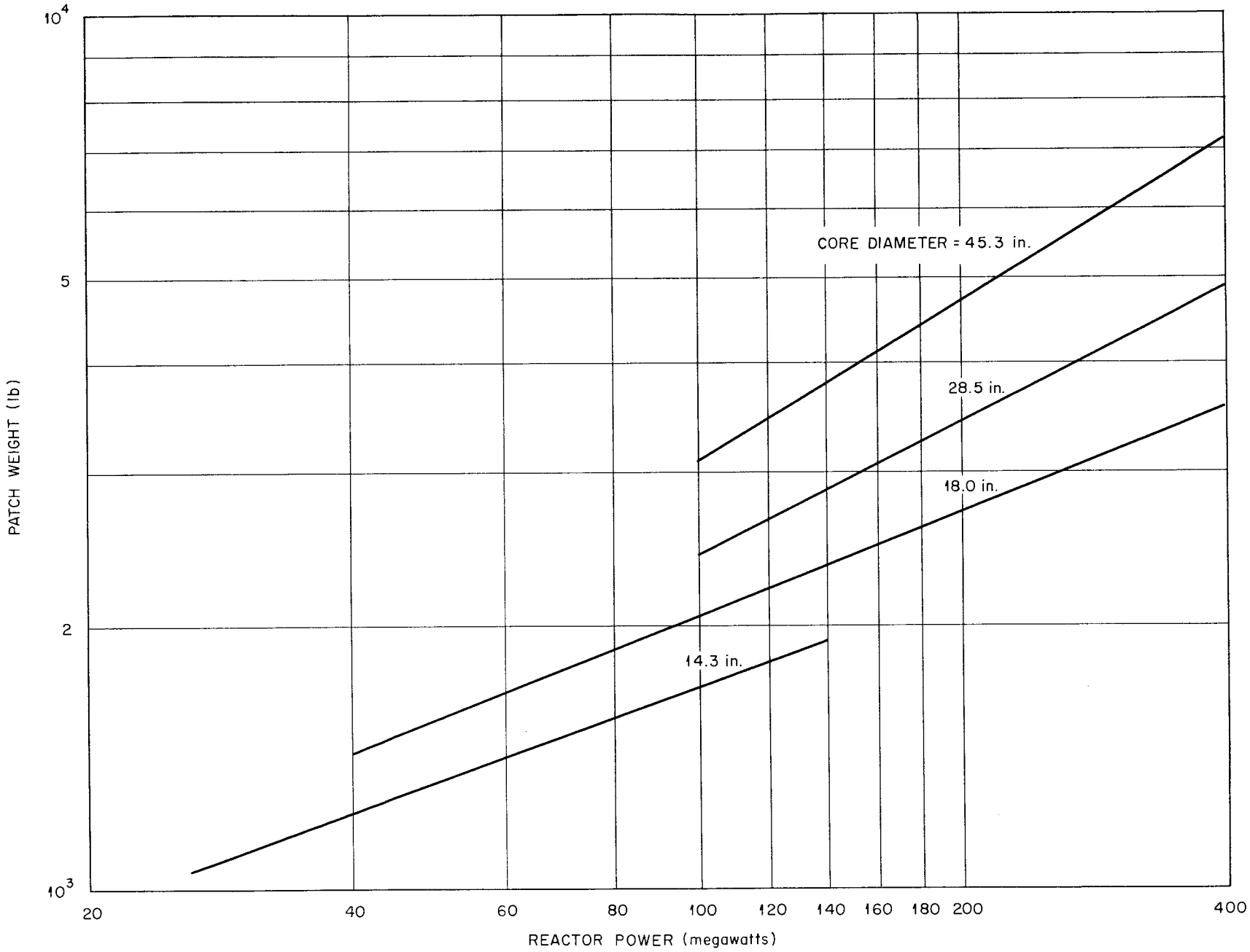

Fig. IV-E-1. Weights of Lead and Water Patches for Fuel and NaK Ducts In RMR-Shield Assemblies With A 3-in. Lead Shield Thickness.

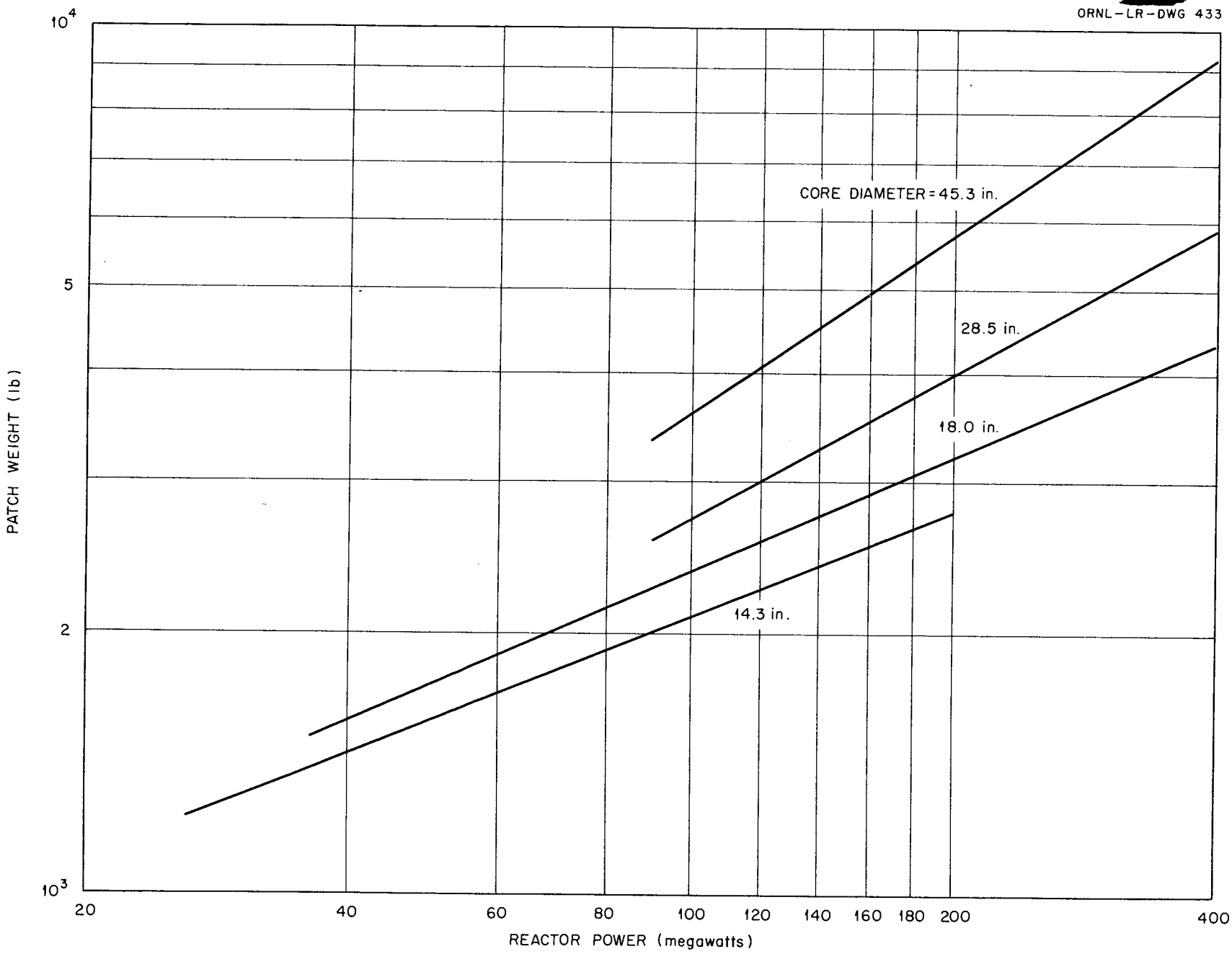

Fig. IV-E-2. Weights of Lead and Water Patches for Fuel and NaK Ducts In RMR-Shield Assemblies With A 6-in. Lead Shield Thickness.

IV-F. REPLACEMENT OF WATER WITH HYDROCARBON FUEL

Since it is contemplated that the reactor shield fuel (or water) will be operated at temperatures of the order of 200°F, it is desirable to utilize a fuel with a relatively high initial boiling point. Further, in order to provide good moderating properties, the hydrogen-to-carbon ratio and the fuel density should be high. The two fuels considered herein are representative of standard American jet engine fuels, but are somewhat higher in density and have higher values of initial boiling point than does the present standard United States jet engine fuel, JP-4. These fuels are JP-3, modified by the National Advisory Committee for Aeronautics,(1) and JP-1, a high boiling point, narrow "cut" from the distillation process.

Some properties of JP-1 and JP-3(mod.) as reported by the NACA are given below:

	JP-1 Fuel	JP-3(mod.) Fuel
Density at 60°F (g/cc)	0.830	0.803
Hydrogen-to-carbon ratio (by wt.)	0.154	0.157
Initial boiling point (°F)	340	210

A comparison between lead-fuel shields and lead-water shields can best be made for shields giving equal external dose; consequently, the neutron and gamma attenuation for both types of shield should be the same. Neutron attenuation lengths are inversely proportional to the removal cross sections of the shield materials and are thus dependent upon the material densities and composition. Using the information given above for jet fuels it is

(1) H. H. Foster, NACA RONE 51A24, Lewis Flight Propulsion Laboratory, Cleveland, Ohio (Mar. 27, 1951).

found that the fuel thickness (x_f) at any temperature required to duplicate the neutron attenuation of a given thickness of water (x_w) is given by

$$x_f = c \frac{\rho_w}{\rho_f} (x_w)$$

where c is a constant taking account of the molecular weights and removal cross sections of the two fuels,

c = 0.83 for JP-1

= 0.82 for JP-3 (mod.),

ρ_w, ρ_f = densities of water and fuel, respectively, at any given temperature.

For equal gamma attenuations $\Sigma_{\mu x}$ for the lead and water or hydrocarbon fuel regions must be the same for both shields, thus

$$\mu_f x_f + \mu_{Pb} x_{Pb_f} = \mu_w x_w + \mu_{Pb} x_{Pb_w}$$

where μ_{Pb}, μ_f and μ_w are the gamma attenuation coefficients of lead, fuel, and water at any given temperature, and x_{Pb_f} and x_{Pb_w} are the required thicknesses of lead for the fuel and water shields, respectively.

If it is assumed that the attenuation coefficient of lead is not a function of temperature and that all the attenuation coefficients are directly proportional to the material densities, the above equations may be reduced to

$$x_{Pb_f} - x_{Pb_w} = \Delta x_{Pb} = \left[1 - c\right] \frac{\rho_w}{\rho_{Pb}} (x_w)$$

where ρ_{Pb} is the density of lead and Δx_{Pb} is the extra thickness of lead which is required by the lead-fuel shield to duplicate the gamma attenuation of the comparison lead-water shield. Although it was not considered in the analysis, both the JP-1 and JP-3 (mod) fuels are capable of being "borated"

with powdered crystalline or amorphous boron with boron concentrations as high as 50% by weight. Boron has been investigated as a fuel additive by the NACA, whose tests indicated superior chemical combustion performance of borated fuels over standard jet fuels.(2)

The fact that some neutron attenuation would be accomplished by the extra lead (Δx_{Pb}) required by the jet fuel shields was neglected in computing the difference in weight between fuel shields at any temperature (t) and a lead-water shield at 60°F. The lead-water shield used as a basis for comparison had a 6 in. thick lead layer with an outer radius of 30.75 in. and an outer shell of water 23.65 in. thick. This shield would be suitable for a 50-megawatt reactor. Further computations were made in order to determine the weight increase necessary to produce lead-water shields at any temperature (t) as effective as the basic 60°F lead-water shield. The results of the computations are shown in Fig. IV-F-1.

It is obvious from Fig. IV-F-1 that the substitution of JP-1 or JP-3 (mod.) jet fuels for water in RMR shields will not be detrimental to the over-all reactor shield weight. The engineering advantages of such a substitution seem quite worth while.

---

(2) A. M. Lord, NACA RME52B01, Lewis Flight Propulsion Laboratory, Cleveland, Ohio (April 28, 1952).

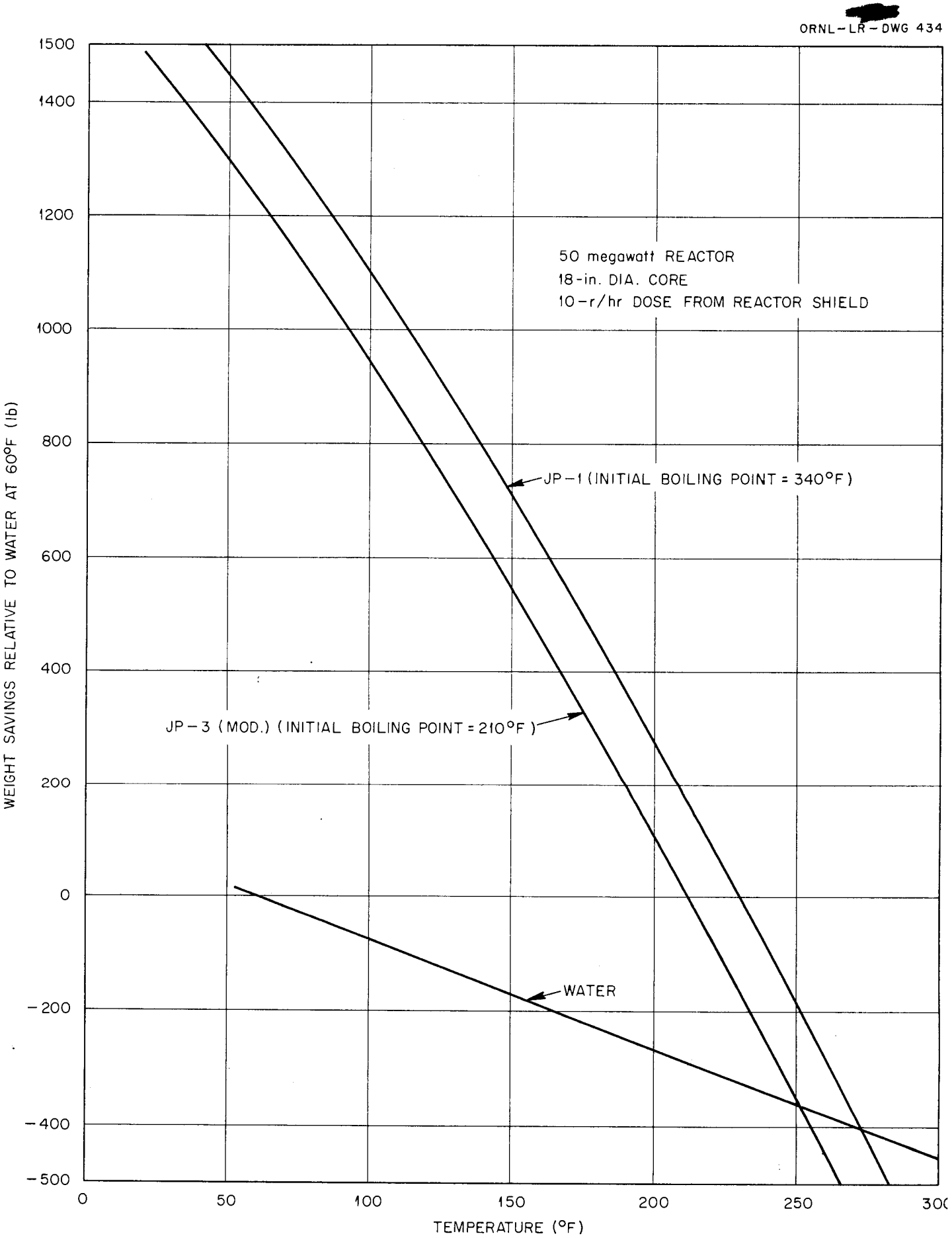

Fig. IV-F-1. Variation in Reactor Shield Weight Due to Use of Jet Fuel.

IV-G. SHIELD COOLING

While the shield cooling problem varies with reactor power output and lead region thickness, it is instructive to examine a typical case. Approximately 150 kw of power will be produced by gamma absorption in the 6 in. thick lead region of a representative 50-megawatt RMR reactor shield. Since all of the heat removed from the lead must eventually be transferred to the air outside the aircraft, and since the stagnation temperature of the air will be roughly 180°F at rated flight conditions of both Mach. = 0.9 at sea level and Mach. = 1.5 at 30,000 ft, in either case it would be necessary to operate the lead cooling system at temperatures greater than 180°F or refrigeration equipment for cooling to lower temperatures would be required. The coolant for the lead region should have a high boiling point, a low viscosity, and good stability in the radiation fields expected. Water seems to be a satisfactory choice for this coolant, provided that the system is operated under pressure in order to raise the boiling point considerably above 212°F. Turbojet engine fuels appear to be seriously damaged in radiation fields of the intensity expected in the lead region and thus do not seem suitable for application there as coolants.

Calculations indicate that a satisfactory lead shield coolant system can be obtained by circulating water through 48 1/4 in. OD aluminum tubes cast 1.25 in. from the inner surface of the 6 in. thick lead region and spaced 7.5 degrees apart on longitude lines. From the lead region the water could flow to an aluminum air radiator with 15 fins/in. and tubes spaced at 2/3 in. on centers. A radiator face area of 4.75 ft^2 and a

depth of 6.6 in. would be required for a water inlet temperature of 280°F and water outlet temperature of 230°F. Air passing through this radiator would be heated from 180 to 220°F. The 230°F outlet water could then be pumped through the jet fuel region of the shield in order to cool the shield fuel, and thence to the cooling tubes in the lead region. The shield jet fuel temperature would be roughly 250°F for this system design. This temperature is well below the initial boiling point of JP-1 fuel at 340°F. The maximum pressure required in the water-cooling circuit would be less than 70 psia.

Since the gamma heating in the hydrogenous region would be only about 3 kw for the above case, a simplified shield jet fuel coolant system would result if the hydrogenous shield were cooled by air flowing over the outside surface of the shield. It appears that satisfactory cooling could be obtained just by free convection from the outside of the shield to the ambient air with a shield to air temperature difference of the order of 60°F. A small air blast properly directed over a portion of the shield surface would suffice to cut this temperature difference to a much lower value.

IV-H. DESIGN PROCEDURE FOR THE CREW COMPARTMENT SHIELD

1. Assumptions and Basic Data

To illustrate the method of crew shield design the following conditions and basic information were assumed:

(1) The crew compartment was assumed to be a right circular cylinder with a rear face area of 50 ft^2 and a side area of 250 ft^2.

(2) The dose rate inside the crew compartment was assumed to be 1 rem/hr of which 0.875 rem/hr was gamma radiation and 0.125 rem/hr was neutron radiation using an RBE of 10.

(3) Four reactor shields giving direct dose rates of 10, 100, 1000 and 10,000 rem/hr at 50 ft from the reactor with a ratio of gamma dose to neutron dose of 7 to 1 in rems were considered. A crew compartment was designed for each of these reactors so that by interchanging crew compartments and reactors total shield weights could be obtained for any desired dose rate or degree of shield division.

(4) Where gamma shadow shields were used an ideal shadow angle of 20° was assumed. It was further assumed in computing weights that the shadow shield area was 42 ft^2 which results when the 20° angle is obtained tangent to the outside of the spherical shell heat exchanger for an 18 in. core. No neutron shadow shielding was assumed, largely because insufficient time was available to investigate the possible savings.

(5) A minimum lead thickness of 0.1 in. was assumed for the sides of the crew compartment as a safety factor against very soft gamma radiation from buildup in the plastic on the crew compartment sides. A lead thickness of 1 in. was considered the minimum thickness on the rear of the crew compartment.

(6) On the basis of the shadow shield experiments in the BSF, it was assumed that it was unrealistic to consider cases in which the direct beam was attenuated largely by the shadow shield with very little lead on the rear of the crew compartment because of the danger of streaming around the shadow shield. An arbitrary rule was used which states that no larger thickness of lead should exist in the shadow shield than on the rear of the crew compartment. This problem is part of the over-all question as to how to select shadow shield angles and attenuations and it appears that satisfactory answers must await experiments in the Tower Shielding Facility.

(7) An assumed borated plastic having a density of 0.93 g/cm^3 and fast-neutron relaxation lengths 10% less than those of full density water was used as a neutron shield material. The resulting relaxation lengths were 4.5 cm for scattered neutrons based on the "skyshine" experiment[1] and 7.2 cm for direct beam neutrons from Lid Tank data. The direct beam gamma relaxation length for plastic was taken as 25 cm including buildup. The lead on the rear of the crew compartment was considered to have a relaxation length for direct beam gammas of 2.37 cm on the basis of the BSF spectral data and NDA buildups. The relaxation length for fast neutrons in this lead was taken as 17 cm including buildup. The gamma relaxation length for the lead shadow disks in water was taken as 2.5 cm from Lid Tank data.

(8) It was assumed that the scattered neutron dose given by the relationship used included the contribution through the front and rear of the crew compartment provided that the plastic thickness on the rear was at least 8/5 of the plastic on the sides, and that the plastic thickness on the front was equal to that on the sides. The latter may be somewhat conservative but the weight penalty is not large.

(1) H. E. Hungerford, "The Skyshine Experiments at the Bulk Shielding Facility," ORNL-1611.

(9) The conversion factor between energy flux and dose rate for gamma rays was taken as independent of energy with a value of 5.5×10^5 $(\text{Mev/cm}^2 \cdot \text{sec})/(\text{r/hr})$.

(10) The reactor source of gammas for air scattering calculations was assumed monoenergetic at 6 mc^2.

(11) Structural scattering of both neutrons and gammas was assumed negligible.

(12) No sources of radiation other than the reactor were assumed.

2. Design Procedure

Since the neutron shielding has quite a large effect upon the gamma dose, while the lead has little or no effect upon the neutron dose, it was convenient to design the plastic first.

The thickness of plastic required on the sides of the crew compartment, t_{ps}, was obtained from the relation derived in section III-E.

$$t_{ps} = 4.5 \ln \left(\frac{2\pi D I_{dn}(D) \overline{(K/\ell)}}{\phi_{sn}} \right)$$

where

D = separation distance (cm) = 1524 cm in this case,

$I_{dn}(D)$ = direct neutron dose rate at 50 ft from reactor,

ϕ_{sn} = desired crew compartment dose rate from scattered neutrons,

$$\overline{\left(\frac{K}{\ell}\right)} = \frac{\int_0^\infty Q \frac{K}{\ell} \, dE_o}{\int_0^\infty Q \, dE_o},$$

Q = number of neutrons per unit energy interval per sec from reactor shield assembly.

The thickness of plastic required on the rear of the crew compartment, t_{pr}, was obtained from

$$t_{pr} = 7.2 \ \ln \frac{I_{dn}(D)}{\phi_{dn}}$$

where ϕ_{dn} is the desired crew compartment dose rate for direct beam neutrons.

Plastic weights were computed for each of the four reactor radiation levels for various combinations of direct and scattered dose. Plotting plastic weight versus the ratios of scattered dose to total dose indicated that 80% scattered and 20% direct dosage was close to optimum for all cases and the plastic thicknesses corresponding to this distribution were used. These thicknesses are shown in Table IV-H-1.

Using the data of section III-E, curves of crew compartment scattered gamma dose per unit reactor source strength, $\phi_{s\gamma}/S_o$, were plotted versus the thickness of lead on the sides of the crew compartment, $t_{\ell s}$, using the plastic thicknesses found above and a 20° shadow shield.

A range of values of the percentage of scattered gamma dose to total gamma dose was chosen from 20% to 80%. The values of $\phi_{s\gamma}/S_o$ required to give this range of doses were then computed and values of $t_{\ell s}$ were read from the curve where possible. In many cases, however, the assumption of the 20° shadow shield resulted in no lead on the sides of the crew compartment. When this occurred, the ratio between the $(\phi_{s\gamma}/S_o)$ required to give the desired gamma scattered dose and the $(\phi_{s\gamma}/S_o)'$ which was read from the curve at the correct plastic thickness and the minimum lead thickness of 0.1 in. was obtained.

In order to handle these cases it was found necessary to return to the data of section III-E and examine the scattered dose contribution from the

first 20° of angle of emission. A plot was made of the ratio of the scattered dose contribution from 0° to 20° to the contribution from 20° to 180° versus the thickness of lead on the sides of the crew compartment for three values of the plastic thickness. This ratio was symbolized by R.

Each crew compartment case was then examined individually and three general cases were found, each of which is discussed below.

Case I

$$\phi_{s\gamma} \frac{(\phi_{s\gamma}/S_o)'}{\phi_{s\gamma}/S_o} < \phi_{s\gamma}$$

Physically this meant that with the minimum lead thickness the air scattering and plastic gamma-ray attenuations were so great that the desired dose was not obtained with a 20° shadow shield. Furthermore,

$$\phi_{s\gamma} \frac{(\phi_{s\gamma}/S_o)'}{\phi_{s\gamma}/S_o} (R + 1) < \phi_{s\gamma}$$

which meant that even eliminating the shadow shield entirely did not bring the scattered dose up to the desired value. The only possible treatment here then was to take the direct dose, $\phi_{d\gamma}'$, to be the total gamma dose, ϕ_{γ}, less the scattered gamma dose with minimum lead on the sides of the crew compartment and no shadow shield; that is

$$\phi_{d\gamma}' = \phi_{\gamma} - \phi_{s\gamma} \frac{(\phi_{s\gamma}/S_o)'}{\phi_{s\gamma}/S_o} (R + 1)$$

The thickness of lead on the rear of the crew compartment was then

$$t_{\ell r} = 2.37 \ln \left[\frac{I_{d\gamma}(D)}{\phi_{d\gamma}'} \frac{1}{e^{t_{pr}/25}} \right]$$

where $I_{d\gamma}(D)$ is the direct gamma dose rate at 50 ft from the reactor.

Case II

Here again

$$\phi_{s\gamma} \frac{(\phi_{s\gamma}/S_o)'}{\phi_{s\gamma}/S_o} < \phi_{s\gamma}$$

However, in this case

$$\phi_{s\gamma} \frac{(\phi_{s\gamma}/S_o)'}{\phi_{s\gamma}/S_o} (R + 1) > \phi_{s\gamma}$$

That is, with a 20° shadow shield the dose from scattered gammas was less than that desired, but elimination of the shadow shield resulted in a dose which was too high. A shadow shield thickness which would give the desired scattered dose was then found as follows.

$$t_{\ell ss} = 2.5 \ln \left[\frac{\phi_{s\gamma} \frac{(\phi_{s\gamma}/S_o)'}{\phi_{s\gamma}/S_o} R}{\phi_{s\gamma} - \phi_{s\gamma} \frac{(\phi_{s\gamma}/S_o)'}{\phi_{s\gamma}/S_o}} \right]$$

and the thickness of lead on the rear of the crew compartment was computed from

$$t_{\ell r} = 2.37 \ln \left[\frac{I_{d\gamma}}{\phi_{d\gamma}} \frac{1}{e^{t_{pr}/25}} \frac{\phi_{s\gamma} - \phi_{s\gamma} \left[(\phi_{s\gamma}/S_o)'/(\phi_{s\gamma}/S_o)\right]}{R\phi_{s\gamma} \left[(\phi_{s\gamma}/S_o)'/(\phi_{s\gamma}/S_o)\right]} \right]$$

Case III

Here the assumption of an essentially black 20° shadow shield was a good one and entering the curve with $(\phi_{s\gamma}/I_o)$ gave the required lead thickness, $t_{\ell s}$. For estimating the weight of the shadow shield, however, some way of defining "essentially black" had to be chosen. For these calculations it was arbitrarily specified that the scattered dose obtained

from the radiation which penetrates the shadow shield should be no more than 2% of the total gamma dose in the crew compartment. This shadow shield thickness was determined as

$$t_{ss} = 2.5 \ln \frac{\phi_{s\gamma} R}{0.02\phi_{\gamma}}$$

and the thickness of lead on the rear of the crew compartment was found from

$$t_{\ell r} = 2.37 \ln \left(\frac{I_{d\gamma}}{\phi_{d\gamma}} \frac{1}{e^{t_{pr}/25}} \frac{0.02\,\phi_{\gamma}}{\phi_{s\gamma} R} \right)$$

The various crew shields arrived at on the basis of different distributions of air-scattered and direct gamma dose were then compared and the lightest crew compartment for each reactor consistent with the previous assumptions and engineering judgement was selected. Thus cases in which a small amount of weight was saved by using a very thin shadow shield, of the order of one centimeter or less, were rejected as being impractical from the engineering point of view. Cases where a very thick shadow shield resulted in a relatively thin lead layer on the rear of the crew compartment were rejected on the basis of assumption 6, p.354. When one crew compartment had been selected for each reactor a check was made to be sure that the scattered gamma dose through the rear of the crew compartment was negligible, using the curves of section III-E.

3. Conclusions

Table IV-H-1 presents the weights, thicknesses, and dose distributions for the selected crew compartments. It should be noted that various dose rates can be obtained by using a given crew shield with various reactors.

Crew compartment design for the divided shield is still plagued with uncertainties which will probably not be resolved until considerable experience with the Tower Shielding Facility has been obtained. Within the framework of these uncertainties and the assumptions used it is believed that these crew shield weights are somewhat conservative but it would be misleading to assign quantitative limits of accuracy. The shadow shield weights given are approximate since they are based on an area of 42 ft^2 which pertains only to an 18-in. core reactor. The shadow shield weight could be obtained rather precisely for any specific reactor once a layout was available, however. All weights given are for shield materials only and do not include any supporting structure.

Table IV-H-1. Characteristics of 1 rem/hr Crew Compartment for Various Degrees of Shielding

8 ft diam. by 10 ft Crew Compartment

Direct Dose 50 ft from Reactor (rem/hr)	Plastic Sides		Plastic Rear		Lead Sides		Lead Rear		Shadow Shield		Total Weight (lb)	Scattered Neutron Dose (% of Total Neutron Dose)	Scattered Gamma Dose (% of Total Gamma Dose)
	W[a] (lb)	T[b] (cm)	W (lb)	T (cm)	W (lb)	T (cm)	W (lb)	T (cm)	W (lb)	T (cm)			
10	3,000	5.3	2,700	28.2	1,500	0.254	3,500	3.0	0	0	10,700	80	8.5
100	8,900	15.6	4,200	44.7	1,500	0.254	8,600	7.5	0	0	23,200	80	28
1,000	14,800	26.0	5,800	16.3	1,500	0.254	11,800	10.2	2,300	2.4	36,200	80	50
10,000	20,800	36.4	7,400	78.0	1,500	0.254	9,500	8.2	10,400	10.7	49,600	80	80

a Weight.
b Thickness.

5 ft diam. by 10 ft Crew Compartment

Direct Dose 50 ft from Reactor (rem/hr)	Weight (lb)		
	Sides	Rear	Total (Includes Shadow Shield)
10	2,700	2,400	5,100
100	6,250	5,000	11,250
1,000	9,800	6,900	19,000
10,000	13,400	6,600	30,400

IV-I. RESULTS

Reactor--intermediate heat exchanger--shield assembly weights were determined for a series of reactor powers, reactor core diameters, and degrees of division of the shielding between the reactor and the crew compartment, i.e., for doses of 1, 10, 100 and 1,000 rem/hr at 50 ft from the reactor shield. The dose was assumed to consist of 7/8 gammas and 1/8 neutrons.

Crew shield weights were calculated for two representative crew compartment configurations, the first consisting of a right circular cyclinder 8 ft in diameter and 10 ft long and the second 5 ft in diameter and 10 ft long. Designs were prepared for attenuation factors of 10, 100, 1,000, and 10,000, respectively.

Total reactor and crew shield weights can be readily obtained by combining the proper reactor and shield combination with the proper crew compartment. This was done to give crew dose rates of both 1.0 and 0.1 rem/hr. Tables IV-I-1 through IV-I-4 summarize the significant weight and dimensional data calculated.

Typical curves were prepared to show the effects of major parameters on shield weight. A careful scrutiny of these leads to the following conclusions:

(1) Dividing the shield makes possible a large savings in total shield weight as the full-power radiation dose 50 ft from the center of the reactor is increased from 1 to 100 r/hr. Further division of the shield results in little if any benefit except for large diameter cores and small crew compartments (see Figs. IV-I-1 and IV-I-2).

(2) The shield weight for a given power output is not very sensitive to the reactor core diameter for cores less than 30 in. in diameter. The shield weight increases rapidly for larger cores (see Figs. IV-I-3 through IV-I-6).

(3) The reactor shield diameter varies quite sensitively with the dose at 50 ft outside of the crew compartment, a factor which will be of considerable interest for supersonic aircraft in which the frontal area must be kept to a minimum (see Fig. IV-I-7).

(4) The shield weight is quite sensitive to reactor power output. Reducing the reactor power makes possible a substantial savings in weight (see Figs. IV-I-3 through IV-I-6).

(5) Reducing the dose in the crew compartment by a factor of 10 imposes a weight penalty from 5,000 to 15,000 lb, depending primarily on crew compartment size (see Fig. IV-I-8).

For most of the designs considered the dose from the activated secondary coolant can be kept quite small. Although activation of the secondary coolant circuit was not included in the above calculations, in no case will it affect the designs for which the dose at 50 ft was 10 r/hr or greater. Its only effect would be to increase the weight of the crew compartments of very nearly unit shields for reactor power outputs of greater than 200 megawatts.

TABLE IV-I-1. REACTOR-INTERMEDIATE HEAT EXCHANGER-SHIELD WEIGHT FOR A DOSE OF 1 rem/hr 50 ft FROM CENTER OF REACTOR WITH DOSE SEVEN-EIGHTHS GAMMAS AND ONE-EIGHTH NEUTRONS

CORE DIAMETER (in.)	POWER (megawatts)	Z (cm)	$\left(\frac{\text{Lid Tank Dose}}{\text{Full-Scale Dose}}\right)$ (Power)	LEAD THICKNESS (in.)		LEAD INSIDE DIAMETER (in.)	LEAD OUTSIDE DIAMETER (in.)	WATER OUTSIDE DIAMETER (in.)	LEAD WEIGHT (lb)	WATER WEIGHT (lb)	REACTOR AND PRESSURE SHELL ASSEMBLY WEIGHT (lb)	BASIC SPHERE WEIGHT (lb)	WEIGHT OF PATCH (lb)	WEIGHT OF STRUCTURE (lb)	TOTAL REACTOR AND REACTOR SHIELD WEIGHT (lb)
				For Core Gammas (Assuming 0.8 r/hr)	For Core Plus Heat Exchanger Gammas										
14.3	25	133.5	1.55	6.25	6.18	44.4	56.8	119.3	20,500	28,650	5,088	54,240	1,200	1,080	56,500
	50	138.0	1.47	7.10	7.03	46.3	60.4	122.9	26,000	30,920	5,852	62,770	1,700	1,260	65,700
	100	145.0	1.36	8.10	8.09	49.4	65.6	128.5	34,000	34,770	7,398	76,770	2,500	1,540	80,800
18	25	130.0	2.16	6.00	5.94	47.8	59.6	120.2	22,100	28,810	6,100	57,000	1,300	1,140	59,400
	50	135.5	2.04	6.70	6.59	49.5	62.7	124.6	26,600	31,880	7,000	65,480	1,800	1,310	68,600
	100	141.5	1.90	7.70	7.65	52.3	67.6	129.2	35,800	34,920	8,300	79,020	2,500	1,580	83,100
	200	149.0	1.75	8.80	8.82	57.0	74.6	135.3	49,200	38,950	11,400	99,550	3,750	1,990	105,300
22.7	50	133.0	2.68	6.55	6.48	53.7	66.7	127.3	30,500	33,370	8,480	72,450	1,850	1,450	75,700
	100	139.0	2.50	7.33	7.26	56.0	70.5	132.1	37,800	36,920	9,900	84,620	2,650	1,690	88,900
	200	146.0	2.32	8.33	8.31	60.2	76.8	137.7	50,900	40,760	13,000	104,660	4,150	2,100	110,900
	400	153.5	2.15	9.70	9.71	67.0	86.4	143.7	73,800	43,860	18,500	136,160	6,400	2,720	145,300
28.5	200	143.5	3.06	8.00	7.97	64.4	80.3	141.5	54,300	43,750	15,300	113,350	4,700	2,260	120,300
	400	151.0	2.84	9.15	9.16	70.4	88.7	147.2	76,000	47,060	20,500	143,560	7,450	2,870	153,900
	800	158.0	2.65	10.6	10.66	79.7	101.0	152.8	114,000	48,210	31,360	193,570	11,200	3,870	208,600
36	200	141.0	4.20	7.55	7.51	70.4	85.4	147.0	59,500	48,520	18,700	128,720	5,300	2,570	136,600
	400	148.0	3.90	8.65	8.65	74.2	91.5	152.5	76,600	52,830	25,200	154,630	8,800	3,090	166,500
	800	155.0	3.64	10.05	10.10	84.0	104.2	158.0	115,500	53,445	34,400	203,440	19,000	4,070	226,500
45.3	200	138.5	5.60	7.15	7.11	78.4	92.6	154.3	67,000	54,720	24,800	146,520	6,300	2,930	155,700
	400	146.0	5.20	8.10	8.08	82.4	98.6	160.2	85,500	59,910	29,400	174,810	12,000	3,500	190,300
	800	152.0	4.90	9.50	9.53	89.7	108.8	164.9	121,100	60,730	39,900	221,730	20,000	4,440	246,200

TABLE IV-I-2. REACTOR-INTERMEDIATE HEAT EXCHANGER-SHIELD WEIGHT FOR A DOSE OF 10 rem/hr 50 ft FROM CENTER OF REACTOR WITH DOSE SEVEN-EIGHTHS GAMMAS AND ONE-EIGHTH NEUTRONS

CORE DIAMETER (in.)	POWER (megawatts)	Z (cm)	$\left(\frac{\text{Lid Tank Dose}}{\text{Full-Scale Dose}}\right)$ (Power)	LEAD THICKNESS (in.)		LEAD INSIDE DIAMETER (in.)	LEAD OUTSIDE DIAMETER (in.)	WATER OUTSIDE DIAMETER (in.)	LEAD WEIGHT (lb)	WATER WEIGHT (lb)	REACTOR AND PRESSURE SHELL ASSEMBLY WEIGHT (lb)	BASIC SPHERE WEIGHT (lb)	WEIGHT OF PATCH (lb)	WEIGHT OF STRUCTURE (lb)	TOTAL REACTOR AND REACTOR SHIELD WEIGHT (lb)
				For Core Gammas (Assuming 6 r/hr)	For Core Plus Heat Exchanger Gammas										
14.3	25	111	2.60	4.70	4.58	43.9	53.1	101.9	13,600	17,260	5,088	35,948	1,100	719	37,767
	50	116	2.42	5.30	5.23	45.8	56.3	105.5	17,900	18,471	5,852	42,223	1,600	844	44,667
	100	122	2.23	5.90	5.81	48.9	60.5	110.3	22,500	21,389	7,398	51,287	2,100	1,026	54,413
18.0	25	108.5	3.60	4.50	4.34	47.3	56.0	103.9	14,900	17,828	6,100	38,828	1,250	776	40,854
	50	114	3.33	5.1	5.03	49.0	59.1	108.0	19,000	19,894	7,000	45,894	1,700	918	48,500
	100	119.6	3.08	5.7	5.65	51.8	63.1	112.0	24,800	21,789	8,300	54,889	2,375	1,098	58,375
	200	125.5	2.86	6.25	6.19	56.5	68.9	117.0	31,600	24,298	11,400	67,298	3,200	1,346	71,850
22.7	50	112	4.37	4.9	4.78	53.7	63.3	110.7	21,400	20,800	8,480	50,680	1,400	1,014	53,400
	100	117.5	4.05	5.45	5.40	55.5	66.4	113.5	26,200	21,661	9,900	57,761	2,300	1,156	61,250
	200	123.3	3.76	6.05	6.02	59.7	71.7	119.9	33,800	25,781	13,000	72,581	3,500	1,452	77,550
	400	129.5	3.50	6.60	6.57	66.5	79.6	124.7	44,800	27,816	18,500	91,116	5,100	1,822	98,020
28.5	200	121.3	4.92	5.80	5.77	63.9	75.4	124.3	36,000	28,647	15,300	79,947	4,000	1,598	85,500
	400	127	4.56	6.5	6.46	69.9	82.8	128.5	49,100	29,547	20,500	99,147	6,000	1,982	107,080
	800	134	4.25	7.2	7.13	79.2	93.5	134.3	69,000	30,883	31,360	131,243	9,900	2,624	143,740
36.0	200	119	6.7	5.55	5.49	69.9	80.9	129.8	40,300	30,845	18,700	89,845	4,600	1,796	96,250
	400	125.3	6.2	6.20	6.13	73.7	86.0	135.0	50,800	34,501	25,200	110,501	7,500	2,210	120,200
	800	131	5.8	6.9	6.87	83.5	97.2	139.2	73,300	34,188	34,400	141,888	11,000	2,840	155,800
45.3	200	117	8.95	5.35	5.23	77.9	88.4	137.5	47,300	35,397	24,800	107,497	5,600	2,150	115,250
	400	123.3	8.3	5.55	5.48	81.9	92.9	143.5	53,800	39,731	29,400	123,931	9,000	2,480	135,400
	800	129	7.8	6.60	6.54	89.2	102.3	146.9	76,600	40,573	39,900	157,073	16,000	3,140	176,200

TABLE IV-I-3. REACTOR-INTERMEDIATE HEAT EXCHANGER-SHIELD WEIGHT FOR A DOSE OF 100 rem/hr 50 ft FROM CENTER OF REACTOR WITH DOSE SEVEN-EIGHTHS GAMMAS AND ONE-EIGHTH NEUTRONS

CORE DIAMETER (in.)	POWER (megawatts)	Z (cm)	$\left(\frac{\text{Lid Tank Dose}}{\text{Full-Scale Dose}}\right)$ (Power)	LEAD THICKNESS (in.)		LEAD INSIDE DIAMETER (in.)	LEAD OUTSIDE DIAMETER (in.)	WATER OUTSIDE DIAMETER (in.)	LEAD WEIGHT (lb)	WATER WEIGHT (lb)	REACTOR AND PRESSURE SHELL ASSEMBLY WEIGHT (lb)	BASIC SPHERE WEIGHT (lb)	WEIGHT OF PATCH (lb)	WEIGHT OF STRUCTURE (lb)	TOTAL REACTOR AND REACTOR SHIELD WEIGHT (lb)
				For Core Gammas (Assuming 50 r/hr)	For Core Plus Heat Exchanger Gammas										
14.3	25	95	2.64	2.95	2.74	44.4	49.9	89.0	7,800	10,984	5,088	23,870	1,000	476	25,300
	50	100	2.44	3.55	3.40	46.3	53.1	93.1	10,800	12,430	5,852	29,080	1,300	580	31,000
	100	105.5	2.24	4.15	4.00	49.4	57.4	97.5	14,800	13,943	7,398	36,140	1,750	720	38,600
18.0	25	93	3.6	2.7	2.38	47.8	52.6	91.2	8,180	11,599	6,100	25,880	1,200	516	27,600
	50	97.5	3.35	3.33	3.19	49.5	55.9	94.8	11,500	12,860	7,000	31,360	1,600	626	33,600
	100	103	3.10	3.95	3.83	52.3	60.0	99.1	15,800	14,323	8,300	38,420	2,100	768	41,300
	200	108.5	2.86	4.50	4.38	57.0	65.8	103.4	21,600	15,519	11,400	48,500	2,800	970	52,300
22.7	50	96	4.40	3.1	2.91	53.7	59.5	98.3	12,000	13,970	8,480	34,450	1,650	688	36,800
	100	101	4.06	3.7	3.59	56.0	63.2	103.0	16,000	15,890	9,900	41,790	2,250	836	44,900
	200	106.5	3.77	4.25	4.18	60.2	68.6	106.6	22,200	16,814	13,000	52,010	3,000	1,040	56,000
	400	112	3.48	4.95	4.83	67.0	76.7	111.0	32,300	17,341	18,500	68,140	4,900	1,362	74,400
28.5	200	104	4.90	4.10	4.00	64.4	72.4	110.4	24,200	18,276	15,300	57,780	3,800	1,156	62,700
	400	110	4.55	4.70	4.62	70.4	79.6	115.1	32,500	19,298	20,500	72,300	5,600	1,446	79,300
	800	116	9.22	5.25	5.20	79.7	91.1	120.0	53,900	18,372	31,360	103,630	8,000	2,072	113,700
36	200	102.5	6.61	3.90	3.74	70.4	77.9	116.7	26,600	21,117	18,700	66,420	4,000	1,128	71,500
	400	108.5	6.10	4.45	4.32	74.2	82.8	121.4	34,200	23,114	25,200	82,510	6,100	1,650	90,300
	800	114	5.70	5.00	5.00	84.0	94.0	125.9	51,000	22,028	34,400	107,430	8,300	2,148	117,900
45.3	200	100.5	8.80	3.65	3.43	78.4	85.3	124.4	33,300	24,664	24,800	82,760	4,800	1,656	89,200
	400	107	8.10	4.20	4.07	82.4	90.5	129.7	39,400	27,256	29,400	96,060	7,600	1,920	105,600
	800	112	7.61	4.85	4.79	89.7	98.3	133.7	49,000	27,240	39,900	116,140	9,000	2,322	127,500

TABLE IV-I-4. REACTOR-INTERMEDIATE HEAT EXCHANGER-SHIELD WEIGHT FOR A DOSE OF 1000 rem/hr 50 ft FROM CENTER OF REACTOR WITH DOSE SEVEN-EIGHTHS GAMMAS AND ONE-EIGHTH NEUTRONS

CORE DIAMETER (in.)	POWER (megawatts)	Z (cm)	$\left(\frac{\text{Lid Tank Dose}}{\text{Full-Scale Dose}}\right)$ (Power)	LEAD THICKNESS (in.)		LEAD INSIDE DIAMETER (in.)	LEAD OUTSIDE DIAMETER (in.)	WATER OUTSIDE DIAMETER (in.)	LEAD WEIGHT (lb)	WATER WEIGHT (lb)	REACTOR AND PRESSURE SHELL ASSEMBLY WEIGHT (lb)	BASIC SPHERE WEIGHT (lb)	WEIGHT OF PATCH (lb)	WEIGHT OF STRUCTURE (lb)	TOTAL REACTOR AND REACTOR SHIELD WEIGHT (lb)
				For Core Gammas (Assuming 500 r/hr)	For Core Plus Heat Exchanger Gammas										
14.3	25	81.3	3.30	1.28	1.12	44.4	46.5	78.4	2,785	7,207	5,088	15,080	700	300	16,100
	50	85.0	3.08	1.85	1.76	46.3	49.8	81.3	5,190	7,939	5,852	18,880	1,150	376	20,400
	100	89.0	2.90	2.33	2.29	49.4	54.0	84.5	7,900	8,424	7,398	23,720	1,500	474	25,700
18.0	25	80.1	4.45	1.05	0.92	47.8	49.6	81.0	2,741	7,723	6,100	16,560	900	330	17,800
	50	83.5	4.23	1.65	1.56	49.5	52.6	83.7	5,190	8,341	7,000	20,530	1,400	410	22,300
	100	87.0	3.98	2.10	2.12	52.3	56.5	86.5	7,940	8,826	8,300	25,060	1,900	500	27,500
	200	91.5	3.71	2.65	2.68	57.0	62.4	90.0	12,360	9,193	11,400	32,950	2,650	858	36,500
22.7	50	82.5	5.46	1.40	1.27	53.7	56.2	87.7	4,840	9,402	8,480	22,720	1,400	454	24,600
	100	85.5	5.16	1.93	1.81	56.0	59.6	90.3	7,720	9,914	9,900	27,530	2,000	550	30,100
	200	90.0	4.82	2.40	2.49	60.2	65.2	93.5	12,610	10,216	13,000	35,830	2,900	716	39,400
	400	94.5	4.46	3.00	3.08	67.0	73.2	96.9	19,570	9,779	18,500	47,840	4,100	956	52,900
28.5	200	88.5	6.20	2.27	2.30	64.4	69.0	98.1	13,120	11,633	15,300	40,050	3,200	800	44,100
	400	93.0	5.80	2.80	2.90	70.4	76.2	102.1	20,000	11,753	20,500	52,250	4,900	1,044	58,200
	800	98.0	5.37	3.30	3.48	79.7	86.7	105.5	30,110	9,881	31,360	71,350	7,200	1,426	80,000
36	200	87.0	8.30	2.05	2.03	70.4	74.5	104.4	13,850	13,528	18,700	46,080	4,200	920	51,200
	400	91.0	7.80	2.65	2.65	74.2	79.5	107.6	20,100	14,055	25,200	59,350	5,600	1,186	66,100
	800	96.0	7.25	3.13	3.33	84.0	90.7	111.6	32,810	12,172	34,400	79,380	8,400	1,586	89,400
45.3	200	85.5	10.68	1.90	1.77	78.4	81.9	112.5	14,400	16,527	24,800	55,730	4,400	1,114	61,200
	400	89.5	10.16	2.40	2.42	82.4	87.2	115.7	22,150	16,317	29,400	67,870	6,900	1,356	76,100
	800	93.5	9.70	2.95	3.11	89.7	95.9	118.9	34,300	15,046	39,900	89,250	10,800	1,784	101,800

[redacted]

ORNL-LR-DWG 456

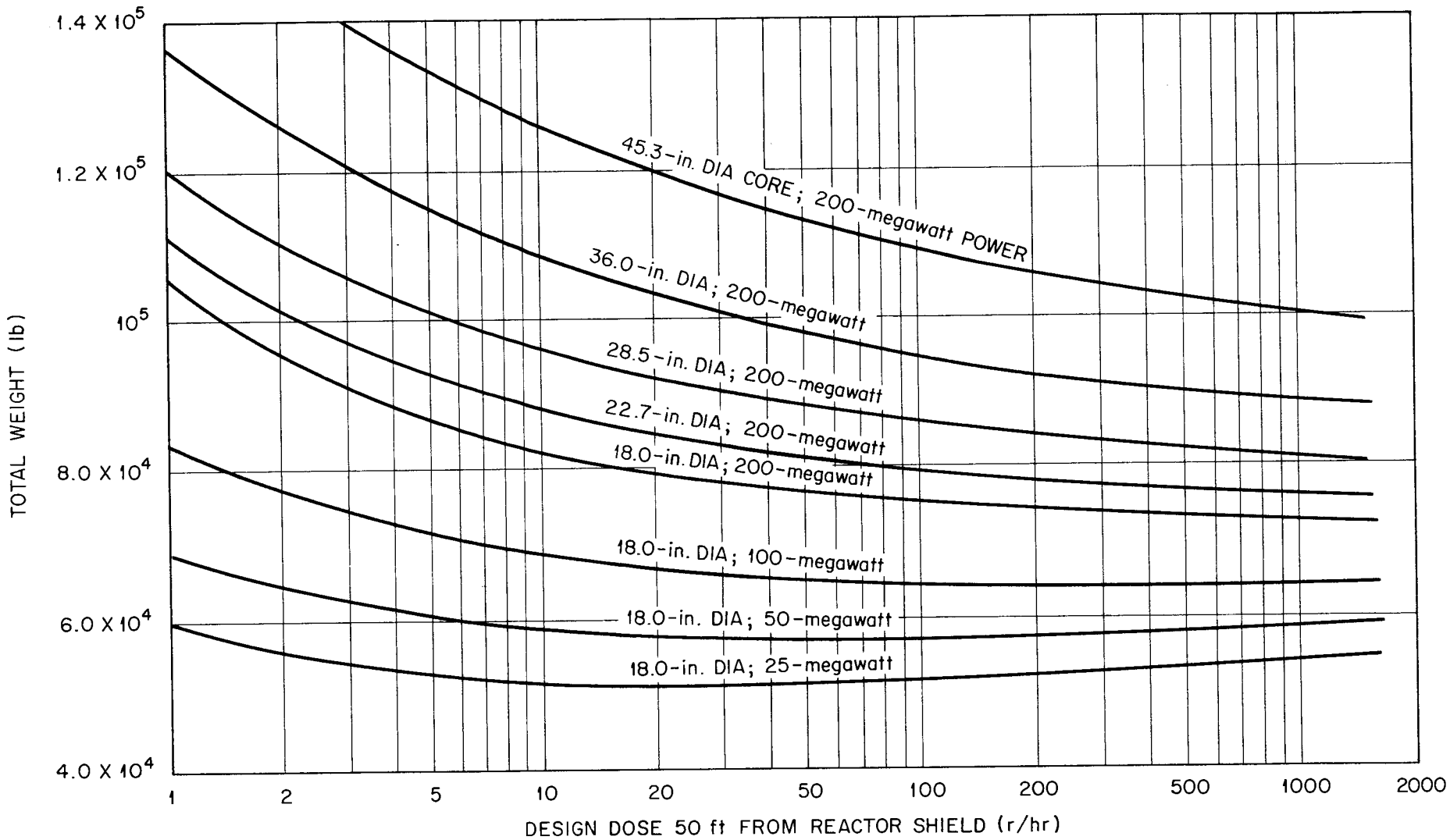

Fig. IV-I-1. Effect of Design Dose from Reactor Shield on Total Reactor-Shield Weight for 1 r/hr in Crew Compartment 8 ft DIA by 10 ft Long.

[redacted]

ORNL-LR-DWG 457

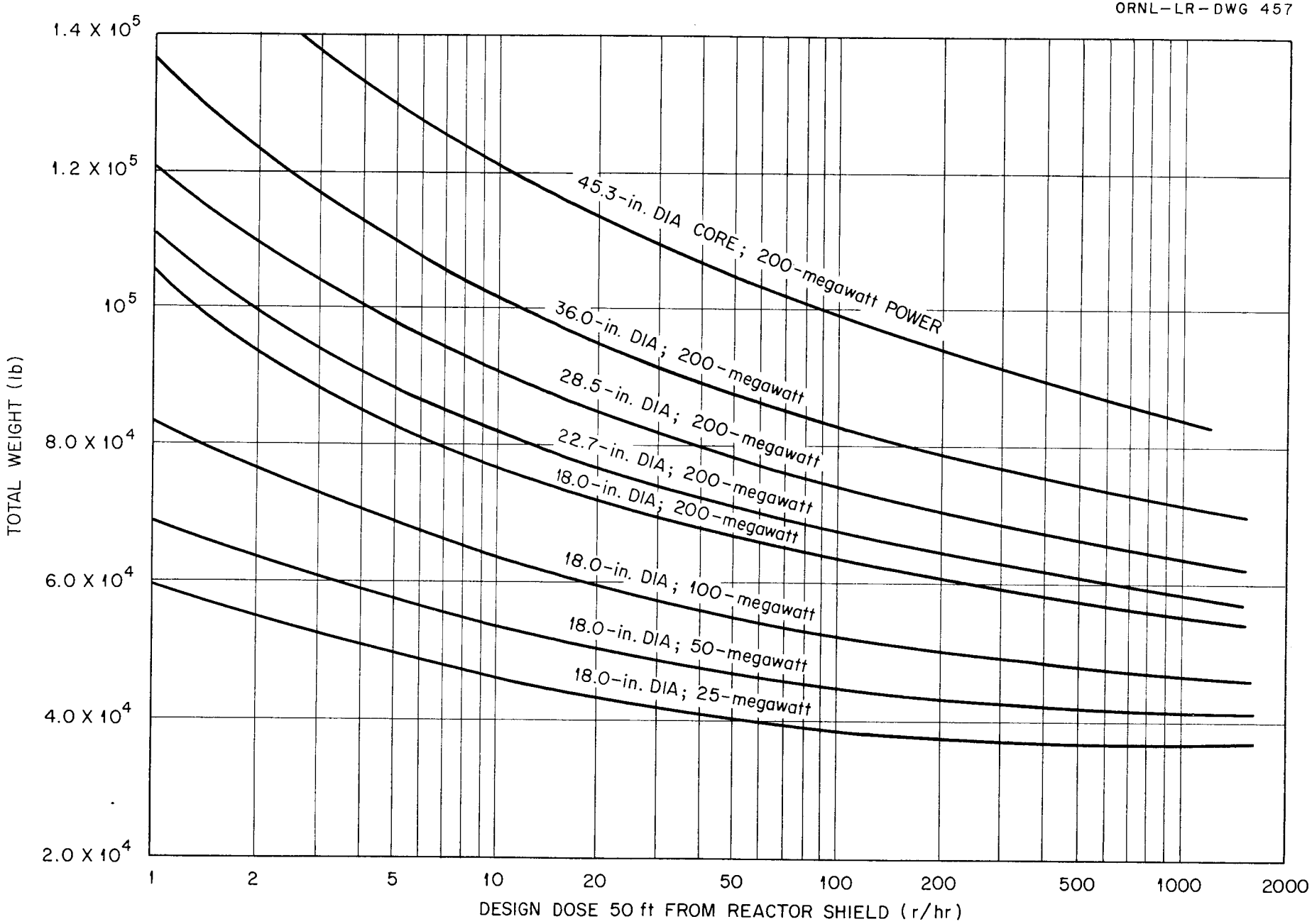

Fig. IV-I-2. Effect of Design Dose from Reactor Shield on Total Reactor-Shield Weight for 1 r/hr in Crew Compartment 5 ft DIA by 10 ft Long.

[redacted]

ORNL-LR-DWG 458

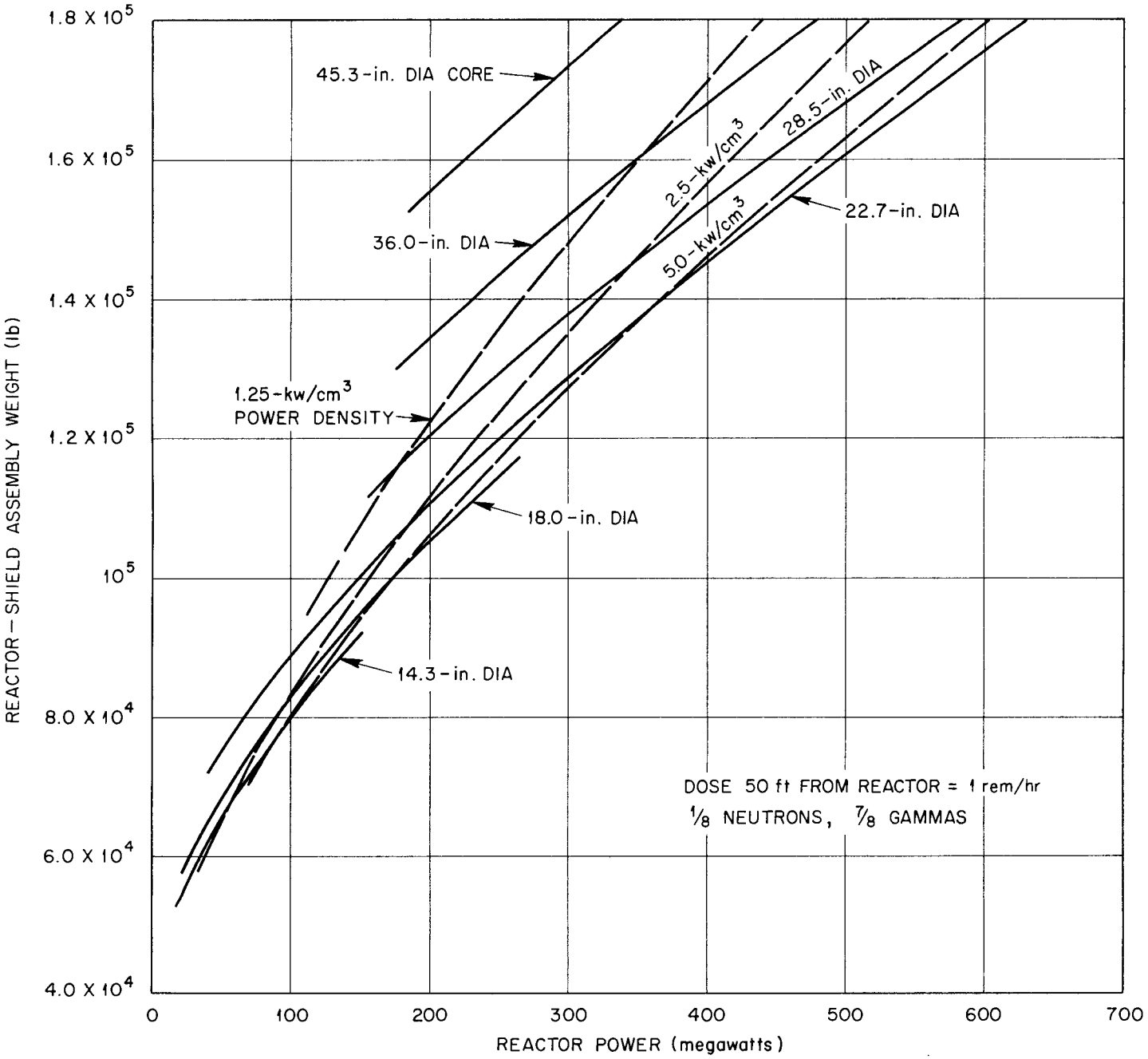

Fig. IV-I-3. Effects of Power Output and Core Diameter on the Weight of the Reactor-Shield Assembly — No Crew Shield.

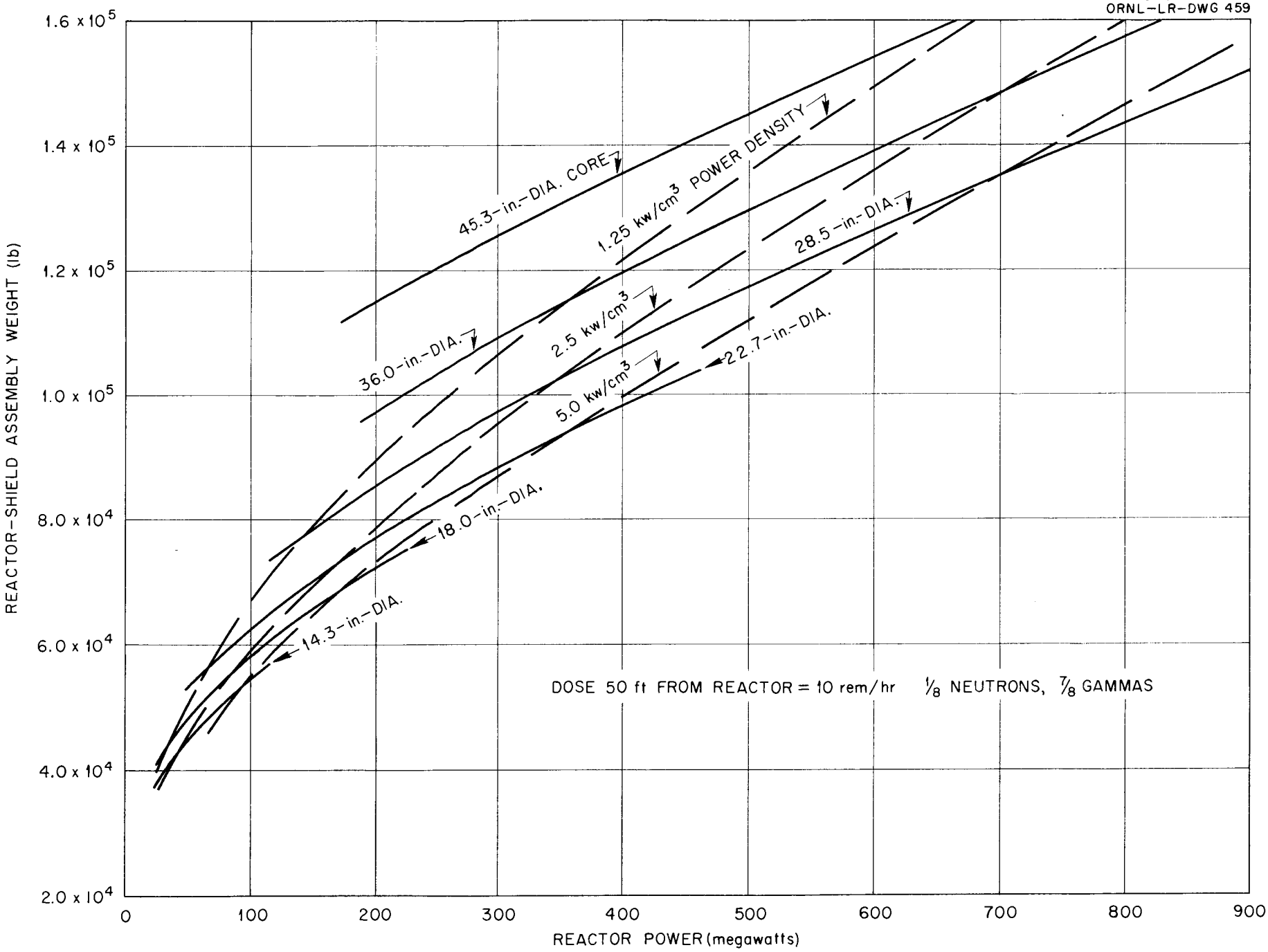

Fig. IV-I-4. Effects of Power Output and Core Diameter on the Weight of the Reactor-Shield Assembly—No Crew Shield.

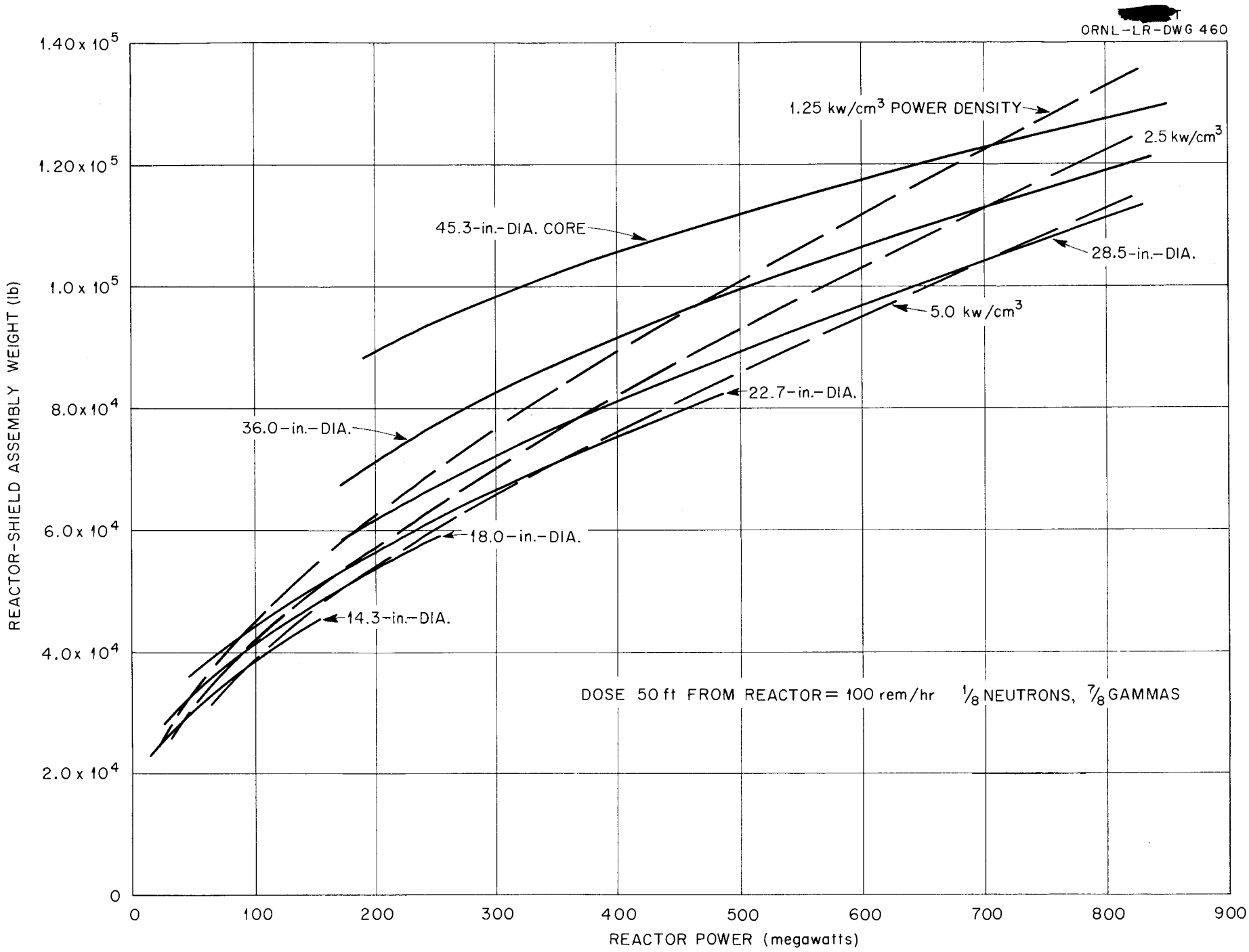

Fig. IV-I-5. Effects of Power Output and Core Diameter on the Weight of the Reactor–Shield Assembly—No Crew Shield.

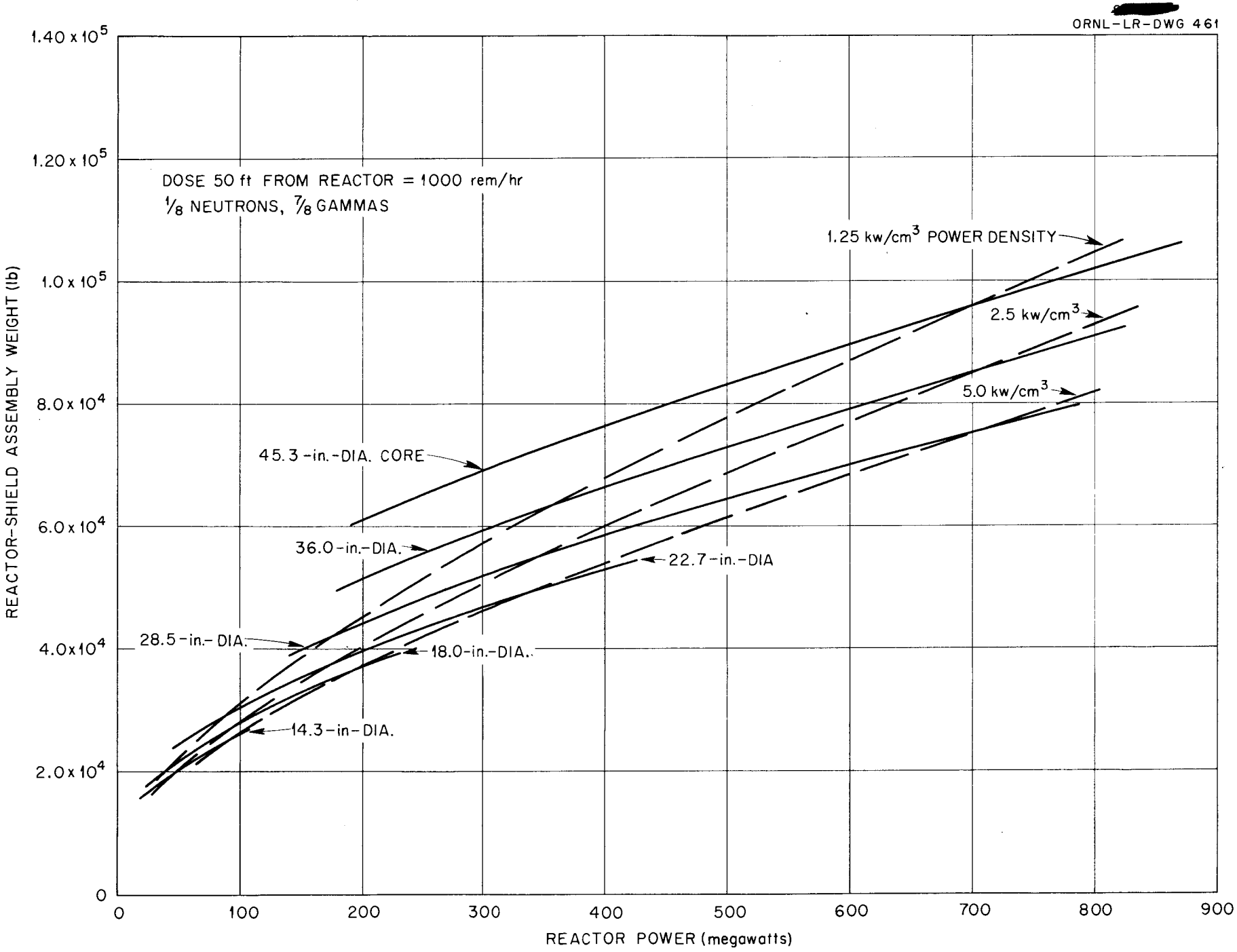

Fig. IV-I-6. Effects of Power Output and Core Diameter on the Weight of the Reactor-Shield Assembly—No Crew Shield.

[redacted]

ORNL-LR-DWG 549

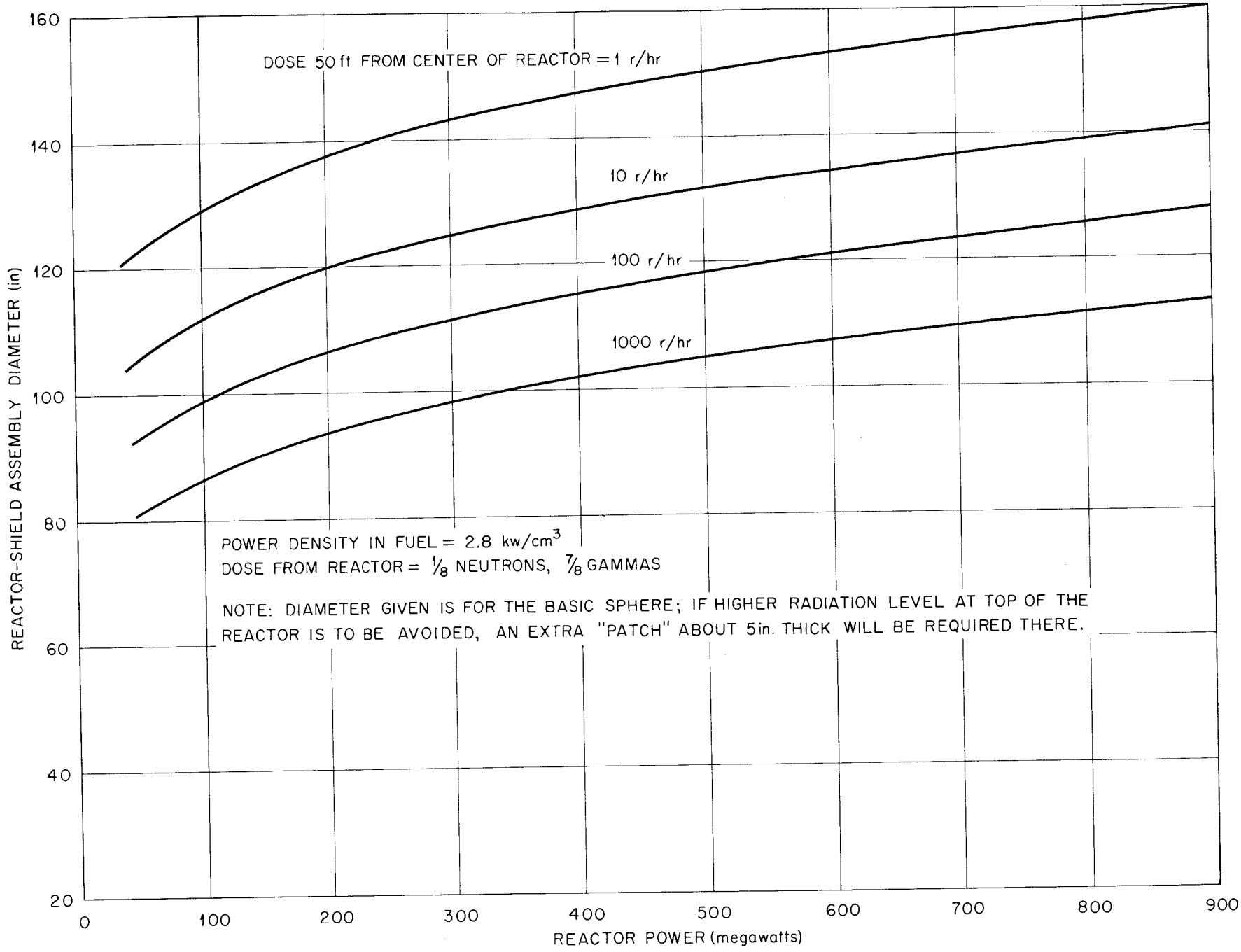

Fig. IV-I-7. Effects of Power Output and Shield Division on the Diameter of the Reactor Shield Assembly.

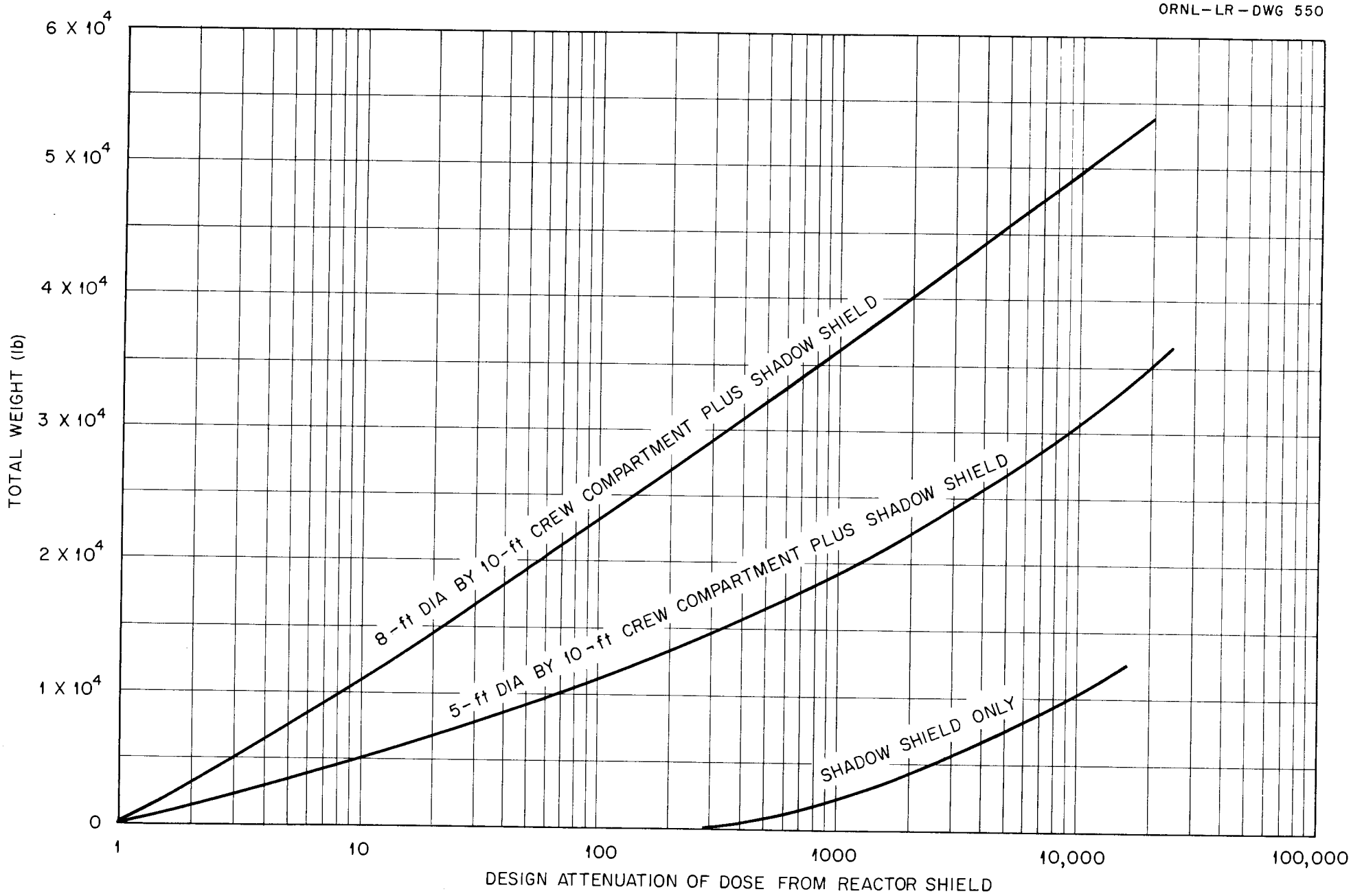

Fig. IV-I-8. Effects of Design Attenuation on Crew and Shadow Shield Weight for Equal Attenuation of Neutrons and Gammas.

V. RECOMMENDATIONS FOR FUTURE RESEARCH

V. RECOMMENDATIONS FOR FUTURE RESEARCH

To date no aircraft shield has been built. No complete mockup has been built and tested. No group of people has been deliberately exposed to the military radiation dose. Until these things have been done no shield design can be considered to be really reliable.

Much of the information which must precede actual shield construction has, however, been obtained. The sources of radiation are largely known. The basic interactions are understood and many of them have been measured. The biological effects of radiation have been observed for some cases. Many aircraft shield designs have been laid down on paper and a submarine reactor has been successfully shielded. But there remain serious hiatuses in our information which can and should be covered by research. Many of these must be found out prior to building the first actual aircraft shield.

1. Determination of Tolerance Dose

While laboratory tolerances can be kept low with relatively little penalty, this obviously is not the case with aircraft. It will be necessary to operate as close to the damage limit as possible, and therefore this limit must be well defined.

Experiments are required to settle questions regarding the following variables:

1. Additivity of the several radiation forms (RBE's).
2. Additivity in time. The effect of allowing recovery periods between successive exposures must be found out.

3. The nature of damage to be expected in the various organs must be known, including those effects which only appear late in life or in succeeding generations.

It is accordingly recommended that a biological program be undertaken to obtain answers to the above problems. Particular attention should be paid to making the results applicable to man in the expected situations, which would seem to legislate toward the use of primates where possible. The extent of the required exposures appears to be such that it will probably be necessary to commandeer the ORNL Tower Shielding Facility for much of the work. That facility should be divided in its application to this problem and those of attenuation measurement for which it was originally intended.

2. Improvement of Computational Methods

Primary Gamma Rays

The moment methods of Fano and Spencer[1] have been exploited notably by NDA for the calculation of gamma-ray buildup factors for a large number of elements. By interpolation between these results it is possible to estimate quite accurately the gamma-ray attenuation in almost any single material. It is possible to obtain a fair estimate also for homogeneous mixtures of materials. No really good methods are yet available, however, for estimating the attenuation in nonhomogeneous media except in rather special cases. Since in aircraft shields it will be not uncommon to use several quite different attenuating regions in juxtaposition, it is very

(1) L. V. Spencer and U. Fano, "Penetration and Diffusion of X-Rays. Calculation of Spatial Distributions by Polynominal Expansion," J. Res. NBS 46, 446 (1951).

important to be able to estimate attenuations to be expected in these shields. The problems are basically of two types. In one the geometry is comparatively simple, such as two or three thick spherical shells inside one another, but the attenuation is large. The approach to this type is much like that to the basic attenuation problem. In the other type, the attenuation is usually not large, but the geometry is difficult to handle. These problems have been attacked most successfully to date with the stochastic (Monte Carlo) methods. Both of these types of problems can very profitably be worked on.

Neutrons

Much of the gamma-ray experience is now being applied to the calculation of neutron attenuations, but these are somewhat hampered by the complexity and lack of knowledge of the interaction processes. It would of course be highly desirable to be able to calculate neutron attenuations in much the same way as is done for gamma rays. To make this possible several things are needed.

Most obvious of course is more information on the differential neutron cross sections. This appears to be coming in as well as can be expected and should not be the immediate concern of those charged with shield development.

It has been demonstrated both experimentally and by computation that it is possible to predict the effect on attenuation of adding a small amount of new material to a hydrogenous shield, making use of a single parameter called the "removal cross section" (see section III-D). This parameter can be measured in facilities such as the ORNL Lid Tank Shielding Facility, and the measurements should be extended until there is essentially little doubt about any material of interest. That this is not out of the question

is evidenced by recent correlations between removal and total cross sections as functions of the atomic weight. These indicate that except for low A materials there will be some smooth relationship between the removal cross section and the total cross section, and perhaps between the removal cross section and the atomic number.

Secondary Gamma Rays

In the attenuation of neutrons, gamma rays are almost always produced, and this complicates considerably the calculation of shield attenuation. Several more or less empirical methods have been devised for optimizing shields in this situation,[2,3] but no calculations have been made which are comparable to those for pure neutrons or pure gamma rays. A start on this calculation was made in 1953 by B. T. Feld,[4] who attempted to reduce the calculation to analytical relationships between a few measurable parameters which take into account neutron attenuation as well as gamma production. If this simplification can be refined and extended, it will afford a cheap method for calculating many pertinent shields.

3. Experimental Program

Removal Cross Sections

The program for measuring fast-neutron removal cross sections should be continued for the reasons given in the preceding part.

(2) L. Tonks and H. Hurwitz, "The Economical Distribution of Gamma Ray Absorbing Material in a Spherical Pile Shield," KAPL-76 (June 8, 1947).
(3) H. Goldstein and E. P. Blizard, "A Criterion for the Experimental Optimization of Two-Component Unit Shields," Reactor Science and Technology, Vol. 1, No. 2, p. 88 (Aug., 1951).
(4) B. T. Feld, forthcoming NDA memo.

Secondary Gamma-ray Parameters

Various shield materials should be examined in a facility such as the Lid Tank to determine comparative propensity for secondary gamma-ray production. This information will assist in choosing materials as well as in calculating multiregion shield attenuations.

Special Geometrical Problems

Special attenuation problems such as the slant penetration of crew shield side walls should be explored experimentally until some rationale is available for general shield design. Another problem has to do with the short-circuiting of gamma radiation around shadow shields. Still another is the attenuation of neutrons and gamma rays in shields which are perforated by ducts.

Divided Shield Mockups

The test of a divided shield on the basis of a full-scale mockup should be performed as soon as practicable. Such questions as the variation of dose within the crew compartment are not satisfactorily calculable and must be left to experiment.

Divided Shield Parameters

Large-scale experiments on a facility such as the ORNL Tower Shielding Facility should be aimed at the determination of the optimum shield shapes. The amount of shield paring which can be permitted, both at reactor and crew, should be determined experimentally. This will of course require a rather detailed knowledge of the attenuation in all parts of the shield, and this information will enable a realistic divided shield optimization.

Structure Scattering

Structure scattering of radiation may either enhance or reduce the attenuation of a divided shield. This should be given careful attention in facilities such as those at Convair.

The Sources of Radiation

Information is still not available on the prompt fission gammas and the gammas from short-lived fission products. These should both be measured as soon as possible. Bremsstrahlung from a Li^7 coolant, which would give off 12-Mev beta rays, has not been satisfactorily measured. If this coolant is to be considered, then an experiment on this phenomenon is in order.

The activation of a secondary coolant by delayed neutrons from a circulating fuel should be measured. The calculations on this phenomenon must be based on poorly known cross sections and the safest procedure is to measure the activation directly.

4. Shield Design Studies

Shield designs should be closely controlled by the results of current research and insurance of this situation is not to be left to small scattered groups at the several interested organizations. By cooperative effort a competent group should be charged with developing shield designs which take into account all the latest experimental evidence. This group should work closely both with the airplane designers and the shield research personnel and should take an aggressive attitude toward making airplane and shielding requirements compatible.

VI. TRENDS IN SHIELD DESIGN

VI. TRENDS IN THE DESIGN OF ANP SHIELDS

The interval since the Shielding Board Session in late 1950 has seen significant advances both in the design of airplane reactor shields and in the tools needed in the designing process. Shield designs of this period have been predominantly of the "divided-shield" type, largely as a result of the report of that Shielding Board. The old idea of placing part of the shielding at the crew position had been ably exploited by W. B. Thomson and H. E. Stern to indicate large savings in weight. The findings of the Board were that these savings were real and, with the tenuous feasibility then believed for ANP, that adoption of the divided configuration appeared to be more or less mandatory. In the absence of attenuation data for the less familiar materials, the composition of the shields appeared to be equally fixed. The early experiments in the ORNL Lid Tank Facility showed that water and lead, as neutron and gamma-ray shields, respectively, out-perform most other materials, while possessing the desirable attributes of cheapness and availability. The Lid Tank tests being conducted at the time of the Board also indicated that boration of the neutron shield would be most helpful in reducing secondary gamma rays.

The pattern thus set by the 1950 Board design has been followed in most shield designs since. The reactor portion of the shield is mainly for attenuating neutron flux and consists of water except for the outer layers. In addition, a lead shield shadowing the reactor core attenuates the gamma rays directly incident on the crew compartment and those which are most likely to contribute to air-scattered flux. The rear face of the crew compartment also has a shield, plastic backed by lead, to reduce the direct

beam. Similar shielding, but of lesser thickness, on the side walls protects against the air-scattered dose. Different cycles have produced variants on this design. For instance, the SCWR has had to have more gamma-ray shielding at the reactor as a result of the pressure shell and its thermal shield. The DCR has naturally emphasized the ducting aspects of the design. But the main features have been the same.

The degree of division of both the gamma-ray and neutron shielding has fluctuated with the core size and nature of the cycle. In the air-cooled reactor the large core size has encouraged a highly divided shield. The ducting for such a cycle through a unit shield would impose excessive weight increases, and this has also emphasized large division. For a reactor of this type the highly divided shield seems to remain the only feasible kind. With small-core cycles, such as the reflector-moderated reactor, the pendulum appears to be swinging back to a more nearly unit type shield. This is a trend that is being welcomed heartily by the ultimate users of ANP vehicles. Not only does it greatly simplify maintenance and operation, but more nearly unit shields are required for newly considered applications, such as cargo and personnel carriers. Present efforts, as exemplified in this report, are to achieve a modified design which does not have excessive radiation fields in the vicinity of the airplane, but which is divided enough to realize most of the weight saving.

The composition of the shield is also being subjected to renewed scrutiny. In large measure, this has been spurred by mounting evidence that ANP practicability (as contrasted with feasibility) may require a reduction in current shield weights as great, proportionately, as that which resulted from the introduction of the divided shield. The most promising region for achieving

this reduction appears to be in the introduction of newer, unfamiliar, shielding materials. At the moment, attention is being paid mostly to the neutron shield. Here beryllium and light element hydrides have given the most promise. If the swing towards a more unit shield, even for gamma radiation, continues there may be a reawakening of interest in the heavy elements too.

The tools available to the designer, both experimental and theoretical, have also shown considerable advance in the last three years. In the fall of 1950 the Lid Tank Shielding Facility provided almost the only means by which bulk shielding tests could be made. In the intervening period the LTSF has been continuously used to capacity and has proved extremely versatile in the many varieties of experiments which can be performed with it. Besides the measurement of simplified versions of shield configurations it has been used to find "removal cross sections," to optimize unit shields, to measure duct properties, to test scattering around bulkheads, and to find the relaxation length for oblique penetration of neutrons, among other applications. At the time of the Shielding Board Meeting the Bulk Shielding Reactor (known as the "swimming pool") was just going into operation. One of the main uses originally envisaged for this facility was the testing of nearly full-scale mockups of shield designs. Certainly, this purpose has occupied a goodly fraction of the facility's time; some of the mockups tested have included an optimized unit shield, the reactor portion of the ANP-53 shield and the SIR top plug. There has been an increasing trend, however, to use the BSF for more fundamental measurements that are made possible only by virtue of the higher fluxes available in the facility. The Lid Tank source plate operates at 6 watts; in contrast the BSR was

started at 10 kw, has been operating routinely at 100 kw, and will probably soon be brought up to 1 megawatt. With this increased source the experiments performed have ranged from simple extensions of Lid Tank results to greater distances, through measurements of prompt fission gamma spectra and activation cross sections, to attempts at measuring air scattering and cataract formation in monkeys.

Full-scale mockup testing in the BSF has proven costly in time and money. For ANP purposes, at least, the emphasis on divided shields and unit shields which are highly assymmetric has also greatly diminished the usefulness of such testing in this facility. The BSF can furnish measurements only on the reactor portion of the shield; complete testing should carry the measurements through air and structure scattering and subsequent penetration into the crew compartment. It is possible in principle to combine calculations of air scattering with detailed energy and angular distributions obtained with the BSF so as to give a measure of the air-scattered dose. This process has been attempted with one mockup, but the measurements and calculations have been so laborious and so freighted with question marks as to underscore the impracticability of the procedure. In consequence a new facility--the Tower Shielding Facility--is being constructed in which it should be possible to measure directly the contribution to the dose in the crew compartment due to direct radiation, air scattering, or even structure scattering. Furthermore, the Tower Shielding Facility can be used for radiations in connection with biological experiments, so that the dose measurements will be the same for biology and shielding. While the trend may be somewhat back to unit shields it is likely that the shielding at the reactor can never be so complete that only the

direct radiation is important. The TSF is therefore likely to be for some time a vital link in the design and testing of ANP shields.

Facilities are of little use unless the accompanying instrumentation keeps pace. From the practical standpoint perhaps the most significant development has been the improvement of the neutron dosimeter for measuring the fast-neutron dose to the point where it is routinely used for measurements where previously only thermal-neutron fluxes could be obtained. Even more significant from the long range point of view may be the advances made in spectroscopy. Gamma-ray spectroscopy, based on two- and three-crystal scintillation spectrometers, has been developed extensively. Measurements with these tools at the BSF have provided much of the basic data for shielding designs and have also been used to check the predictions of theoretical calculations. Neutron spectroscopy is in a less happy state, although the progress made in the last three years has been far from negligible. So far, no counter, either gas discharge or scintillation, has yet been devised which has an output determined solely by the incident neutron energy, which has a good efficiency for neutrons but is insensitive to gamma rays, and which does not require collimation of the neutrons. The most successful device to date, the proton-recoil spectrometer, is insensitive to gamma radiation and provides reasonable energy resolution, but the efficiency is quite low (since the recoil radiator must be thin) and neutron collimation is necessary. The latter drawback would not be so disadvantageous were the efficiency higher, for then angular distributions could be measured as with gamma rays. At present the spectrometer has only sufficient sensitivity to measure the spectra at around 50 cm from the BSR and then only looking directly at the reactor. These limitations on the spectrometer

hinder comparison of the measurements with theory but some useful clues are nonetheless provided. An efficient method for the spectroscopy of the uncollimated neutrons is still very greatly to be desired.

The extent of the help which the designer can obtain from bulk shielding experiments depends on how successfully they have been understood. Interpretation has perhaps not kept in step with the huge volume of experimental data, but some advances can be noted. The concept of fast-neutron "removal cross section" which had barely been introduced by the fall of 1950 has found widespread favor and application. A continuing measurement program in the LTSF has provided by now removal cross sections for a large number of elements. Because it permits fast-neutron attenuation to be described by a single parameter, the removal cross section idea has been quite successful. One might almost say it has been too successful, for this one property of a material has overshadowed other shielding attributes which have so far defied parametric characterization, such as secondary gamma production.

About the time of the 1950 Shielding Board the first trials had begun on experimentally optimizing a unit shield by Lid Tank tests. Since that time the theoretical basis of such empirical optimization procedures has been firmly established. The method has been extended in principle also to optimization of more complete airplane shields. It is expected that trials of this procedure will be made once the TSF is constructed and in operation.

Ducting was a subject which was in a state of near chaos three years ago. The design of ducts has not yet been reduced to handbook routine, by far; significant progress has been made, however. Numerous experiments have been performed both at ORNL and at the Brookhaven shielding facility. More important, simple empirical representations have been developed which cover a

fair fraction of the situations encountered in design. One applies particularly well to neutron attenuation and might be called the albedo approach. Here the particle is considered to propagate along the duct by successive reflection at the turns and bends in the duct; the reflection process being described by a simple albedo. Where the turns are so many and the duct so narrow that the transmission by such reflections is very small, the effect of the duct can often be obtained by assuming it acts only to reduce the density of the overall shield.

Some experiments other than in bulk shielding facilities have proven directly helpful for shielding design. Measurements have been made at NBS and BNL on the penetration of gamma rays obliquely incident on slabs simulating the sides of crew compartments. These results combined with theoretical calculations of air scattering enable the designer to predict accurately the dose received by the crew once the energy and angular distributions of the photons emitted from the reactor are known. Similar experiments for neutrons are in progress.

Fundamental shielding theory has made great strides in the last three years. The results are just now reaching the point of becoming helpful to the practical designer and give promise of much greater usefulness in the future. Two developments have made this progress possible. One is the amount of microscopic data which is becoming available to serve as the raw input of the theoretical calculations. The other is the application of high-speed computing machines to shielding problems.

It was once the perhaps unspoken feeling that completely theoretical calculations were of little use since the microscopic data needed were unknown. There is much less force to this point at the present and likely

to be still less in the near future. In 1950 there were few gamma-ray absorption coefficients which were known to better than 6%, and each worker had his own pet table of cross sections. Today the average accuracy is closer to 2% (or a factor of 1.5 in 20 mean free path lengths) and there exists a compilation of the NBS which bids fair to become an "industry wide" standard. Progress in neutron cross section measurements can be dramatically demonstrated by comparison of Adair's 1950 compilation(1) with the latest revised version of AECU-2040.(2) The prospect for the future is even brighter. Intensive experimental effort is being put on the measurements of interest for shielding -- gamma-ray spectra, angular distributions of scattered neutrons, and inelastic cross sections. Techniques of gamma-ray spectroscopy have reached the stage where it is reasonable to ask for most of the spectra needed for shielding studies, such as prompt fission gamma rays or capture gamma-ray spectra. The small trickle of angular distribution measurements has grown to a healthy stream now. Only the measurement of inelastic processes has so far defied successful solution, mainly for lack of a good neutron spectrometer. One cannot complain for lack of attention to the problem, however; one of the techniques now being studied will probably be successful.

The physicist has the data with which to calculate, and the methods of calculation are also being developed. The pre-1950 era was one in which many unsuccessful searches were made for quick approximate solutions to the fundamental transport equation. With the rise of the high-speed automatic

(1) R. K. Adair, "Neutron Cross Sections of the Elements," Revs. Mod. Phys. 22, 249 (1950).
(2) "Neutron Cross Sections," AECU-2040 (May 15, 1952).

computing machines it has been possible to devise seminumerical methods to obtain quite accurate solutions. In the realm of gamma-ray penetration particularly, it has been possible to provide almost complete solutions to all problems involving a single infinite medium. The same methods are now being successfully applied to similar neutron penetration problems. As our knowledge of the potentialities of extensive calculations with high-speed machines increases, there is reason to believe the several-media problem can also be tackled. These calculations already supplement and extend bulk shielding experiments, and they can be expected to do so to an ever increasing extent in the coming years. One bright expectation of 1950 that failed to materialize was the development of Monte Carlo techniques, also using high-speed computers. Some early failures and misapplications of the method caused a regretable loss of interest. Recently there has been a renaissance of attention to the technique and its application to more suitable problems.

Specific problems yet to be tackled belong in the section on recommendations for future research, but an attempt at a general glance into the future may not be amiss here. Some things are easy to predict. The next few years will surely see the Tower Shielding Facility in operation and the testing of mockups of complete airplane shields. It is most likely that procedures for calculating neutron penetration, and even combined neutron-gamma propagation, in infinite media will be reduced to a nearly routine basis. The neutron cross section picture can be expected to improve much as it has in the past few years even perhaps to the point of seeing the inelastic problem licked.

Some predictions must be in the nature of hopes rather than firm beliefs. It is to be hoped that the next few years will see rational

interpretations of most of the large output of bulk shielding experiments, so that the designer can utilize these results with varied source geometry and leakage, and with not too large perturbations in configuration and composition of the shield. One would hope that some method can be devised for the design of shadow shields that is more reasonable than the present conservative practice based on ignorance. Another need which should be fulfilled in the next few years is a careful and concerted search for new shielding materials, a search which makes use of all the improvements in shielding lore gained up till now. One would also like to see the methods of computation for the fundamental attenuation problem extended to cover several media. Without this extension the basic theory will fall short of maximum usefulness to the designer. And it is to be hoped the Monte Carlo method can be developed to handle some of the meaner geometries encountered in actual shields.

One can only guess at the form of shield design in, say, 1956. If the trend to smaller cores continues it is likely the shield will be closer to "unit" than at present, with little shielding on the crew compartment. It is also likely that the dose rates demanded inside the crew compartment will tend to be lower than now allowed. It seems reasonable to predict that the kinds of shielding mechanisms employed will be the same as now, i.e., fast neutrons removed by first slowing down and then capturing, gamma rays absorbed in heavy elements which play only a minor role in neutron attenuation. Reduction in shield weights is more likely to come rather from the careful employment of materials now moderately unfamiliar and by detailed optimization of the various components. It also seems reasonable to predict that as the day for actually constructing an airplane shield comes closer, increasing attention will have to be paid to engineering details now so blithely

overlooked. And it is a reasonable extrapolation from submarine experience to predict that these details will threaten large weight increases which will need to be combated by all the cleverness and skill the shield and reactor designers can muster.

VII. BIBLIOGRAPHY AND ACKNOWLEDGMENTS

BIBLIOGRAPHY

Abernathy, F. H., and H. Reese, Jr., "The (n,γ) Cross Section for Na^{23} at 500-600 Kev," ORNL-CF-53-8-22 (Aug. 4, 1953).

Adair, R. K., "Neutron Cross Sections of the Elements," Revs. Mod. Phys. 22, p. 249 (1950).

"Aircraft Nuclear Propulsion Project Quarterly Progress Report for Period Ending June 10, 1953," ORNL-1556.

"The Aircraft Nuclear Propulsion Project at the Oak Ridge National Laboratory," ORNL-768 (Aug. 14, 1950).

"Aircraft Nuclear Propulsion Project Quarterly Progress Report for Period Ending September 10, 1953," ORNL-1609.

Albert, R. D., and T. A. Welton, "A Simplified Theory of Neutron Attenuation and Its Application to Reactor Shield Design," WAPD-15 (Nov. 30, 1950).

Baldinger, E., P. Huber, and W. G. Proctor, "Streuung von schnellen Neutronen an O^{16}," Helv. Phys. Acta 25, p. 142 (1952).

Banus, M. D., R. W. Bragdon, and T. R. P. Gibb, Jr., "Preparation of Quaternary Ammonium Borohydrides from Sodium and Lithium Borohydrides," J. Am. Chem. Soc. 74, p. 2346 (1952).

Blizard, E. P., and T. A. Welton, "The Shielding of Mobile Reactors (I)," Reactor Sci. Tech. 1, No. 3, p. 15, TID-73 (1951).

Blizard, E. P., H. L. F. Enlund, and J. H. Wyld, "Ammonia as an Aircraft Shield Component," Reactor Sci. Tech. 2, No. 1, p. 79, TID-2001 (1952).

Blizard, E. P., "Introduction to Shield Design, Parts I and II," CF-51-10-70 (1952).

Blizard, E. P., "Reactor Leakage for Shielding Calculations," CF-53-7-170 (Nov. 27, 1953).

Blizard, E. P., "The Tower Shielding Facility," Reactor Sci. Tech. 3, No. 2, p. 279, TID-2009 (1953).

Bly, F., and F. C. Maienschein, "A Calculation of Gamma Radiation Reaching the ANP-53 Crew Shield," ORNL-CF-53-5-117 (May 23, 1953).

Bockelman, C. K., D. W. Miller, R. K. Adair, and H. H. Barschall, "Total Cross Sections of Light Nuclei for p, T-Neutrons," Phys. Rev. 84, p. 69 (1951).

Born, J. W., "Closure Report (on) Plastic and Elastomeric Materials as Shielding Components for Nuclear Reactors," B. F. Goodrich Co., ORO-80 (July 2, 1952).

Bouricius, W. G., "Void Theory of Ducts," NEPA-1536 (Aug. 24, 1950).

Brennan, James T., et al., "The Biological Effectiveness of Thermal Neutrons on Mice," LA-1408 (Feb. 15, 1952).

Brittan, R. O., et al., "Technical Review of ZPR-1 Accidental Transient: The Power Excursion, Exposures, and Clinical Data," ANL-4971 (Jan. 26, 1953).

Clifford, C. E., "Gamma Attenuation Behind 3.8-, 7.6-, and 11.4-cm Solid Lead Shadow Shields in Pure Water as a Function of Water Reflector Thicknesses," CF-52-5-163 (May 20, 1952).

Coon, J. H., E. R. Graves, and H. H. Barschall, "Total Cross Sections for 14-Mev Neutrons," Phys. Rev. 88, p. 562 (1952).

"Engineering Progress Report No. 2; October 1, 1951 -- December 31, 1951," Aircraft Nuclear Propulsion Project, DC-51-12-25, p. 130 (Dec., 1951).

Enlund, H. L. F., "Energy Absorption of Capture Gammas," CF-52-6-99 Supplement (Oct. 16, 1952).

Fano, U., "Gamma-Ray Attenuation," Nucleonics 11, No. 8, p. 8 (1953).

Feld, B. T., H. Feshbach, M. L. Goldberger, H. Goldstein, and V. F. Weisskopf, "Final Report of the Fast Neutron Data Project," Nuclear Development Associates NYO-636 (Jan. 31, 1951).

Fishler, M. C., et al., "Therapeutic Effect of Rat Bone Marrow Injection in Rats Exposed to Lethal Whole-Body X Radiation," USNRDL-410 (Sept. 8, 1953).

Flynn, J. D., and G. T. Chapman, "Attenuation by Lead of Fast Neutrons from a Fast Fission Source," ORNL CF-53-3-166 (Mar. 10, 1953).

Foster, H. H., NACA RONE 51A24, Lewis Flight Propulsion Laboratory, Cleveland, Ohio (Mar. 27, 1951).

Fraas, A. P., and M. E. LaVerne, "Heat Exchanger Design Charts," ORNL-1330 (Dec. 7, 1952).

Fraas, A. P., "Three Reactor -- Heat Exchanger -- Shield Arrangements for Use with Fused Fluoride Circulating Fuel," Y-F15-10 (June 30, 1952).

Goldstein, H., and E. P. Blizard, "A Criterion for the Experimental Optimization of Two-Component Unit Shields," Reactor Sci.Tech. 1, No. 2, p. 88, TID-72 (1951).

Goldstein, H., and R. Aronson, ORNL-1179 (to be published).

Goldstein, H., J. E. Wilkins, Jr., and L. V. Spencer, "Systematic Calculations of Gamma-Ray Penetration," Phys. Rev. 89, p. 1150 (1953).

Goldstein, H., J. E. Wilkins, Jr., and Stanley Preiser, "Interim Report on the NDA-NBS Calculations of Gamma Ray Penetration," NDA Memo 15C-20 (Sept. 8, 1953).

Goldstein, H., "Notes on the Transformation from Sphere to Plane Isotropic Source," NDA Memo 12-5 (Sept. 23, 1953).

Gray, L. H., "An Ionization Method for the Absolute Measurement of Gamma-Ray Energy," Proc. Roy. Soc. (London) 156A, p. 578 (1936).

Ham, W. T., Jr., "Radiation Cataracts," Arch. Opthalmol. (Chicago) 50, p. 618 (1953).

Handbook of Chemistry and Physics, 35th ed., Chemical Rubber Publishing Co., Cleveland, Ohio, 1953.

Hartree, Mem. Proc. Manchester Lit. and Phil. Soc. 80, p. 85 (1935).

Heitler, W., Quantum Theory of Radiation, Oxford University Press, New York, 1944.

Held, K., "Polymethylene as Shielding Material," NDA-71 (May 20, 1953).

Held, K., "Shielding Materials," NDA-10-52 (March 21, 1953).

Henshaw, P. S., E. F. Riley, and G. E. Stapleton, "The Biologic Effects of Pile Radiations," Radiology 49, p. 349 (1947).

Hoffman, J. G., "Radiation Doses in the Pajarito Accident of May 21, 1946," LA-687 (May 26, 1948).

Hughes, D. J., W. D. B. Spatz, and N. Goldstein, "Capture Cross Sections for Fast Neutrons," Phys. Rev. 75, p. 1781 (1949).

Hungerford, H. E., "Bulk Shielding Facility Data Work Sheets," CF-52-2-37 (Feb., 1952).

Hungerford, H. E., "Some Ground Scattering Experiments Performed at the Bulk Shielding Facility," ORNL-CF-52-4-99 (April 16, 1952).

Hungerford, H. E., "The Skyshine Experiments at the Bulk Shielding Facility," ORNL-1611.

Kern, F. S., et al., "Oblique Attenuation of X-Rays from Co^{60} and Ce^{137} in Polyethylene, Concrete and Lead," National Bureau of Standards, NBS-2125 (Dec. 23, 1952).

Kouts, H. J., "Theory of Flux Perturbations by Voids in Shields," BNL Log No. C-6459 (Sept. 15, 1952).

Latter, R., and H. Kahn, "Gamma-Ray Absorption Coefficients," R-170 (Sept. 19, 1949).

Lord, A. M., NACA RME52B01, Lewis Flight Propulsion Laboratory, Cleveland, Ohio (April 28, 1952).

Lorenz, E., "Some Biologic Effects of Long Continued Irradiation," Am. J. Roentgenol. Radium Therapy 63, p. 176 (1950).

Maienschein, F. C., "Gamma-Ray Spectral Measurements with the Divided Shield Mockup," Part I, ORNL-CF-52-3-1 (March 3, 1952); Part III, ORNL-CF-52-8-38 (August 8, 1952); ...and T. A. Love, Part IV, ORNL-CF-52-11-124 (Nov. 17, 1952).

Mela, R., private discussion with Mr. Landolt of Metalloy Corp. re Lithium Hydride, NDA-10-59 (Feb. 11, 1954).

Mills, C. A., "Fast Neutron Dosimetry in a Small Tissue Equivalent Phantom," to be published in Nucleonics.

Mittelman, P., "Gamma Rays Resulting from Thermal Neutron Capture," NDA-10-99 (Oct. 6, 1953).

Morgan, K. Z., "Radiation Safety Measures in an Atomic Energy Plant," Eng. J. 31, No. 3 (1948).

Motz, J. W., "Gamma-Ray Spectra of the Los Alamos Reactors," Phys. Rev. 86, p. 753 (1952).

Nereson, N., and S. Darden, "Average Neutron Total Cross Sections in the 3- to 12-Mev Region," Phys. Rev. 89, p. 775 (1953).

"Neutron Cross Sections," AECU-2040 (May 15, 1952).

"Nuclear-Powered Flight; A Report of the Atomic Energy Commission," LEXP-1 (Sept. 30, 1948).

Oaks, W. R., and C. C. Lushbaugh, "Course of Testicular Energy Following Accidental Exposure to Nuclear Radiations; Report of a Case," Radiology 59, p. 737 (1952).

"Permissible Dose from External Sources," Handbook 55, National Bureau of Standards.

"Physics Division Quarterly Progress Report for Period Ending December 20, 1952," ORNL-1477 (Secret).

"Physics Division Quarterly Progress Report for Period Ending December 20, 1952," ORNL-1496 (Unclassified).

"Physics Division Quarterly Progress Report for Period Ending June 20, 1952," ORNL-1365.

"Physics Division Quarterly Progress Report for Period Ending September 20, 1952," ORNL-1415.

Placzek, G., and Gertrude Blanch, "The Functions $E_n(x) = \int_1^\infty e^{-xu} u^{-n} du$ and Their Fourier and Laplace Transforms," Montreal Laboratory, MT-1.

Plesset, M. S., and S. T. Cohen, "Scattering and Absorption of Gamma-Rays," J. Applied Phys. 22, p. 350 (1951).

Plesset, M. S., "Scattering of Gamma Rays and Neutrons," Douglas Aircraft Company, Inc., Project Rand, RAD-196 (Aug., 1947).

Pratt, W. W., and H. J. Kouts, "Leakage of Gamma Radiation Through Spherical and Cylindrical Voids," BNL Log No. C-6456 (Aug. 25, 1952).

Reactor Handbook, Vol. 1, RH-1, Technical Information Service, U. S. Atomic Energy Commission (June, 1953).

"Recommendations of the International Commission on Radiological Protection and of the International Commission on Radiological Units, 1950," Handbook 47, National Bureau of Standards (June 29, 1951).

"Recordings of Genetic Society of America," No. 22 (1953).

"Report of the ANP Shielding Board for the Aircraft Nuclear Propulsion Program," ANP-53 (Oct. 16, 1950).

"Report of the Physics Section for December 1952, January and February 1953," Knolls Atomic Power Laboratory, KAPL-909.

"Report of the Technical Advisory Board," ANP-52 (Aug. 5, 1950).

Roe, G. M., "The Penetration of Neutrons Through an Empty Cylindrical Duct in a Shield," KAPL-712 (Mar. 29, 1952).

Rossi, H. H., "The n Unit and Energy Absorption in Tissue," Radiology 61, p. 93 (1953).

Russell, W. L., "Mammalian Radiation Genetics," Symposium on Radiobiology, Oberlin College, Wiley, New York, 1952.

Russell, W. L., L. B. Russell, J. S. Gower, and C. W. Sheppard, "Neutron Induced Dominant Lethals in the Mouse," Genetics 38, p. 688 (1953).

Sakamoto, S., "Tafel der Funktionen $y = e^{x^2}/x \int_0^x e^{\alpha^2} d\alpha$ und $z = e^{-x^2} \int_0^x e^{\alpha^2} d\alpha$ im Intervall $x = 0$ bis $x = 10$," Ber. Verhandl. Akad. Wiss. Leipzig, Math-naturw. Kl. 80, 217 (1928).

Simon, A., and C. E. Clifford, "The Attenuation of Neutrons by Air Ducts in Shields, Part I, Theory," ORNL-1217 (Nov. 28, 1952).

Simon, A., and R. H. Ritchie, "Background Calculations for the Proposed Tower Shielding Facility," ORNL-1273 (Oct. 15, 1952).

Snyder, W. S., and J. L. Powell, "Absorption of γ-Rays," ORNL-421 (March, 1950); also issued as AECD-2739.

Snyder, W. S., "Calculated Depth Dose Curves in Tissue for Broad Beams of Fast Neutrons," to be published in Brit. J. Radiology.

Snyder, W. S., "Calculations for Maximum Permissible Exposure to Thermal Neutrons," Nucleonics 6, p. 46 (1950).

Spencer, L. V., and U. Fano, "Penetration and Diffusion of X-Rays. Calculation of Spatial Distributionsby Polynomial Expansion," J. Res. NBS 46, p. 446 (1951).

Stone, R. S., "Neutron Therapy and Specific Ionization," Am. J. Roentgenol. Radium Therapy 59, No. 6, p. 771 (1948).

Tait, J. H., "Calculation of the Energy Deposition by Fast Neutrons in Soft Tissue," Brit. J. Radiology 23, No. 269, p. 282 (1950).

Tonks, L., and H. Hurwitz, "The Economical Distribution of Gamma Ray Absorbing Material in a Spherical Pile Shield," KAPL-76 (June 8, 1947).

Tonks, L., "Enhancement of Leakage by Internal Voids in a Shield," KAPL-107 (Jan. 17, 1949).

Trice, J. B., "The Importance of Twice Scattered Gamma Rays Arriving at the Crew Position of a Nuclear Powered Aircraft," NEPA-1297 (Feb. 27, 1950).

Welton, T. A., and E. P. Blizard, "The Shielding of Mobile Reactors (II)," Reactor Sci. Tech. 2, No. 2, p. 73, TID-2002 (1952).

Whitcombe, D. W., "A Diffusion Solution for the Cylindrical Ducting Problem of Infinite Geometry," ORNL-668 (April 19, 1950).

White, G. R., "X Ray Attenuation Coefficients from 10 Kev to 100 Mev," NBS-1003 (May 13, 1952).

Zirkle, R. E., "Radiobiological Additivity of Various Ionizing Radiations," Am. J. Roentgenol. Radium Therapy 63, p. 170 (1950).

[redacted]

ACKNOWLEDGMENTS

We who participated in this summer session wish to express our appreciation for all the assistance which was tendered us by our associates both at Oak Ridge and at our other parent organizations.

In the preparation of the section on radiation tolerances, K. Z. Morgan, Director of the ORNL Health Physics Division, made many helpful suggestions. Some of the material appearing therein is taken from his article for the "Handbook on Physics" to be published by the National Research Council. The section was also read and improved by J. Furth, W. L. Russell, L. B. Russell, and A. Upton, of the ORNL Biology Division.

Various portions of the manuscript have been read in various stages of preparation by L. A. Wills, C. Klahr, A. Stathopolis, and P. Mittelman, all of NDA. Their many suggestions have been very valuable in improving the text.

Thanks are due to R. K. Osborne for assistance in preparation of the treatment of sodium activation in the heat exchanger. The chapter on shield design for the RMR was very carefully reviewed by Lt. R. M. Spencer and Lt. F. M. Westfall, and they added some very useful material to the text. Their suggestions, furthermore, added considerably to the utility of the subject matter.

For technical editing and assimilation of our diverse contributions our thanks are due to Mrs. L. S. Abbott. During the session the Laboratory personnel were particularly cooperative with the visiting participants, making their stay an enjoyable one. Particular mention should be made of Miss Rebecca Rickman for her continued assistance to the participants during their stay here and for the typing of this report.

The Editors

[redacted]